The regulation of Mps1 kinase during mitosis

Davinderpreet Singh Mangat

Lincoln College

University of Oxford

A thesis submitted for the degree of Doctor of Philosophy,

Michaelmas 2017

I would like to dedicate this thesis to my parents,
without whom I would never have even imagined doing a PhD.

You taught me to dream big and work hard.

Now I'll be a Doctor which is incredible, but most of all
I'm glad I'll be able to fulfil one of your dreams.

Thanks for giving me the opportunities you never had,
This is for you Mum and Dad

Acknowledgements

During the course of this PhD I struggled more than I ever have before. I am delighted to get this opportunity to thank all the people who made it possible for me to finish this PhD. Without a doubt I couldn't have done this without you.

To my **parents** to whom this thesis is dedicated, thanks for the constant support, the lessons, the nagging, and the kicks up the backside when necessary. To my older sisters, **Harpreet** and **Gurpreet**. Thanks for all the encouragement, advice and for being great examples to follow. It's amazing to think that before you two our families only qualification was Dad's O-level in poultry farming. To my little sister and best friend, **Baljit**. Being a good role model to you has been somewhat of a driving force this past decade. I hope you're proud and inspired.

To my best friend **Christy**, without your support, your jokes and your hugs I would never have managed to get through this part of my life. We swore a pact almost 3 years ago to finish the PhD together no matter what and I can't believe we're one down. I simply couldn't have done this without you. I'm glad you're my best mate and that I agreed to your pact that night. You're the best Christy.

To my teammates, at **Oxford University Quidditch Club**. Playing Quidditch with you in the rain, cold and mud was the best possible way to spend my weekends. As always, Volate Pulchre. To my friends at the board game club, **Kerry**, **Luke**, **Xin**, **Martin**, **Fran**, **Phil** and **Jana**. It has been a pleasure playing board games with you these last few years and was one of the highlights of my week. To **Dan**, thanks so much for your counsel and advice. To **John and the boys**, thanks for welcoming me as a guest and providing me with a great setting to write this thesis.

I would like to thank my **department** and **college** for their funding. Finally, I would like to thank **Dr Ulrike Gruneberg** for having me in her group and for providing me with my scientific training. I really enjoyed working on our scientific questions.

Table of contents

Declaration of Authorship

Except where stated to the contrary, the work described in this thesis is my own.

Both the mass spectrometry experiments and analysis were done in collaboration with Christina. H. Y. Barnard.

List of figures and tables.

Abbreviations

3’ UTR	3’ Untranslated region
APC/C	Anaphase promoting complex/cyclosome
Bub1	Budding uninhibited by benzimidazoles 1
Bub3	Budding uninhibited by benzimidazoles 3
BubR1	Budding uninhibited by benzimidazoles related 1
CDK	Cyclin dependent kinase
CPC	Chromosome passenger complex
CIN	Chromosomal instability
CENP	Centromere protein
CCAN	Constitutive centromere associated network
CH	Calponin homology domain
DMEM	Dulbecco’s modified eagle medium
DMSO	Dimethyl Sulfoxide
EC	Error correction
FRAP	Fluorescence recovery after photobleaching
FRET	Fluorescence resonance energy transfer
GFP	Green fluorescent protein
H2A	Histone 2A
HEC1	Highly expressed in cancer 1
IF	Immunofluorescence
IP	Immunoprecipitation
K-MT	Kinetochore-microtubule attachments
KMN	Knl1-Mis12-Ndc80 network

KNL1	Kinetochore scaffold 1
KD	Kinase dead
MAPs	Microtubule associated proteins
MCC	Mitotic checkpoint complex
MAD1	Mitotic arrest defect 1
MAD2	Mitotic arrest defect 2
MELT	Met-Glu-Leu-Thr motifs on Knl1
MIS12 complex	Consisting of Nsl1, Nfn1, Dsn1 and Mis12
MPS1	Monopolar spindle 1
MR	Middle region domain of Mps1
MTOC	Microtubule organising centre
NEB	Nuclear envelop breakdown
NDC80 complex	Consisting of Hec1, Nuf2, Spc24 and Spc25
NTE	N-terminal extension domain of Mps1
NUF2	Nuclear filament-related 2
PPP	Phospho-protein phosphatases
PLK1	Polo like kinase 1
RZZ	Rod-Zwilch-Zw10
SAC	Spindle assembly checkpoint
SKA	Spindle and kinetochore associated network
SiRNA	Small interfering RiboNucleic Acid
T-loop	Activation loop of a kinase
TPR	Tetratricopeptide domain
WT	Wildtype

Abstract

The spindle assembly checkpoint (SAC), a conserved surveillance system, ensures genomic stability by delaying anaphase entry until all sister chromatids are attached to the mitotic spindle. The SAC network is active at unattached kinetochores and a complex signalling cascade culminates in the production of a diffusible 'wait anaphase' signal. Regulation of protein:protein interactions by reversible phosphorylation is critical in this signalling pathway. The checkpoint kinase Mps1, a central regulator of the SAC, plays a positive role in enabling protein interactions. Mps1 builds the SAC network by phosphorylating multiple kinetochore targets and in doing so it coordinates mitotic exit with microtubule binding. Given the critical role Mps1 plays in SAC activation, precise regulation of the activity and localisation of Mps1 must be key in controlling the activation status of the SAC.

Mps1 binds to unattached kinetochores and is activated by autophosphorylation of its T-loop. However, once chromosomes are attached to the spindle and the SAC is satisfied Mps1 is switched off. The mechanisms controlling the inactivation of Mps1 were unknown. Here, it is shown that phosphorylation of T676, located on the activation loop of Mps1, is important in controlling Mps1 activity and SAC signalling. A PP2A-B56 phosphatase complex opposes Mps1 activation by directly dephosphorylating its activation loop both *in vitro* and *in vivo*. The interaction of PP2A-B56 with BubR1 is essential for this dephosphorylation event. Moreover, preliminary results from experiments combining Mps1 immunoprecipitations with mass spectrometry indicate that phosphate groups are globally lost from Mps1 when the SAC is inactive. The binding of interaction partners is a common mechanism used by kinases to regulate their function. Knl1 is present in Mps1 complexes by immunoprecipitation and mass spectrometry. While these results are still preliminary it is clear from siRNA depletion that Knl1 plays a previously unidentified role in regulating the localisation of Mps1. Together, these results signify an important advance in our knowledge of how the function of Mps1 is controlled.

1.

INTRODUCTION

1.1 The Cell Cycle

The generation of a new cell involves the duplication of a cell that already exists (Morgan, 2007). This concept first discussed in the middle of the nineteenth century, has shaped our understanding of the evolution of life on Earth. Life began with a single ancestral cell 3 to 4 billion years ago and every unicellular and multicellular organism that has evolved since is simply a product of repeated rounds of cell growth and division. In each duplication, cells grow, replicate their genetic material (DNA) and then evenly distribute this genetic information between two daughter cells. This process is called the cell cycle (**figure 1.1**). Faithful execution of the cell cycle is fundamental for the creation and survival of all organisms. In unicellular organisms, such as yeast and bacteria, a single cell division produces a completely new organism (Lara-Gonzalez et al., 2012). In multicellular organisms, long and complex sequences of cell division are needed to create the muscles, tissues and organs that make up a functional organism. After development, cell division is essential for continued survival replacing the millions of cells that die per second. In fact, if cell division stopped in a person, for example by exposing someone to large levels of radiation, they would die within days (Alberts B et al, 2014).

The introductory section of this chapter will provide an overview of the cell cycle, the checkpoints that guard progression and will lead onto an in-depth discussion of mitosis. Howard and Pelc first proposed the existence of four stages in the cell cycle: pre-replication growth (G1), DNA replication (S), pre-mitotic gap phase (G2) and cell division or mitosis (M) (**figure 1.1**) (Dubrovsky and Ivanov, 2003). The order of phases in the cell cycle varies from organism to organism, for example, in archaea and bacteria the two genomes are segregated while DNA replication is underway (Lara-Gonzalez et al., 2012). In Xenopus embryos, cells use an inherited protein rich cytoplasm to undergo cell division without needing to enter growth phases. While the cell cycle can vary between organisms each cell has the fundamental task of replicating its DNA and evenly segregating it

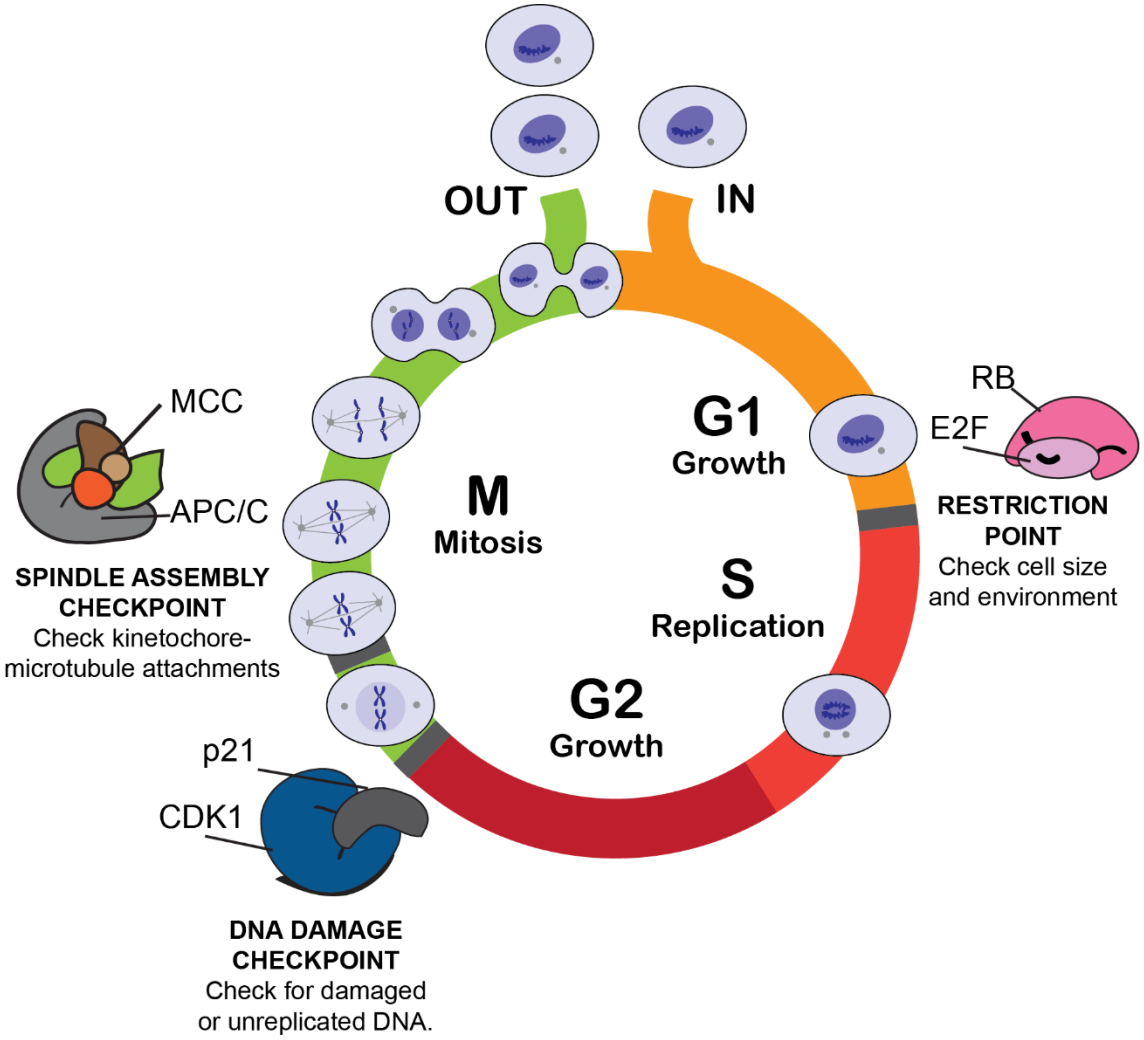

Figure 1.1. The metazoan cell cycle. A cartoon showing how cells progress through the cell cycle. The cell cycle has four major phases and three checkpoints: the restriction point, the cell interprets environmental cues, the DNA damage checkpoint, when the cell assesses the quality of the DNA and the spindle assembly checkpoint (SAC), when the cell ensures chromosomes are properly attached to the mitotic spindle prior to segregation.

between daughter cells. The introductory discussion here will focus on the cell cycle of eukaryotes specifically of humans, which are most relevant to this study.

1.1.2 THE CDK ENGINE

The four stages of the cell cycle are divided by three switch-like transitions: at the onset of S phase, mitotic entry and exit (Hochegger et al., 2008). Progression through the cell cycle is driven by members of a family of protein kinases called the cyclin-dependent kinases (CDKs). CDKs are the engines that drive the cell cycle. In modified yeast cells lacking the canonical regulatory networks, oscillations in an engineered monomolecular CDK was sufficient to drive orderly cell cycle progression (Coudreuse and Nurse, 2010). While CDKs are the engines of the cell cycle their respective regulatory subunits called cyclins, make up the gears that control transitions between phases (Hochegger et al., 2008). The cyclins form bipartite complexes with their cognate CDKs, to activate the kinase and target it to specific substrates. The concentration of cyclins rise and fall during the cycle and subsequently specific Cyclin:CDK heterodimers are only present at certain points (**figure 1.2**). Cyclical changes in the concentration of cyclins turns their respective CDKs on and off to trigger cell cycle transitions. In addition to cyclin binding, CDKs are also activated by phosphorylations on the activation loop of the kinase. CDKs can be inactivated through multiple methods including the proteasome-dependent degradation of its respective cyclin (Peters, 2006), inhibitory phosphorylations such as Tyr14 and Tyr15 on CDK1 (Kellogg, 2003) and by CDK inhibitors (Besson et al., 2008). The precise details of how Cyclin B-CDK1 is regulated has been studied extensively and has additional layers of regulation (**figure 1.2**). The different CDKs are switched on and off as the cell progresses through the cycle, resulting in timely changes in the phosphorylation of cell cycle regulators and the subsequent activation or inactivation of signalling networks that control major cellular events. The Cyclin B:CDK1 is activated at the G2/M transition and degradation of its cognate Cyclin is the key step in mitotic exit.

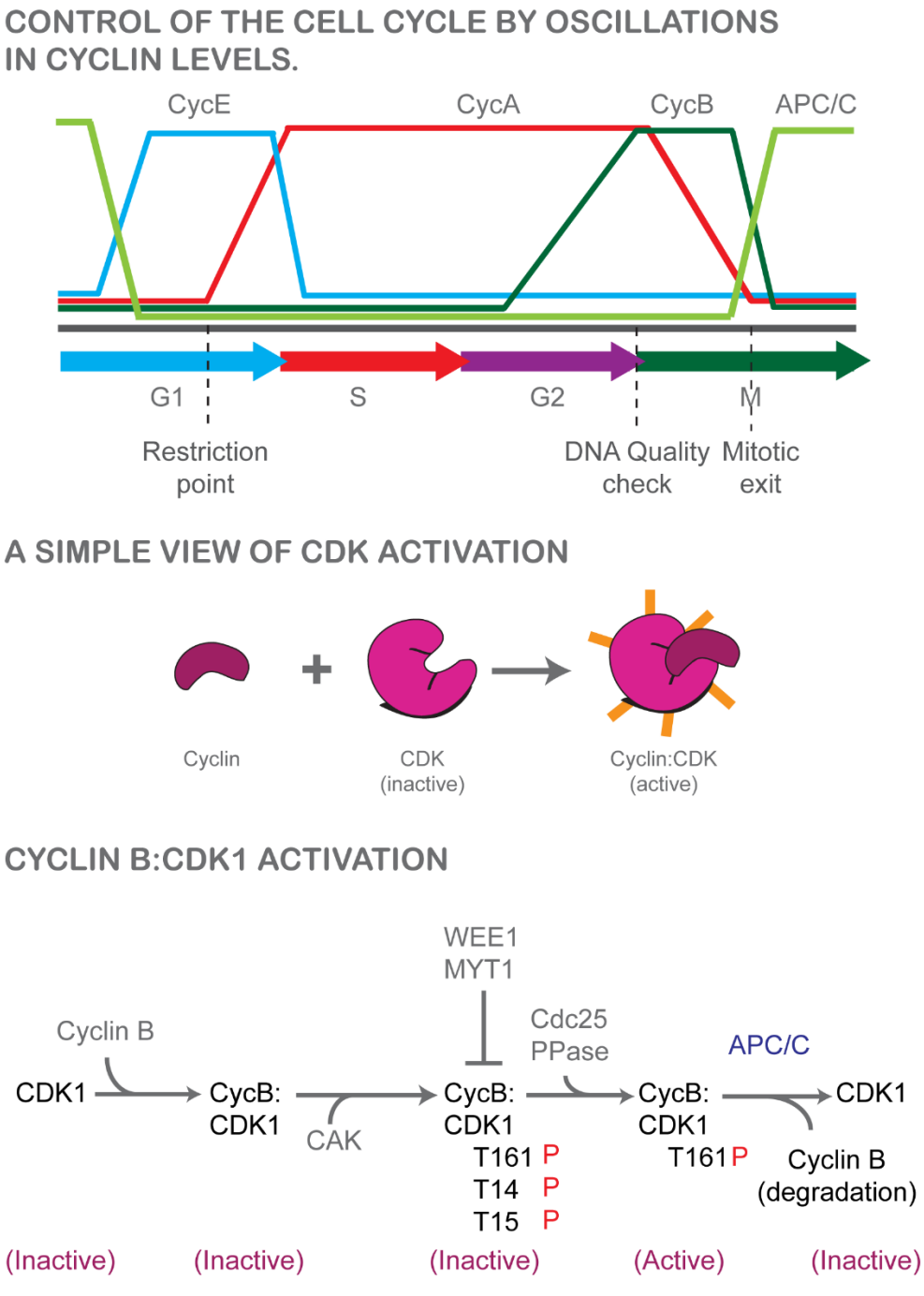

Figure 1.2. The cell cycle oscillator. Periodic oscillations in the concentration of cyclins and subsequently the activity of their respective kinases regulates the cell cycle. Cyclins are expressed and degraded at specific points of the cell cycle. The binding of cyclins to CDKs activates the kinase, however, some additional level of control is needed, for example, Cyclin B: CDK1 is regulated by several other kinases, the Cdc25 phosphatase as well as by the APC/C.

1.1.3 CHECKPOINTS

In human cells, DNA held in the form of 46 chromosomes is replicated during a Synthesis or S phase and chromosomes are segregate during mitosis or M phase. There are two gap phases, G1 and G2, which separate DNA synthesis and mitosis. Importantly, these gap phases are not periods of inactivity, but signify important time points when the cell manufactures protein machinery, evaluates its environment and corrects any errors made during replication to ensure the fidelity of daughter cells. It is essential that all these complex cellular events occur in a sequence so that DNA is replicated, corrected and segregated at the correct time. To ensure genetic fidelity, cells have evolved complex surveillance mechanisms called cell cycle checkpoints (**figure 1.1**). When these checkpoints are active cell cycle progression is halted providing time for the cell to check an earlier process (Hartwell and Weinert, 1989). Cell cycle checkpoints have three crucial components: a surveillance mechanism, that detects any errors made: an enforcement mechanism to stop the cell cycle, providing time to make corrections and lastly an error correction pathway, to resolve the problem.

The first of these checkpoints functions at the G1/S transition. During G1, cells increase in size (Wood and Nurse, 2015), repair any damaged DNA (Kastan and Bartek, 2004), and synthesise the proteins needed for DNA replication (White-Gilbertson et al., 2009). Towards the end of G1, cells evaluate a diverse range of metabolic, stress and environmental signals and then decide on whether to commit to entering the cell cycle, this is called the restriction point. The second of these checkpoints, the DNA damage checkpoint, is active at the S/G2 transition and during S phase. This checkpoint detects DNA damage that can occur due to spontaneous chemical reactions in nucleotides, errors introduced during replication and exposure to radiation. DNA damage stimulates effector kinases that propagate a wait signal by phosphorylating many target proteins (Wang et al., 2015). A hallmark of cancer cells is an array of defects in the DNA repair machinery and this is associated with increased genomic instability (Hanahan and Weinberg, 2011).

The final checkpoint is active at mitosis and ensures chromosome segregation occurs with high fidelity. During mitosis, replicated chromosomes are segregated to opposite sides of the cell. Chromosome segregation is coordinated by the mitotic spindle, a microtubule-based structure, which attaches to the kinetochores of sister chromatids. When kinetochore-microtubule (K-MT) attachments are complete, the cohesin ring, which holds sister chromatids together, is cleaved and the mitotic spindle distributes chromosomes between the two poles (Michaelis et al., 1997; Foley et al., 2011). The spindle assembly checkpoint (SAC), a cell cycle surveillance mechanism, has evolved to ensure efficient chromosome segregation. The SAC monitors K-MT attachments and blocks anaphase entry in response to even a single unattached kinetochore. To do this the SAC inhibits the anaphase promoting complex (APC/C), an E3 ubiquitin ligase that targets cyclin B and securin for degradation (Lara-Gonzalez et al., 2012) (**figure 1.3**). The phosphorylation of many substrates by Cyclin B:CDK1 is required for mitotic entry and conversely the dephosphorylation of these substrates by PP1 and PP2A-B55 is needed for mitotic exit (Wu et al., 2009; Heim et al., 2015; Cundell et al., 2013, 2016). Securin the other major target of the APC/C is an inhibitor of a protein called separase, which as the name suggests separates sister chromatids by cleaving the cohesin ring holding them together (Uhlmann et al., 2000). When the SAC is active a “wait anaphase” signal, the mitotic checkpoint complex (MCC), comprising the SAC proteins BubR1, Bub3, Mad2 and the obligatory APC/C accessory subunit Cdc20, is assembled at unattached kinetochores (Sudakin et al., 2001; Kulukian et al., 2009). The MCC diffuses into the cytoplasm where it binds and inhibits the APC/C to prevent the degradation of cyclin B and securin to maintain a mitotic state. The attachment of chromosomes to the bipolar spindle switches the SAC off. The production of the MCC stops and as a result inhibition of the APC/C is relieved. Active APC/C proceeds to ubiquitinate Cyclin B and securin marking them for the proteasome pathway. The loss of Cyclin B inactivates CDK1, a core component of the cell cycle oscillator system, while separase-mediated cleavage of cohesin is a prelude for chromosome segregation. Together the destruction of these two targets drives mitotic exit.

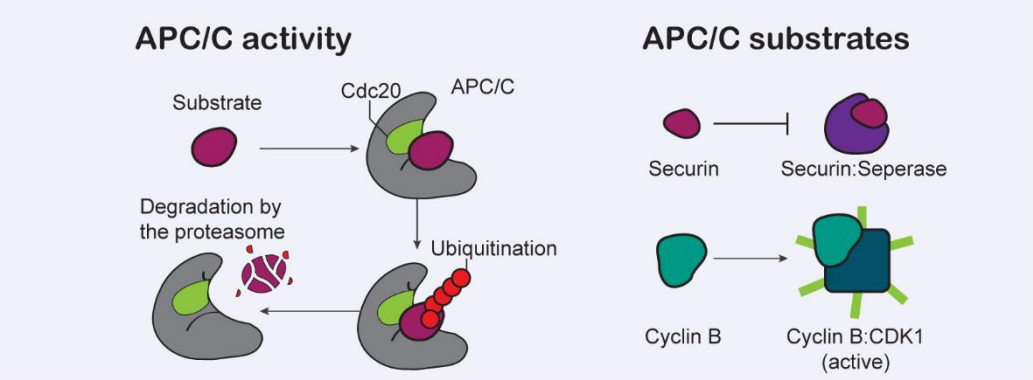
APC/C activity
Substrate
Cdc20
APC/C
Degradation by
the proteasome
Ubiquitination
APC/C substrates
Securin
Securin:Seperase
Cyclin B
Cyclin B:CDK1
(active)

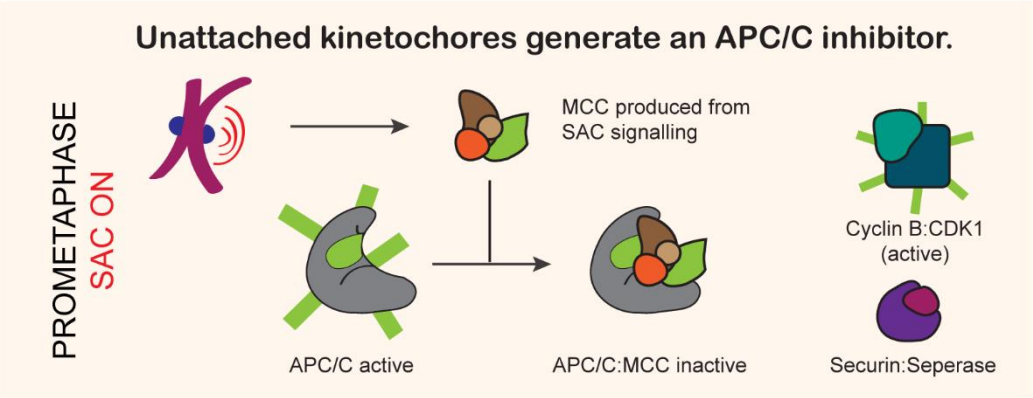
Unattached kinetochores generate an APC/C inhibitor.
PROMETAPHASE
SAC ON
MCC produced from
SAC signalling
APC/C active
APC/C:MCC inactive
Cyclin B:CDK1
(active)
Securin:Seperase

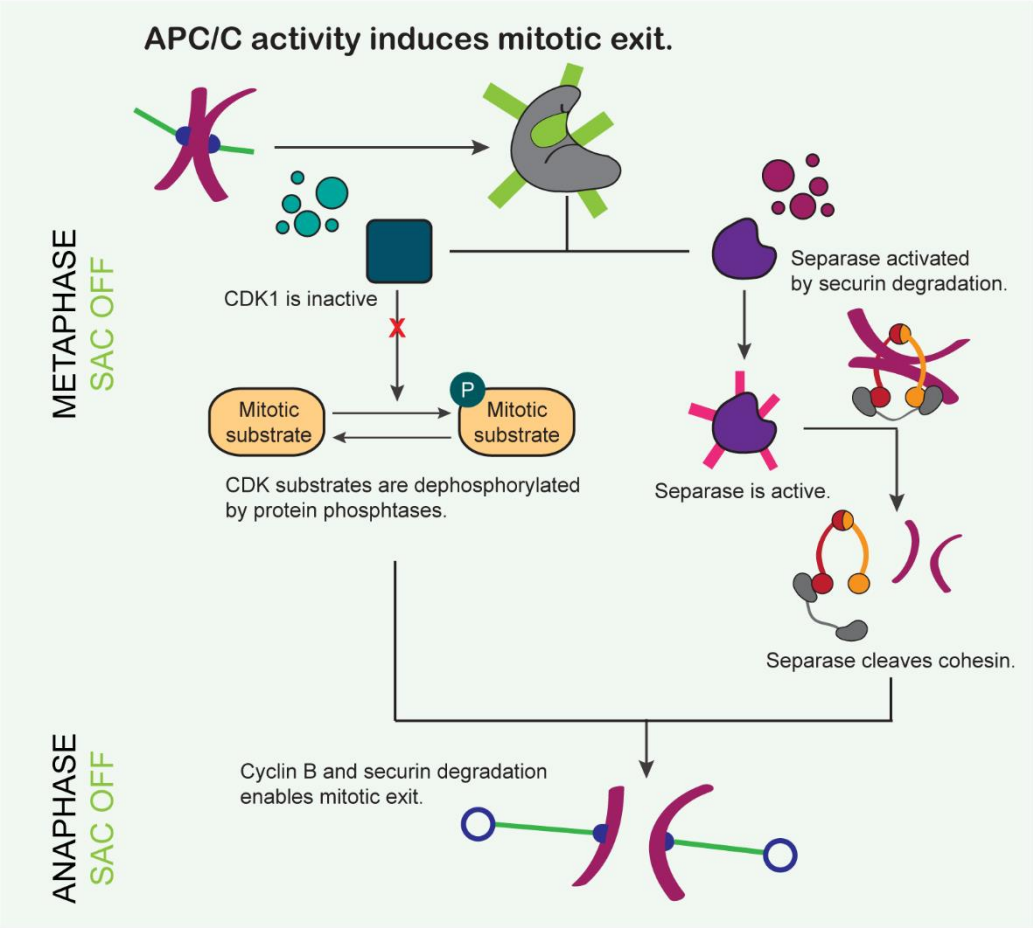
APC/C activity induces mitotic exit.
METAPHASE
SAC OFF
CDK1 is inactive
Separase activated
by securin degradation.
Mitotic
substrate
P
Mitotic
substrate
CDK substrates are dephosphorylated
by protein phosphtases.
Separase is active.
Separase cleaves cohesin.
ANAPHASE
SAC OFF
Cyclin B and securin degradation
enables mitotic exit.

Figure 1.3. Molecular control of mitosis. The Anaphase promoting complex (APC/C) promotes mitotic exit by regulating Cyclin B and securin. When kinetochores are unattached they generate the MCC, a diffusible anaphase inhibitor that binds and inhibits the APC/C. Upon microtubule attachment, the checkpoint is satisfied, and APC/C inhibition is relieved. Active APC/C proceeds to ubiquitylate its targets and target them for proteasome-dependent degradation. Cyclin B degradation inactivates CDK preventing the phosphorylation of mitotic substrates that are needed to maintain anaphase. Degradation of securin releases active separase which cleaves the cohesion complex, a prerequisite for separating kinetochores.

1.1.4 MITOSIS

Arguably, the segregation of sister chromatids between the opposite spindle poles during mitosis is one of the most dramatic and important events in a cells life. Fundamentally mitosis ensures that the replicated sister chromatids generated in S phase are evenly distributed into two pools so that daughter cells inherit identical copies of the original genome. After DNA replication (S) and a short gap phase (G2), cells enter mitosis with two sets of identical chromatids and two microtubule organising centres called centrosomes. The mitotic spindle, a microtubule network, emanating from centrosomes binds to kinetochores of chromosomes - large, specialised protein complexes embedded on centromeres. Once sister chromatids are attached to opposite poles, chromosomes are said to be bi-oriented and are then transported to opposing poles by the mitotic spindle. Chromosome segregation is a huge challenge for cells requiring them to: attach each of the 92 chromatids to microtubules, aligning these chromosomes at the equator of the cell and then transporting sister chromatids to the opposite spindle poles (Walczak et al., 2010). To orchestrate these cellular events complex signalling pathways are written into the mitotic programme to correct K-MT attachments (error-correction pathway) and importantly to couple the completion of K-MT attachments at each centromere to the cell cycle oscillator (SAC pathway). In this section, I will provide an overview of how cells orchestrate mitosis, a description of the molecular machinery used and a detailed discussion of the regulatory mechanisms that ensure accurate chromosome segregation.

During prophase, the first stage of mitosis, replicated chromosomes undergo immense structural remodelling in a process called chromosome condensation (**figure 1.3**). The condensation of chromosomes is a prerequisite for the accurate segregation of chromosomes in subsequent stages of mitosis. Cytologically, the DNA undergoes a striking transformation from a mass of chromatin to tightly compact sets of rod-shaped chromosomes in which identical sister chromatids are linked together. The condensation process is largely controlled by the condensin family and cohesin. Condensin I and II are required to further coil

chromosomes into highly compact structures (Hirano, 2005), while the cohesin ring holds sister chromatids together (Haering et al., 2008). The cohesin complex consisting of four core components, Smc1, Smc3, Scc1 and Scc3, traps sister DNA molecules in its tripartite ring (Nasmyth and Haering, 2005). Sister chromatid cohesion is essential for the bi-orientation of chromosomes and prevents chromatid separation until load bearing attachments are established at subsequent stages. Once chromosomes are properly bi-oriented, it is equally important that sister chromatid cohesion is lost so that chromatids can migrate independently at the metaphase-anaphase transition (Nasmyth and Haering, 2009). Outside the nucleus, the two centrosomes move apart and the mitotic spindle, a bipolar assembly of microtubules, is organised. The mitotic spindle binds to kinetochores on sister chromatids and will later pull them to the two poles.

The following phase prometaphase, starts with the breakdown of the nuclear envelope (NEBD) – triggered by the CDK-dependent phosphorylation of nuclear lamins (Guttinger et al., 2009). The mitotic checkpoint is activated at unattached kinetochores and generates a diffusible ‘wait anaphase’ signal (Malureanu et al., 2009; Kulukian et al., 2009). Microtubules emanating from the spindle poles undergo cycles of growth and shrinkage as they ‘search’ for a target. In a stochastic search process, the microtubule will eventually ‘capture’ a chromosome by binding to its kinetochores (Kirschner and Mitchison, 1986). The ‘search-and-capture’ mechanism first proposed in the 1980s has since been refined to a ‘biased-search-and-capture’ to account for the required speed of capture (Wollman et al., 2005; Kirschner and Mitchison, 1986). Kinetochore-microtubules, a subset of microtubules, bind directly to the kinetochore to form K-fibers. The K-fibers are created by two ways: microtubule bundles grow from spindle poles until they find kinetochores or preformed microtubules emanating from kinetochores are captured by the mitotic spindle. Multiple mechanisms have been uncovered that promote microtubule nucleation at kinetochores to make K-fibers (Heald and Khodjakov, 2015; Maiato et al., 2004a). Laser ablation experiments demonstrated that K-fibers growing from kinetochores are integrated

into the mitotic spindle to enhance the rate of kinetochore capture (Maiato et al., 2004a). Eventually, the mitotic spindle captures each chromosome so that sister kinetochores are connected to opposite poles.

Metaphase is characterised by the congression and bi-orientation of chromosomes at the equator of the cell to form a metaphase plate. It is essential that chromosomes are bi-oriented (attached to microtubules form opposite poles) prior to chromosome segregation. Chromosomes congress at the equator by two modes: direct and peripheral congression. The pathway selected largely depends on the location of the chromosome at NEBD. Chromosomes at roughly equal distance between the two poles are favourably positioned for bi-orientation and are directly captured by the mitotic spindle. While the peripheral congression pathway is needed to move chromosomes that were located at the nuclear periphery when the envelope fragmented. Although bi-orientation could eventually be achieved by the classical 'search-and-capture' model, in cells the rate of bi-orientation is increased by transporting these peripheral chromosomes to the equator where the probability of bi-orientation is higher (Maiato et al., 2004a). This pathway is independent of end-on attachments with microtubules and is instead driven by the action of the kinetochore motors Dynein and CENP-E. In addition to chromosome movement, organisation of the mitotic spindle is completed by metaphase with three types of spindle microtubules present. These microtubules are: kinetochore microtubules which extend from each spindle pole and bind to kinetochores, interpolar microtubules that reach from one pole to almost the other functioning as the structural scaffold and lastly, astral microtubules which connect the spindle pole to the membrane. At the end of metaphase, cells have connected their chromosomes to the mitotic spindle, the mitotic checkpoint has been satisfied and cells are now ready to distribute their chromosomes.

During anaphase, chromosome cohesion is lost, and sequentially sister chromatids are segregated by the mitotic spindle to opposite poles of the cell. On a molecular level, the metaphase-anaphase transition is marked by activation of

the APC/C that targets many proteins for proteasome-dependent degradation including cyclin B, to turn off the cell cycle oscillator, and securin, to stop sister chromatid cohesion. Phenotypically anaphase can be divided into two distinct phases: anaphase A, the poleward movement of chromosomes towards the spindle poles due to the shortening of kinetochore-microtubules, and anaphase B, the two poles push away from one another to further define two separate pools of chromosomes. In anaphase A, kinetochore transport has been described by two mechanisms: the 'Pac Man' model in which kinetochores chew microtubules to reach the poles, and the 'microtubule flux' model, in which depolymerisation at centrosomes creates a treadmilling effect to pull chromosomes towards the poles (Khodjakov and Kapoor, 2005; Liu and Onuchic, 2006). Anaphase B is characterised by the sliding apart of overlapping interpolar microtubules to form the mid-zone, while astral microtubules pull centrosomes towards the cell membrane. These changes in microtubule assembly create the force needed to complete chromosome segregation (Scholey et al., 2016).

In the final stages of mitosis, the cell prepares to divide into two daughter cells. In telophase, the two pools of chromosomes delivered in anaphase are repackaged into new nuclei by the reassembly of the nuclear envelope (Guttinger et al., 2009). Meanwhile, overlapping interpolar microtubules detach from spindle poles and are organised into antiparallel bundles by many different microtubule associated proteins (MAPs) and molecular motors – this assembly constitutes the central spindle (Fededa and Gerlich, 2012). The central spindle recruits the necessary factors to activate the RhoA protein which directs the assembly of a contractile actin-myosin ring at the mid-zone. The contractile ring constricts to create a cleavage furrow and the ring holding the dividing cells shrinks. At its smallest point the cytoplasm remains connected by a matured midbody and during abscission the cytoplasm is completely divided into two (Green et al., 2012). Even this brief description of the principle cell cycle events, highlights that coordination of the order and timing of the many cellular events is a remarkable feat. In the next section, we will discuss the molecular machinery that the cell uses to segregate its chromosomes.

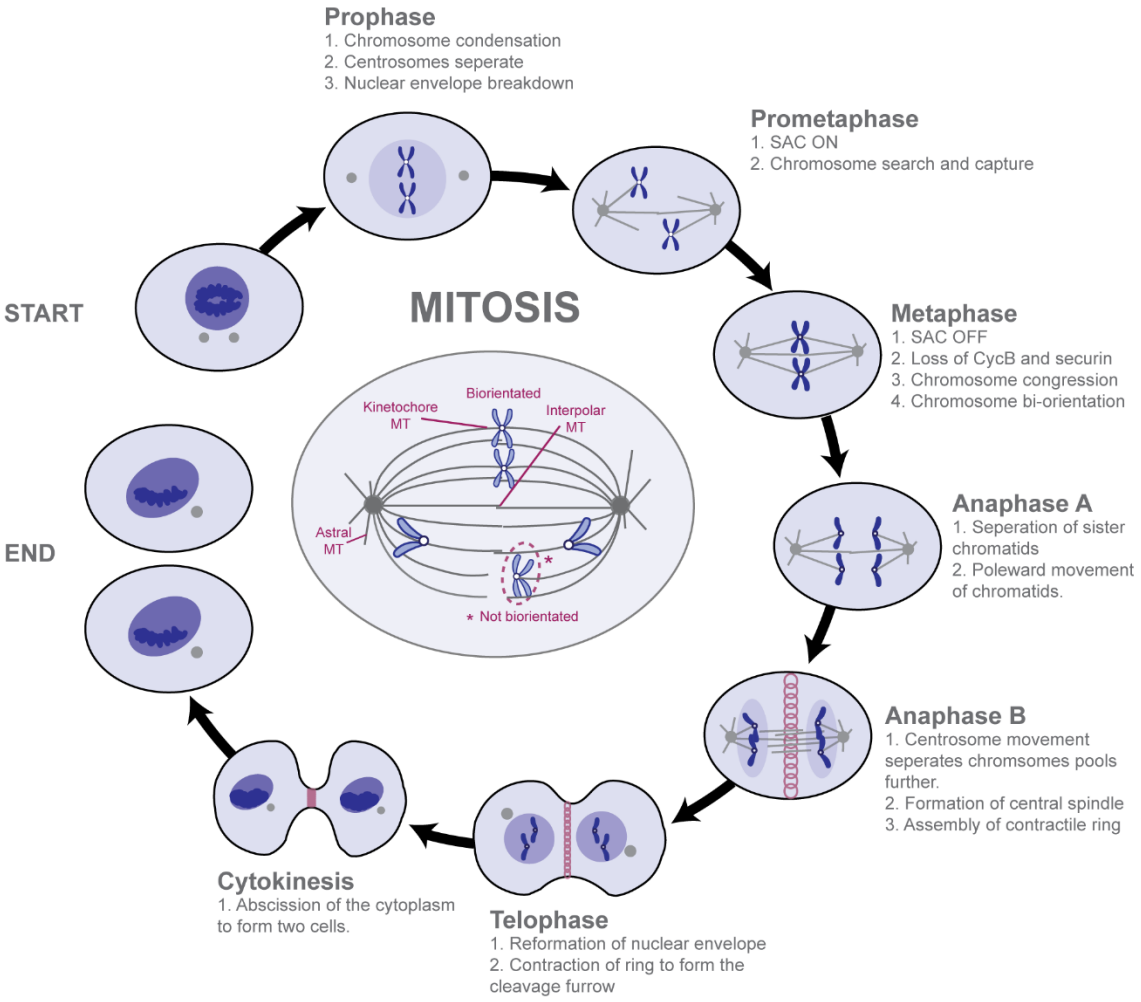

Figure 1.4. Mitosis in metazoans. Prophase, begins with the movement of the centrosomes to opposite poles of the cell, chromatin condenses, and then nuclear envelope breakdown ensues. After nuclear envelope breakdown, microtubules of the mitotic spindle search and capture chromosomes by binding to kinetochores. Metaphase cells are characterised by chromosomes lining up at the equator of the cells with sister kinetochores being attached to microtubules from either centrosome. At this point cells are ready to divide their DNA and during anaphase sister chromatids are split between the two poles. Two genetically equal pools of chromatids are packaged during telophase and the cell gets ready to divide its cytoplasm. During cytokinesis, cells are divided into two.

1.2 THE MOLECULAR MACHINERY.

1.2.1 KINETOCHORES.

Kinetochores are large, specialised protein complexes, assembled on centromeric chromatin, that connect chromosomes to the mitotic spindle and this is fundamental for the faithful segregation of chromosomes. The main function of kinetochores is to mediate load-bearing attachments between chromosomes and microtubules (Santaguida and Musacchio, 2009). In addition to providing an interface to bind microtubules, kinetochores are mechano-sensors that stabilise microtubule attachments in response to tension. Besides physically linking chromosomes to the mitotic spindle, kinetochores act as a platform for two intricate signalling networks: the error correction pathway, to correct erroneous microtubule attachments, and the spindle checkpoint, to coordinate mitotic exit with chromosome bi-orientation. Kinetochores can functionally be divided into two regions: an inner kinetochore, that associates with the centromere, and the outer kinetochore which binds microtubules and SAC proteins. The composition of the kinetochore dynamically changes between an unattached and attached state (**figure 1.5 & 1.6**).

1.2.1.1 INNER KINETOCHORE

The inner kinetochore proteins are responsible for connecting the kinetochore to the centromere. The centromeric DNA is specified by many tandem repeats called α-satellites and the centromere specific histone variant CENP-A (Sullivan et al., 1994). CENP-A, the innermost component of the kinetochore, is essential and sufficient for the hierarchical recruitment of all other kinetochore components (Howman et al., 2000; Liu et al., 2006; Fachinetti et al., 2013; Heun et al., 2006). The constitutive centromere associated network (CCAN) comprised of a network of proteins at the inner kinetochore recognises CENP-A and couples it to the outer kinetochore (McAinsh and Meraldi, 2011). Dissection of the CCAN network by biochemical reconstitution and reciprocal dependency experiments

demonstrated that the CCAN can be subdivided into four parts: the CENP-LNS complex, CENP-CHIKM, CENP-TW and CENP-OPQRU (**figure 1.5**) (Musacchio and Desai, 2017; Weir et al., 2016; Hori et al., 2008; McAinsh and Meraldi, 2011). Recognition of CENP-A is exclusive to two subunits CENP-C (Falk et al., 2016; Kato et al., 2013) and CENP-N (Carroll et al., 2009, 2010). CENP-N binds solely to the CENP-A centromere targeting domain (CATD) and has considerable selectivity for CENP-A over H3 (Carroll et al., 2009, 2010), whereas, CENP-C associates with the C-terminal tail of CENP-A as well as acidic patches in H2A and H2B (Musacchio and Desai, 2017). The CENP-HIKM complex also contributes to DNA binding, however, it lacks specificity unlike CENP-C and CENP-N (Weir et al., 2016).

The CCAN network is also responsible for interacting with components of the outer kinetochore to link them with the inner kinetochore. The KMN (Knl1, Mis12 and Ndc80) network constitutes the stable components of the outer kinetochore and is comprised of three parts: Knl1, Ndc80 and Mis12 which are connected to members of the CCAN. CENP-T and CENP-C are thought to be the major CCAN effectors for the binding of the KMN network of proteins. The Mis12: CENP-C interaction is perhaps the best studied of these, cocrystal structures revealed that an ~45 residue N-terminal motif of CENP-C is needed to form interactions with members of the Mis12 complex (Petrovic et al., 2016). Moreover, this interaction is stabilised by the Aurora B kinase through phosphorylation of positively charged residues in a disordered loop on Dsn1, to increase its affinity for CENP-C (Kim and Yu, 2015; Yang et al., 2008; Welburn et al., 2010). CENP-T, on the other hand, associates with the RWD domains on Spc24 and Spc25 of the Ndc80 complex. This interaction is mediated by the N-terminal extension region in CENP-T and is sensitive to CDK phosphorylation (Schleiffer et al., 2012; Nishino et al., 2013; Malvezzi et al., 2013; Kim and Yu, 2015). Recently, it was shown that CENP-T is also needed for the recruitment of the Mis12 complex, however, presently it’s not clear why there are two CCAN receptors for the Mis12-complex (Rago et al., 2015; Suzuki et al., 2015; Huis in ’t Veld et al., 2016).

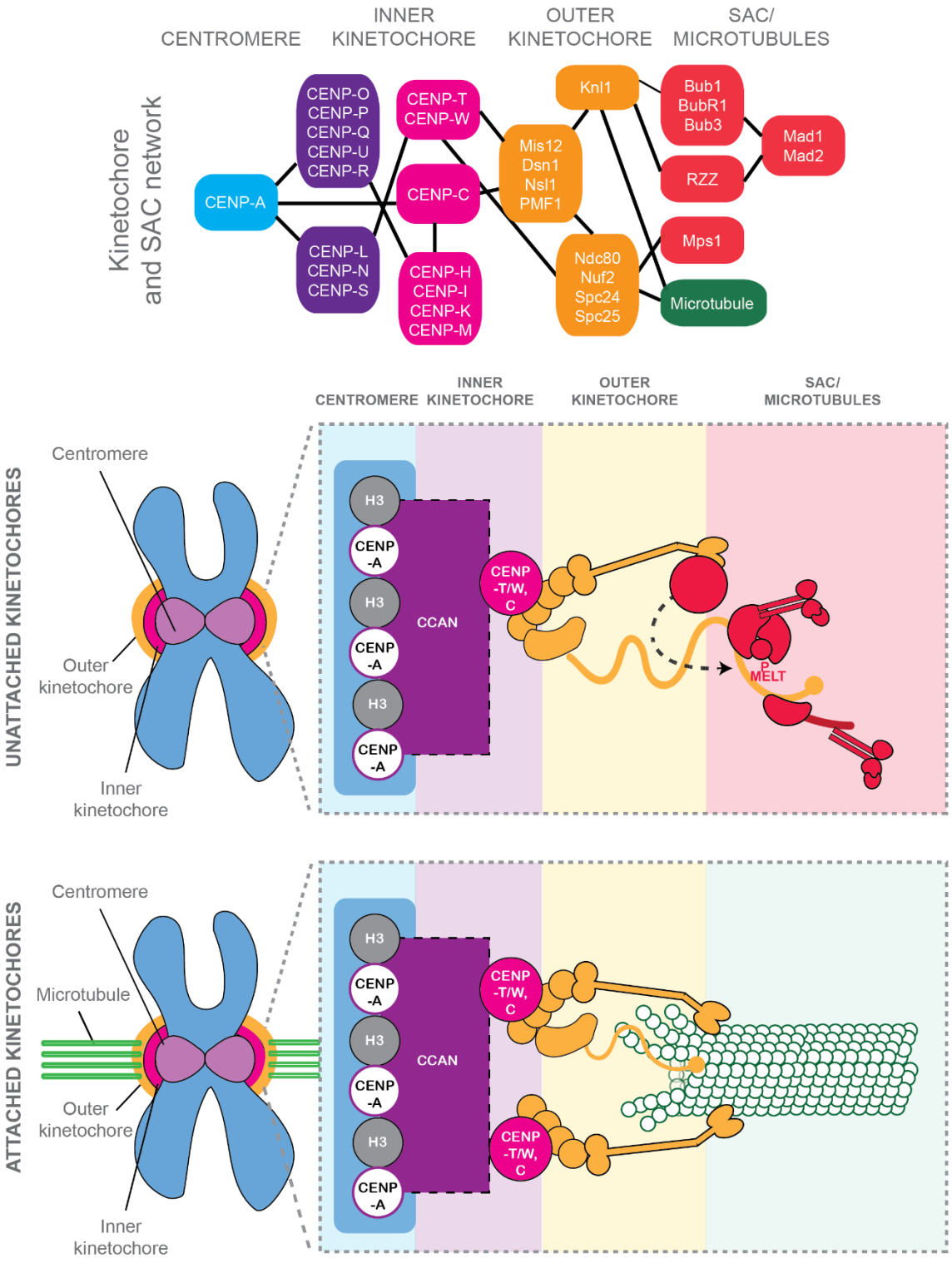

Figure 1.5. Composition of an unattached or attached kinetochore. Kinetochore composition when microtubules are or are not attached to the kinetochore. The centromere, inner kinetochore and the KMN network of the outer kinetochore are stable at kinetochores. SAC proteins bind when kinetochores are unattached, but are ejected upon microtubule binding.

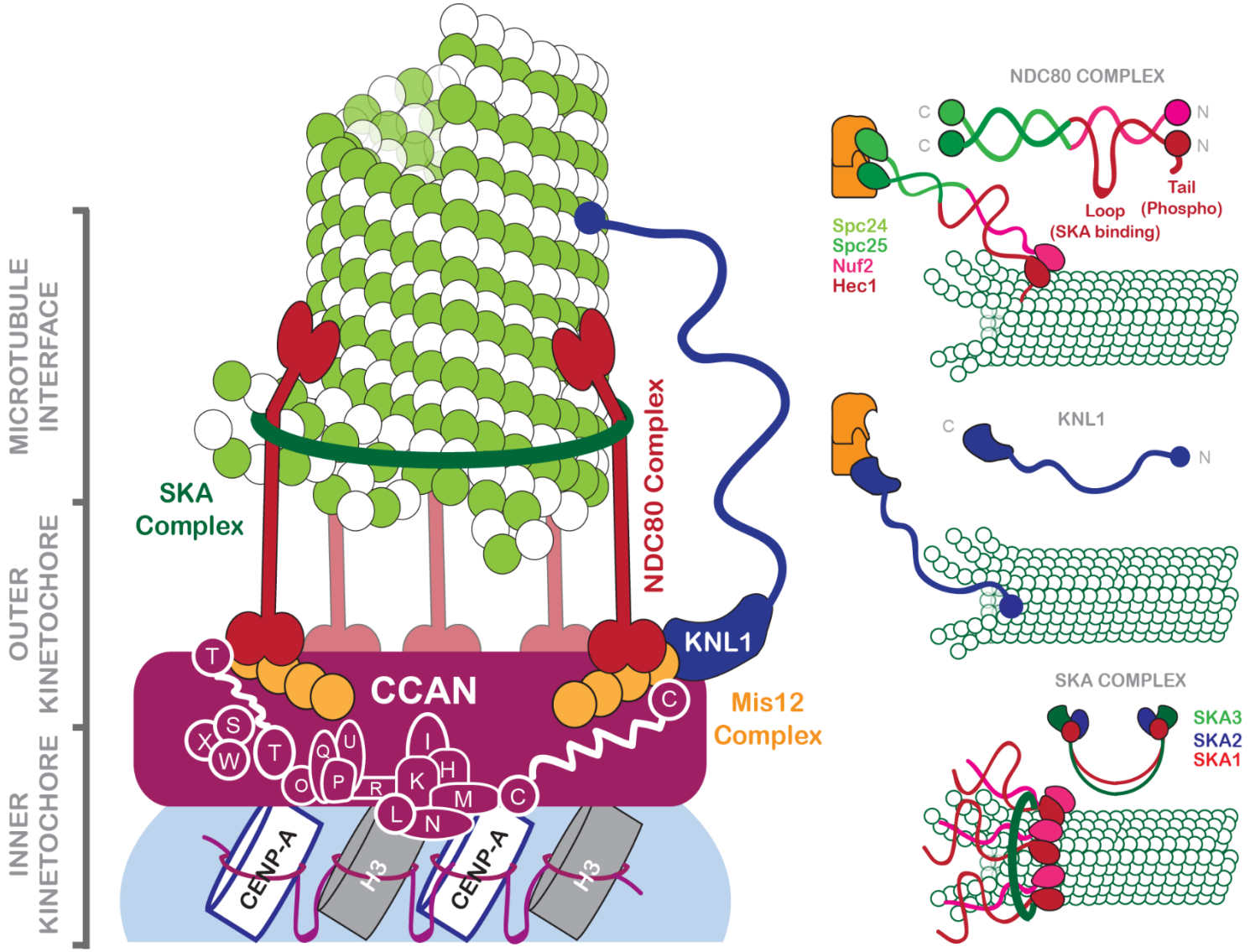
MICROTUBULE INTERFACE
OUTER KINETOCHORE
INNER KINETOCHORE
SKA Complex
NDC80 Complex
KNL1
CCAN
Mis12 Complex
T
S
X
W
T
Q
U
O
P
R
I
H
K
M
L
N
C
CENP-A
H3
CENP-A
H3
NDC80 COMPLEX
C
C
N
N
Tail
Loop
(Phospho)
(SKA binding)
Spc24
Spc25
Nuf2
Hec1
KNL1
C
N
SKA COMPLEX
SKA3
SKA2
SKA1

Figure 1.6. The kinetochore-microtubule interface. A diagram showing the structure of an attached kinetochore and specifically the proteins that coordinate microtubule binding. Kinetochores can be roughly divided between the inner and outer kinetochore. Inner kinetochore proteins mainly comprise of the CCAN network of proteins which link the outer kinetochore to the centromeric DNA. The outer kinetochore proteins are responsible for forming attachments with microtubules and providing a scaffold for the SAC pathway. The Ndc80 complex has been identified as the major effector of microtubule binding at kinetochores and its components are shown on the right. Knl1 also contributes to microtubule binding and the SKA complex binds to microtubules and Hec1 to stabilise the interaction between outer kinetochore proteins and microtubules.

1.2.1.2 OUTER KINETOCHORE

The outer kinetochore is the primary site for microtubule binding by the kinetochore and provides a platform to transduce signals from the error correction and mitotic checkpoint pathways. The KMN network, a 9-subunit protein assembly, constitutes the core components of the outer kinetochore (**figure 1.7**). The three subcomplexes provide different functions: Knl1, the platform for SAC signalling, the Ndc80 complex, that mainly regulates microtubule binding, and the Mis12 complex, an interaction hub that links the members of the KMN network together and with the CCAN.

1.2.1.3 NDC80 COMPLEX

The Ndc80 complex is the main kinetochore effector of end-on microtubule attachments. Depletion of members of the Ndc80 complex compromises the structural integrity of the outer kinetochore and disrupts the formation of K-MT attachments. The Ndc80 complex is made up of four subunits, Ndc80 (Hec1 in humans), Nuf2, Spc24 and Spc25 that are connected to one another by highly conserved coiled coil regions. At one end of the complex, Spc24 and Spc25 interact with the CCAN subunit, CENP-T, to link the Ndc80 complex to central kinetochore components (Schleiffer et al., 2012; Nishino et al., 2013). On the other end, the Ndc80 and Nuf2 proteins constitute a microtubule binding interface (Cheeseman et al., 2006; Wei et al., 2006; Ciferri et al., 2008).

Determination of the crystal structure of the globular domains of the Ndc80 complex and of Ndc80 mutants lacking the coiled-coil regions indicated that the microtubule binding surface is composed of the calponin-homology (CH) domains of the Nuf2 and Hec1 subunits (Wei et al., 2006; Ciferri et al., 2008; Musacchio and Desai, 2017). A more detailed picture was obtained by cryo-electron microscopy of the $Ndc80^{Bonsai}$ mutant bound to microtubules. This showed that the CH domain of Hec1 directly interacted with both tubulin monomers of the microtubule lattice. This interaction relies on a region of the CH domain referred

to as the toe, the toe recognises a site between tubulin monomers and contributes positively charged residues to mediate the high affinity binding of microtubules (Alushin et al., 2010). The CH domain is not the only region in Hec1 that contributes to microtubule binding, recently it was shown that the basic N-terminal tail (residues 1-80) is functionally important for microtubule binding (Alushin et al., 2012). A stretch of positively charged residues between residues 47-68 form electrostatic interactions with negatively charged E-hooks of the tubulin protomers (Alushin et al., 2012). Further to this, the stretch of residues adjacent to the E-hook binding region are essential for coupling Ndc80 complexes. The clustering of the Ndc80 complex provided new insight into how microtubules are bound by the kinetochore (Alushin et al., 2010, 2012). The Ndc80 complex, specifically the Hec1 internal loop, regulates the recruitment of the Ska complex to strengthen the K-MT interface (Tooley and Stukenberg, 2011; Tang and Toda, 2013; Zhang et al., 2012). The Ska complex, a W-shaped dimer formed of coiled-coil interactions between the Ska1, Ska2 and Ska3 subunits, is essential for microtubule attachment and subsequently chromosome segregation (Jeyaprakash et al., 2012; Hanisch et al., 2006; Welburn et al., 2009). The Ska complex binds both microtubules and the Ndc80 complex to seal the kinetochore-microtubule interface.

In addition to regulating microtubule binding, the Ndc80 complex has been implicated as the major kinetochore binding site for the Mps1 kinase – the key SAC transducer (Hiruma et al., 2015; Ji et al., 2015; Zhu et al., 2013; Saurin et al., 2011; Martin-Lluesma et al., 2002). In the current model, Mps1 competes with microtubules to bind to the CH domains of Hec1 and Nuf2 (Hiruma et al., 2015; Ji et al., 2015). The affinity of the Ndc80 complex for Mps1 or microtubule binding is determined by phosphorylation by the Aurora B kinase (DeLuca et al., 2011; Zhu et al., 2013; Saurin et al., 2011; Long et al., 2017; Zaytsev et al., 2015). The Aurora B kinase, the main effector of the error correction pathway, phosphorylates nine sites on the N-terminal tail of Hec1 to neutralise its positive charge and this reduces its affinity for microtubules (DeLuca et al., 2011; Zaytsev et al., 2015). Phosphorylated Ndc80 favours an interaction with the Mps1 kinase

which in turn activates the SAC pathway (Hiruma et al., 2015; Ji et al., 2015; Zhu et al., 2013; Saurin et al., 2011; Martin-Lluesma et al., 2002). The Aurora B mediated phosphorylation of Hec1 and the subsequent recruitment of Mps1 kinase will be discussed in more detail in later chapters. Even from this brief explanation it is apparent that the Ndc80 complex is one of the most important components of the kinetochore. The Ndc80 complex bridges microtubule attachment sensing to the error correction pathway, triggers the SAC pathway and subsequently it indirectly regulates the cell cycle oscillator. Control of its modifications and its binding partners is critical in coordinating microtubule binding with SAC activity.

1.2.1.4 MIS12 COMPLEX

The Mis12 complex consists of four subunits, Nsl1, Dsn1, Nnf1 and Mis12, that are structural paralogs with conserved helical regions. The Mis12 complex is a protein interaction hub, that links the KMN network (outer kinetochore) with the CCAN (inner kinetochore) (Petrovic et al., 2010). Visualisation of the Mis12 complex by electron microscopy revealed that it appears as a 22nm rod (Petrovic et al., 2010). Moreover, crystal structure determination of the complex demonstrated that at one end of the tetramer the subunits split into two pairs Dsn1:Nsl1 and Mis12:Nnf1 that join at a central stalk to form a rod-shaped complex (Dimitrova et al., 2016; Petrovic et al., 2016). As discussed before, the Mis12 complex binds to two CCAN subunits CENP-C and CENP-T and this interaction is essential for proper chromosome segregation (Rago et al., 2015; Suzuki et al., 2015; Huis in ’t Veld et al., 2016; Tanaka et al., 2009; Kim and Yu, 2015). At the tip of the central stalk, C-terminal residues of the Nsl1 and Dsn1 subunits are contact points for the Spc24 and Spc25 subunits of the Ndc80 complex (Malvezzi et al., 2013; Petrovic et al., 2010; Dimitrova et al., 2016). In addition to this, the Mis12 complex is needed to bind Knl1 and this is mediated by the central stalk together with the C-terminal tail of Nsl1 (Petrovic et al., 2010, 2014). The Mis12 complex is a core interaction hub that holds the KMN network together and connects it to the CCAN network

1.2.1.5 KNL1

The final member of the KMN network, Knl1 is a large, scaffolding protein that serves as the platform for the SAC signalling pathway. Knl1 the largest subunit of the outer kinetochore (2316 residues in humans), is mainly unstructured except for ~500 C-terminal residues (Musacchio and Desai, 2017). The functional importance of intrinsically disordered proteins in signalling networks has only recently come to light. It has been postulated that large regions of disorder function to increase the surface area for interactions with multiple binding partners, provide conformational flexibility and the fine control of binding affinities (V Caldas et al., 2013). Consistently, Knl1 has an array of protein:protein interaction motifs including: a PP1 binding motif (RVSF and SILK) (London et al., 2012; Rosenberg et al., 2011; Liu et al., 2010; Pinsky et al., 2006), KI motifs to enhance the binding of SAC proteins (Krenn et al., 2014, 2012), MELT motifs to bind the Bub complex (Vleugel et al., 2013; Yamagishi et al., 2012; Primorac et al., 2013; Shepperd et al., 2012; Zhang et al., 2014), an RWD domain (Petrovic et al., 2010, 2014), to associate with the Mis12 complex, and a coiled-coil region that interacts with the RZZ complex (Silió et al., 2015; Varma et al., 2013). Depleting Knl1 disrupts the assembly of the kinetochore and the recruitment of the SAC proteins (Varma and Salmon, 2012; Cheeseman et al., 2008, 2004; Desai et al., 2003). In addition to SAC signalling, Knl1 may also play a role in microtubule binding, however, evidence for this function is still lacking in humans. In yeast, Knl1 has a more established role in microtubule binding by interacting with microtubules and their associated proteins to regulate chromosome segregation (Pagliuca et al., 2009). Although biochemical reconstitution of the core microtubule binding site showed that human Knl1 is necessary for high affinity binding of microtubules, this is yet to be demonstrated in human cells (Cheeseman et al., 2006).

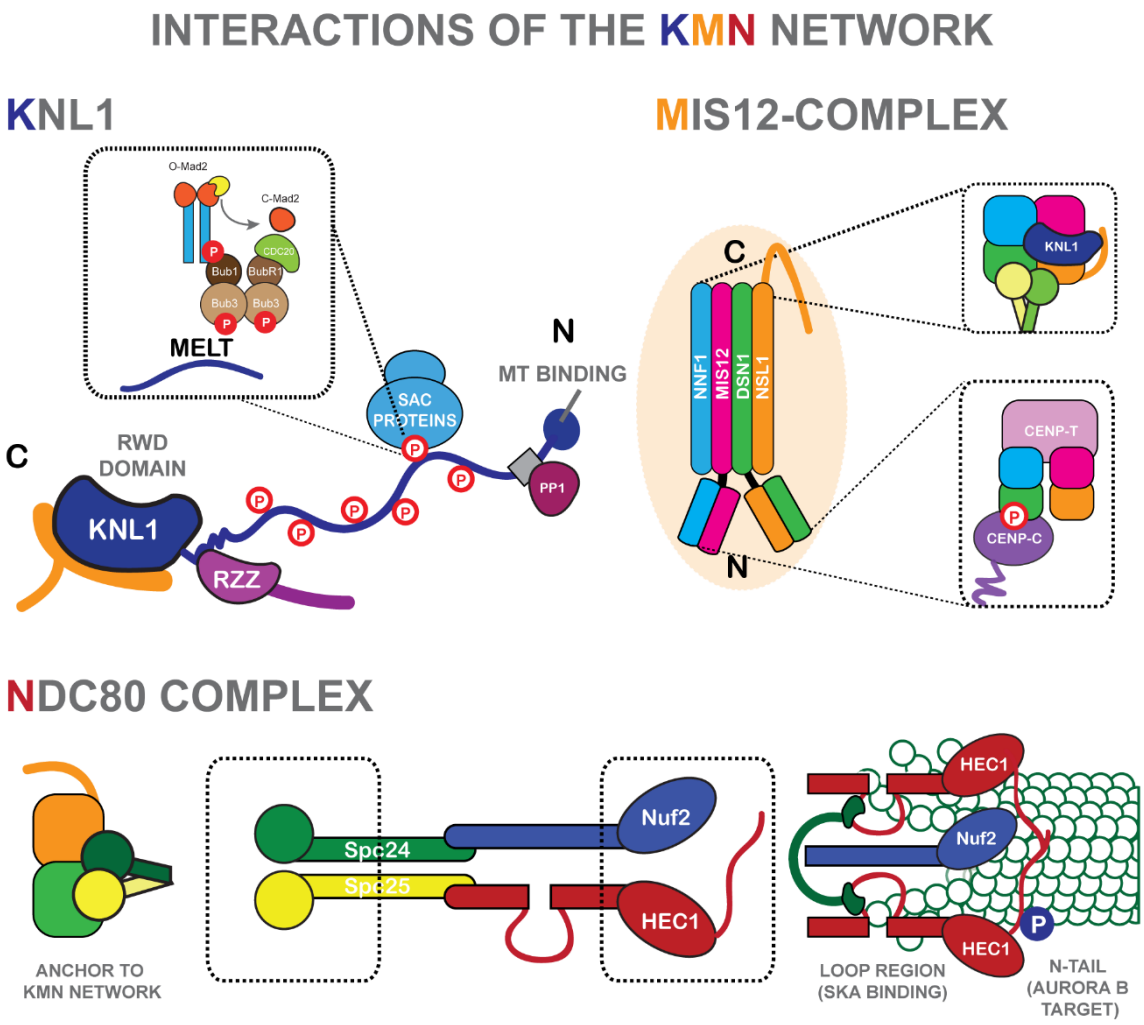

Figure 1.7. The interactions of the KMN network. The KMN network consists of Knl1, the Mis12-complex and the Ndc80 complex. Knl1 is a platform for the SAC pathway and is associated with the Mis12 complex. The Mis12 complex, an interaction hub, joins the KMN network with the CCAN. The Ndc80 complex is the primary effector of microtubule binding.

1.2.2 THE MITOTIC SPINDLE

1.2.2.1 MICROTUBULES

The mitotic spindle coordinates chromosome segregation by capturing chromosomes, and following the loss of sister chromatid cohesion, it pulls chromatids poleward to opposite sides of the cell. Microtubules, 24nm hollow cylindrical structures, are built by joining 13 parallel protofilaments, each of which is composed of αβ-tubulin heterodimers that make up the microtubule building blocks (**figure 1.8**) (Alberts B et al, 2014). To assemble protofilaments, αβ-tubulin heterodimers stack head to tail to make a protein polymer. In this classic model: the α-tubulin (head) subunit of a new heterodimer binds to the exposed region of β-tubulin (tail) in a growing microtubule. To build a microtubule, 13 protofilaments line up side-by-side and lateral contacts are formed between like-monomers. Microtubule protofilaments are polar protofilaments with a negative end (minus or - end) that has exposed α-tubulin subunits and a positive end (plus or + end) that exposes β-tubulin - where new tubulin heterodimers are added. The minus end of a microtubule binds to the microtubule organising centre (MTOC) through interacting with a nucleating tubulin variant called γ-tubulin. The γ-tubulin binds to two additional proteins GCP2 and GCP3 as well as other accessory proteins to make the γ-tubulin ring complex (γ-TuRC) (Kollman et al., 2011). In addition to this, microtubules interact with many other proteins collectively referred to as microtubule associating proteins (MAPs) to coordinate cellular events (Maiato et al., 2004b).

1.2.2.2 DYNAMIC INSTABILITY

In cells microtubules are highly dynamic and switch between phases of growth and catastrophic phases when the polymer disassembles. While both α and β tubulin monomers bind GTP, the hydrolysis of the GTP bound to β-tubulin is important for the stability of the microtubule lattice. Hydrolysis of the high energy

phosphate on the guanosine group is relatively slow in free tubulin dimers; however, this is accelerated when tubulin is incorporated into microtubules. In microtubules, when the GTP:β-tubulin is hydrolysed, GDP remains bound and the energy from hydrolysis is stored as strain along the microtubule lattice. As more tubulin dimers are hydrolysed the strain in microtubules increases to make disassembly energetically favourable. The tips of growing microtubules have GTP:β-tubulin that forms a protective GTP-cap. However, when the rate of hydrolysis exceeds the addition of new GTP:β-tubulin microtubules enter a catastrophic phase and are depolymerised. Dynamic changes in the organisation of microtubules is essential for proper chromosome segregation. On one hand, microtubules must grow from spindle poles and form load bearing end-on attachments with kinetochores. On the other hand, depolymerising microtubules pull sister-chromatids poleward. Microtubule stabilisers, such as Taxol, or destabilising drugs including colchicine and nocodazole have a profound impact on mitosis to the extent that dividing cells die when treated with these drugs (Gascoigne and Taylor, 2009; Blajeski et al., 2002). Thus, the dynamic polymerisation and depolymerisation of microtubules is essential for chromosome segregation.

1.2.2.3 CENTROSOMES

The centrosome is the main MTOC in cells; it is built from two centrioles at its core and surrounded by pericentriolar material. During the cell cycle, centrosomes form the two poles of the cell and organise the bipolar mitotic spindle, this is key for the segregation of chromosomes to opposite sides of the cell. Like DNA, centrosomes are duplicated during S phase of the cell cycle and it is important that this happens once, and only once per cycle (Nigg, 2007; Nigg and Stearns, 2011). Centrosomes are made up of a pair of centrioles, each consisting of nine microtubule triplets organised around a central cartwheel structure in a nine-fold symmetrical arrangement. Surrounding this pair of core centrioles is the pericentriolar material (PCM) which is formed of a matrix of proteins. Proteomic analysis revealed that this matrix is formed of hundreds of

proteins (Jakobsen et al., 2011; Andersen et al., 2003) with different functions including cell cycle regulators, signalling molecules (Arquint et al., 2014), as well as proteins required for the nucleation and organisation of microtubules (Conduit et al., 2015). Although the PCM contains hundreds of proteins, surprisingly few proteins are needed to assemble a centriole. Genetic screens in C.elegans identified five core components that are strictly needed for centriole biogenesis: PLK4, SAS-5, SAS-6, SAS-4 and CEP135 (Nigg and Stearns, 2011). The Plk4 kinase initiates the assembly of a daughter centriole by recruiting SAS-6 and SAS-5 which configure the central cartwheel scaffold (Ohta et al., 2014; Kratz et al., 2015; Dzhindzhev et al., 2014). In turn, SAS-4 is recruited to the central cartwheel scaffold and organises the surrounding centriolar microtubules with help from CEP135 (Lin et al., 2013; Tang et al., 2011).

In addition to duplication in S phase, the centrosome is further matured before cells enter mitosis. Interphase centrosomes contain only ~15-40% of the proteins of that of a mitotic centrosome. The dramatic expansion of the PCM as cells prepare for mitosis is termed centrosome maturation. The mitotic kinases Plk1 and Aurora A play key roles in this maturation process. Plk1 targets several proteins at the centrosome including two PCM scaffold proteins, pericentrin and Cnn to assemble the PCM and recruit the γ-tubulin to nucleate microtubules (Lee and Rhee, 2011; Conduit et al., 2014). On the other hand, Aurora A is needed to stabilise the minus end of microtubules by phosphorylating the microtubule stabiliser TACC3 (Kinoshita et al., 2005; Barros et al., 2005). Production of two mature centrosomes relies on the action of mitotic kinases and a vast number of protein:protein interactions. The proper assembly of centrosomes is needed to organise a bipolar spindle and to efficiently segregate chromosomes. Centrosome abnormalities are thought to promote tumorigenesis by increasing the frequency of chromosome mis-segregations (Gönczy, 2015).

.

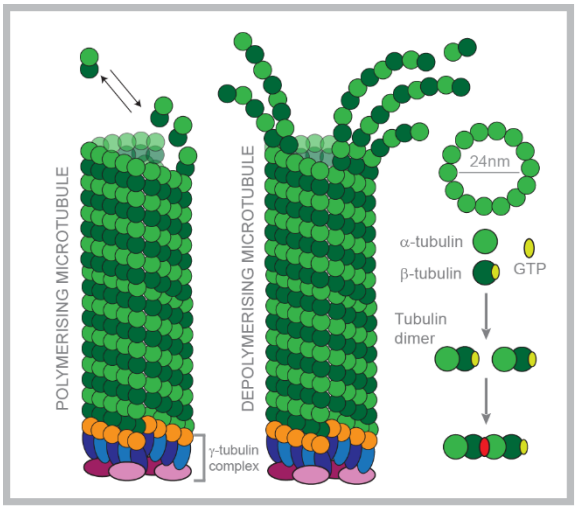
POLYMERISING MICROTUBULE
DEPOLYMERISING MICROTUBULE
24nm
α-tubulin
β-tubulin
GTP
Tubulin dimer
γ-tubulin complex

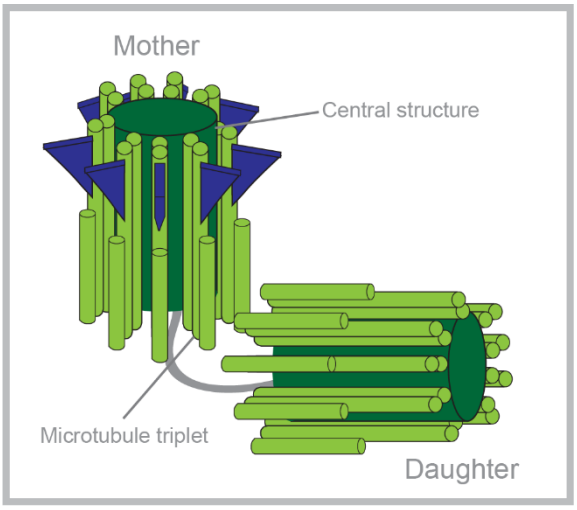
Mother
Central structure
Microtubule triplet
Daughter

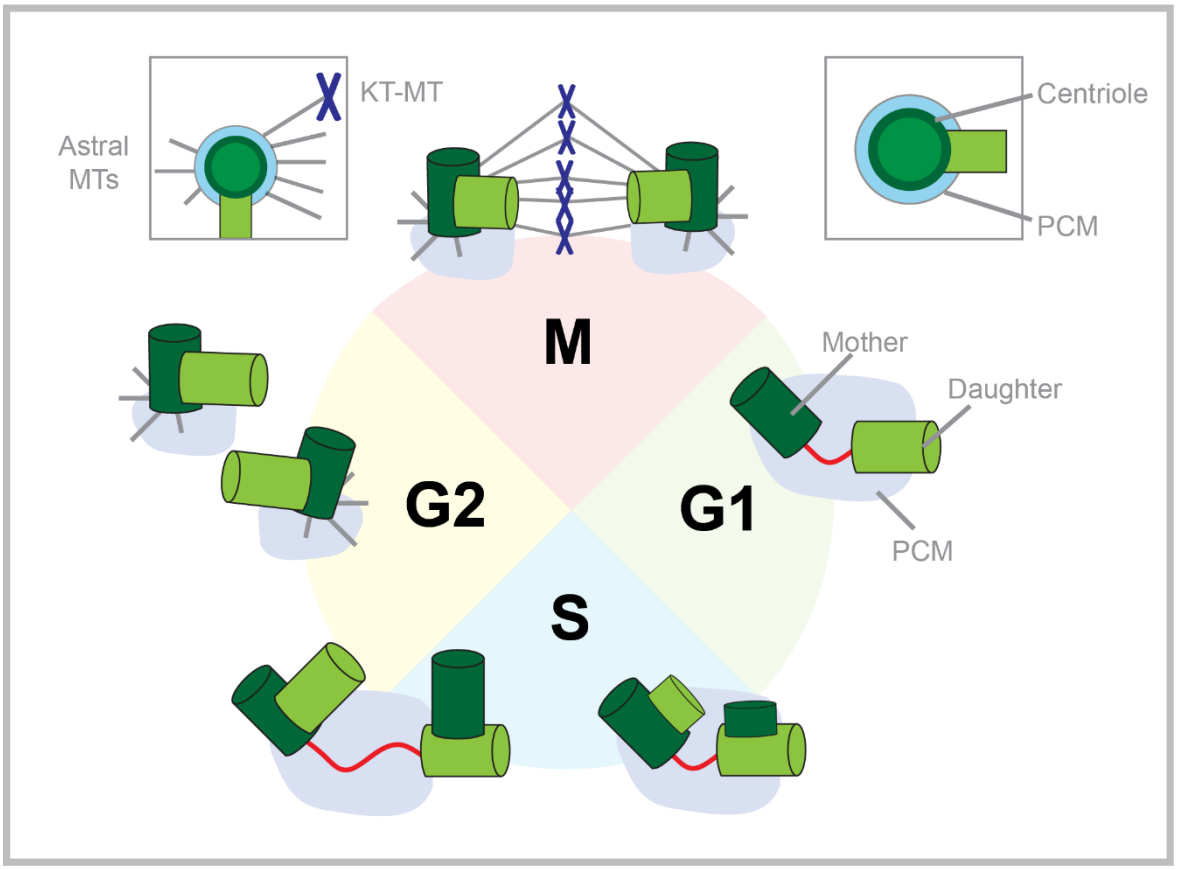
Astral MTs
KT-MT
Centriole
PCM
M
Mother
Daughter
G2
G1
PCM
S

Figure 1.8. Microtubules and centrosomes. Microtubules are 24nm wide hollow cylindrical structures produced from the polymerisation of αβ tubulin dimers to the plus-end of microtubules. Microtubules are nucleated from γ-tubulin complexes. Microtubules depolymerise when the hydrolysis of β tubulin-GTP (yellow) to GDP (red) surpasses the addition of new αβ tubulin dimers. Centrosomes are microtubule organising centres, formed from two centrioles, that are surrounded by a PCM. Each centriole contains microtubule triplets arranged around a central cartwheel structure by nine-fold symmetry. The centrosome is duplicated during S phase so that two centrosomes can organise a bipolar spindle during mitosis. Kinetochores attach to the microtubules emanating from the centrosomes to become bi-oriented and then are segregated between the two poles. This figure was inspired by (Conduit et al., 2015).

1.2.3 CORRECTING MICROTOUBULE ATTACHMENTS.

1.2.3.1 TYPES OF ATTACHMENT

Accurate chromosome segregation requires the formation of proper amphitelic attachments, by which sister kinetochores attach to microtubules radiating from opposite spindle poles (**figure 9**). The generation of amphitelic attachments requires intermediate steps. Initially, kinetochores interact with the lateral surface of microtubules to generate tenuous lateral attachments that are converted into mature load-bearing end-on attachments. Lateral attachments require molecular motors including members of the Kinesin-14 family, the kinetochore-associate dynein and CENP-E (Shrestha and Draviam, 2013; Yang et al., 2007b). Importantly, these lateral attachments facilitate the sliding of chromosomes towards the equator of the cell to increase the likelihood of bi-orientation (peripheral congression). Often chromosomes enter a transient state referred to as monotelic state, whereby only one kinetochore of the chromosome is connected to a single pole. During prometaphase, the spindle encounters two types of erroneous kinetochore attachments called syntelic and merotelic attachments. In syntelic attachments, both sister kinetochores of a chromosome attach to the same spindle pole. In merotelic attachments, one sister kinetochore is attached to both poles. These attachments states occur frequently during mitosis and therefore it is essential that the cell has a correction mechanism in place to make sure chromosomes are not mis-segregated (Santaguida and Musacchio, 2009; Walczak et al., 2010). When sister chromatids fail to properly bi-orient, chromosomes are mis-segregated generating aneuploid daughter cells that have gained or lost chromosomes.

1.2.3.2 THE ERROR CORRECTION PATHWAY

Erroneous syntelic and merotelic attachments occur frequently during mitosis (Godek et al., 2015). The error correction pathway is a mechanism, whereby, erroneous attachments are eliminated and amphitelic attachments are selectively

stabilised. Kinetochores act as mechano-sensors that detect tension between chromosomes and spindle poles generated by the end-on attachment of microtubules. The error-correction (EC) pathway is active when kinetochores are unattached or lack tension, but is inactive when kinetochores make end-on microtubule attachments that are under sufficient tension. Importantly, only amphitelic attachments produce sufficient tension to turn the EC pathway off. The KMN network makes up the major microtubule binding site. The KMN-microtubule interaction must be sufficiently dynamic to release improper attachments. Aurora B is a chief effector of the EC pathway and its inhibition results in the stabilisation of incorrect attachments (Kallio et al., 2002; Hauf et al., 2003; Tanaka et al., 2002; Biggins and Murray, 2001). At tension-less kinetochores, Aurora B phosphorylates several microtubule binding proteins reducing their affinity for microtubules and severing this interaction. In contrast, the phosphorylation of Aurora B substrates is reduced as kinetochores come under tension. The Aurora B kinase is the catalytic component of a multi-subunit complex called the chromosome passenger complex (CPC). The other three proteins that make up the CPC include: INCENP, that acts as a scaffold protein, Survivin, that localises the CPC to the centromere and Borealin, that mediates interactions with additional proteins (Carmena et al., 2012). The CPC localises to centromeres through Survivin which binds to a short N-terminal motif of H3 that must be phosphorylated at Thr3 by the Haspin kinase (Yamagishi et al., 2010; Wang et al., 2010; Jeyaprakash et al., 2011). The phosphorylation of Thr120 of H2A by Bub1 kinase is also important for targeting CPC to the centromere (Yamagishi et al., 2010; Kawashima et al., 2010).

Centromere localised Aurora B has several kinetochore substrates including components of the KMN network (Welburn et al., 2010), microtubule binding proteins (Zaytsev et al., 2014) and microtubule depolymerases (Hunter et al., 2003). Aurora B-mediated phosphorylation of these substrates: 1) reduces their affinity for microtubules, 2) weakens the kinetochore-microtubule interface and 3) breaks erroneous connections. To reduce the affinity of the Ndc80 complex to microtubules, Aurora B phosphorylates three components of the KMN network,

Hec1, Knl1 and Dsn1, at tension-less kinetochores (Welburn et al., 2010). Hec1, a member of the Ndc80 complex, is differentially phosphorylated at its positively charged N-terminal tail depending on attachment status (Zaytsev et al., 2015, 2014). The phosphorylation of nine serine residues on the Hec1 tail, neutralises its positive charge to disrupt electrostatic interactions with the negatively charged E-hooks of tubulin dimers (DeLuca et al., 2011; Long et al., 2017). It was recently postulated that the phosphorylation of the Hec1 tail acts as a 'rheostat,' to increase the microtubule-binding affinity of Hec1 by 20 to 100-fold as it transitions from a phosphorylated to dephosphorylated state (Zaytsev et al., 2015). Consistent with this model, cells expressing the non-phosphorylatable mutant Hec1-9A are unable to correct erroneous attachments and subsequently mis-segregate chromosomes (DeLuca et al., 2011; Guimaraes et al., 2008). In addition to this, phosphorylation of the N-terminal tail of Hec1 favours the binding of Mps1 kinase to initiate the SAC pathway and thus links the EC and SAC pathways (Saurin et al., 2011; Hiruma et al., 2015; Ji et al., 2015). The kinetochore-microtubule interface is sealed by the Ska complex in higher eukaryotes (Kalantzaki et al., 2015; Chan et al., 2012) and the analogous Dam1 complex in yeast (Grishchuk et al., 2008), as well as, the Astrin-SKAP complex (Schmidt et al., 2010; Dunsch et al., 2011). Aurora B negatively regulates the association of these complexes with the outer kinetochore to weaken the kinetochore-microtubule interface. Lastly, Aurora B positively regulates the kinesin-13 family member mitotic centromere-associated kinesin (MCAK). MCAK is a microtubule depolymerase which catalyses the depolymerisation of microtubules to destabilise erroneous attachments (Hunter et al., 2003; Ems-McClung et al., 2013).

1.2.3.3 THE SPATIAL SEPERATION MODEL

Aurora B binds to the centromere-inner kinetochore interface and phosphorylates substrates located in the outer kinetochore. To regulate error-correction Aurora B must be close by to its kinetochore targets. When kinetochores are unattached or lack tension, Aurora B is sufficiently near to its substrates, whereas

kinetochores with amphitelic attachments are pulled outwards so that Aurora B can no longer reach its targets (Krenn and Musacchio, 2015). In Hela cells, immunofluorescence analysis showed that proper microtubule attachments increased the distance between inner kinetochore proteins from 0.9um in prometaphase to 1.4um upon bi-orientation at metaphase (Liu et al., 2012). Initial experiments using an engineered Aurora B FRET sensor fused to CENP-B or the Mis12 complex demonstrated that an increased distance from the CPC correlated with reduced phosphorylation of the FRET sensor (Zaytsev et al., 2016). In line with this, observations of known Aurora B targets confirmed that phosphorylation is reduced as they are pulled away from Aurora B when tension arises. Thus, Aurora B substrates, specifically those of the KMN network that regulate the EC and SAC pathway, are physically uncoupled from the Aurora B kinase as kinetochores are bi-oriented. The uncoupling of the Ndc80 complex from Aurora B activity encourages its dephosphorylation by the PP2A-B56 phosphatase (Foley et al., 2011). The dephosphorylated form of the Ndc80 complex has reduced affinity for Mps1, but increased affinity for microtubules. The stretching of kinetochores at bi-orientation stops the Aurora B dependent phosphorylation of target proteins and in doing so stabilises end-on attachments as well as stopping further initiation of the SAC pathway.

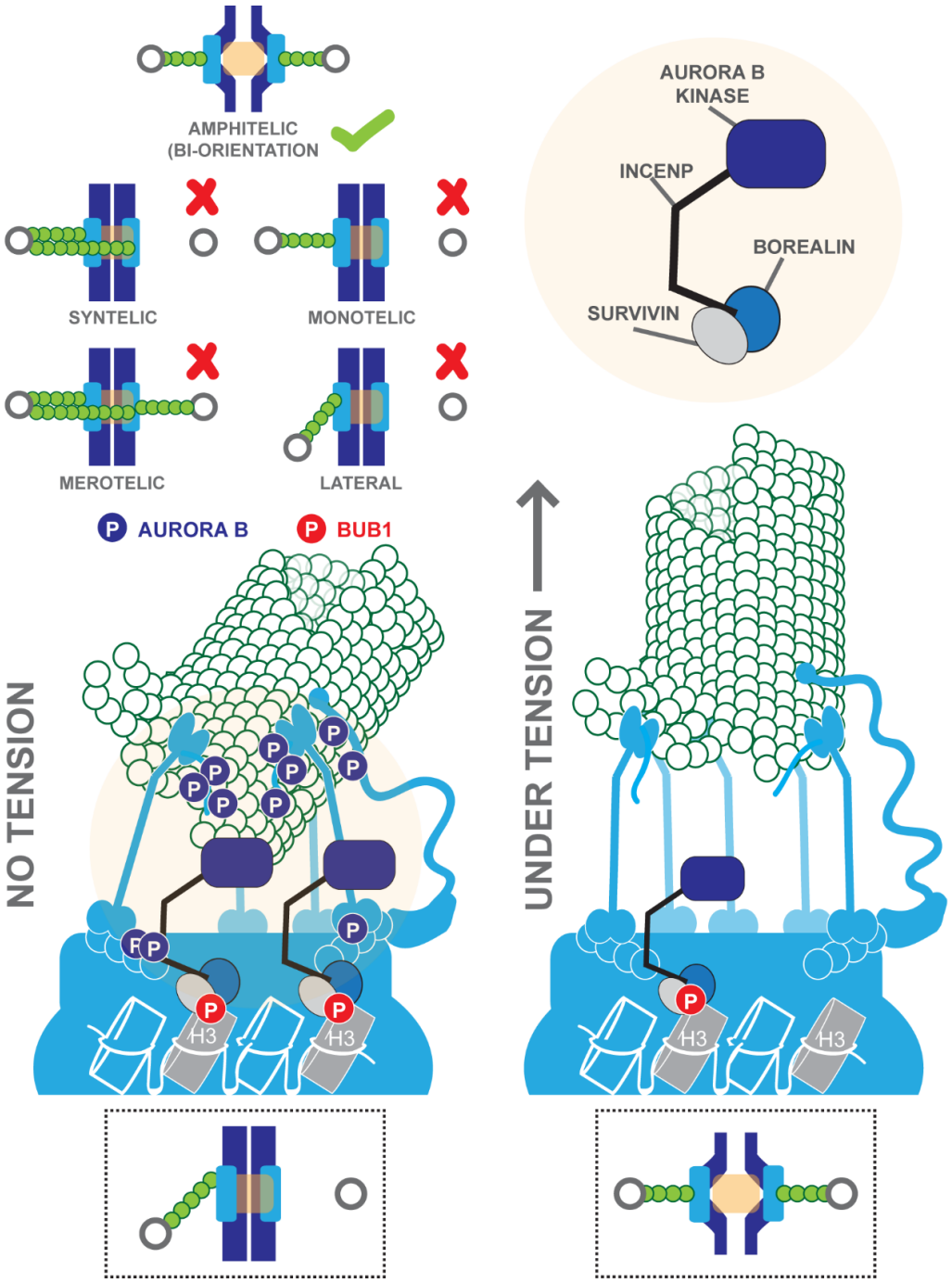

Figure 1.9. The error correction pathway. A schematic showing the formation of different types of microtubule attachments. Incorrect attachments as depicted are corrected by the error-correction pathway of which the CPC complex is the main effector. A lack of tension allows Aurora B to phosphorylate Hec1, Knl1 and components of the Mis12 complex because they are near. When kinetochores are under tension they stretch, and Aurora B is further away from its targets and as a result there is less phosphorylation.

1.3 THE SPINDLE ASSEMBLY CHECKPOINT

The SAC, a cell cycle surveillance mechanism, has evolved to ensure efficient chromosome segregation. Ultimately the SAC pauses the cell cycle to give cells time to properly bi-orient their chromosomes before cell division (**figure 1.10**). The SAC monitors kinetochore-microtubule attachments and blocks anaphase onset in response to even a single unattached kinetochore (Rieder et al., 1995). Similar to other checkpoint pathways, the SAC has a sensory mechanism, to detect unattached kinetochores and an effector system that inhibits the cell cycle oscillator to halt the cell cycle. When kinetochores are not attached to microtubules, the checkpoint sensor initiates the hierarchical recruitment of the SAC module. The assembled SAC module catalyses the production of a 'wait anaphase' signal that blocks the basic cell cycle oscillator, this signal constitutes the SAC effector system. While cell cycle progression is suspended by the SAC effector, the error correction pathway replaces erroneous attachments with correct amphitelic attachments (Musacchio, 2015).

Pioneering genetic screens in budding yeast were essential for the identification of the SAC network. These screens identified core SAC components including the kinase Bub1 and the non-kinases Bub3, Mad1 and Mad2 (Hoyt et al., 1991; Li and Murray, 1991). Monopolar spindle 1 or Mps1 was originally identified as a gene responsible for controlling spindle pole duplication (Winey et al., 1991), however, it soon became apparent that Mps1 was in fact a key SAC protein (Stucke et al., 2002). Initially it was unclear what these proteins did, how they interacted in a pathway and even the molecular target of the SAC was a mystery. Elegant experiments in higher eukaryotes, involving micro-manipulation, biochemical reconstitutions and laser ablation experiments, demonstrated that unattached kinetochores were the signalling centres for the SAC pathway (Li and Nicklas, 1995; Rieder et al., 1995; Kulukian et al., 2009). Consistent with this, immunofluorescence analysis of the SAC proteins revealed that they were dynamically recruited to unattached kinetochores at the start of prometaphase

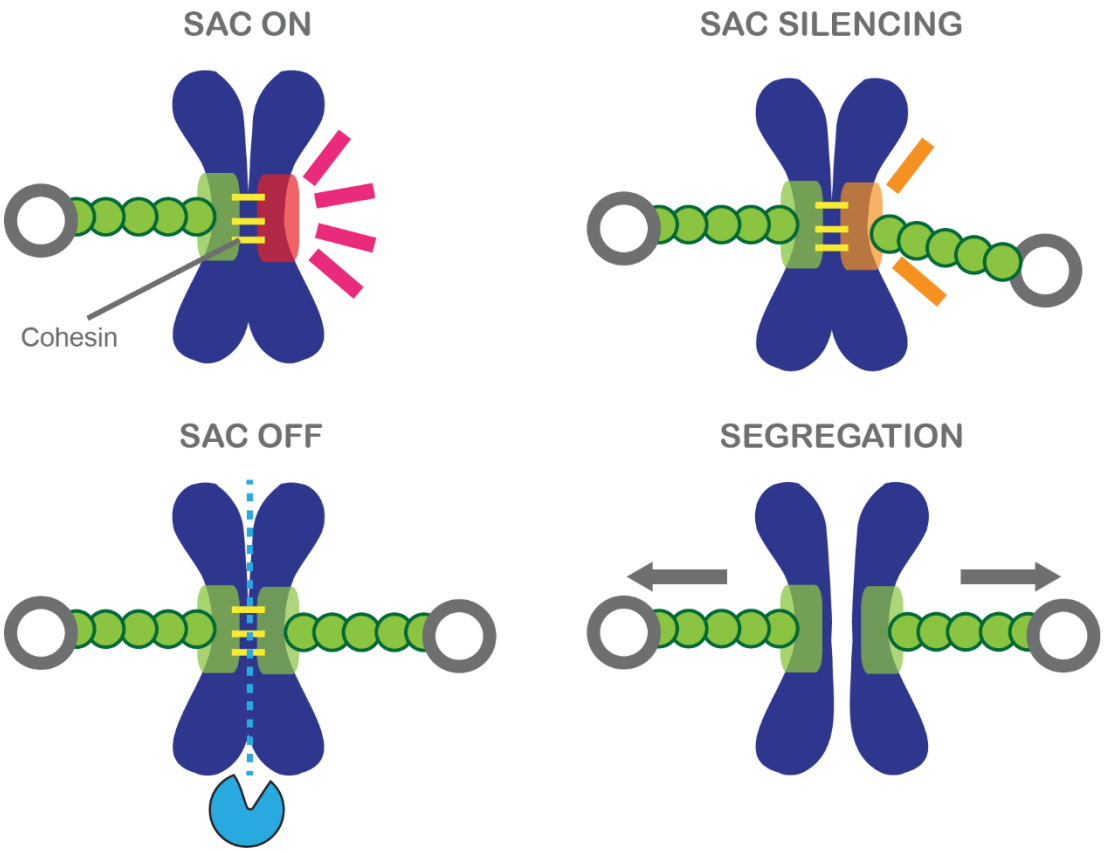

Figure 1.10. Integration of SAC signalling and chromosome segregation. The SAC pathway is active at unattached or incorrectly attached kinetochores. Kinetochores are eventually captured by the mitotic spindle and initial tenuous attachments mature to for intimate end-on attachments. In parallel to the stabilisation of microtubule attachments, the SAC is silenced. At metaphase, the SAC is turned off, chromosomes are attached to both spindle poles and cohesion between sister chromatids is lost due to the activation of the APC/C-separase pathway. In anaphase, chromatids are segregated between the two poles.

and were released as microtubule attachments ensued so that metaphase plates were devoid of SAC proteins (Howell et al., 2004). The Mps1 kinase is the master regulator of SAC signalling and is responsible for the recruitment of all major SAC transducers (Tighe et al., 2008; Kwiatkowski et al., 2010; Maciejowski et al., 2010; Sliedrecht et al., 2010; Hewitt et al., 2010). Once the SAC module is assembled, BubR1, Bub3, Mad2 and the obligatory APC/C accessory subunit Cdc20 assemble the MCC (Sudakin et al., 2001). The MCC binds and inhibits the APC/C and in doing so prevents the degradation of cyclin B and securin (**figure 1.3**). Following chromosome bi-orientation the SAC must be switched off to allow mitotic exit. However, how the SAC is silenced is an unsolved problem.

Perturbations in the mitotic checkpoint causes chromosome mis-segregation, aneuploidy and potentially contributes to tumorigenesis (Kops et al., 2005b; Salmela and Kallio, 2013). Aneuploidy, the gain or loss of chromosomes, and chromosomal instability (CIN) occurs at a higher frequency in cells with a compromised SAC and is a hallmark of many cancer cells (Dominguez-Brauer et al., 2015). In the rare human condition, mosaic variegated aneuploidy, inactivation of the SAC regulator BubR1 predisposes an individual to cancer (Hanks et al., 2004). More commonly cancer cells have genetic or epigenetic changes that disrupt the function of SAC components and this generally weakens the checkpoint rather than completely inactivating it (Torres et al., 2008; Shichiri et al., 2002). Cells with a weakened checkpoint divide with a higher frequency of mis-segregations, whereas, turning off the SAC completely compromises genomic stability to the extent that it becomes lethal to tumour cells (Manchado et al., 2012). Targeting key SAC components is a current anticancer strategy that is being investigated and the Mps1 kinase is the most promising drug target. Inhibiting Mps1 with small molecules disrupts the SAC pathway causing cells to exit mitosis before chromosomes are bi-oriented, resulting in severe chromosome mis-segregation and aneuploidy (Colombo et al., 2010; Jemaa et al., 2013; Hewitt et al., 2010; Kwiatkowski et al., 2010). Surprisingly, Mps1 kinase is also over-expressed in several human tumours and this is expected to contribute towards the survival of aneuploid cells (Salvatore et al., 2007). Mps1

has multiple functions at prometaphase including regulating SAC signalling, MCC assembly and chromosome alignment, therefore, it's perhaps less surprising that having too little or too much of Mps1 is detrimental. The development of Mps1 inhibitors as anti-cancer therapeutics is an active area of research and some inhibitors have progressed as far as clinical trials (Naud et al., 2013; Tardif et al., 2011). The current strategy being developed is to couple SAC inhibitors with microtubule-targeting agents to drive chromosome segregation errors above the threshold needed to kill cells (Manchado et al., 2012; Maia et al., 2015). Given the clinical relevance of Mps1 inhibitors as developing anti-cancer drugs, a greater understanding of how Mps1 is regulated may give valuable insight into the outcome of such strategies.

1.3.1 THE ROLE OF MPS1 KINASE

Like many signalling pathways, reversible protein phosphorylation is a central theme in the SAC signalling network. Protein kinases catalyse the transfer of a high-energy phosphate group from ATP molecules to the side chains of three amino acids: serine, threonine and tyrosine. The less studied protein phosphatases catalyse the reverse reaction and recently their role in signalling networks has emerged. The addition of phosphate groups can modify the function of a target protein by directly modifying its activity or indirectly by modulating its interaction partners. At kinetochores, phosphorylation often influences the available binding partners for a protein, which in turn regulates the targets activity, localisation or stability. The SAC consists of a cascade of phosphorylation events catalysed mainly by the Mps1 kinase which facilitate new protein:protein interactions to build the SAC network. Phosphoamino acids alter the charge and topology of a protein so that it can be recognised by new binding partners. Negatively charged phosphate groups form electrostatic interactions or hydrogen bonds with positively charged residues on interactors. The reversibility of phosphorylation makes it ideal for the SAC pathway because rapid phosphorylation and dephosphorylation allows cells to toggle between an on and off state (Hunter, 2012).

At unattached kinetochores, phosphorylation of SAC proteins, by mitotic kinases, is a prerequisite for protein:protein interactions. Recently, Mps1 has emerged as the chief SAC kinase, which recruits all downstream checkpoint proteins including the Bub proteins, the Mad1:Mad2 heterodimer and the RZZ complex (**figure 1.11**) (Abrieu et al., 2001; Stucke et al., 2002). When the checkpoint is active Mps1 phosphorylates Knl1, a scaffolding protein, to recruit Bub1, Bub3 and BubR1 to the kinetochore (Primorac et al., 2013; Yamagishi et al., 2012; Vleugel et al., 2013; Shepperd et al., 2012; London et al., 2012). In *S. cerevisiae* and *C. elegans*, kinetochore localised Bub1 is sequentially phosphorylated by Mps1 to facilitate its interaction with the Mad1:Mad2 heterodimer (London and Biggins, 2014; Moyle et al., 2014; Ji et al., 2017). The SAC signalling cascade culminates in the kinetochore association of the Mad1:Mad2 heterodimer which acts as a template to convert open-Mad2 (O-Mad2) to closed-Mad2 (C-Mad2). In the final step of SAC signalling, a recent study revealed that Mps1 phosphorylates the Mad1:Mad2 heterodimer to increase the conversion of O-Mad2 to C-Mad2 (Faesen et al., 2017). In addition to this, proteomic analysis has identified other Mps1 SAC targets, as well as, microtubule binding proteins and microtubule motors (Maciejowski et al., 2017). The molecular mechanism by which Mps1 transduces the SAC signal is an active area of research; however, how Mps1 itself is regulated is not known. The aim of my research is to gain a greater understanding of how the activity and localisation of Mps1 is modulated during SAC silencing. In this section, a general overview of SAC signalling will be given with particular emphasis on the Mps1 kinase which is the focus of this study.

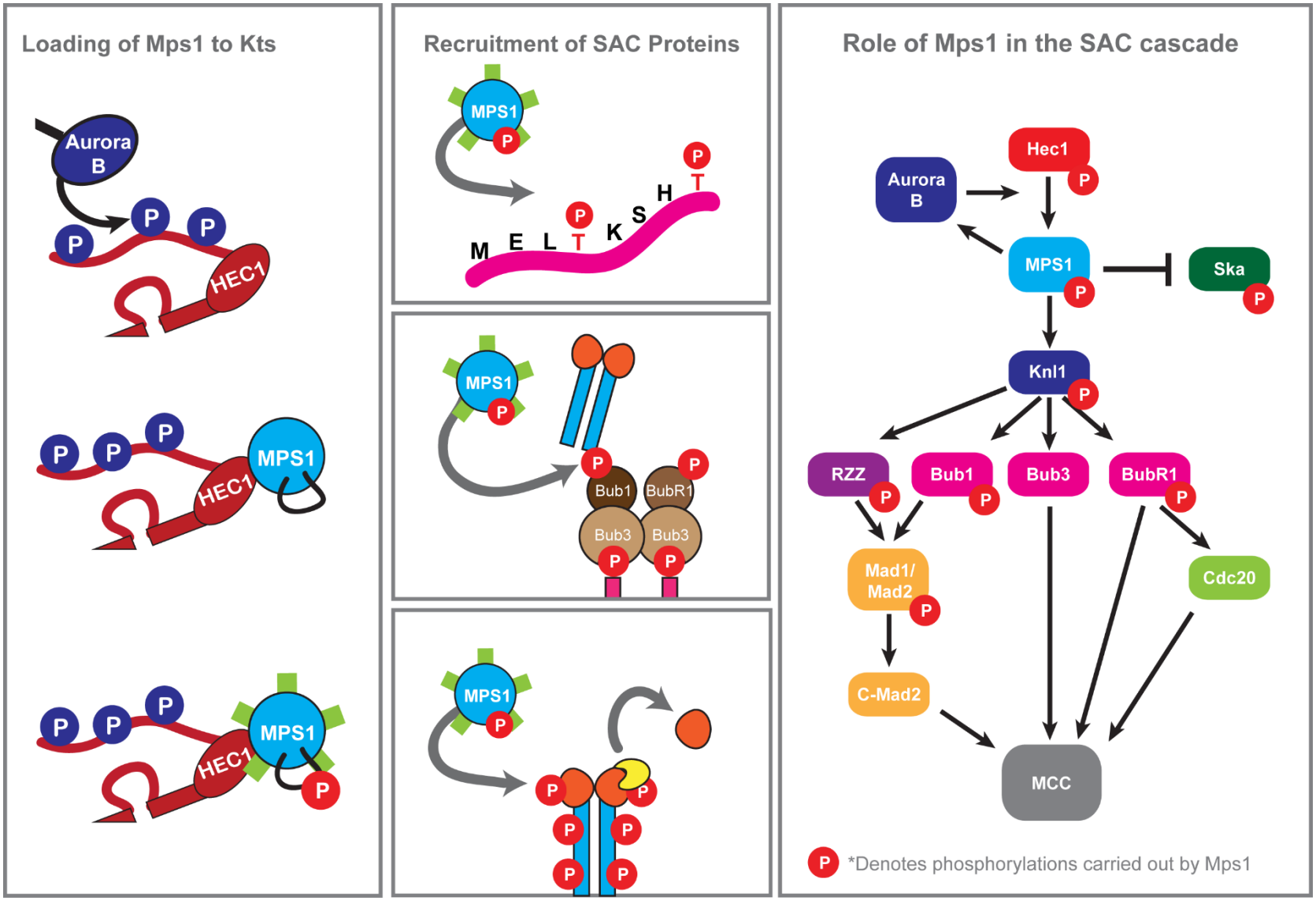
Loading of Mps1 to Kts
Aurora B
HEC1
MPS1
Recruitment of SAC Proteins
M E L T K S H T
Bub1
BubR1
Bub3
Role of Mps1 in the SAC cascade
Hec1
Aurora B
MPS1
Ska
Knl1
RZZ
Bub1
Bub3
BubR1
Mad1/ Mad2
C-Mad2
Cdc20
MCC
*Denotes phosphorylations carried out by Mps1

Figure 1.11. Mps1-dependent SAC signalling. Mps1 docks to the microtubule binding site of the Ndc80 complex facilitated by Aurora B phosphorylation. Mps1 is activated at kinetochores and then phosphorylates target proteins. The key SAC targets include the MELT motifs of Knl1, to recruit Bub1, which is then sequentially phosphorylated to recruit the Mad1:Mad2 complex. Further phosphorylation of the Mad1:Mad2 heterodimer is needed to enhance its template ability. Mps1 controls the SAC cascade and proteomic analysis has further identified new substrates.

1.3.2 SAC INITIATION

When the checkpoint is on, Mps1 is dynamically recruited to kinetochores where it is fully activated (**figure 1.11**) (Stucke et al., 2002). Early FRAP experiments revealed that Mps1 is one of the most dynamic SAC proteins with a turnover of ~2s (Howell et al., 2004; Jelluma et al., 2010). However, exactly how Mps1 binds to kinetochores is not fully understood. The ~200 N-terminal residues constitute the kinetochore binding domain of Mps1 and consist of an N-terminal extension (NTE) and tetratricopeptide repeat (TPR) motif (Nijenhuis et al., 2013). The localisation of Mps1 to kinetochores is the first and perhaps most critical step in SAC signalling. Mps1 specifically localises to unattached kinetochores during prometaphase and is released as attachments are formed so that metaphase plates are devoid of Mps1 (Stucke et al., 2002). When the SAC is turned off Mps1 is released from kinetochores. Blocking the release of Mps1 from kinetochores prevents the SAC from being turned off and perturbs anaphase onset (Ito et al., 2012; Jelluma et al., 2010; Maldonado and Kapoor, 2011). Understanding how the SAC senses microtubule attachments and how this is relayed to inactivate the checkpoint was a major challenge. Recently, complementary work by the Yu and Kops labs showed that the Mps1 kinase competes with microtubules for a single binding site on the Ndc80 complex providing the long-awaited answer to this question (Hiruma et al., 2015; Ji et al., 2015). This work built upon previous studies that showed, using chemical inhibitors and siRNA knock-down, that the kinetochore localisation of Mps1 relied on the Aurora B dependent phosphorylation of the N-terminal tail of Hec1 (Nijenhuis et al., 2013; Zhu et al., 2013; Saurin et al., 2011).

The current consensus is that Aurora B is active at unattached kinetochores, and phosphorylates kinetochore components including the N-terminal tail of Hec1 to recruit Mps1. The phosphorylation of Hec1 weakens its affinity for microtubules and favours the recruitment of Mps1 (Zhu et al., 2013; Saurin et al., 2011; DeLuca et al., 2011). Biochemical experiments using purified fragments of Mps1 and Hec1 have provided a detailed understanding about the domains involved in the

Mps1 and Hec1 interaction. Purified fragments of the N-terminal of Mps1 directly interact with the CH domains of Hec1 (Zhu et al., 2013; Hiruma et al., 2015; Ji et al., 2015). This interaction is promoted when the fragments are phosphorylated and negatively regulated by the introduction of microtubules. In addition to this, mutating basic patches in the CH domain of Hec1 abrogates the localisation of Mps1 in cells. Additionally, Ji et al., 2015, identified a distinct region in Mps1 the middle region (MR), C-terminal to the TPR domain, that is required to bind the CH domain of Nuf2 (Ji et al., 2015). The competition of Mps1 and microtubules provides an elegant system whereby Mps1 senses unattached kinetochores because of the presence of an unoccupied binding site. For this model to accommodate microtubule binding, Mps1 must be repeatedly released and bound to kinetochores, and it is therefore, important to understand how Mps1 leaves kinetochores. An important clue is that Mps1 kinase somehow negatively regulates its own localisation (Hewitt et al., 2010; Jelluma et al., 2010), but this negative feedback mechanism is yet to be defined. Once kinetochore-microtubule attachments are complete, Mps1 must be removed from kinetochores to stop the recruitment of downstream checkpoint proteins (Jelluma et al., 2010). How Mps1 is released from kinetochores is a point of discussion.

When the SAC is on, kinetochore localised Mps1 is phosphorylated at many residues (Stucke et al., 2002; Wang et al., 2009) and these phosphorylations are expected to regulate the activity and localisation of Mps1 (Kang et al., 2007; Mattison et al., 2007; Tyler et al., 2008; Wang et al., 2009, 2014). Phospho-proteomic analysis of phosphorylated Mps1 revealed that it is phosphorylated at different regions of the protein (Kang et al., 2007; Jelluma et al., 2008b; Dou et al., 2011; Mattison et al., 2007). Like other kinases Mps1 kinase has a regulatory activation loop or T-loop in its kinase domain and phosphorylation of its T-loop is associated with maximum kinase activity (Bayliss et al., 2012). At kinetochores, clusters of Mps1 molecules dimerise and activate each other's kinase domain by trans-autophosphorylation of the activation loop residue T676 (Kang et al., 2007; Mattison et al., 2007; Wang et al., 2009). This empowers Mps1 kinase with increased catalytic activity to promote further autophosphorylation, as well as,

facilitating the phosphorylation of other kinetochore substrates. Phosphorylation of T676 has been shown to be an important auto-activation mechanism in several studies (Kang et al., 2007; Mattison et al., 2007; Wang et al., 2009). *In vitro*, a non-phosphorylatable mutant (T676A) shows significantly reduced kinase activity. Moreover, cells expressing Mps1 T676A have a weakened checkpoint and mis-segregate chromosomes more frequently (Kang et al., 2007; Jelluma et al., 2008b). At the start of this study, the mechanism by which Mps1 is turned off had not been investigated and was a major unresolved question.

1.3.3 SAC RECRUITMENT

During prometaphase, SAC proteins are dynamically recruited to kinetochores by Mps1 kinase. In recent years, considerable progress has been made in understanding mechanistically how Mps1 builds the SAC module. Proteomic analysis has revealed that Mps1 orchestrates SAC signalling by phosphorylating multiple target proteins (Maciejowski et al., 2017). There are three fundamental steps in the assembly of the SAC module: 1) the binding of the Bub proteins, that are packaged into the MCC, 2) the loading of the Mad1:Mad2 heterodimer, which in turn catalyses 3) the conversion of open-Mad2 to closed-Mad2 (**figure1.12**). We will briefly discuss how the SAC module is assembled by the checkpoint kinase Mps1.

1.3.3.1 MELT MOTIFS

Among these targets, Knl1, the largest subunit of the 9-subunit KMN network, is the most studied Mps1 target. Initial studies in budding yeast demonstrated that Mps1 drives the recruitment of the Bub proteins by phosphorylating the highly conserved Met-Glu-Leu-Thr (MELT) motifs on Knl1 (Shepperd et al., 2012; London et al., 2012). The presence of an array of MELT motifs is a characteristic feature of Knl1 across different species (Cheeseman et al., 2004). Consistently, studies in human cells found that the Mps1 dependent phosphorylation of the MELT motifs on Knl1 was indeed required for the recruitment of the Bub proteins

(Yamagishi et al., 2012). Although human Knl1 has a total of 19 MELT repeats, many of these have deteriorated and it is predicted that only 6-7 MELTs recruit substantial levels of the Bub proteins (Zhang et al., 2014; Vleugel et al., 2015). While the MELT motif is simple and compact in budding yeast, in humans active repeats are further specified by two flanking sequences TΦΦΩ (where Φ denotes a hydrophic residue) and SHT motifs. Extensive analysis of the human MELT repeat expanded this repeat to DKTΦΦΩS[ED]x[ED]xxM[DE]ΦTKSHTΦxΦ (where X refers to any amino acid, Φ refers to a hydrophobic residue and Ω refers to an aromatic residue) (Vleugel et al., 2013, 2015). In this sequence, Mps1 phosphorylates the threonine residues of both the MELT and SHT and this is critical for the binding of the Bub proteins in cells.

1.3.3.2 THE BUB COMPLEX

How phosphorylated MELT motifs were interpreted as a signal by downstream SAC proteins was an important question. It was shown by crystal structure data that Bub3 directly recognises phosphorylated MELT motifs on the surface of Knl1 and binds them with high affinity (Primorac et al., 2013). This promotes the successive recruitment of Bub1 and BubR1 that form heterodimers with Bub3 bound to Knl1 (Overlack et al., 2015). Crystal structure determination of a ternary complex between the pMELT2 motif and a Bub1:Bub3 construct provided insight into how pMELT motifs are recognised. In this structure, the pMELT2 motif docks between two blades of the 7-bladed β-propeller structure of Bub3. At this highly conserved interface, extensive contacts between the MELT motif and side chains of Bub3 are formed. Bub3 is highly selective for phosphorylated MELT motifs. The phosphate group binds to a basic region of Bub3 where it is coordinated by three highly conserved and positively charged arginine residues to form strong electrostatic interactions. Mutating residues at this interface abrogated the localisation of Bub3 and Bub1 and caused a checkpoint defect. Bub3 serves at least three functions at kinetochores including recognising pMELT motifs, recruiting Bub1 and BubR1 as well as being a core component of the MCC (Primorac et al., 2013).

Bub1 is a SAC kinase, recruited by Bub3, that positively regulates the localisation of Aurora B to link the SAC with the error-correction machinery (Yamagishi et al., 2010). In addition to this, Bub1 has been implicated in the localisation of other SAC members to kinetochores including Mad1:Mad2 (Zhang et al., 2017; London and Biggins, 2014; Moyle et al., 2014; Ji et al., 2017), potentially the RZZ complex (Zhang et al., 2015) and more recently it was shown that it regulates the kinetochore association of BubR1(Overlack et al., 2015). The SAC components, Bub1 and BubR1, are paralogous proteins and therefore, are conserved at the sequence and domain level. While both Bub1 and BubR1 form heterodimers with Bub3, only Bub1 contributes to the Bub3:pMELT interaction (Overlack et al., 2015; Primorac et al., 2013). This function is confined to the B3BD domain of Bub1 and although BubR1 has its own B3BD domain, structural changes during evolution mean its unable to carry out this function. As a consequence, BubR1 uses a different binding mechanism, whereby, it is stabilised at kinetochores with help from Bub1. Bub1 and BubR1 interact via their GLEB and B3BD domains and this interaction relies on both forming hetero-dimers with Bub3 (Overlack et al., 2015).

1.3.3.3 LOADING OF THE MAD1:MAD2 TEMPLATE

When the SAC is active, the Mad1:Mad2 heterodimer docks onto unattached kinetochores, where it catalyses the conversion of O-Mad2 to C-Mad2 (De Antoni et al., 2005). It had been known for some time that Mps1 regulates Mad1 binding (Hewitt et al., 2010; Kwiatkowski et al., 2010; Santaguida et al., 2010; Maciejowski et al., 2010; Sliedrecht et al., 2010), however, specific details about how this is achieved have only recently come to light. Given the crucial role that the Mad1:Mad2 heterodimer plays in SAC signal transduction, the identity of its kinetochore associated receptor has been an active area of research. In the current model, Mad1 binds to two independent sites, one consists of a phosphorylated region on Bub1 and the other is through the RZZ complex.

Initial studies in yeast, proposed that the Bub1 protein is the kinetochore receptor for Mad1 (Brady and Hardwick, 2000) and follow-up studies have shown that this mechanism is conserved in other organisms including C. elgans and humans (Ji et al., 2017; Zhang et al., 2017; Moyle et al., 2014). The central region (CD1) of Bub1 is sufficient to target Mad1 to kinetochores. The CD1 domain is regulated by Mps1 and its phosphorylation is a strict requirement for the binding of Mad1 (London and Biggins, 2014; Zhang et al., 2017). Mutating the phosphosite on CD1 to alanine abrogated Mad1 binding and caused a checkpoint defect (Zhang et al., 2017). There is considerable evidence to suggest that Bub1 is the main receptor for Mad1:Mad2 at kinetochores. In contrast, other studies have described a close relationship between the colocalisation of the RZZ complex and the Mad1:Mad2 template (Buffin et al., 2005). The RZZ complex depends on a structural protein, ZW10-interacting protein 1 (Zwint1), to bind to the kinetochore which interacts with Knl1 (Foley and Kapoor, 2013). There is some evidence to suggest that the RZZ complex is needed to load the Mad1:Mad2 heterodimer. Depleting components of the RZZ complex by siRNA causes a significant decrease in the localisation of Mad1 and Mad2 to kinetochores (Varma et al., 2013; Défachelles et al., 2015; Caldas et al., 2015). The functional importance of the RZZ complex is somewhat confusing because although RZZ proteins are important SAC regulators in mammalian cells (Kops et al., 2005a), they are not conserved in many other organisms (Karess, 2005). It is possible that the RZZ-Mad1 interaction may be a metazoan creation that has evolved to provide an additional layer of regulation. Recently Millar and colleagues postulated that both these receptors exist in human cells, however, there are mechanistic differences between them (Silió et al., 2015). They postulate that the RZZ receptor is needed for the initial binding of Mad1 at unattached kinetochores, whereas, Bub1 binds Mad1 more strongly at misaligned kinetochores. The precise contribution of Bub1 and the RZZ complex to Mad1 loading requires additional clarity. Nonetheless, these studies have provided considerable insight into how the Mad1:Mad2 heterodimer is loaded onto kinetochores.

1.3.4 SAC: CATALYSIS

SAC signal transduction at kinetochores culminates in the catalysis of O-Mad2 to C-Mad2 by the Mad1:Mad2 template. Mad2 can exist in two distinct conformations: an open configuration O-Mad2, this cytosolic pool makes up the bulk of Mad2 present in cells, and a closed configuration C-Mad2, stabilised by the binding of interaction partners. In the 'Mad2 template model,' the dimerisation of cytosolic O-Mad2 with C-Mad2 at kinetochores causes a conformational change in O-Mad2 that encourages it to adopt the closed configuration (De Antoni et al., 2005). Newly formed C-Mad2 is incorporated into the MCC (Sudakin et al., 2001). The conversion of O-Mad2 to C-Mad2 is the rate limiting step in the production of the MCC. To undergo this transition O-Mad2 undergoes large topological changes including relocation of the C-terminal tail termed the 'safety belt' (Sironi et al., 2002; Luo et al., 2002). Given these structural changes, the conversion of O-Mad2 to C-Mad2 requires a large activation energy and thus, *in vitro* is very slow (Simonetta et al., 2009; Musacchio, 2015). In the 'Mad2 template model,' the Mad1:Mad2 complex catalyses this reaction by lowering the energy barrier needed to achieve the closed conformation.

A recent study revealed that Mps1 activity was needed to accelerate the rate of O-Mad2 to C-Mad2 conversion (Faesen et al., 2017; Hewitt et al., 2010). Previously, *in vitro* studies observed that the Mad1:Mad2 complex catalysed this reaction by a factor of only 10 (Simonetta et al., 2009; Musacchio, 2015) and that MCC assembly took several hours (Kulukian et al., 2009; Simonetta et al., 2009). In contrast, MCC assembly must be rapid in cells to establish a SAC response in a timeframe of a few minutes (Dick and Gerlich, 2013). Biochemical reconstitution experiments in which the core components required for MCC assembly were phosphorylated by Mps1, demonstrated that Mps1-mediated phosphorylation accelerated the conversion of Mad2. Multiple phosphorylation sites were found on Mad1 and mutating these sites to alanine ablated the catalytic role of Mad1 (Faesen et al., 2017). In a multi-step process Mps1 induces the conversion of O-Mad2 to C-Mad2 by phosphorylating MELT motifs to create docking sites for

Bub1, sequentially phosphorylating Bub1 to load the Mad1:Mad2 heterodimer, and finally by phosphorylating Mad1:Mad2 to activate the template.

1.3.5 SAC: EFFECTOR MECHANISM

The MCC, comprising the SAC proteins BubR1, Bub3, Mad2 and the obligatory APC/C accessory subunit Cdc20, constitutes the major SAC effector system. Recruitment of these core components to kinetochores is an important step in the assembly of the MCC complex. The MCC opposes APC/C activity by two ways: firstly, the MCC sequesters a molecule of Cdc20, an APC/C coactivator, and secondly, the MCC acts as a pseudo-substrate inhibitor (Musacchio, 2015). The BubR1 protein, the largest of the four subunits, has multiple interaction motifs so that it can facilitate the assembly of a core MCC. Functionally important motifs in BubR1 include two KEN boxes (KEN1 and KEN2), a TPR domain, a GLEB motif (Bub3 binding domain) and a D-box, to act as a pseudo-substrate. The crystal structure of fission yeast MCC represented a milestone in the mechanistic understanding of the MCC/APC/C interaction (Chao et al., 2012). In this structural analysis, the HLH motif of the KEN1 box of BubR1 is sandwiched between the β-propeller of Cdc20 and an α-helix of Mad2. The BubR1 TPR domain forms additional contacts with both Cdc20 and Mad2. The Mad2 safety belt associates with the N-terminal of Cdc20 through its Mad2-interacting motif. The Bub3 subunit binds to the GLEB domain of BubR1 a distinct site to other components (Musacchio, 2015). Collectively, these interactions cooperate to assemble the stable core MCC complex. Recent studies, revealed that the core MCC binds a second Cdc20 subunit, through BubR1s second KEN box, to form MCC^{2Cdc20} (Izawa and Pines, 2015). Interestingly, this second Cdc20 can already be bound to active APC/C, and this therefore, explains how the MCC inhibits active APC/C complexes. Structural data has since confirmed the presence of two Cdc20 subunits in the MCC (Yamaguchi et al., 2016; Alfieri et al., 2016). Recent developments in cryo-electron microscopy have provided greater insight into how the MCC molecule docks into the APC/C. These structures demonstrate that inhibitory motifs in BubR1 including KEN 2, D-box 2 and the A1 motif, are

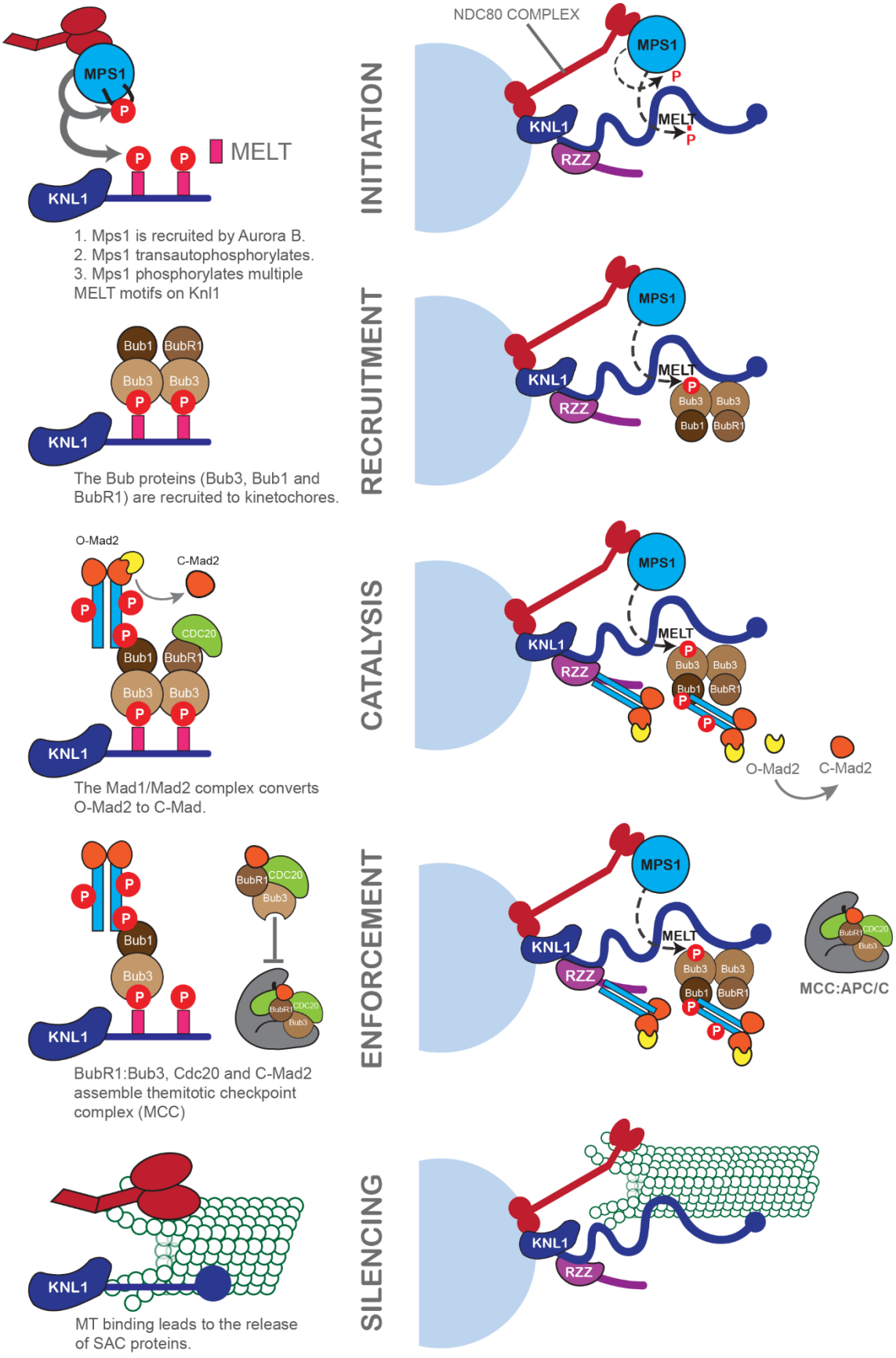
MPS1
P
MELT
KNL1
1. Mps1 is recruited by Aurora B.
2. Mps1 transautophosphorylates.
3. Mps1 phosphorylates multiple MELT motifs on Knl1
Bub1
BubR1
Bub3
The Bub proteins (Bub3, Bub1 and BubR1) are recruited to kinetochores.
O-Mad2
C-Mad2
CDC20
The Mad1/Mad2 complex converts O-Mad2 to C-Mad.
BubR1:Bub3, Cdc20 and C-Mad2 assemble themitotic checkpoint complex (MCC)
MT binding leads to the release of SAC proteins.
INITIATION
RECRUITMENT
CATALYSIS
ENFORCEMENT
SILENCING
NDC80 COMPLEX
RZZ
MCC:APC/C

Figure 1.12. The SAC pathway. Assembly of the spindle assembly checkpoint. The binding of Mps1 kinase to Hec1 is required for the hierarchical recruitment of all other components. Mps1 phosphorylates itself to become active and the scaffolding protein Knl1 on its MELT motifs. The phospho-MELT motifs act as docking sites for the Bub proteins and further phosphorylation of Bub1 recruits the Mad1-Mad2 heterodimer. C-Mad2 at kinetochores catalyses the conversion of surrounding cytoplasmic O-Mad2. The newly formed C-Mad2 binds to other kinetochore-localised proteins including Bub3, BubR1 and Cdc20 to form the mitotic checkpoint complex. The MCC binds and inhibits the APC/C to deny the onset of anaphase. The SAC is turned off when microtubules bind with tension and the SAC proteins are evicted from kinetochores.

recognised by Cdc20 bound to the APC/C. The binding of BubR1 blocks the Cdc20 coactivator from recognising substrates and is therefore, a competitive inhibitor. In addition to this, BubR1 prevents association of an accompanying E2 enzyme UbcH10 to disable APC/C activity (Alfieri et al., 2016). The MCC, a diffusible inhibitor, connects microtubule sensing and SAC signalling with the inhibition of cytosolic APC/C to pause the central cell cycle control network.

1.3.6 SAC: SILENCING

As chromosomes attach to the bi-polar spindle the mitotic checkpoint is satisfied and the transduction of a 'wait anaphase' signal stops. SAC inactivation is controlled by three distinct mechanisms involving Dynein-mediated stripping, the p31-comet inhibitor and the activity of SAC phosphatases.

1.3.6.1 DYNEIN MEDIATED STRIPPING

The composition of the kinetochore changes dramatically upon microtubule binding. The microtubule motor Dynein, a minus-end directed motor, walks along microtubules to transport SAC proteins from kinetochores towards centrosomes. This process is called Dynein-mediated stripping and has been suggested to be important in SAC silencing (McHugh and Welburn, 2017). Importantly, inhibiting dynein-mediated stripping prevents the removal of the Mad1:Mad2 heterodimer from kinetochores (Howell et al., 2001) and blocks the inactivation of the SAC (Maldonado and Kapoor, 2011). The RZZ complex, that regulates Mad1:Mad2 binding, is the kinetochore target of this process (Karess, 2005). However, Dynein alone is not sufficient to move SAC proteins and it utilises a cargo adaptor protein called Spindly. Consistently, Spindly depletion abrogates Dynein recruitment and the successive removal of the RZZ complex and the Mad1:Mad2 template (Griffis et al., 2007; Barisic et al., 2010; Gassmann et al., 2010). Until recently, a mechanistic understanding of how the Spindly-Dynein complex interacted with the RZZ complex was lacking. Now, biochemical binding assays and crystal structures have revealed a direct interaction between the C-terminus of Spindly

and the β propeller region of Rod, a subunit of the RZZ complex (Mosalaganti et al., 2017; Gama et al., 2017). This interaction can be strengthened by farnesylation of cysteine residues on Spindly, however, the role of kinases in regulating this interaction is yet to be determined (Mosalaganti et al., 2017). Recent progress has given a more detailed mechanistic understanding for the removal of the Mad1:Mad2 heterodimer through the RZZ-Dynein stripping pathway. How Mad1:Mad2 is removed from Bub1 is yet to be determined.

1.3.6.2 p31-COMET

The p31-comet protein, a SAC inactivator, was originally identified in a yeast two-hybrid screen for Mad2 interactors. The overexpression of p31-comet blocks the SAC signal and conversely depletion of p31-comet by siRNA extends mitosis (Hagan et al., 2011; Jia et al., 2011; Westhorpe et al., 2011). To inactivate the SAC, the association of p31-comet with Mad2 is essential – mutants unable to bind Mad2 do not influence checkpoint signalling (Westhorpe et al., 2011; Yang et al., 2007a). Crystal structures demonstrated that p31-comet binds C-Mad2 at its dimerisation interface to 'cap' Mad2 and stops it recruiting O-Mad2 (Mapelli et al., 2006). Some observations conflicted with the model that p31-comet inhibited the SAC simply by 'capping' Mad2 (Westhorpe et al., 2011), and more recent studies have focused on the role of p31-comet downstream of kinetochores. A role for p31-comet in MCC disassembly has been proposed. *In vitro* p31-comet has been shown to negatively regulate the assembly of the MCC, moreover, it is thought that p31-comet actively extracts Mad2 from preassembled MCC (Westhorpe et al., 2011). To extract Mad2 from the MCC, p31-comet partners with TRIP13, an ATPase, to catalyse the conversion of C-Mad2 back to O-Mad2 to destabilise the MCC (Westhorpe et al., 2011; Teichner et al., 2011; Eytan et al., 2014; Liu Hang). Precise details on how p31-comet controls the SAC pathway and MCC disassembly are still lacking, however, it is clear that it achieves SAC inactivation largely by antagonising the function of C-Mad2.

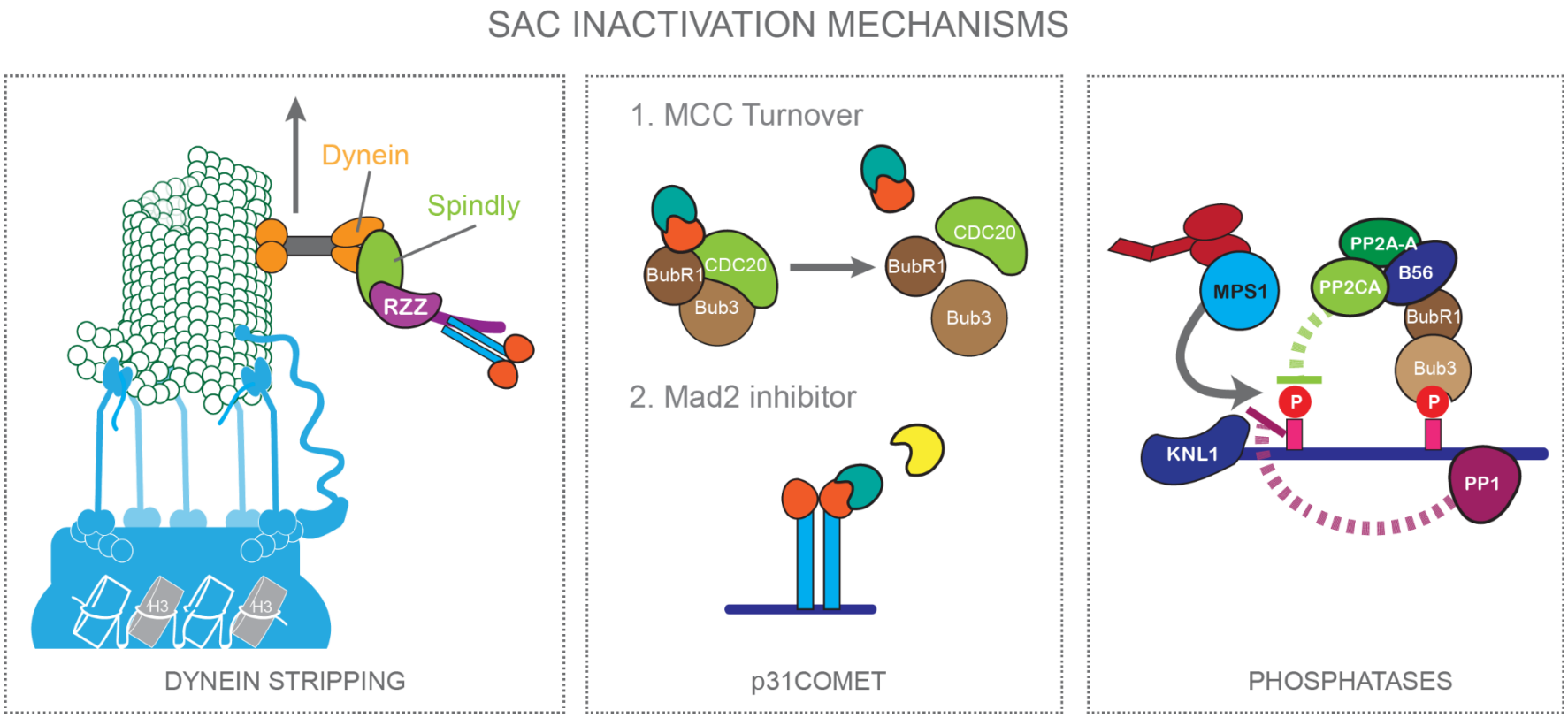

Figure 1.13. Silencing the checkpoint. The SAC is inactivated by three main mechanisms. The most studied of these, is Dynein mediated stripping of the RZZ:Mad-Mad2 complex from kinetochores. The p31Comet protein, a competitive inhibitor of O-Mad2, binds to C-Mad2 blocking the conversion of Mad2 from an open to a closed state. More recently, the function of the PP2A-B56 and PP1 phosphatases in SAC silencing was bought to light.

1.3.6.3 SAC PHOSPHATASES

The mitotic kinases Mps1 and Aurora B, master regulators of the SAC and error-correction pathways respectively, are essential for the proper bi-orientation of chromosomes. Mitotic protein phosphatases work antagonistically to remove phosphate groups previously placed by a mitotic kinase and in doing so play a pivotal function in switching off these pathways. The interplay between kinase and phosphatase activity is critical in creating a complex signalling network involving multiple negative feedback loops, priming events and dynamic changes in kinetochore composition (Nijenhuis et al., 2014; Espert et al., 2014; Funabiki and Wynne, 2013). A strict balance between kinase and phosphatase activity acts as the fulcrum in regulating SAC output. While the contribution of SAC kinases has been widely studied, less is known about the SAC phosphatases. The phospho-protein phosphatase (PPP) family, a group of serine/threonine phosphatases, have been implicated in mitosis (Picard et al., 1989; Axton et al., 1990). Of these phosphatases, PP1 and PP2A complexes have a known role in phospho-regulation of the SAC. Based on present studies the individual contribution of PP1 and PP2A to the SAC is unclear because they seem to play overlapping functions. Moreover, this has been further confused by differences in phosphatase requirements in different organisms, for example budding yeast rely heavily on the PP1 phosphatase. There is considerable evidence to suggest these mitotic phosphatases are critical in stabilising correct K-MT attachments and more recently modulating SAC signalling (Foley et al., 2011; Espert et al., 2014; Nijenhuis et al., 2014). To stabilise microtubule attachments PP1 and PP2A oppose the Aurora B mediated phosphorylation of subunits of the KMN network (Liu et al., 2010; Foley et al., 2011; Foley and Kapoor, 2013). To inactivate the spindle checkpoint PP1 and PP2A oppose Mps1 activity. The phosphorylation of MELT motifs on Knl1 by Mps1 is the most studied phosphorylation event in the SAC pathway (Yamagishi et al., 2012; Shepperd et al., 2012; London et al., 2012; Primorac et al., 2013; Vleugel et al., 2013). This phosphorylation is negatively regulated by the action of PP1 and PP2A phosphatases to stop the Mps1 dependent recruitment of downstream SAC components (Nijenhuis et al., 2014; Espert et al., 2014). However, recent studies have highlighted that there are many

other phosphorylation events during the recruitment of the SAC proteins and potentially these may also be regulated by the SAC phosphatases (Maciejowski et al., 2017; Faesen et al., 2017; Ji et al., 2017). The role of protein phosphatases will be discussed in-depth in Chapter 4.

1.4 Aim of Thesis

After over two decades of research into the SAC, the Mps1 kinase has emerged as the master regulator. While we had uncovered some of the functions of Mps1 very little was known about how Mps1 itself was modulated. Given that Mps1 is crucial to SAC signalling I hypothesised that regulatory mechanisms must be in place to control its function. Thus, the primary aim of this project was to identify and characterise these regulatory mechanisms. There are five potential points at which Mps1 may be regulated: its recruitment to, activation and inactivation at, release from kinetochores and its association with interaction partners. There was a significant gap in our understanding of how Mps1 is inactivated at kinetochores and thus, this was the initial focus of my research. Parallel to this work, I searched for novel interactors of Mps1 and this work led us onto an investigation into how the localisation of Mps1 is controlled.

The two main scientific questions investigated in this thesis are:

1) How is Mps1 inactivated during SAC silencing?

2) What proteins, if any, does Mps1 interact with at kinetochores?

2.
MATERIALS AND METHODS

2.1 Cell culture

2.1.1 General tissue culture

HeLa and HEK-293T cells were grown in DMEM containing 10% fetal bovine serum at 37^{o}C. To synchronise cells in G1/S phase, cells were incubated with 2 mM thymidine for 18-24 hrs to block the cell cycle. Cells were released into mitosis by washing with 3 x PBS and finally cells were transferred into fresh DMEM. To arrest cells in mitosis after a thymidine release, 100 ng/ml (330 nM) nocodazole was added alongside 20 µM MG132. Cells were also arrested in mitosis overnight (o/n) by adding 100 ng/ml nocodazole for 10-16 hrs.

2.1.2 siRNA treatments

For RNAi experiments, cells were transfected with oligofectamine and 20 nM of the indicated siRNA oligonucleotides for 48h-72 hrs. SiRNA oligonucleotides are listed in table 2.2.

2.1.3 Inhibitor treatment

For immunofluorescence experiments, cells were treated for 5 mins with 2 µM AZ3146, 10 mins with 2 µM ZM447439 and 8 mins with 25 nM calyculin. In immunoprecipitation experiments cells were treated for 1 hour with 20 µM MG132 and DMSO vehicle control or with MG132 and AZ3146 or ZM447439.

2.2 GFP-Mps1 cell lines

2.2.1 Cloning

Mps1 was previously amplified from human testis cDNA and placed in the pSC-A plasmid (Espert et al., 2014). For the generation of Mps1 mutants, site-directed mutagenesis was performed using the QuickChange mutagenesis system (Agilent technologies). DNA mutagenesis primers were obtained from Invitrogen (table 2.3). WT-Mps1 and the different phospho-mutants were sub-cloned into a pCDNA5/FRT/TO vector (Invitrogen) modified to contain an EGFP reading frame.

2.2.2 Production of stable cell lines

For the generation of stable HeLa cell lines, HeLa-Flp-in TRex parental cells cells (a kind gift from Stephen Taylor's lab (Tighe et al., 2008)) were transfected with the relevant Mps1-pCDNA5/FRT/TO vector and the POG44 plasmid (encodes Flip-in recombinase) in a ratio of 1:9. Transfected cells were seeded as single cells on 15 cm dishes and selected with Blasticidin 4 µg/ml and Hygromycin 200 µg/ml. Colonies were grown and picked using cloning discs (thermo-fisher). Next, colonies were screened for an expression level comparable to endogenous Mps1 and immunofluorescence was used to identify colonies with homogenous expression levels. The most suitable colonies were picked, and a single colony was used in future experiments. GFP-BubR1, GFP-BubR1$^{L669A/I672A}$ and GFP-CenpA cells had been produced previously in the lab.

2.3 Rescue experiments

2.3.1 Mitotic index

GFP-Mps1 cells were seeded at a density of 60,000 cells per 2 ml well 24 hrs prior to siRNA transfection. Cells were depleted of endogenous Mps1 by 3' UTR siRNA for a total of 48 hrs. Doxcycline was added 4 hrs before siRNA transfection to induce the expression of transgenes. The ability of transgenes to restore the SAC was assessed by incubating cells with nocodazole for a further 10-12 hrs. Fields of cells were imaged under a tissue culture microscope (5 fields in three separate experiments). Cells were judged to be mitotic based on a characteristic rounded morphology and the proportion of mitotic cells was quantified.

2.3.2 SAC rescue assay

GFP-BubR1 or GFP-Mps1 cells were depleted of the relevant endogenous protein by siRNA for 48 hrs. Doxycycline was added to induce the expression of the indicated transgene 4 hrs before transfection. Cells were synchronised in mitosis by the standard thymidine-release protocol, but additionally doxycycline was added to the fresh medium in the final step. After 7 hrs of release, MG132 and nocodazole were added for a final 2 hrs to block mitotic exit and to activate

the SAC. Finally, cells were fixed, stained by immunofluorescence as indicated and imaged.

2.4 Image processing and analysis

2.4.1 Fixed Imaging

Cells were fixed for 15 mins in PTEMF fixation buffer (20 mM Pipes-KOH, pH 6.8, 0.2% Triton X-100, 1 mM $MgCl_2$, 10 mM EGTA, and 4% formaldehyde) at room temperature (RT). Coverslips were blocked in PBS with 2% BSA for 30 minutes at RT. Primary and secondary antibody incubations were carried out for 1 hour at RT. Coverslips were dried and mounted onto microscopy slides using moviol. Microscope slides were imaged using a 60 x 1.35 NA oil immersion objective lens on a DeltaVision core microscope system equipped with an Olympus IX-71 and a Photometrics CoolSNAP HQ2 camera. The microscope was fitted with filter sets for DAPI, Alexa Fluor 488, Alexa Fluor 555, Alexa Fluor 647. Representative images were taken for at least 5 cells per condition in three different experiments (n=15). For each cell analysed a z-stack comprising 12 images was taken. In ImageJ the maximum intensity in each stack was projected to obtain a single image for each channel. The kinetochore intensities were measured in ImageJ by circling kinetochores using a 7x7 pixel circle. For each quantification 5 representative cells were chosen per condition and the intensity of 20 kinetochores per cell was measured. The kinetochore intensity obtained was corrected for background staining in Microsoft Excel. The antibody signals were normalised to CENP-A or CREST, kinetochore markers and graphs were plotted using Graphpad prism. For figure production, the maximum intensities were projected from a z-stack in ImageJ and the projected images were uniformly scaled, cropped and imported into Adobe illustrator CS4 for figure production.

2.4.2 Cold stable assays

GFP-Cenp A cells were depleted of the indicated proteins by siRNA and released into mitosis by a standard thymidine-release protocol. Upon mitotic entry cells were treated with the indicated inhibitors and MG132 to block mitotic exit. Before PTEMF fixation, cells were incubated in 4ºC DMEM for 10 mins to destabilise

unattached microtubules. Following cold-treatment, cells were fixed, and immunofluorescence was performed as described before. Images were processed in ImageJ and the final figure was built in Adobe Illustrator.

2.4.3 Live Cell Imaging

Cells were depleted of Mps1 by siRNA and rescued by expressing doxycycline inducible versions of GFP-Mps1. For live cell imaging, GFP-Mps1 cells were grown in 35 mm dishes with coverglass bottoms and following a 18hr thymidine block were released in mitosis. To stain for DNA, SiR-Hoechst (150 nM) was added 8 hrs prior to imaging. Live cell imaging was performed using a Deltavision Elite microscope system which has filter sets for DAPI, Alexa Fluor 488, Alexa Fluor 555, Alexa Fluor 647 and is equipped with a Photometrics Evolve 512 Delta EMCCD camera. Cells were placed in the environmental chamber (Imaging Solutions), mounted to the microscope stage, at 37ºC and 5% CO2. Imaging was performed using a heated 60 x 1.4Na oil immersion lens. On average 7-8 points were selected per condition and imaged every 2 mins for 12 hrs. Maximum intensity projections for each channel were generated using ImageJ and these projected images were cropped and copied into Adobe Illustrator. Still image figures were produced in Adobe Illustrator and calculations for mitotic timing were performed in Microsoft Excel.

2.4.4 FRAP analysis

GFP-Mps1 cells were plated in imaging dishes with coverglass windows in the bottom (Mattek corpotation) and placed in a 37ºC AND 5% CO2 environmental chamber. Cells were arrested in mitosis by the addition of MG132 and Nocodazole. FRAP analysis was performed using a spinning disc confocal system (Ultraview Vox PerkinElmer) attached to an inverted microscope (IX8 Olympus). Imaging was performed using a 60 x 1.4Na lens and the system was controlled by Volocity software. Cells were excited and bleached using the 488-laser. Excitation was carried out at 15% 488-laser power. Areas of 25x25 pixels were defined and bleached for 200 ms at 60% 488-laser power for 10 iterations. The recovery of the GFP signal was recorded every 0.2 secs. For analysis, the kinetochore intensity of the image taken before photo-bleaching was set as 100%

kinetochore signal and the signal after bleaching was normalised to this value. The kinetochore intensity was measured in ImageJ, calculations were done in Microsoft Excel and the graphs were plotted in GraphPad Prism.

2.5 Protein purifications

2.5.1 Phosphatase purification

The B55α and B56γ regulatory subunits were cloned into pCDNA5/FRT/TO-Flag vectors. Flag constructs, and an empty flag vector, were transfected into HEK-293T cells, using Mirus LT1 transfection agent. Transfected HEK-293T cells were lysed for 30 mins on ice in lysis buffer (20 mM Tris-HCl, pH 8.0, 150 mM NaCl, 1% triton X-100 and 1 x protease inhibitor cocktail). Flag tagged proteins were immunoprecipitated by incubating cleared lysate with Flag (M2)-agarose beads (Sigma) for 3 hours at 4^{o}C. Beads were then pelleted and washed with lysis buffer (TBS + 0.1% TritonX-100). Phosphatase complexes were eluted from Flag (M2)-agarose by incubating with elution buffer (20 mM Tris-HCl, 150 mM NaCl, 1 mM MnCl2 and Flag peptide 200 µg/ml (Sigma, F3290)) at room temperature for 30 mins.

2.5.2 Mps1 purification

Baculoviruses encoding 6-His-tagged WT or KD Mps1, cloned into the expression vector pACSG2 (BD technologies), were generated using the BaculoGold system (BD technologies). Recombinant WT and KD Mps1 were purified from Sf9 insect cells infected with the respective viruses. After 60hr of infection, cells were pelleted and lysed for 10min in IMAC-20 buffer (20 mM TrisCl, pH 8.0, 200 mM NaCl, and 20 mM imidazole, 0.1% Triton-x100) supplemented with a protease inhibitor cocktail (Sigma-Aldrich). Lysate was cleared by centrifuging cells for 30 mins at 100,000 xg at 4°C using an Optima-Max-XP ultracentrifuge (Beckman Coulter). His-Mps1 was pulled down by incubating cleared lysate with NiNTA beads (Qiagen). The Mps1- NiNTA beads were washed with IMAC20 and His-Mps1 was eluted from columns with 12x 1 ml IMAC200 buffer (20 mM Tris-Cl, pH 8.0, 200 mM NaCl, and 200 mM imidazole). The eluted fractions were run on an SDS PAGE gel and stained with coomassie

Instant blue (Sigma). The peak fractions were collected and dialysed overnight in PBS at 4°C.

2.5.3 Hec1 and Knl1 fragment purifications

Hec1 and Knl1 fragments were cloned into a GST-tagged expression vector pGEX-5X-1. The plasmids were transformed into JM109-pRIL cells and 4 litres of each construct was cultured in L-broth. Cultures were incubated with 0.5 mM IPTG to induce protein expression. Cells were pelleted and lysed in lysis buffer (PBS, 0.5 mg/ml lysozyme and protease inhibitors) and homogenised. Lysate was cleared, and the supernatant was incubated with glutathione-agarose beads (Life technologies) for 2 hours at 4°C. The bound GST-proteins were purified from beads by eluting with elution buffer (100 mM Tris-HCL pH 7.4, 150 mM NaCL and 15 mM reduced glutathione). The peak fractions were pooled and dialysed in PBS overnight at 4°C.

2.6 Biochemical assays

2.6.1 λ Phosphatase dephosphorylation of Mps1

KD and WT Mps1 were incubated in the absence or presence of λ phosphatase (New England Biolabs (NEB)). The reaction was carried out for 30 mins at 25°C in NEB's 1 x PMP buffer (50 mM HEPES, 100 mM $NaCl_2$, 2 mM DTT, 0.01% Brij 35 pH 7.5) supplemented with 1 mM $MnCL_2$.

2.6.2 In vitro dephosphorylation of Mps1

Reaction tubes were pre-blocked with 2 mg/ml BSA for 30 mins at RT. Recombinant phosphorylated WT Mps1 was added to the reaction buffer (Tris 50 mM pH 7.35, 0.1 mM $MnCl_2$, 1 mM $MgCl_2$, 1 mM DTT, 0.1% TX-100, 20 mM AZ3146, 150 mM NaCl and a protease inhibitor cocktail). WT-Mps1 was incubated for 1h at 37^{o}C with purified phosphatases PP2A-B55 and PP2A-B56 as well as whole cell extracts with comparable amounts of phosphatase.

2.6.3 *In vitro* binding assay

GST-tagged Hec1 and Knl1 fragments were bound to GST-agarose beads and incubated with His-WT-Mps1 in the reaction buffer (PBS and 0.2% TX-100) for 2 hrs at 4°C. Following the incubation, beads were washed 3xPBS to remove unbound proteins and boiled in SDS buffer to analyse on a coomassie gel and by western blot.

2.6.4 Immunoprecipitation experiments.

Cells were grown in 5x15cm dishes per condition. A mitotic shake-off was performed to harvest cells. Cells were pelleted at 500 xg for 5 min at 4ºC and washed 3 x PBS. Pellets were lysed in lysis buffer (Tris 20 mM, $NaCl_2$ 150 mM, PMSF 0.2 mM, 0.1%TX-100 micrococcal nuclease and a protease inhibitor cocktail (Sigma)) for 30 mins at 4ºC and then 20 mins at RT. Phosphatase inhibitors including Calyculin 100 nM and a phosphatase inhibitor cocktail (Sigma) were added when appropriate. Lysates were clarified at 14,000rpm for 15 mins at 4ºC. 4 mg of cleared lysate was incubated with 4 µg of the relevant antibody (homemade sheep anti-Mps1 or Genetex anti-Hec1) and Protein G Dynabeads (Invitrogen) for 2 hrs. Species specific controls were used to identify proteins non-specifically pulled down (i.e. a negative control). Following the incubation step, protein-beads were washed in 3 x lysis buffer and 3x wash buffer (lysis buffer without 0.1% TX-100). To run samples on western blot, SDS buffer was added to the Dynabeads and proteins were denatured for 5 mins at 95ºC. The protein complexes were eluted from Dynabeads by glycine elution and processed for mass spectrometry.

2.7 Mass spectrometry.

2.7.1 Glycine elution

After immunoprecipitation beads were washed 3 x lysis buffer (Tris 20 mM, $NaCl_2$ 150 mM, PMSF 0.2 mM and 0.1% TX-100) and 3 x wash buffer (Tris 20 mM, NaCl2 150 mM and PMSF 0.2 mM). Protein complexes were eluted from beads by 3 x 30 mins incubations in 0.1 M Glycine pH 2.6 with vigorous shaking (1500rpm). The eluted fractions were pooled and neutralised with the addition of

an equal amount of Tris pH 8.5. Urea was added to a final concentration of 2M to denature protein structure.

2.7.2 FASP

The eluates were loaded onto FASP columns, reduced with 4 mM dithiothreiotol (Fluka) for 30 mins and alkylated with 8 mM chloroacetamide for 30 mins in the dark. Proteins were digested with 1.5 mg of Trypsin (Promega) for 12 hrs at 37^{o}C.

2.7.3 Di-methyl labelling

Digested peptides were loaded onto SepPak C18 columns and then labelled with light or heavy methyl labels (Boersema et al., 2009). The heavy and light labels were alternated between experiments to ensure labelling did not influence the result.

2.7.4 Titanium Dioxide phospho-enrichment

For phospho-enrichment a titanium dioxide micro-spin column (TopTip, Glygen) was used. Labelled peptides were loaded onto columns in loading buffer (5% trifluoracetic acid, 1 M glycolic acid and 80% acetonitrile). Columns were washed with 2 x wash buffer (0.2% trifluoracetic acid and 80% acetonitrile) and once with wash buffer 2 (0.2% trifluoracetic acid). Phospho-peptides were eluted from columns using elution buffer (5% ammonia solution) into 5% formic acid.

2.7.5 Mass spectrometer processing

Peptides were run on either an Orbitrap Elite mass spectrometer or a Q-Exactive mass spectrometer (Thermo Fischer Scientific). MaxQuant was used to process the data and the processed data was analysed in Microsoft Excel. Perseus was used to generate graphs on the Mps1 interaction partners. Mass spectrometry figures were produced in Adobe Illustrator.

Table 2.1 Antibodies used during this study.

Target	Species	Supplier
Primary antibodies		
Mps1	Mouse	Millipore
Mps1 pT676	Sheep	Homemade
Mps1 pT33/S37	Invitrogen	Rabbit
CREST	Human	Millipore
Cenp-A	Mouse	Abcam
Tubulin (DM1A)	Mouse	Abcam
Actin HRP	Mouse	Abcam
Cyclin-B	Mouse	Abcam
PP1CA	Rabbit	Bethyl
PP1CB	Rabbit	Bethyl
PP1CC	Goat	Santa Cruz Biotechnology
PP2CA/B	Mouse	BD transduction laboratory
PP4C	Rabbit	Bethyl
PP5C	Rabbit	Bethyl
PP6C	Sheep	Homemade
PP2R1A/B	Goat	Santa Cruz Biotechnology
B55α	Mouse	Cell signalling
B56γ	Rabbit	Bethyl
Flag	Rabbit	Sigma-Aldrich
H3	Mouse	Abcam
Hec1	Mouse	Genetex
Hec1 pSer55	Rabbit	Genetex
Nuf2	Rabbit	Abcam
Eg5	Mouse	BD transduction laboratory
Bub1	Rabbit	Bethyl
Knl1	Sheep	Homemade
Mad1	Rabbit	Genetex
Secondary antibodies		
Donkey anti-sheep Alexa Fluor 488	Donkey	ImmunoResearch laboratories
Donkey anti-mouse Alexa Fluor 555	Donkey	ImmunoResearch laboratories
Donkey anti-human Alex Fluor 647	Donkey	ImmunoResearch laboratories
Donkey anti-mouse HRP	Donkey	Jackson laboratories
Donkey anti-rabbit HRP	Donkey	Jackson laboratories
Donkey anti-sheep HRP	Donkey	Jackson laboratories

Table 2.2 siRNA sequences for genes depleted.

Gene name	Gene ID	Accession number	Supplier	Sequence
Mps1_1 3'UTR	7272	NM_001166691	Qiagen	UUGGACUGUUA UACUCUUGAA
Mps1_2 3'UTR	7272	NM_001166691	Qiagen	GUGGAUAGCAA GUAUAUUCUA
Mps1_3 3'UTR	7272	NM_001166691	Dharmacon	CUUGAAUCCC UGUGGAAAU
Mps1 Smart pool	7272	NM_001166691	Dharmacon	GAUAGUUGAUGGAAUGCUA CGAGUUAACCUUCUAAAUA GCAAUACCUUGGAUGAUUA GAUAAGAUCAUCCGACUUU
PP2CA	5515	NM_002715	Dharmacon	GAACUUGACGAUACUCUAA GCUUGUAGCUCUUAAGGUU GGCAAGAUAUUUCUGAGAC GCAAAUCACCAGAUACAA
PP2CB	5516	NM_004156	Dharmacon	CACGAAAGCCGACAAAUA UUUAGUAGAUGGACAGAUA CCAGAACGCAUUACAAUAU GAACCAGGCUGCUAUCAUG
B55A (PPP2R 2A)	5520	NM_002717	Dharmacon	CAUACCAGGUGCAUGAAUA GUAUAGAGAUCCUACUACA GCAAGUGGCAAGCGAAAGA AGACAUAACCCUAGAAGCA
B55B (PPP2R 2B)	5521	NM_181676	Dharmacon	UCGAUUACCUGAAGAGUUU GGGUCGGGUUGUAAUAUUU GAAUGCAGCUUACUUUCUU CCACACGGGAGAAUUACUA
B55C (PPP2R 2C)	5522	NM_001206994	Dharmacon	CGGAGGAUCUUUGCCAAUG GAUACAACCUGAAGGAUGA CCAACAACCUGUACAUCUU GAAGAUUACCGAACGAGAU
B55D (PPP2R 2D)	55844	NM_001003656	Dharmacon	GUAGGUCCUUCUUCUCAGA UCGGAUAGCGCCAUCAUGA GAGACUACCUGUCGGUGAA GAGAACGACUGCAUCUUUG
B56A (PPP2R 5A)	5525	NM_006243	Dharmacon	GCUCAAAGAUGCCACUUCA CAAUACAAGUGCCGAAUAA UGAAUGAACUGGUUGAGUA GGAAAUGAAUGGCAAGCUU

B56B (PPP2R 5B)	5526	NM_006244	Dharmacon	CGCAUGAUCUCAGUGAAUA UCAAGUCGCUGUCUGUCUU CAAACCAUCGUAUCACUGA GAACAAUGAGUAUAUCCUA
B56C (PPP2R 5C)	5527	NM_178588	Dharmacon	GGAUUUGCCUUACCACUAA GGAAGAUGAACCAACGUUA CAUCAGAAUUUGUGAAGAU CAGAAGUAGUCCAUAUGUU
B56D (PPP2R 5D)	5528	NM_180977	Dharmacon	GUACAUCGACCAGAAGUUU UCCAUGGACUGAUCUAUAA UGACUGAGCCGGUAAUUGU GUAGGCAGAUCAACCACAU
PPP2R5 E	5529	NM_006246	Dharmacon	UUAAUGAACUGGUGGACUA GCACAGCUGGCAUAUUGUA GACACGCUAUCUGAUCUUA GGAUAAAGUAGACGGAUUU
PPP1CA	5499	NM_206873	Dharmacon	GCAAGAGACGCUACAACAU GAGCAGAUUCGGCGGAUCA CAUCUAUGGUUUCUACGAU GAACGACCGUGGCGUCUCU
PPP1CB	5500	NM_206877	Dharmacon	GCAAAGUUAUGGUCGAUUU GCUGAGCGAUUUCUAAUAA GUGCUUAACUGUCUAAUAU GAGAAGAGACUUAAUCCAA
PPP1CC	5501	NM_002710	Dharmacon	GCGGAGAGUUUGACAAUGC CGAAUUAUGCGACCAACUG UAGAUAAACUCAACAUCGA UGACAUCCAUGGACAAUAC
PPP4C	5531	NM_002720	Dharmacon	GCACUGAGAUCUUUGACUA GACAAUCGACCGAAAGCAA GCACUUAAGGUUCGCUAUC GGAGCCGGCUACCUAUUUG
PPP5C	5536	NM_006247	Dharmacon	GGGCGUGAGCUGUCAGUUU GACCAACCCCUAUAUAUUU UGUACGAGCUCUUUAGCGA GAUCUACGGUUUCGAGGGU
PPP6C	5537	NM_002721	Dharmacon	CUAAAUGGCCUGAUCGUAU CGCUAGACCUGGACAAGUA GUUUGGAGACCUUCACUUA CGAACGGAAUCAGGAAAUU
BubR1	701	NM_001211	Dharmacon	GCAATCAAGTCTCACAGAT
Hec1	10403	NM_006101	Dharmacon	UUGUCUCAGUA AAGUGUAAUU
Knl1	57082	144508	Dharmacon	CCACCAUUGGAACAACCAA

Table 2.3 Primers used in this study.

Primer name	Gene ID	Accession number	Sequence
Mps1 WT FWD + RV	7272	NM_001166691	GGCGGATCCCCATGGAAT CCGAGGATTTAAGTGGCAG GGCCTCGAGTCATTTTTTT CCCCTTTTTTTTTCAAAAG
Mps1 KD FWD + RV	7272	NM_001166691	ATGCTAAAGCTAATTGC TTTTGGGATTGCAAAC GTTTGCAATCCCAAAAG CAATTAGCTTTAGCAT
Mps1 T676A FWD + RV	7272	NM_001166691	ATGCAACCAGATACAG CAAGTGTTGTTAAAGAT ATCTTTAACAACACTTG CTGTATCTGGTTGCAT
Mps1 T676D FWD + RV	7272	NM_001166691	ATGCAACCAGATACA GATAGTGTTGTTAA ATCTTAACAACACTAT CTGTATCTGGTTG
Mps1 T676E FWD + RV	7272	NM_001166691	ATGCAACCAGATACAGA AAGTGTTGTTAAAGAT ATCTTTAACAAACTTC TGTATCTGGTTGCAT
Mps1 T676S FWD + RV	7272	NM_001166691	ATGCAACCAGATACATC AAGTGTTGTTAAAGAT ATCTTTAACAACACTAG TTGTATCTGGTTGCAT
Hec1 1-80 FWD + RV	10403	NM_006101	GGCTGATCATTATGAA GCGCAGTTCAGTTT GGCCTCGAGCTAGATTTTCT CAGAACTGGAAAATATAC
Hec1 1-196 FWD + RV	10403	NM_006101	GGCTGATCATTATGAA GCGCAGTTCAGTTT GGCCTCGAGCTAAGT ATGTATCTTGATGCA

Hec1 81-196 FWD + RV	10403	NM_006101	GGCTGATCATTATGAAGG ACCCGAGACCACTTAAT GGCCTCGAGCTAAGTA TGTATCTTGATGCA
Hec1 81-642 FWD + RV	10403	NM_006101	GGCTGATCATTATGAAGG ACCCGAGACCACTTAAT GGCTGATCATTATGGCCA TGAAAGAAAGCTCACC
Hec1 197-642	10403	NM_006101	GGCTGATCATTATGGCCA TGAAAGAAAGCTCACC GGCCTCGAGCTACATTCT TCAGAAGACTTAATTAGAG
Knl1 1-350	57082	144508	GGGATCCCCATGGATG GGGTGTCTTCAGAG GGCCTCGAGCTAGACTGTT CGGTTCCTTGGAATAAATAG
Knl1 350-728	57082	144508	GGCTGATCATTATGACCTG CAACAGGTAATTTTTCTG GGCCTCGAGCAGTAG ACTATATTATG

3.

THE IMPORTANCE OF MPS1 T-LOOP PHOSPHORYLATION

3.1 Introduction

During mitosis, kinetochore localised Mps1 is hyper-phosphorylated (Stucke et al., 2002; Wang et al., 2009) and these phosphorylations are expected to be key in regulating Mps1-dependent SAC signalling (Kang et al., 2007; Mattison et al., 2007; Tyler et al., 2008; Wang et al., 2009). Phospho-proteomic analysis has revealed that Mps1 phosphorylates a number of kinetochore targets (Maciejowski et al., 2017) and so far, Knl1 is the most studied Mps1 target. Once bound to kinetochores, Mps1 phosphorylates Knl1 at multiple Met-Glu-Leu-Thr (MELT) motifs (Shepperd et al., 2012; Yamagishi et al., 2012; London et al., 2012; Vleugel et al., 2013) creating binding sites for the Bub proteins (London and Biggins, 2014; Primorac et al., 2013). Phosphorylation of additional substrates initiates the hierarchal recruitment of all other SAC proteins culminating in the kinetochore-binding of the Mad1:Mad2 heterodimer and the production of C-Mad2 (Ji et al., 2017; London and Biggins, 2014; Moyle et al., 2014; Zhang et al., 2017) (see chapter 1.3). Inhibiting Mps1 by chemical genetics, with small molecule inhibitors or RNAi-dependent knockdown of Mps1 demonstrated its importance to SAC signalling (Tighe et al., 2008; Sliedrecht et al., 2010; Hewitt et al., 2010; Kwiatkowski et al., 2010; Santaguida et al., 2010; Maciejowski et al., 2010). When Mps1 is inhibited the SAC module is disassembled and all SAC proteins are lost from kinetochores. How Mps1 is switched on and off was not known but given the importance of Mps1 kinase activity to SAC signalling addressing this question was key in understanding how the SAC is controlled.

While several studies highlight a tight link between Mps1 phosphorylation status and kinase activity (Stucke et al., 2002; Kang et al., 2007; Mattison et al., 2007; Tyler et al., 2008; Wang et al., 2009), exactly how Mps1 is activated is a point of debate. In the current model, the clustering of Mps1 molecules at unattached kinetochores facilitates dimerisation and subsequently promotes trans-autophosphorylation (Kang et al., 2007) (**figure 3.1**). Mass spectrometry analysis of phosphorylated Mps1 revealed that autophosphorylation occurs at many places across the protein (Kang et al., 2007; Jelluma et al., 2008b; Dou et al., 2011; Mattison et al., 2007). Mps1 has four conserved domains including the N-

terminal extension (NTE), tetratricopeptide repeat (TPR), middle region (MR) and kinase domain. The NTE, TPR and MR domains are required for localisation, whereas the kinase domain is needed for catalytic activity (**figure 3.1A**). The kinase domain is auto-phosphorylated at two important residues, pT676 and p-T686 (**figure 3.1A-B**). The pT676 residue is located at a conserved loop in the kinase domain called the activation loop or T-loop that is important for kinase activity, whereas, p-T686 is located on the P+1 loop and is expected to play a role in catalysis (Wang et al., 2009) (**figure 3.1C**). Many serine/threonine kinases require phosphorylation of their activation loops to switch to an active configuration and thus become fully active kinases (Bayliss et al., 2012). Generally, the phosphorylated residue on the activation loop forms canonical interactions with the basic residues of three motifs the αC-helix, the β9 strand and the HRD motif (**figure 3.1D-E**). However, it is unclear how the Mps1 activation loop functions, because Mps1 lacks most of the motifs that usually coordinate the phosphorylated activation loop in other kinases (Bayliss et al., 2012). It has been postulated that basic residues in a nearby disordered loop (loop connecting αF and αEF) interacts with the activation loop of Mps1 to promote an active configuration. Indeed mutating two basic residues on this loop, K708 and K710, to alanine substantially reduces kinase activity(Wang et al., 2009). While inactive structures of the Mps1 kinase domain have provided some insight into its activation mechanism, resolution of the crystal structure of active Mps1 is needed for a more complete understanding of the specific mechanism by which T-loop phosphorylation stabilises the active kinase.

Although phosphorylation of T676 is associated with active Mps1 kinase studies on the precise contribution of T676 phosphorylation to kinase activity *in vivo* have produced conflicting results (table 3.1). So far, all studies agree that the phospho-null mutant, T676A, has reduced kinase activity in *in vitro* phosphorylation assays. *In vivo,* Kang et al., 2007, observed that cells expressing the T676A mutants did not arrest in mitosis after treatment with nocodazole, a microtubule depolymerising agent. This indicates that the checkpoint is no longer functional in T676A mutants. In contrast, Jelluma et al., 2007, found that Mps1-T676A cells arrested in mitosis at a level comparable to wild-type (WT) Mps1 cells despite

having a very similar experimental set-up. Further to this, in colony growth assays Mps1 T676A cells grew at a normal rate albeit it with a higher frequency of chromosomal abnormalities (Jelluma et al., 2008b). A third study, showed that mutation of the corresponding residue T591 to alanine in yeast, inhibited Mps1 activity *in vitro* and *in vivo* colony growth was blocked (Mattison et al., 2007). Given these conflicting reports, determining the precise contribution of T676 to Mps1 activity was a prerequisite to future experiments.

Aims:

- Optimisation of Mps1 depletion by siRNA to remove endogenous Mps1 for rescue experiments.
- Creation of the phospho-null mutant T676A and phospho-mimetic mutants T676D and T676E to compare the effect of a loss of or gain of Mps1 function.
- Rescue experiments to quantify the SAC response in the Mps1-T676A, Mps1-T676D and Mps1-T676E phospho-mutants.
- Live cell imaging of Mps1 phospho-mutants to observe phenotypic changes in chromosomal segregation and mitotic timing.

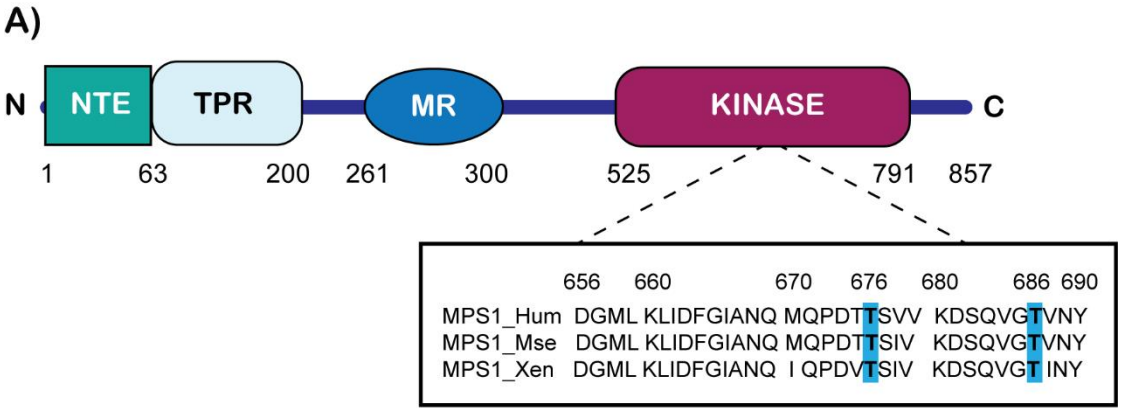
A)
N
NTE
TPR
MR
KINASE
C
1
63
200
261
300
525
791
857
656 660 670 676 680 686 690
MPS1_Hum DGML KLIDFGIANQ MQPDTTSVV KDSQVGTVNY
MPS1_Mse DGML KLIDFGIANQ MQPDTTSIV KDSQVGTVNY
MPS1_Xen DGML KLIDFGIANQ I QPDVTSIV KDSQVGT INY

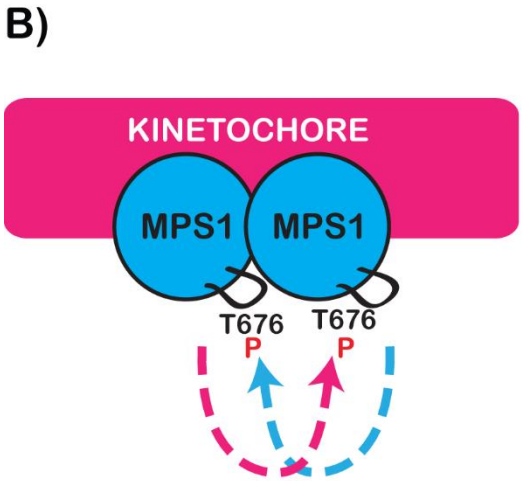
B)
KINETOCHORE
MPS1
MPS1
T676
T676
P
P

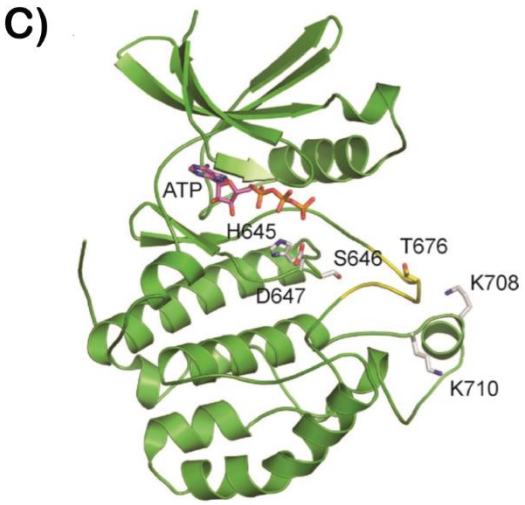
C)
ATP
H645
S646
T676
D647
K708
K710

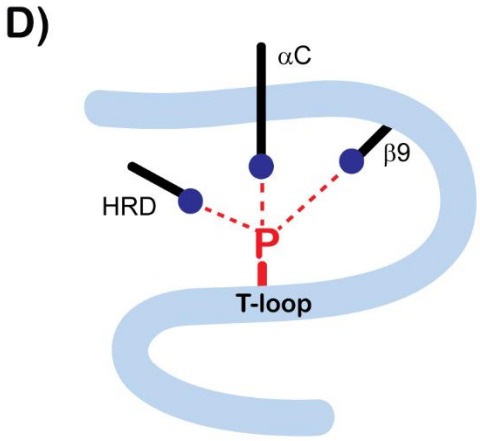
D)
αC
β9
HRD
P
T-loop

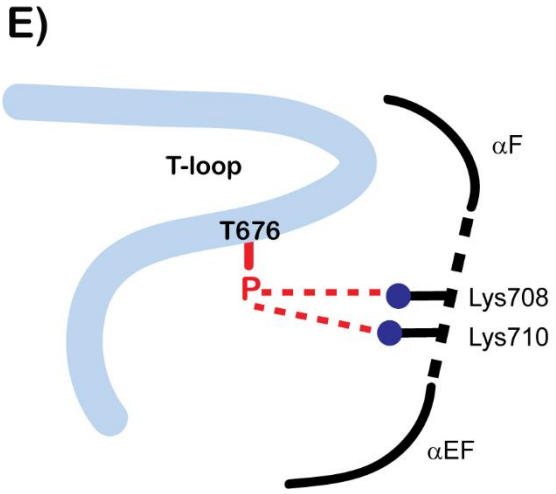
E)
T-loop
αF
T676
P
Lys708
Lys710
αEF

Figure 3.1. Autoactivation of Mps1 kinase. The auto-activation mechanism of Mps1 and the structure of its kinase domain. **(A)** Schematic representation of the domains of Mps1 including the N-terminal extension (NTE), tetratricopeptide repeat (TPR), middle region (MR) and kinase domain. **(B)** In the current model, Mps1 is recruited to kinetochores where it undergoes trans-autophosphorylation to become an active kinase. **(C)** Diagram model of the kinase domain of Mps1 in complex with ATP (taken from Kang et al., 2007). **(D)** Diagram of the canonical kinase motifs and their interaction with the phosphorylated residue on the activation loop (blue circles represent basic residues and the red dotted lines signify an electrostatic interaction with the negatively charged phosphate group labelled in red). **(E)** Diagram showing the expected model for the Mps1 activation loop; basic residues from a nearby disordered loop interact with pT676. D and E were adapted from Bayliss et al., 2012.

Table 3.1. A comparison of published studies on T676 phosphorylation.

Reference	Findings	Mutants used.	*In vitro* expts	*In vivo* expts
Jelluma et al., 2007, PlosOne (HeLa cells)	Overall, they found that T676A showed decreased activity *in vitro*, but failed to see this effect *in vivo* by mitotic index or colony growth assays.	KD, T676A, T676D, T686A	*Dephosphorylation assay:* • KD decreased activity • T676A decreased activity. • T676D still partially active • T686A decreased activity.	*Mitotic index assay:* • WT (100%) • KD reduction (~5%) • T676A no change (~90-100%) • T686A reduction (~10%) Live cell assay: • KD chromosomal abnormalities • T676A had some chromosomal abnormalities. *Colony growth assay:* • KD no growth • T676A still grow • T686A no growth
Kang et al., 2007, PNAS (HeLa cells)	Overall, they found that T676A was needed for kinase activity both *in vitro* and *in vivo*.	KD, T676A	*Dephosphorylation assay:* • Decreased activity in both KD and T676A.	*Mitotic index assay:* • Both KD and T676A show reduced mitotic indices compared to WT. *SAC assay:* • Reduced BubR1 signalling in KD and T676A compared to WT.
Mattison et al., 2007, The Journal of Biological Chemistry (HeLa cells and Yeast)	Overall, T676A mutants showed reduced kinase activity. T676D and T676E mutants were active kinases.	Human: KD, T676A, T686A Yeast: T591A, T591D, T591E	*Dephosphorylation assay* • -KD, T676A and T686A all displayed reduced kinase activity *in vitro.* • -T591A also showed reduced kinase activity.	Colony growth (yeast): • T591A shows reduced growth • T591D and T591E form colonies.

3.2 RESULTS

3.2.1 Optimisation of siRNA mediated depletion of Mps1.

Establishing an efficient and reliable method to deplete Mps1 was a prelude to any future rescue experiments on Mps1 phospho-mutants. In previous studies, involving the replacement of Mps1 with a transgene, the endogenous Mps1 was removed by different methods, using siRNA (Kang et al., 2007; Tighe et al., 2008), targeting endogenous Mps1 or alternatively by simultaneously expressing shRNA Mps1 and an RNAi insensitive Mps1 allele from their respective plasmids (Sliedrecht et al., 2010; Jelluma et al., 2008b).

Here, I used an siRNA-based approach to deplete Mps1. To this end, I tested the efficiency of three siRNA oligonucleotides (table 2.2) targeting the 3'UTR of Mps1 to specifically knock-down the expression of endogenous Mps1, but not the Mps1 transgenes to be expressed later. HeLa cells were incubated for 48 hrs with the three single siMps1 3'UTR oligonucleotides and a commercial Mps1-Smartpool (table 2.2). In the final 2 hrs of this incubation step, a proteasome inhibitor (MG132) and a microtubule depolymerising agent (nocodazole) were added to block mitotic exit and activate the SAC pathway respectively. Immunofluorescence analysis of total Mps1 showed that we had achieved a ~90% reduction in kinetochore-localised Mps1 in each condition (**figure 3.2A-B**). To exclude that this reduction was not simply due to the removal of Mps1 from kinetochores, western blot analysis of siRNA treated samples was performed. Indeed, the protein levels of Mps1 were reduced in all conditions, however, faint bands could still be observed (**figure 3.2C**). Unexpectedly, in functional SAC assays Mps1 cells depleted individually with 3'UTR siRNAs did not display a physiologically significant reduction in Mps1-dependent SAC signalling (**figure 3.2D**). HeLa cells depleted of Mps1 were treated with nocodazole to activate the checkpoint and if Mps1 had been depleted sufficiently cells should not have arrested in mitosis because the SAC has been abrogated. However, cells depleted of Mps1 using the single siRNA oligonucleotides arrested in mitosis indicating that small amounts of residual Mps1 were adequate to support a

functional SAC. The Mps1_1 oligo was the most potent of the three and blocked mitotic arrest in half of the treated cells. Although the total amount of Mps1 was reduced by 90% this remaining pool of Mps1 was sufficient for cells to mount a checkpoint response.

Next, I tested whether the siRNA protocol could be optimised to more efficiently deplete Mps1. As a starting point, the siRNA incubation was extended from 48 hrs up to 72 hrs and cells were seeded at a range of densities, but this failed to improve the depletion efficacy. Unexpectedly, treating cells with a cocktail of all three 3'UTR oligonucleotides proved to be a very effective way to further reduce the level of Mps1. Western blot analysis showed that the amount of Mps1 was reduced in these cells (**figure 3.2C**). Most importantly, in functional SAC assays most cells treated with the Mps1 siRNA cocktail did not arrest in mitosis (**figure 3.2D**) because Mps1 had been depleted below a critical threshold. I have established an effective siRNA-based protocol to knock-down Mps1 and this approach was used in all subsequent experiments.

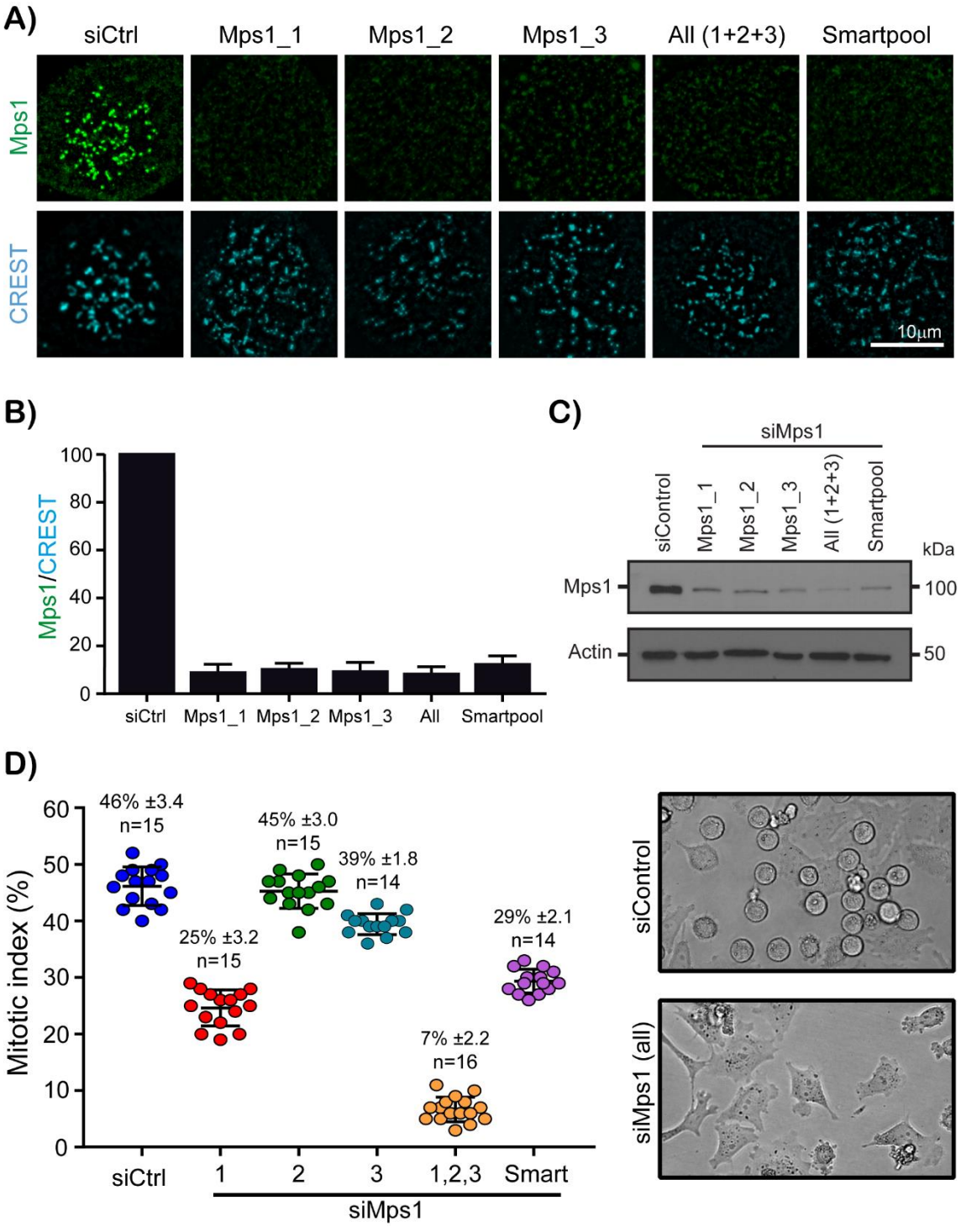
A)
siCtrl
Mps1_1
Mps1_2
Mps1_3
All (1+2+3)
Smartpool
Mps1
CREST
10µm
B)
Mps1/CREST
100
80
60
40
20
0
siCtrl
Mps1_1
Mps1_2
Mps1_3
All
Smartpool
C)
siMps1
siControl
Mps1_1
Mps1_2
Mps1_3
All (1+2+3)
Smartpool
kDa
Mps1
100
Actin
50
D)
Mitotic index (%)
60
50
40
30
20
10
0
46% ±3.4
n=15
25% ±3.2
n=15
45% ±3.0
n=15
39% ±1.8
n=14
7% ±2.2
n=16
29% ±2.1
n=14
siCtrl
1
2
3
1,2,3
Smart
siMps1
siControl
siMps1 (all)

Figure 3.2. Efficient depletion of Mps1 by siRNA using 3' UTRs. **(A)** HeLa cells were treated with control siRNA, individually with three different siRNAs targeting the 3'UTR of Mps1, a mix of all three siRNAs or a smartpool targeting different regions in Mps1. Mitotic exit was blocked by the addition of MG132 and the SAC was activated by the addition of nocodazole. Using an Mps1 antibody immunofluorescence analysis was carried out in siMps1 treated cells. **(B)** Quantification of the Mps1 kinetochore signal in (A) (n=300 kinetochores per condition) and (**C)** analysis of the protein levels of Mps1 after siRNA mediated depletion. **(D)** HeLa cells depleted of Mps1 were treated with nocodazole for 10 hours to activate the SAC and on average 5 fields of cells (n) were imaged under a tissue culture microscope. Cells were judged to be mitotic if they displayed the characteristic rounded morphology. Consistent with (C) depletion of Mps1 using a cocktail of Mps1 siRNAs targeting the 3' UTR leads to greater depletion of Mps1 and as a result fewer cells arrest in mitosis when treated with all three Mps1 siRNAs.

3.2.2 Generation of GFP-Mps1 phospho-mutants.

The role of T676 phosphorylation in modulating Mps1 activity remained a point of debate, and therefore, I generated several phospho-mutants to investigate its importance. We aimed to knockdown endogenous Mps1 by siRNA and replace it by transiently expressing GFP-Mps1 mutants. All cell lines were generated using the Flp-In TREx system (parental cells were a kind gift from S. Taylor) that allows the tetracycline-inducible expression of the inserted gene from a defined promoter (**figure 3.3**). Given that Mps1 activity is essential for cell viability it was critical that Mps1 was only replaced transiently. Another benefit of this system was that all transgenes were controlled by the same promoter, and therefore, expression levels of the individual Mps1 transgenes were comparable.

As a starting point, five GFP-Mps1 cell lines were made including wild-type (WT), kinase-dead (KD), T676A, T676D and T676E Mps1 (**figure 3.4A**). To see the consequence of not phosphorylating T676 I mutated the threonine residue to alanine by site directed mutagenesis (see Chapter 2.2) similar to previous studies (Kang et al., 2007; Mattison et al., 2007; Jelluma et al., 2008b). If phosphorylation at T676 was important for activity the phospho-null mutant T676A should show reduced kinase activity. To test the effect of constitutive phosphorylation at T676, threonine was replaced with two charged residues aspartate (T676D) and glutamate (T676E) to mimic phosphorylation. In principal, these mutations should activate the kinase domain, however, in practice these sites often play an important structural role and consequently mutants are often poor phospho-mimetics (Bayliss et al., 2012). In previous studies, T676D was reported to be a poor phospho-mimetic (Jelluma et al., 2008b), but in yeast the corresponding T591D and T591E mutants appeared to be active kinases (Mattison et al., 2007). Therefore, I created the T676E mutant to test whether it was a more appropriate phospho-mimetic in human cells. In line with previous studies, the GFP-Mps1 kinetochore signal was substantially increased in KD, T676A, T676D and T676E Mps1 mutants (**figure 3.4B-C**) (Jelluma et al., 2010; Wang et al., 2014). The kinetochore enrichment of Mps1 is a characteristic feature of inactive

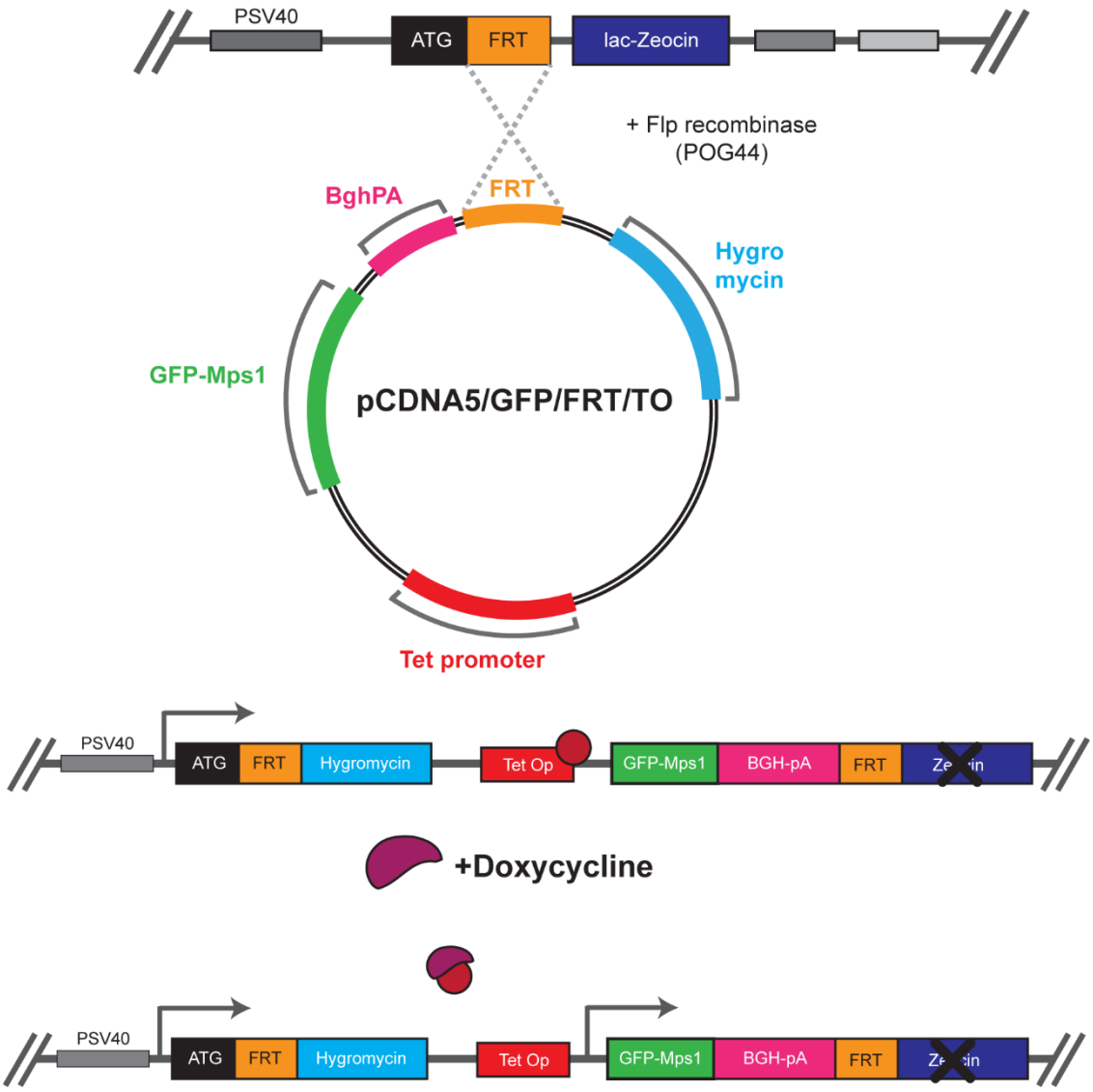

Figure 3.3. Generation of GFP-Mps1 phospho-mutants using the Flp-In TREx system. Schematic representation of the Flp-In TREx system. Different versions of GFP-Mps1 were transfected into host cell lines to generate stable cells. GFP-Mps1 expression was placed under the control of the Tet-repressor system and could be induced by adding doxycycline (purple). In uninduced cells the tet-repressor (red circle) binds to the tet-operon to prevent the expression of the GFP-tagged protein. When doxycycline is added it binds to and inhibits the tet-repressor to promote the expression of the transgene.

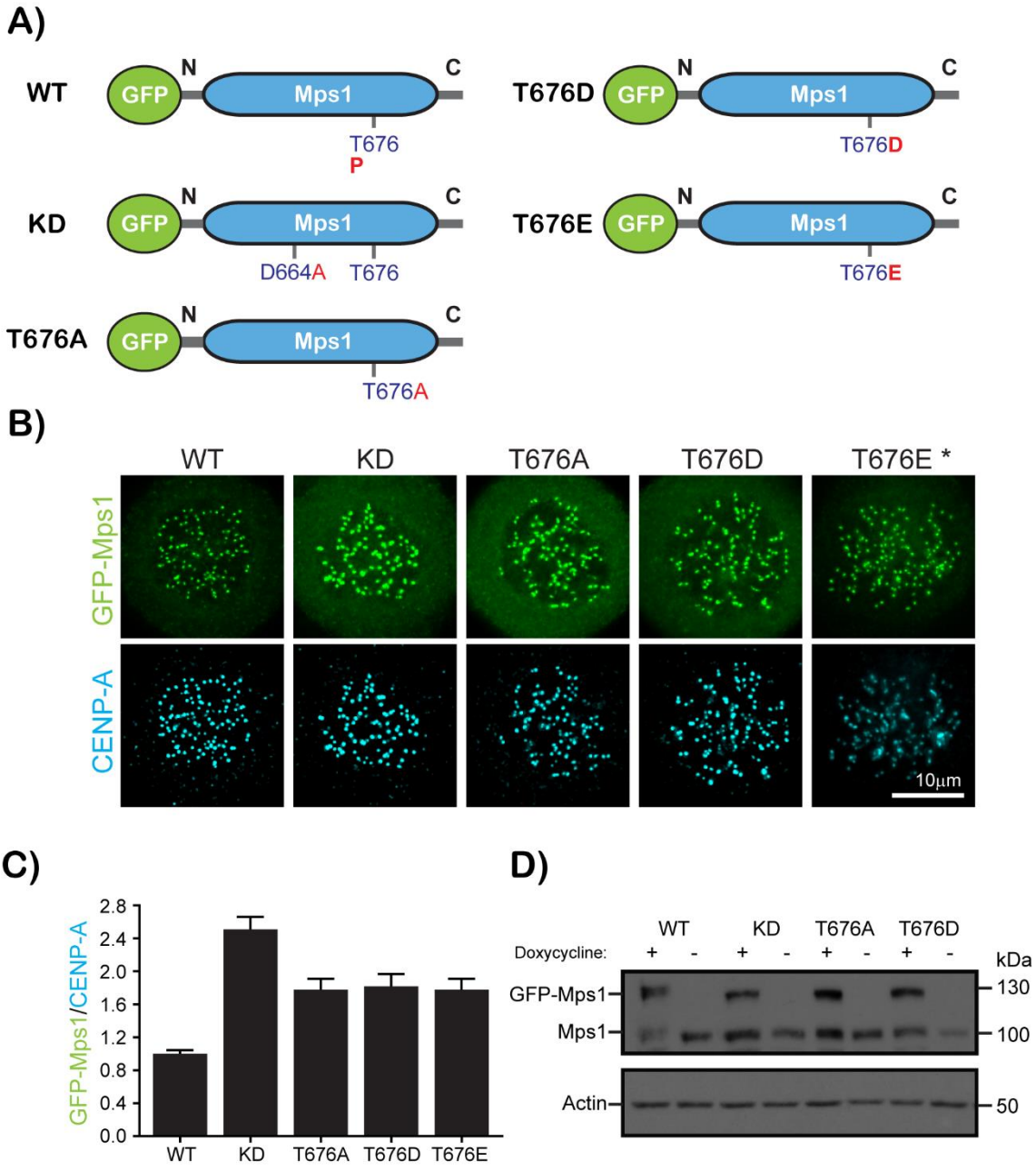

Figure 3.4. The generation of GFP-Mps1 cell lines. **(A)** Diagrams showing the structure of GFP-Mps1 phospho-mutants generated. Charged residues and phosphorylations are marked red. **(B)** Mps1 phospho-mutants were arrested in mitosis by nocodazole treatment. Immunofluorescence analysis of mitotic cells was used to quantify. The T676E* was made after these initial experiments and therefore, was analysed separately for protein expression. **(C)** the relative GFP-Mps1 kinetochore signal between different phospho-mutants. **(D)** The protein levels of endogenous Mps1 and GFP-Mps1 transgenes.

Mps1 kinase (Hewitt et al., 2010; Tighe et al., 2008; Santaguida et al., 2010; Saurin et al., 2011).

3.2.3 SAC signalling is disrupted in Mps1 phospho-mutants.

To assess the significance of T-loop phosphorylation on Mps1 kinase activity, we analysed the checkpoint in the phospho-null and phospho-mimetic mutants. Endogenous Mps1 was depleted from cells by a mix of Mps1 siRNA oligonucleotides and rescued with the relevant GFP-Mps1 variant. Next, cells were synchronised in mitosis by a thymidine-block release protocol, trapped in mitosis by the addition of MG132 and Mps1 was recruited to kinetochores by depolymerising microtubules with nocodazole (**figure 3.5A**). If an active form of Mps1 is expressed SAC proteins are sequentially recruited to unattached-kinetochores to generate the wait-anaphase signal and cells should arrest in mitosis. The kinetochore localisation of the SAC proteins BubR1 and Mad2, which are recruited by Mps1 dependent SAC-signalling, provided a read-out of how active the relevant Mps1 variants were and the level of checkpoint response achieved. As expected, immunofluorescence analysis of the SAC markers showed that GFP WT-Mps1 could recruit SAC proteins at a level comparable to untreated control cells. KD-Mps1 recruited the lowest amount of BubR1 (3%) and Mad2 (10%) confirming that the checkpoint is perturbed when Mps1 is catalytically inactivated (**figure 3.5B**). As predicted, the phospho-null mutant T676A-Mps1 had substantially reduced kinase activity compared to WT-Mps1 (BubR1 5%, Mad2 38%). Like the phospho-null mutant, the T676D-Mps1 and T676E-Mps1 mutants had significantly less BubR1 and Mad2 at kinetochores compared to cells expressing WT-Mps1. Based on this result neither the T676D-Mps1 or T676E-Mps1 work as appropriate phospho-mimetic mutant. It seems possible that the T676 residue is important structurally because mutating it to aspartate or glutamate also abrogated kinase activity. In T676 Mps1 mutants I observed a reduced recruitment of other downstream SAC proteins and this can be interpreted as these mutants having weakened kinase activity.

Whether the recruitment of this reduced pool of SAC proteins was sufficient to arrest cells in mitosis was an outstanding question, and therefore I performed a complementary functional SAC assay. When Mps1 was depleted uninduced control cells exited mitosis despite the presence of unattached kinetochores (mitotic index=2%) because Mps1 kinase was not present to induce a wait anaphase signal. Depleted cells were treated with doxycycline to express an Mps1 variant and cells were treated with nocodazole to activate the SAC and cause cells to arrest in mitosis only if the SAC is sufficiently active (**figure 3.6**).

The SAC can be fully restored by expressing GFP WT-Mps1 and cells arrest in mitosis to almost the same level as untreated control cells (mitotic index=48%). Consistent with previous results, cells expressing KD-Mps1 did not arrest in mitosis (mitotic index=5%) and this was due to a lack of BubR1 and Mad2 recruitment (Kang et al., 2007; Jelluma et al., 2008b). In agreement with Kang et al., 2007, I observed that far fewer cells expressing the T676A-Mps1 mutant arrested in mitosis (mitotic index=12%) indicating that phosphorylation at this residue was essential to SAC signalling. Both T676D-Mps1 and T676E-Mps1 cells arrested in mitosis at similar levels to the T676A-Mps1 mutants (mitotic index=13% and 10% respectively) confirming that these mutations do not activate the kinase domain of Mps1.

Together, these results indicated that the T676A-Mps1 mutant was unable to support a functional checkpoint and this was due to a reduced recruitment of SAC proteins. Moreover, functionally this reduction in the kinetochore recruitment of SAC proteins abrogates SAC signalling and consequently cells exit mitosis even in the presence of unattached kinetochores. Like other studies I struggled to produce a valid phospho-mimetic mutant as T676D-Mps1 and T676E-Mps1 mutants rescued Mps1 activity poorly. A more detailed analysis was required to see the physiological consequence of not phosphorylating T676 and so live cell microscopy was performed on these cells.

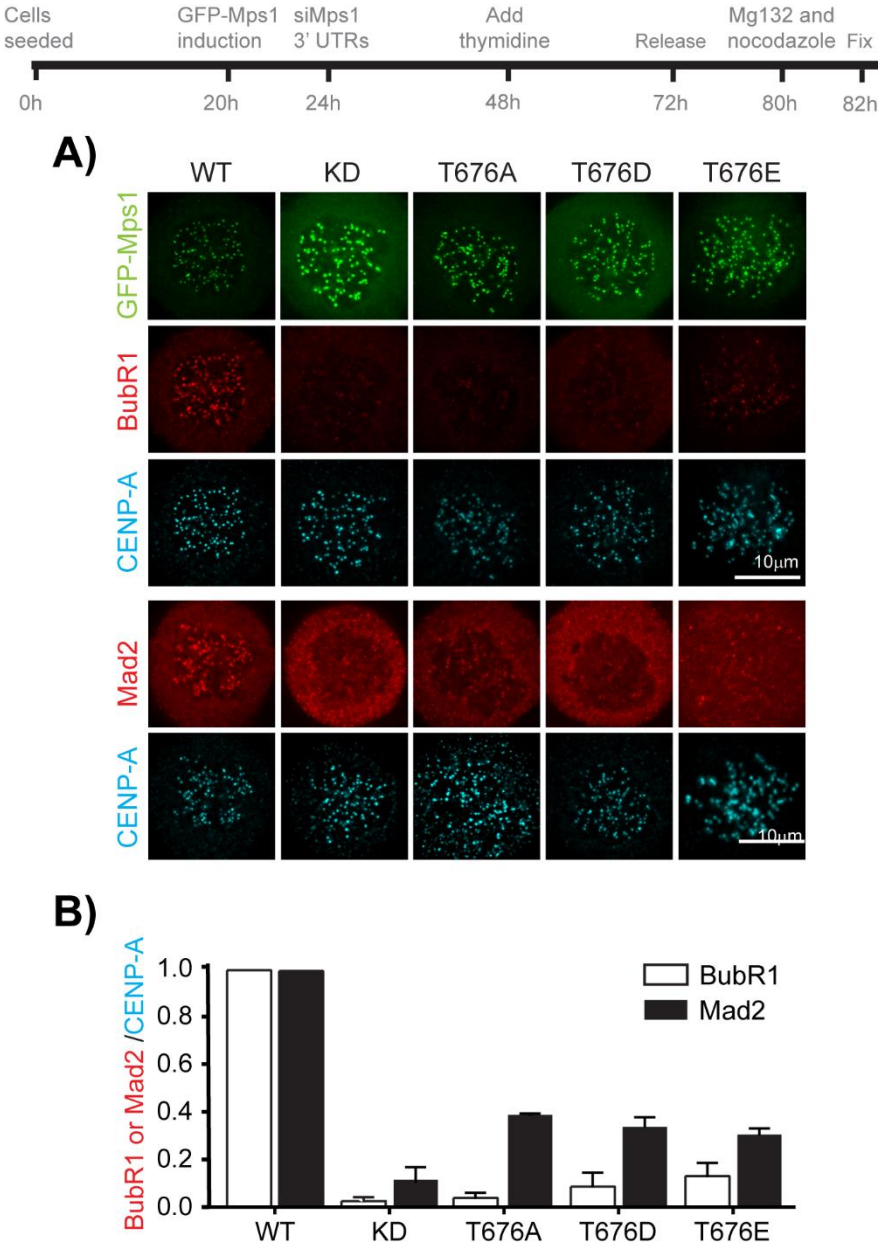

Figure 3.5. SAC proteins are not recruited to kinetochores in GFP-Mps1 phospho-mutants. (A) SAC activity assays were performed as depicted. Endogenous Mps1 was replaced with GFP-Mps1 transgenes and released into mitosis using a thymidine-block and release protocol. Mitotic exit was blocked by the addition of MG132 and the SAC was activated by nocodazole. Immunofluorescence analysis of BubR1 and Mad2 was used to measure SAC activity in the GFP-Mps1 mutants. **(B)** Quantification of BubR1 and Mad2 kinetochore signals in Mps1 mutants (n=300 kinetochores from 15 cells).

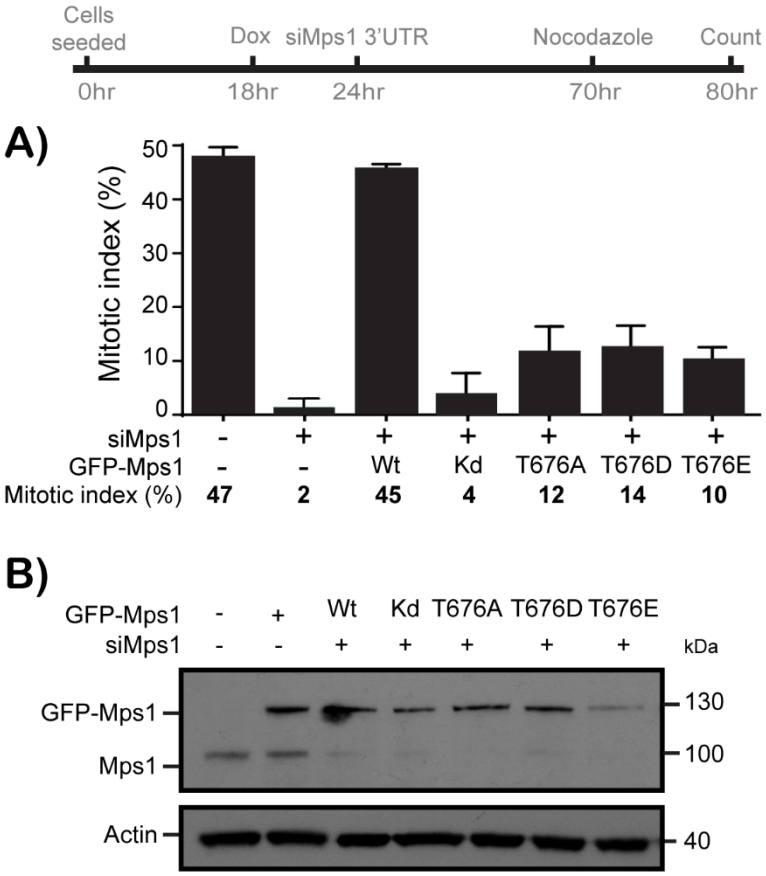

Figure 3.6. Mitotic arrest in GFP-Mps1 phospho-mutants. (A) The Mps1 rescue assay was carried out as depicted in the diagram. Endogenous Mps1 was depleted by siRNA and replaced by different versions of GFP-Mps1 via doxycycline induction. GFP-Mps1 cells were treated with nocodazole and the percentage of mitotic cells were counted in fields of cells (n=15 from 3 experiments). The results were presented as a graph. **(B)** Samples were taken for these rescue experiments and analysed to determine the levels of endogenous Mps1 and the corresponding transgene.

3.2.4 Live cell imaging of the T676A-Mps1 mutant.

Here, I showed that phosphorylation at T676 was important for Mps1 function and was critical for proper SAC signalling (**figure 3.5 and 3.6**). Next, the contribution of T676 phosphorylation in mitosis was studied in greater detail by following T676A-Mps1 cells through an unperturbed mitosis by fluorescence live cell microscopy. Endogenous Mps1 was replaced with GFP-Mps1 mutants and cells were stained with SiR-Hoechst to visualise DNA (**figure 3.7A**). In an unperturbed mitosis, the mitotic checkpoint is activated immediately after nuclear envelope disassembly and each kinetochore produces a wait anaphase signal that prevents anaphase onset. A single unattached kinetochore is sufficient to activate the checkpoint and silencing of the SAC occurs only once every kinetochore is attached to the spindle.

In GFP Mps1-WT cells, there is a rapid influx of Mps1 at NEB and as kinetochore-microtubule attachments are stabilised Mps1 is removed such that metaphase plates are devoid of Mps1 (**figure 3.7A**). Most chromosomes align 14 mins after NEB with the final chromosomes aligning at ~30 mins. Anaphase onset ensued 20-30 mins after chromosomes were aligned and on average mitosis took 57 mins on average (**figure 3.7B**). In contrast, KD-Mps1 (24 min) and T676A-Mps1 (21 min) cells exited mitosis in less than half the time of cells expressing WT-Mps1 (**figure 3.7A**). An accelerated mitosis is characteristic of perturbed SAC signalling, and consistently cells depleted of BubR1 and Mad2 exit mitosis in ~20 mins (Kops et al., 2004). Prematurely exiting mitosis does not give sufficient time for chromosomes to attach to the mitotic spindle or to correctly align. In line with this, cells rescued with KD-Mps1 or T676A-Mps1 displayed a range of striking chromosome abnormalities. Chromosome alignment was severely impaired and 90% of T676A-Mps1 cells underwent anaphase with multiple lagging chromosomes. As a result, the number of chromosomes split between daughter cells varied greatly with some cells receiving a significantly higher proportion of the total chromosomes as shown in **figure 3.7A**. Many of the daughter cells generated from mitosis in the T676A-Mps1 mutant mis-segregated their chromosomes. These defects in chromosome segregation may in part be due to

a lack of PP2A-B56 recruitment, which has a known role in regulating kinetochore-microtubule attachments, rather than solely due to mitotic timing (Foley et al., 2011). Thus, it would be interesting to follow these cells in the presence of MG132 to analyse defects in chromosome alignment when mitotic exit is no longer a factor (similar to (Jelluma et al., 2008b)). Together, the results presented here demonstrate that T676 phosphorylation on Mps1 is critical for mitotic timing and proper chromosome segregation.

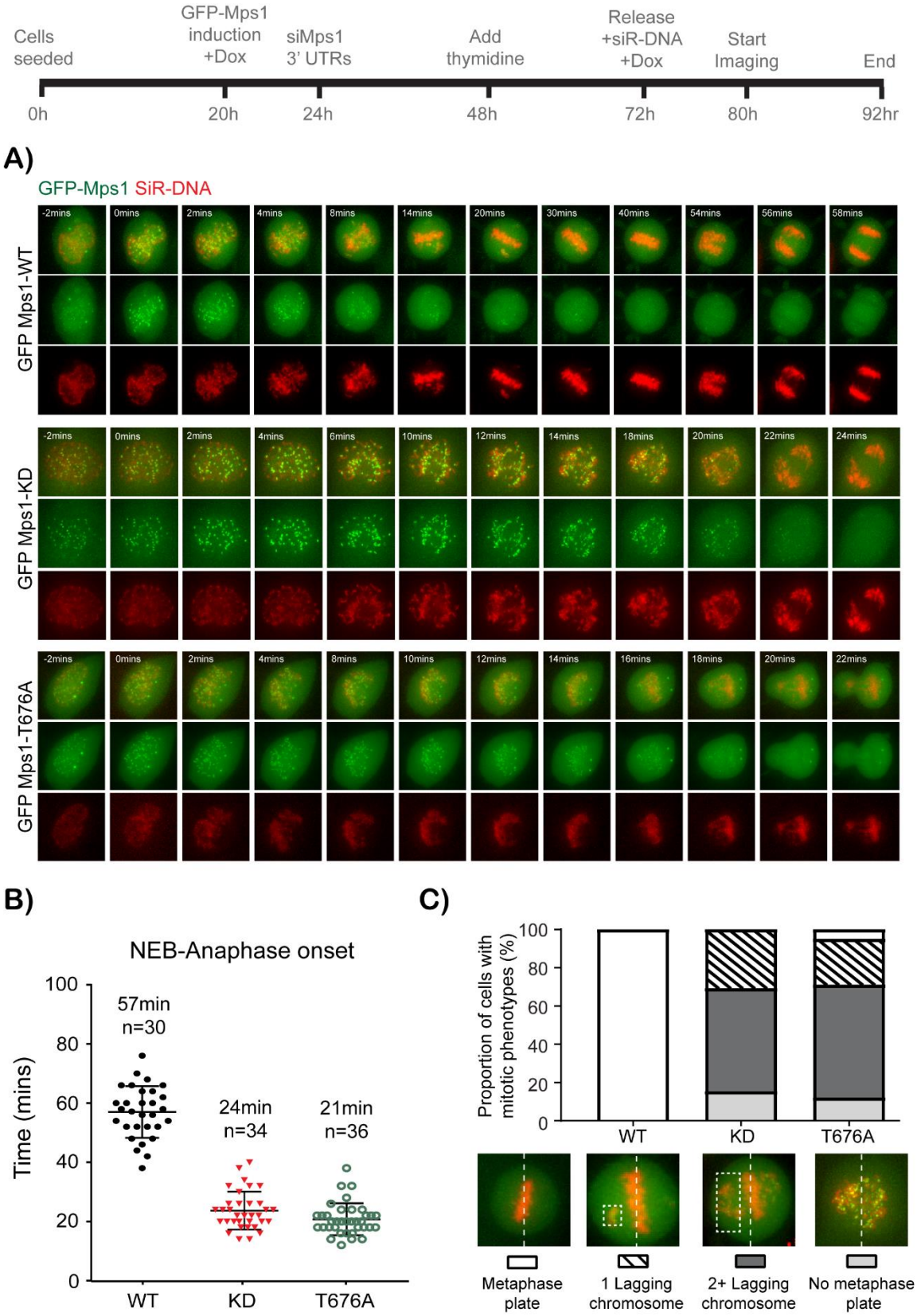
Cells seeded
GFP-Mps1 induction +Dox
siMps1 3' UTRs
Add thymidine
Release +siR-DNA +Dox
Start Imaging
End
0h
20h
24h
48h
72h
80h
92hr
A)
GFP-Mps1 SiR-DNA
GFP Mps1-WT
GFP Mps1-KD
GFP Mps1-T676A
B)
NEB-Anaphase onset
Time (mins)
57min n=30
24min n=34
21min n=36
WT
KD
T676A
C)
Proportion of cells with mitotic phenotypes (%)
WT
KD
T676A
Metaphase plate
1 Lagging chromosome
2+ Lagging chromosome
No metaphase plate

Figure 3.7. Live cell imaging of GFP-Mps1 variants. (A) Endogenous Mps1 was replaced with either WT-Mps1 or KD-Mps1 as described previously. DNA was stained with SiR-Hoechst and visualised alongside GFP-Mps1 using a live cell microscopy during mitosis. **(B)** Quantification of mitotic timing for GFP-Mps1 cells from nuclear envelope breakdown (NEB) to anaphase onset (WT n=30, KD n=34 & T676A=31). **(C)** The proportion of chromosomal abnormalities in GFP-Mps1 cells were quantified (WT n=30, KD n=34 & T676A=31). Representative images of cells with aligned metaphase plates, a single lagging chromosome, 2+ lagging chromosomes and cells lacking a metaphase plate are shown.

3.2.5 A link between Mps1 activity and localisation.

Like others (Hewitt et al., 2010; Jelluma et al., 2010), I observed that inactive versions of Mps1 displayed higher levels of Mps1 at kinetochores (**figure 3.4C**). This suggests that somehow Mps1 kinase activity negatively regulates its own localisation, however, details of this negative feedback loop remain elusive. An increase in Mps1 kinetochore localisation can indicate that more Mps1 was recruited to kinetochores or that inactive Mps1 was more stably bound and released at a slower rate. Of the SAC proteins, Mps1 is the most dynamic with the fastest turnover rate as demonstrated by FRAP analysis (Howell et al., 2004). Consistent with previous studies, inhibiting Mps1 increased its recovery to kinetochores from 4 secs to 6 secs indicating that the turnover of Mps1 was decreased. KD-Mps1, T676A-Mps1 and T676D-Mps1 had an increased half-life of 6.5 secs, 5.5 secs and 6.5 secs respectively consistent with these mutants being inactive. Intriguingly, in each condition GFP-Mps1 recovered to only 70% after photo-bleaching suggesting that there may be two pools of Mps1 a stably bound pool and a transiently bound pool. Overall, these results suggested that the exchange rate of Mps1 kinase was at least in part influenced by its kinase activity and further research is needed to dissect this negative feedback mechanism.

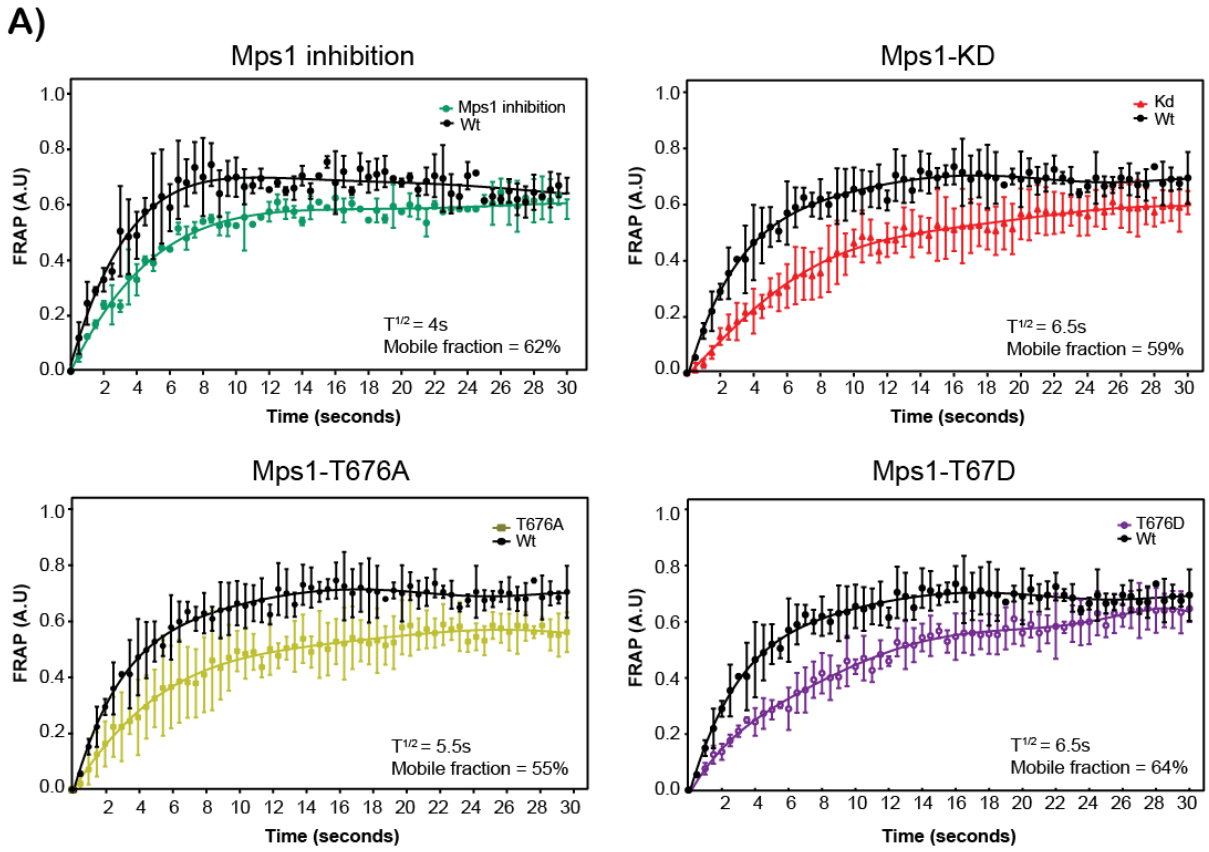
A)
Mps1 inhibition
Mps1 inhibition
Wt
FRAP (A.U)
Time (seconds)
T1/2 = 4s
Mobile fraction = 62%
Mps1-KD
Kd
Wt
T1/2 = 6.5s
Mobile fraction = 59%
Mps1-T676A
T676A
Wt
T1/2 = 5.5s
Mobile fraction = 55%
Mps1-T67D
T676D
Wt
T1/2 = 6.5s
Mobile fraction = 64%

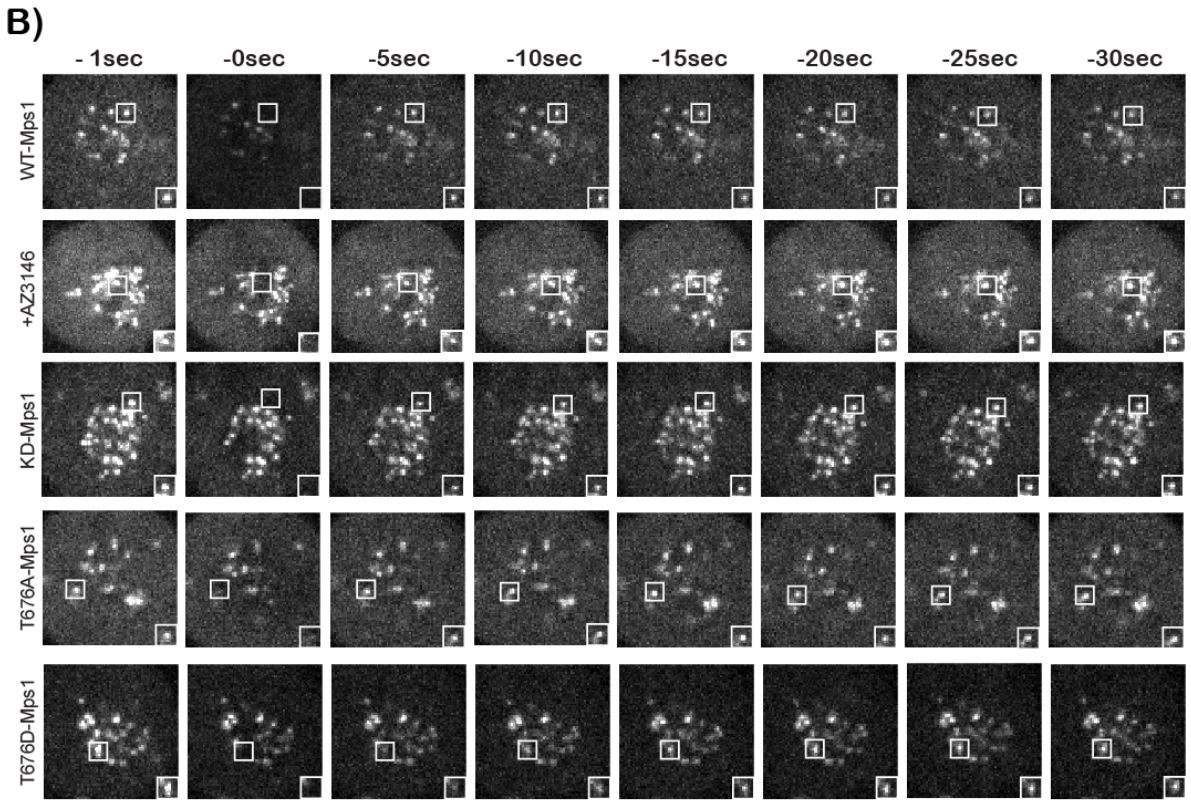
B)
- 1sec
-0sec
-5sec
-10sec
-15sec
-20sec
-25sec
-30sec
WT-Mps1
+AZ3146
KD-Mps1
T676A-Mps1
T676D-Mps1

Figure 3.8 FRAP analysis of Mps1 phospho-mutants. **(A)** GFP-Mps1 variants were photobleached at kinetochores and the recovery time was recorded and plotted (n=50 kinetochores over three separate experiments per condition). Mps1 inhibitor was added as indicated. In each case a WT-Mps1 control has been shown (black). The recovery of Mps1 after inhibitor treatment (green), KD-Mps1 (red), T676A-Mps1 (yellow) and T676D-Mps1 (purple) were analysed. **(B)** Representative still images of cells analysed by FRAP (kinetochores photobleached are indicated).

3.3 Discussion

3.3.1 Summary

Using an siRNA-based approach and the Flp-In TREx system I have established a method to effectively replace endogenous Mps1 with GFP-tagged Mps1 variants. Rescue experiments on a phospho-null mutant T676A-Mps1 demonstrated that phosphorylation at this site was critical for full kinase activity and overall SAC signalling. T676A-Mps1 mutants were unable to recruit sufficient amounts of BubR1 and Mad2 to kinetochores and thus a wait anaphase signal was not generated at kinetochores. Therefore, T676A-Mps1 cells exited mitosis prematurely and as a result some chromosomes were segregated before they were properly attached to the spindle and aligned at the equator. The daughter cells produced from cells expressing T676A were aneuploid because they had gained or lost chromosomes during mitosis. Aneuploidy is a hallmark of many cancer cells which underlines the physiological consequence of improper phosphorylation at T676.

3.3.2 Discussion

The initiation and sustained activity of Mps1 at kinetochores is a critical step in turning the SAC on and is needed to assemble a functional signalling network. The localisation of Mps1 to kinetochores is the first step in Mps1 regulation and this is directly followed by its autoactivation. Inhibiting Mps1 activity disrupts the recruitment of the entire SAC pathway and has a profound consequence on mitotic progression (Hewitt et al., 2010; Tighe et al., 2008; Maciejowski et al., 2010; Kwiatkowski et al., 2010). In this study, we aimed to understand how the activity of Mps1 is modulated during mitosis. Like other mitotic kinases Mps1 is phosphorylated at its T-loop and this was predicted to be key for its activation. However, from the limited crystal structure data, precisely how this phosphorylation stabilises an active kinase is unclear. The activation loop of Mps1 lacks most of the motifs needed to form the canonical interactions (Bayliss et al., 2012). Moreover, *in vivo* there had been conflicting results reported on the biological relevance of this phosphorylation event (Jelluma et al., 2008b; Kang et al., 2007; Mattison et al., 2007) (refer back to table 3.1).

As a prelude to future experiments investigating the regulation of Mps1 activation, the importance of phosphorylation at the T-loop of Mps1 was assessed. While optimising the siRNA-based depletion of Mps1 I identified difficulties in removing endogenous Mps1 to a physiologically significant level (**figure 3.2**). In agreement with Kang et al., 2007, I found that mutating this residue to alanine substantially reduced kinase activity to the extent that the SAC no longer halted cells in mitosis even in the presence of unattached kinetochores (**figure 3.5 & 3.6**). The most obvious explanation for discrepancies between the results reported here and by Kang et al., 2007 with those of Kops et al., 2008 is that in the latter study they failed to deplete endogenous Mps1 below a critical threshold. As a result, it is possible that low levels of residual WT Mps1 obscured the contribution of T676 phosphorylation in the study by Jelluma et al., 2008, other possibilities include differences in the expression level of Mps1 transgenes. While Mps1 mutants have low kinase activity, it is possible that overexpression of these proteins above normal levels may be sufficient to support a functional checkpoint. At the start of

this study, the efficient depletion and replacement of Mps1 posed a technical challenge and may explain why there are discrepancies between other studies. We developed a reliable method to deplete Mps1 below a critical threshold and established an effective system to express GFP-Mps1 transgenes at similar levels to endogenous Mps1.

The T676A-Mps1 mutant had significantly reduced kinase activity *in vivo* and subsequently in rescue experiments recruited much less BubR1 and Mad2 to kinetochores (**figure 3.5**). While SAC proteins were more concentrated at kinetochores in T676A-Mps1 cells compared to KD-Mps1 mutants, this was still not sufficient for cells to arrest in mitosis when kinetochores are unattached (**figure 3.6**). As reported by Kang et al., 2007, and Jelluma et al., 2008, neither the T676D nor the T676E mutant acted as a phospho-mimetic mutant as they were inactive kinases. Generation of a true phospho-mimetic mutant at T676 would provide insight into the effect of upregulated Mps1 kinase activity and may provide further insight into its function. While cancer cells usually harbour mutations inactivating SAC proteins to weaken the checkpoint, some cancers also overexpress Mps1 to increase their survival (Salvatore et al., 2007). Therefore, analysing the phenotypic consequence of a loss or gain of function Mps1 mutants may be of clinical relevance.

A more detailed analysis of the T676A-Mps1 mutant, was carried out by following these cells through an undisturbed mitosis by fluorescence live cell microscopy. Strikingly, T676A-Mps1 mutants exited mitosis rapidly (21mins) in the presence of many lagging chromosomes and often without forming a proper metaphase plate. Premature mitotic exit is characteristic of perturbed SAC signalling, and consistently cells where the SAC has been abrogated by BubR1 and Mad2 depletion exit mitosis in ~20 mins (Kops et al., 2004). In contrast, wild-type cells took more than twice as long to enter anaphase (57 mins) and in agreement with previous work even the presence of a single unattached kinetochore was sufficient to prevent mitotic exit (Rieder et al., 1994). In line with previous studies, T676A-Mps1 mutants mis-segregated chromosomes at a much higher frequency. I observed a more pronounced phenotype compared to others, with T676A cells

undergoing mitosis with multiple lagging and misaligned chromosomes concluding in a clearly uneven distribution of chromosomes between daughter cells. Whether problems in chromosome alignment are solely due to an accelerated mitosis is an intriguing question. Thus, it would be interesting to follow these cells in the presence of MG132 to analyse defects in chromosome alignment when premature anaphase onset is no longer a factor. Another possibility is that a reduction in Mps1 activity stops the kinetochores localisation of BubR1 and subsequently prevents PP2A-B56 binding (Espert et al., 2014). It is possible that chromosome alignment defects seen in T676A-Mps1 mutants are in part due to reduced kinetochore recruitment of the PP2A-B56 phosphatase. The PP2A-B56 phosphatase has a defined role in controlling K-MT attachments by dephosphorylating members of the KMN network (Foley et al., 2011). Taken together, the results presented here show that T676 phosphorylation on Mps1 is critical for mitotic timing and correct chromosome alignment. It seems likely that modulating Mps1 activity is key in switching the SAC on and off. How Mps1 is turned off during SAC silencing was unknown, and therefore, I investigated this question to further our understanding of SAC regulation.

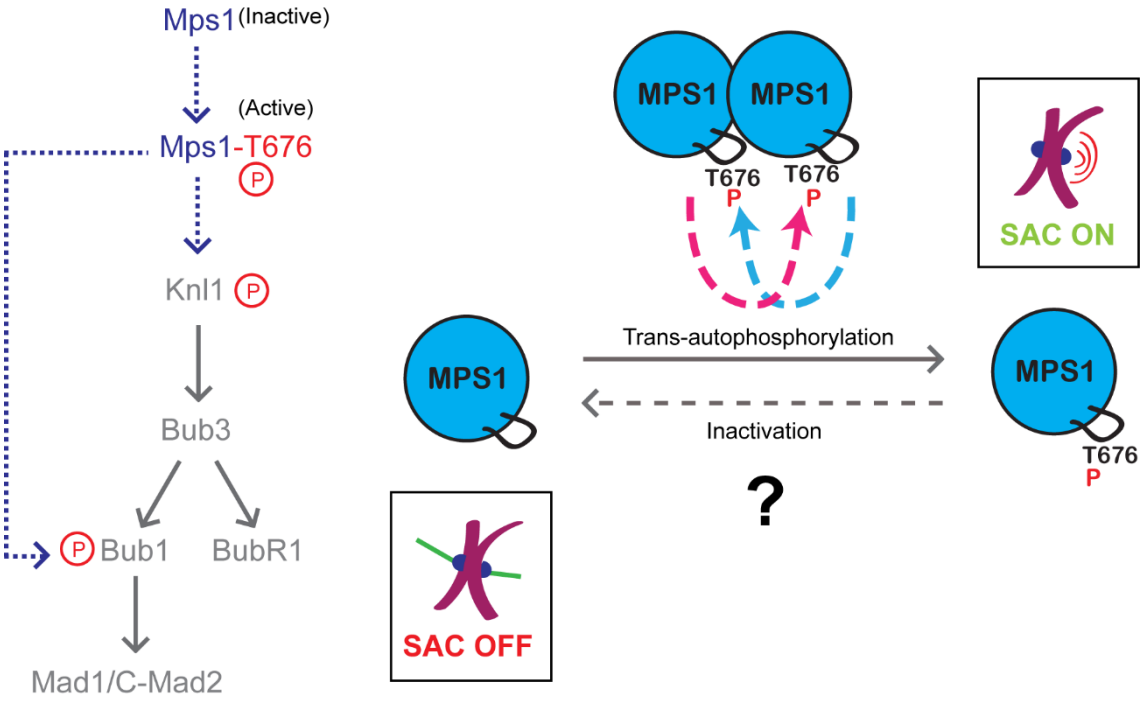

Figure 3.9. Model of Mps1 inactivation. Mps1 is activated by trans-autophosphorylation on T676 to become an active kinase. The active Mps1 is responsible for a SAC ON state because it recruits all downstream SAC proteins. We postulate that a mechanism is in place to inactivate Mps1 to turn off the checkpoint.

4.

A PP2CA-B56 PHOSPHATASE REGULATES THE ACTIVITY OF MPS1 KINASE

4.1 Introduction

The reversible phosphorylation of a variety of components at the kinetochore is a key mechanism in modulating the mitotic checkpoint. The interplay between kinase and phosphatase activity is critical in creating a complex signalling network involving multiple negative feedback loops, priming events and dynamic changes in kinetochore composition (Nijenhuis et al., 2014; Espert et al., 2014; Funabiki and Wynne, 2013). While the contribution of SAC kinases has been widely studied, less is known about their counterparts, the SAC phosphatases. The phospho-protein phosphatase (PPP) family (**figure 4.1A**), a group of serine/threonine phosphatases, have been implicated in mitosis (Picard et al., 1989; Axton et al., 1990). Of these phosphatases, the role of PP1 and PP2A holoenzymes in mitotic regulation is the best characterised. There is considerable evidence to suggest these mitotic phosphatases are involved in stabilising correct K-MT attachments and more recently modulating SAC signalling (Foley et al., 2011; Espert et al., 2014; Nijenhuis et al., 2014).

4.1.1 The role of PP1 in mitosis.

The PP1 phosphatases are highly conserved in eukaryotes and are responsible for a diverse range of functions including DNA replication, the DNA damage response and cell cycle progression (reviewed in Cuelemans and Bollen 2004). This subfamily consists of three isoforms PP1α, PP1β and PP1γ which can bind to a number of regulatory subunits (150-200 validated) to create many combinations of phosphatase holoenzymes (Bollen et al., 2010). At the kinetochore, PP1 is expected to be involved in the regulation of K-MT attachments as well as silencing the SAC. PP1 docks to the kinetochore by binding to the RVSF and SILK motifs on the N-terminus of Knl1 and this can be inhibited by Aurora B phosphorylation of these sites (Liu et al., 2010). Tethering PP1γ to kinetochores stabilised microtubule attachments and conversely PP1 docking mutants failed to form load-bearing attachments (Espeut et al., 2015). While it has been suggested that PP1 is involved in K-MT attachments, details about how it regulates the stability of K-MT attachments are yet to be determined.

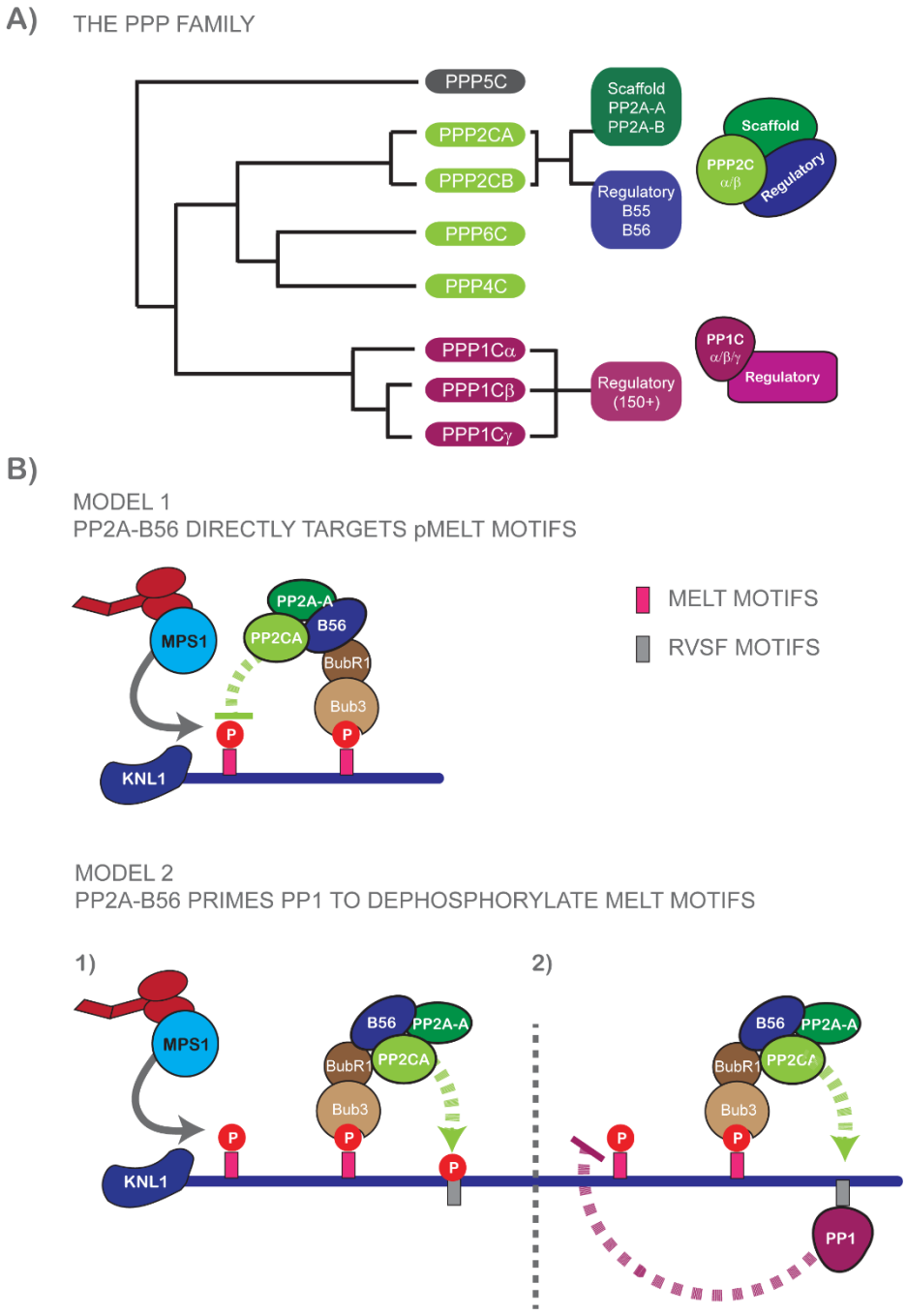

Figure 4.1. Protein phosphatases in mitosis. (A) The PPP family of phosphatases control Knl1 MELT phosphorylation. Diagram to show the subgroups in the PPP family. The PP1 and PP2 phosphatases form holoenzymes with regulatory subunits. Adapted from Barr et al., 2011. **(B)** The PP1 and PP2A-B56 phosphatase have been associated with the dephosphorylation of Knl1 MELT motifs. In one model PP2-B56 directly dephosphorylates MELT motifs Espert et al., 2014. In a second model PP2A-B56 dephosphorylates RVSF motifs for PP1 and then PP1 dephosphorylates MELT motifs Nijenhuis et al., 2014.

In budding and fission yeast, there is strong evidence to support a role for Glc7 (PP1 homologue) in SAC silencing (Meadows et al., 2011; London et al., 2012; Rosenberg et al., 2011). Genetic disruption of the PP1-Knl1 interaction provided initial evidence that PP1 is needed to release Bub proteins and is essential for cell viability in yeast (Meadows et al., 2011; Rosenberg et al., 2011). Further work revealed that PP1 turns off the checkpoint by directly targeting the Knl1 MELT motifs to release Bub1 from kinetochores (London et al., 2012). The exact contribution of PP1 in mammalian cells is unclear. In one model of SAC regulation, PP1 collaborates with PP2A-B56 to regulate K-MT attachments and SAC silencing (Nijenhuis et al., 2014). This idea relies on PP2A-B56 priming the kinetochore for PP1 binding by opposing Aurora B activity. The PP2A-B56 phosphatase removes phosphate groups from the RVSF and SILK motifs of Knl1 (**figure 4.1**). PP1 binds to non-phosphorylated RVSF and SILK motifs and catalyses the dephosphorylation of the MELT motifs on Knl1. The dephosphorylation of MELT motifs evicts SAC proteins from kinetochores and turns the checkpoint off. In human cells, PP2A-B56 directly dephosphorylates the MELT motifs on Knl1 (Espert et al., 2014). Differentiation between the contribution of PP1 and PP2A-B56 during SAC silencing is needed to better understand their individual roles.

4.1.2 The role of PP2A-B56 in mitosis.

The PP2A phosphatases have a number of roles during the cell cycle including controlling central-spindle growth (Nunes Bastos et al., 2014), mitotic exit (Cundell et al., 2013) and most importantly SAC silencing (Espert et al., 2014). PP2 phosphatases function as heterotrimeric complexes composed of a catalytic subunit PP2CA or PP2CB, a scaffolding subunit PP2A-A or PP2A-B and a regulatory subunit from the B55 or B56 subfamilies (Barr et al., 2011). The PP2A-B55 phosphatase opposes CDK1 activity to promote the onset of cytokinesis by dephosphorylating the PRC1 protein (Cundell et al., 2013). Recently, proteomic analysis identified a wider list of PP2A-B55 substrates. Importantly, PP2A-B55 does not have kinetochore targets and this is probably because it is not localised to kinetochores (Cundell et al., 2016). In addition to this, PP2A-B55 is kept

inactive by the biological inhibitor ENSA and therefore, I will focus on the B56 subunit which is more relevant at this stage of mitosis. There are five B56 isoforms (α,β,γ,δ,ε) in mammalian cells with a characteristic pseudo-HEAT repeat that can function redundantly (Barr et al., 2011). Kinetochore-localised PP2A-B56 has a recognised role in controlling K-MT attachments and silencing the SAC pathway (Foley et al., 2011; Espert et al., 2014). PP2A-B56 promotes mitotic progression by dephosphorylating several different targets including microtubule binding regulators (Foley et al., 2011), central spindle motors (Nunes Bastos et al., 2014) and SAC proteins (Espert et al., 2014).

There are two pools of PP2A-B56 in human cells, Sgo1-associated PP2A-B56 (Kitajima et al., 2006) and a BubR1-associated pool of PP2A-B56 which is critical in mitosis (Kruse et al., 2013). Generally, the B56 subunit serves two functions, 1) it interacts with other proteins to control the cellular location of the phosphatase complex and 2) it recognises substrates which are in turn dephosphorylated by the PP2A catalytic subunit. At unattached kinetochores, PP2A-B56 binds to a conserved LxxxIxE motif on the KARD domain of BubR1 (Hertz et al., 2016) and this is upregulated by Plk1 phosphorylation (Kruse et al., 2013). Disrupting the BubR1-B56 interaction, by deleting the KARD domain, disrupts the PP2A-B56 mediated regulation of K-MT attachments and the SAC pathway (Suijkerbuijk et al., 2012; Espert et al., 2014). The PP1 and the PP2A-B56 phosphatases play overlapping roles in removing Aurora B phosphorylations on the KMN network to stabilise end-on attachments (Foley et al., 2011; Foley and Kapoor, 2013; Liu et al., 2010). In human cells, depleting PP2A-B56 by siRNA reduces the stability of K-fibres and cells display numerous misaligned chromosomes consistent with defects in the formation of K-MT attachments. Interestingly, inhibition of Aurora B using the chemical inhibitor ZM447439 was sufficient to restore K-fibre stability in PP2A-B56 depleted cells (Foley et al., 2011). This data indicated that PP2A-B56 works antagonistically to Aurora B to stabilise kinetochore microtubule binding. Moreover, Aurora B-mediated phosphorylation of Knl1 and Dsn1 was increased in PP2A-B56 depleted cells (Foley et al., 2011). Taken together these observations indicate that PP2A-B56 activity is required to stabilise K-MT-

attachments and that this is associated with the dephosphorylation of Aurora B substrates.

Recent work in our group demonstrated that PP2A-B56 is the major SAC phosphatase in mammalian cells (Espert et al., 2014). Like PP1 in yeast, the mammalian PP2A-B56 phosphatase opposes Mps1 activity by catalysing the release of BubR1 from kinetochores (Espert et al., 2014). It was shown that PP2A-B56 does this by directly dephosphorylating the MELT motifs of Knl1 both *in vitro* and *in vivo.* These data indicate that in human cells a PP2A-B56 holoenzyme is responsible for regulating the release of the SAC proteins. In contrast to Nijenhuis et al., 2014, I found that the depletion of PP1 failed to rescue the BubR1 signal at kinetochores. This contradicts a role for PP1 in controlling pMELT motifs at least in human cells. Moreover, using BubR1 mutants unable to bind B56 we demonstrated that pMELT sites are controlled by a BubR1 associated pool of PP2A-B56. So far, dephosphorylation of Knl1 MELT motifs is the most studied point in SAC signalling, however, there are many other key phosphorylation events that may be controlled by SAC phosphatases. Protein phosphatases are important to regulate the activity of some mitotic kinases, for example, PP6C inactivates Aurora A by dephosphorylating its activation loop (Zeng et al., 2010). I hypothesised that a yet to be identified protein phosphatase was required to regulate the activity of Mps1 during mitosis.

Aims:

- Screen for a SAC phosphatase regulating the phosphorylation of T676 on Mps1 kinase.
- Determine how PP2A-B56 achieves substrate specificity
- Study the consequence of a lack of pT676 dephosphorylation using an engineered T676S-Mps1 mutant.

4.2 An siRNA-based screen to determine the protein phosphatase complex modulating T676 phosphorylation.

In the last chapter, I showed that phosphorylation of the T-loop of Mps1 on T676 was indeed an essential step in regulating Mps1-dependent SAC signalling. Given that SAC signalling is highly sensitive to K-MT attachments we expect that Mps1 activity is continuously turned on and off as the mitotic spindle captures chromosomes. I hypothesised that a mechanism is in place to dynamically regulate the phosphorylation status of T676, and thus, toggle Mps1 kinase on and off as microtubule attachments are tested. Since the activation of Mps1 is a phosphorylation dependent event, I reasoned that a protein phosphatase may control the reverse reaction. The most likely candidate was a member of the PPP family of phosphatases given that we and others had previously uncovered their role in SAC regulation (Espert et al., 2014; Nijenhuis et al., 2014).

4.2.1 Validation of the specificity of the pT676 antibody.

To investigate a role for a PPP family phosphatase in controlling Mps1 activity, I generated a phospho-specific antibody against T676 phosphorylation to read-out Mps1 kinase activity. Antibodies generated against total Mps1 and pT676 were tested by immunofluorescence. In agreement with previous work, Mps1 was active and kinetochore localised during prometaphase when the checkpoint was on, whereas, it was delocalised at metaphase when chromosomes have aligned and the checkpoint is turned off (Stucke et al., 2002). The kinetochore signal of both antibodies was absent in cells depleted of Mps1 (**figure 4.2A-B**) indicating that these antibodies specifically recognise Mps1. The Mps1-pT676 antibody also detected non-specific centrosome staining which remained in cells depleted of Mps1. In addition to this, both Mps1 and pT676 signals were lost after inhibition of the upstream kinase Aurora B (**figure 4.2C**). In contrast, Mps1 inhibition resulted in the loss of pT676, but a characteristic increase in the level of total Mps1 associated with the previously described negative feedback loop (see 1.3.2) (Jelluma et al., 2010; Hewitt et al., 2010). To further validate the phospho-specificity of pT676, I tested its sensitivity to phosphorylation. Phosphorylated

and unphosphorylated versions of recombinant Mps1 were incubated in the presence or absence of λ phosphatase (**figure 4.2D**). As anticipated, the pT676 antibody specifically detected phosphorylated Mps1, but not unphosphorylated forms of Mps1. Together these results indicated that the pT676 antibody was highly phospho-specific and was therefore, an accurate readout of the Mps1 T-loop phosphorylation status.

4.2.2 Mps1 T676 phosphorylation is controlled by a PPP phosphatase.

Next, I investigated the role of PPP phosphatases in regulating the pT676 phospho-site (**figure 4.3A**). To screen for a SAC phosphatase opposing Mps1 auto-activation, an assay was set up to measure Mps1 activity during checkpoint silencing. As before, doxycycline inducible GFP-Mps1 was expressed in HeLa Flp-in cells that were arrested in mitosis by an overnight treatment with nocodazole. SAC activated cells were then treated with the proteasome inhibitor MG132, to block mitotic exit, or MG132 and AZ3146 (Mps1 inhibitor). Mps1 inhibition stopped further autophosphorylation to recapitulate SAC inactivation and poised the checkpoint towards phosphatase mediated dephosphorylation (**figure 4.3B**). A short pulse (5 mins) of AZ3146 was sufficient to cause the loss of the pT676 signal and a characteristic increase in total Mps1 levels was observed. If Mps1 phosphorylation was under the control of a protein phosphatase, then inhibition of such a phosphatase would logically prevent the loss of the pT676 signal. Since, the PPP family of phosphatases had a known role in SAC signalling we investigated whether they also controlled the T-loop of Mps1. Intriguingly, treating cells with Calyculin A, a general PPP family inhibitor, for 3minutes before Mps1 inhibition prevented the loss of the pT676 signal (**figure 4.3B-C**) while the GFP-Mps1 signal was unaffected (**figure 4.3D**). When both kinase and phosphatase activity was blocked by chemical inhibitors pT676 was retained. This result indicated that a PPP family phosphatase was responsible for controlling pT676 dephosphorylation, however, the composition of the specific phosphatase holoenzyme was unknown.

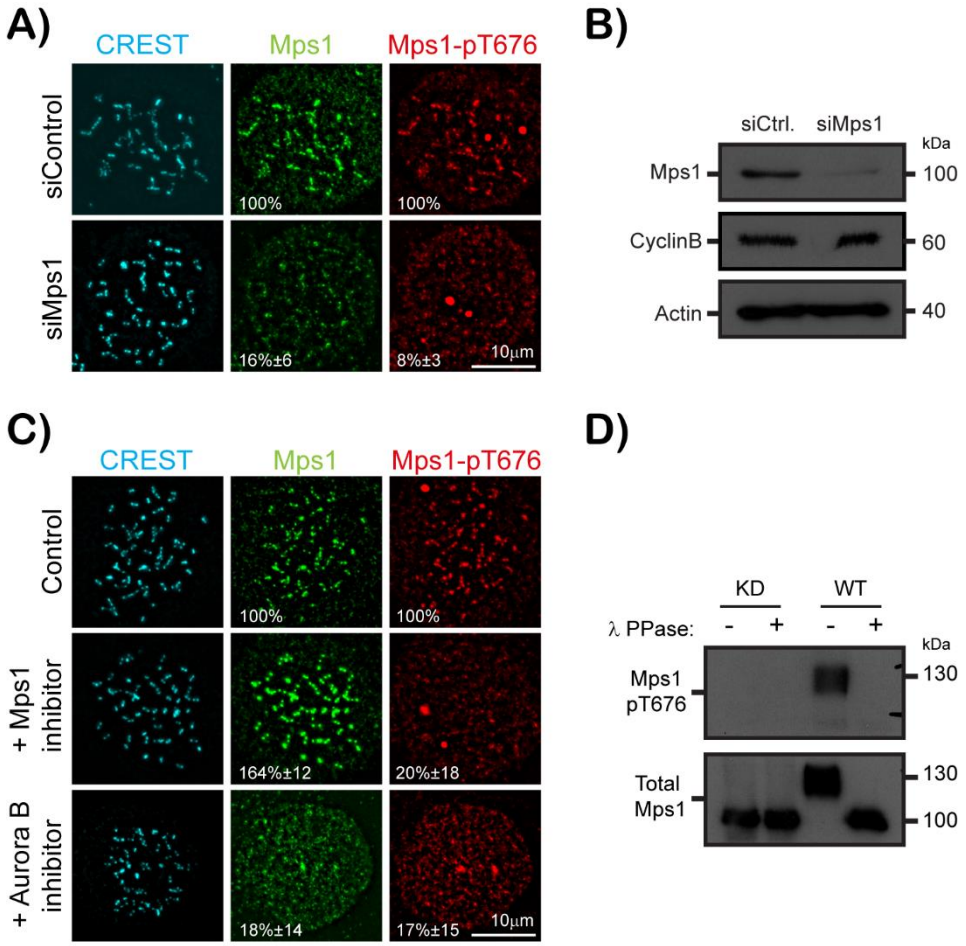

Figure 4.2. Production and validation of the Mps1 and phospho-Mps1 antibodies. (A) The specificity of antibodies generated for total Mps1 and p-T676 Mps1 was tested by analysing cells depleted of Mps1 and treated with nocodazole. **(B)** Confirmation of Mps1 depletion by western blot analysis. **(C)** As expected the kinetochore signal of the Mps1 antibody was increased after Mps1 inhibiton and lost when Aurora B was inhibited. The phospho-T676 antibody signal was lost in both cases consistent with previous work. **(D)** *In vitro* dephosphorylation of kinase dead (kd) and wild-type (wt) Mps1 demonstrated that pT676 Mps1 is phospho-specific Mps1 antibody.

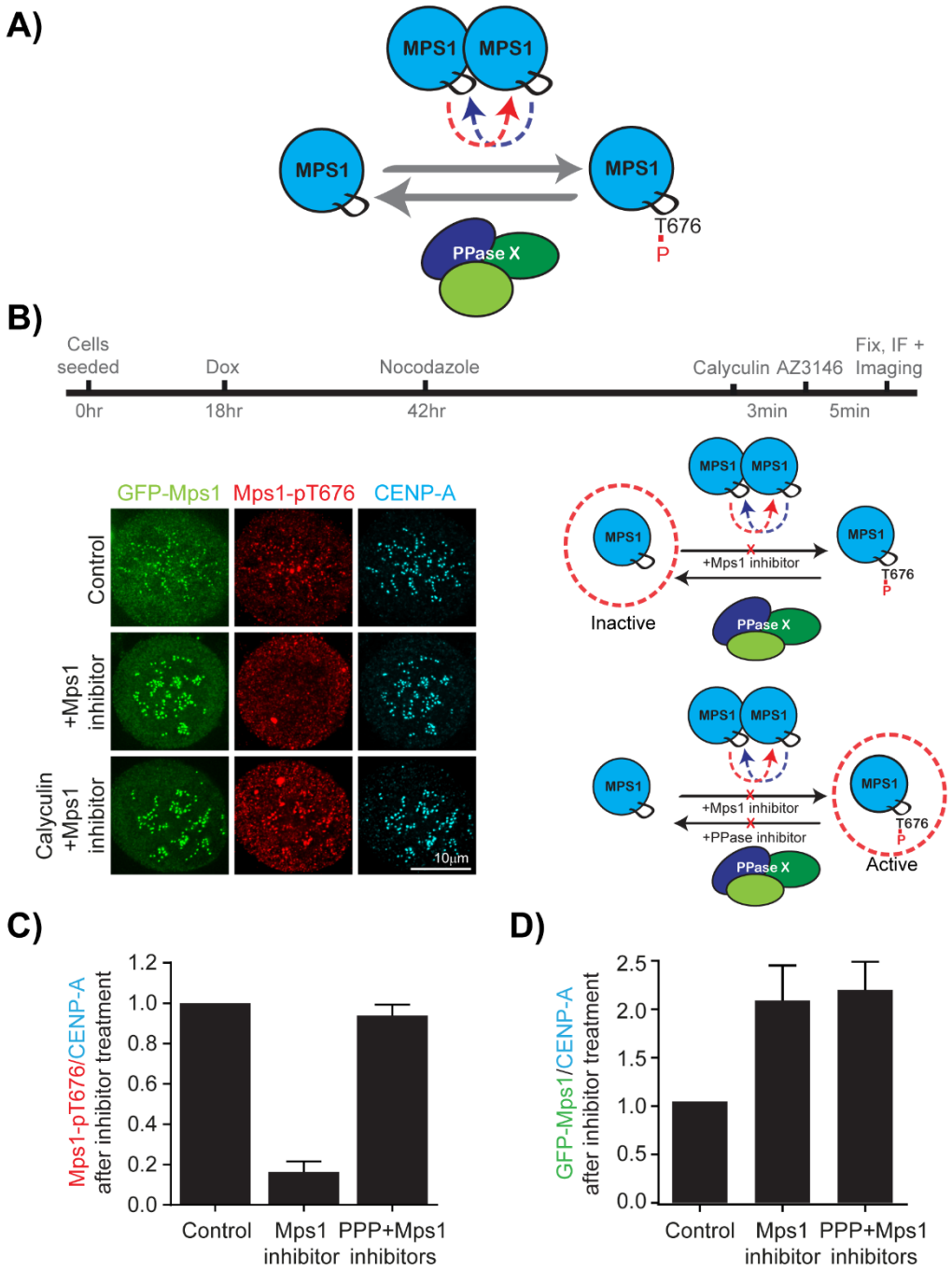

Figure 4.3. A PPP family member dephosphorylates the T-loop of Mps1. Calyculin treatment conserved pT676 kinetochore signal demonstrating that a PPP family phosphatase controls pT676. **(A)** Model to show the regulation of Mps1 phosphorylation. Mps1 kinase autophosphorylated and potentially dephosphorylated by an unknown protein phosphatase. **(B)** Mps1 inhibition causes the loss of pT676 signal, however, this can be prevented by the addition of 25nM Calyculin before Mps1 inhibitor treatment. **(C-D)** Quantification of pMps1 and total Mps1 levels in inhibitor treated cells compared to MG132 controls.

4.2.3 A PP2CA-B56 holoenzyme dephosphorylates the T-loop of Mps1.

An unbiased siRNA-based approach was used to determine the specific catalytic subunit which dephosphorylates pT676 on Mps1. GFP Mps1 cells were depleted of individual or combinations of the PPP family catalytic subunits by siRNA. To achieve high synchronisation, cells were arrested in mitosis by the addition of nocodazole, treated with either MG132 or MG132 and Mps1 inhibitor as before and analysed for the pT676 signal. Mps1 inhibition resulted in the loss of pT676 signal in control cells, however, the pT676 signal was retained in Mps1-inhibited cells depleted of PP2Cα (**figure 4.4A**). The depletion of other catalytic subunits including PP1α and γ co-depletions did not rescue the pT676 signal and so, PP2CA is the relevant catalytic subunit. A novel function has been delineated for a PP2CA-based phosphatase in opposing the trans-autophosphorylation of Mps1 kinase. Consistent with our previous work, PP1 phosphatases did not influence the phosphorylation status of this phospho-site (Espert et al., 2014).

PP2 phosphatases function as heterotrimeric complexes consisting of a catalytic, scaffolding and regulatory subunit. The PP2CA phosphatase had been shown to be the necessary catalytic subunit, however, the identity of the scaffolding and regulatory subunits was yet to be determined. There are two forms of the scaffolding subunit, PP2A-A and PP2A-B, of which PP2A-A is predominant, while the two regulatory subunit families, B55 and B56, have four (α,β,γ,δ) and five (α,β,γ,δ,ε) members respectively (Barr et al., 2011). Given that B56 is kinetochore localised and had previously been shown to dephosphorylate pMELT motifs, it was the most obvious candidate (Foley et al., 2011; Espert et al., 2014). Moreover, at this stage of mitosis the B55 subunit is kept inactive by the biological inhibitor ENSA (Gharbi-Ayachi et al., 2010; Mochida et al., 2010). Indeed, when cells were depleted of all subunits of the B56 family the pT676 signal was retained after Mps1 inhibition, whereas pT676 is lost when all B55 subunits are knocked-down (f**igure 4.5A-E**). So far, it was shown that a holoenzyme consisting of the PP2A catalytic subunit, the B56 regulatory subunit and a scaffolding subunit, most likely PP2A-A, was required to dephosphorylate the T-loop of Mps1.

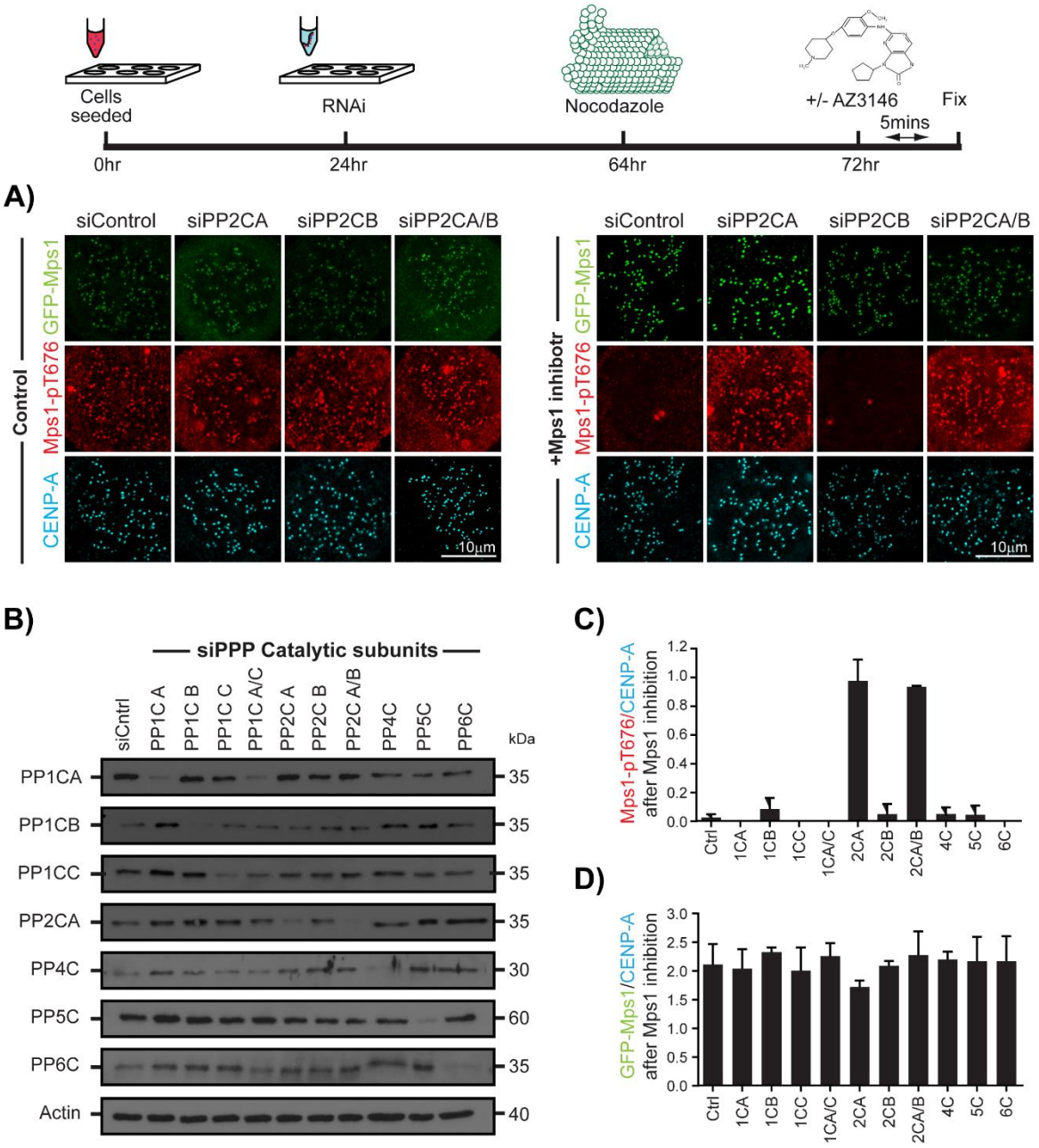

Figure 4.4. A PP2CA-specific protein phosphatase controls pT676 phosphorylation. (A) Cells were depleted of the different PPP catalytic subunits, treated with Mps1 inhibitor and stained for pMps1. Depletion of PP2CA was sufficient to restore pT676 signal despite Mps1 inhibition indicating that a PP2CA based phosphatase complex is important in dephosphorylating the activation loop of Mps1. **(B)** The PPP catalytic subunits were efficiently depleted as demonstrated by western blot analysis. **(C-D)** Quantification of GFP-Mps1 and pMps1 kinetochore levels in inhibitor treated cells compared to MG132 controls.

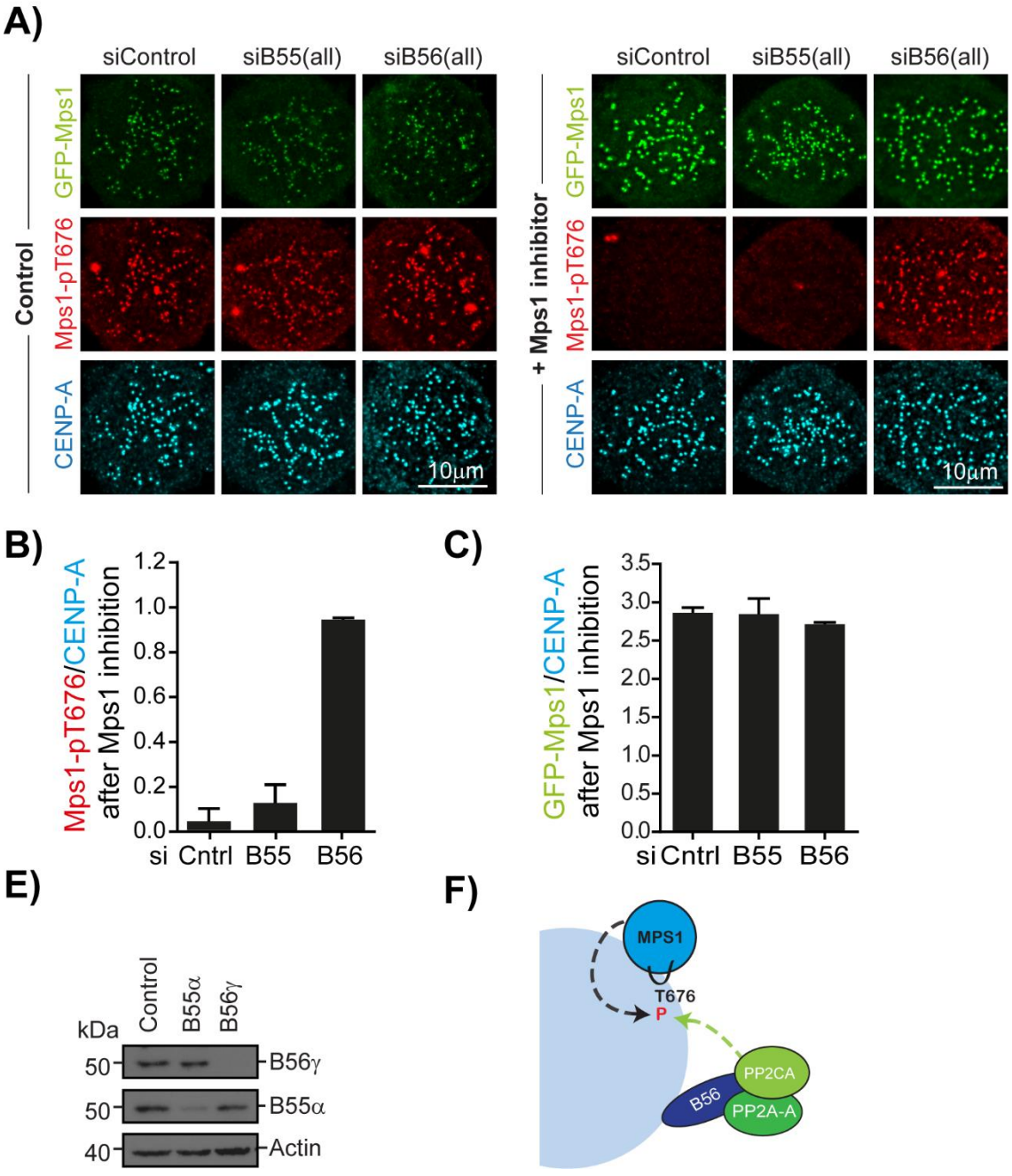

Figure 4.5. The B56 regulatory subunit is the key regulatory subunit. (A) Depletion of the B56 subunit, but not the B55 subunits, maintains pT676 signal in cells where Mps1 is inhibited because it is the necessary regulatory subunit. **(B-C)** Quantification of pMps1 and total Mps1 levels at kinetochores in inhibitor treated cells compared to controls. **(E)** B56 is efficiently depleted after siRNA. **(F)** A PP2CA-B56 phosphatase complex dephosphorylates the activation loop of Mps1.

4.2.4 PP2A phosphatases directly dephosphorylate Mps1 *in vitro*

To test biochemically whether the T-loop of Mps1 was indeed a direct substrate of PP2CA phosphatases, an *in vitro* dephosphorylation assay using purified PP2CA-B55α and PP2CA-B56γ holoenzymes was carried out. Phosphorylated recombinant Mps1 was purified from insect cells treated for 1 hour with Calyculin A to prevent Mps1 dephosphorylation. Flag tagged versions of the B55α and B56γ regulatory subunits were transiently expressed in HEK-293T cells and the heterotrimeric phosphatase complexes were isolated by anti-Flag immunoprecipitation. Analysis of the elution fractions by coomassie blue staining and western blotting confirmed the efficient purification of phosphatase holoenzymes (**Figure 4.6A-B**). Having successfully purified the PP2CA-B55α and PP2CA-B56γ holoenzymes, an assay was set up to dephosphorylate recombinant Mps1 *in vitro*.

Phosphorylated recombinant Mps1 was treated with AZ3146 to block further autophosphorylation. Increasing, but comparable, amounts of PP2CA-B55α, PP2CA-B56γ and mitotic cell extract were incubated with purified phosphorylated Mps1 (**Figure 4.6C**). Unexpectedly, both purified PP2CA-B55α and PP2CA-B56γ had the same level of activity as phosphatases present in the mitotic cell extract. This result confirmed that Mps1-pT676 was indeed a substrate for PP2CA phosphatases, however, it was intriguing that there was no clear difference between PP2CA-B56γ and PP2CA-B55α phosphatase activities. For some substrates the regulatory subunit is crucial for substrate recognition, for example the B55 subunit largely contributes to PRC1 (Cundell et al., 2013) and Tau recognition (Xu et al., 2008b). A more in-depth analysis of the kinetics of Mps1 dephosphorylation by B55 and B56 phosphatases may highlight differences in their ability to catalyse this reaction. In addition to substrate recognition, the B56 regulatory subunit also provides specificity by controlling the cellular location of the PP2A catalytic subunit.

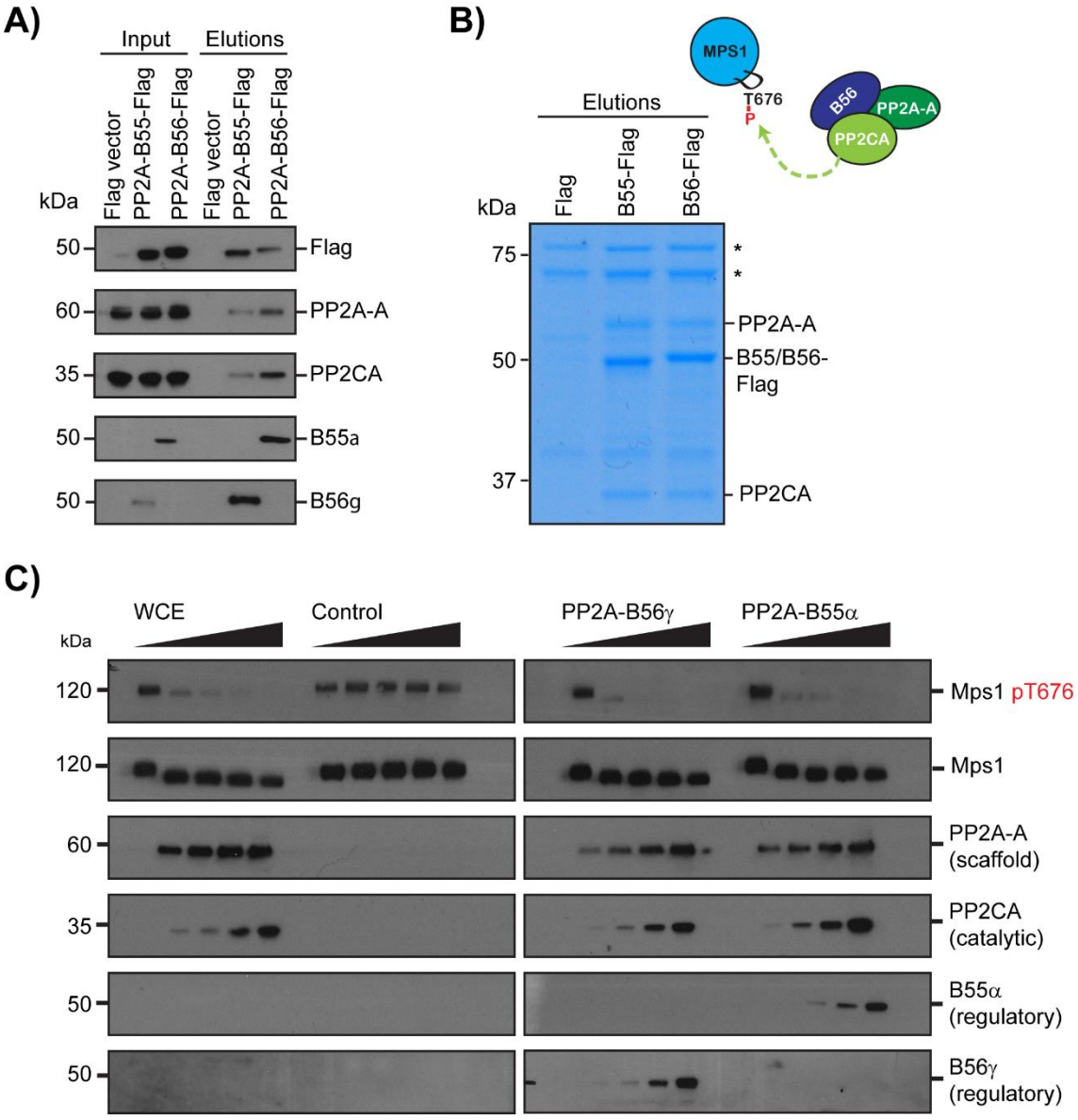

Figure 4.6. *In vitro* dephosphorylation of Mps1. (A) PP2CA-B56 and PP2A-B55 phosphatases were Flag-tagged and purified from HEK293T cells. **(B)** Coomassie analysis demonstrates that purifications contain few impurities. Asterisks denote non-specific bands. **(C)** *In vitro* dephosphorylation of Mps1 with increasing concentrations of PP2CA-B56 and PP2A-B55 phosphatases 0nM, 2.0nM, 4.0nM, 6.0nM and 8.0nM. Whole cell extract (WCE) was added so that there was an equal amount of PP2CA as judged by western blot analysis. Flag-control was added at an equal volume to the purified phosphatases. An hour incubation with the PP2A-B55 and PP2A-B56 phosphatases at 30^{o}C is sufficient to dephosphorylate Mps1 completely.

In mammalian cells, there are two distinct pools of PP2A-B56: a centromere-associated pool bound to Sgo1 and a kinetochore-localised fraction bound to BubR1. The Sgo1-PP2A-B56 pool protects the cohesin complex from premature disassociation, whereas BubR1-PP2A-B56 catalyses the dephosphorylation of pMELT motifs on Knl1 and the dephosphorylation of other members of the KMN network (Foley et al., 2011; Espert et al., 2014). Since BubR1 associated PP2A-B56 had a known function in SAC signalling it seemed highly likely that this pool also controlled the dephosphorylation of T676 on Mps1. To dock to BubR1 the B56 subunit binds a conserved phosphorylated sequence LxxxIxE on the KARD domain (Kruse et al., 2013; Hertz et al., 2016). Mutating the leucine and isoleucine residues of this motif to alanine disrupts the interaction between B56 and BubR1 (Kruse et al., 2013). Therefore, BubR1 was replaced with the B56 binding mutant BubR1$^{L699A/I672A}$ and the pT676 signal was analysed. As expected, the pT676 signal was retained in the BubR1 mutant due to decreased B56 binding and phosphatase activity.

Here, a novel function has been revealed for a BubR1-associated PP2A-B56 phosphatase in controlling Mps1-dependent SAC signalling. PP2A-B56 opposes Mps1 activity in a two-step process. Firstly, PP2A-B56 inactivates Mps1 kinase by dephosphorylating its T-loop, preventing further recruitment of downstream SAC proteins, and secondly PP2A-B56 removes phosphorylations on Knl1 to drive the release of SAC proteins present at the kinetochore. PP2A-B56 regulates both kinetochore-microtubule attachment and SAC inactivation by opposing the activity of Aurora B and Mps1 respectively; thus this phosphatase may provide a link between sensing microtubule attachments and turning off the SAC signal.

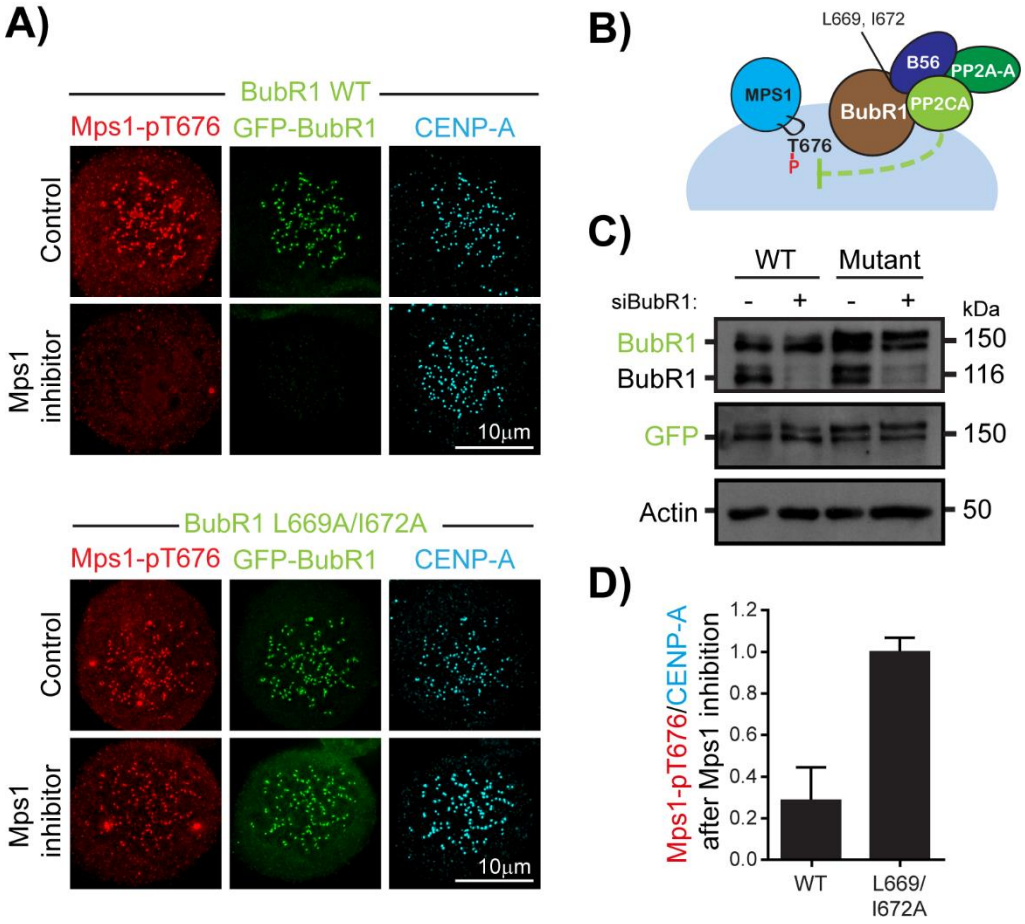

Figure 4.7. A BubR1 bound PP2A-B56 phosphatase controls Mps1 dephosphorylation. (A) Expressing a mutant BubR1, incapable of binding PP2CA-B56 (L669A/I672A) conserved the pMps1 signal after Mps1 inhibition. **(B)** Model showing L669 and I672 mutations in BubR1 that disrupt B56 binding to the kinetochore. **(C)** Western blot analysis of replacement of endogenous BubR1 with mutant BubR1 and **(D)** quantification of pT676 signal. Replacing BubR1 with the L669A/I672A BubR1 mutant preserved the pT676 signal in Mps1 inhibited cells. This demonstrated that a BubR1 associated pool of PP2CA-B56 regulates the dephosphorylation of T676 on Mps1. Quantification of pMps1 and levels in Mps1 inhibitor-treated cells compared to controls.

4.2.5 Analysis of the Mps1 T676S mutant.

Previous work in our lab analysed the mitotic phenotype of cells expressing the B56 binding mutant BubR1$^{L699A/I672A}$. This mutant was generated to understand the consequence of not having B56 dependent phospho-regulation of the SAC (Espert et al., 2014). The BubR1$^{L699A/I672A}$ mutant clearly demonstrated that removal of B56 from kinetochores prevents SAC silencing and consequently cells take much longer to exit mitosis. In addition to SAC silencing, a decrease in PP2A-B56 activity also disrupts K-MT attachments to hyperactivate the SAC (Foley et al., 2011). Here it has been shown that PP2A-B56 modulates the SAC by controlling the phosphorylation of at least two substrates: the MELT motifs of Knl1 (Espert et al., 2014) and T676 on Mps1 (shown in this study). While this mutant shows the physiological consequence of losing all PP2A-B56 activity at kinetochores, the specific contribution of T676 dephosphorylation to this phenotype was unclear. To uncouple the impact of perturbed T676 phosphorylation I aimed to analyse a hyperphosphorylated T676 Mps1 mutant. As described previously (chapter 3), mutating threonine to aspartate or glutamate had yielded poor phospho-mimetic mutants, and therefore I designed a novel mutant to answer this question. Given that some cancers overexpress Mps1, studying a mutant with constitutive Mps1 activity may provide insight into how increased kinase activity helps tumour cells to survive.

We generated a novel Mps1 mutant, Mps1-T676S, to precisely investigate the consequence of blocking T-loop dephosphorylation. This mutant was designed on two assumptions, firstly, the serine residue would be autophosphorylated as normal and secondly, that phosphoserine would not be dephosphorylated by PP2A-B56 because of phospho-amino acid specificity. Given that serine differs from threonine by a single methyl group, it is unsurprising, that threonine to serine substitutions are well tolerated. Threonine to serine mutations in other studies have yielded active proteins (Bondoc et al., 2017; Lück-Vielmetter et al., 1990). Recently, proteomic analysis demonstrated that PP2A-B55 phosphatases are selective for phosphothreonine over phosphoserine (Cundell et al., 2016). Mutating residues from threonine to serine on PRC1 and TPX2 dramatically

reduced the rate of PP2A-B55 dephosphorylation. I hypothesised that the B56 subunit may also show a strong preference for phosphothreonine versus phosphoserine. Based on these ideas I created the T676S mutant which we predicted would be trans-autophosphorylated as normal, but not dephosphorylated by PP2A-B56. If this mutant behaved as expected, Mps1 should be constitutively active and therefore, T676S cells should spend longer in mitosis.

As before, SAC activity assays were performed on cells expressing GFP T676S-Mps1. Initial results were promising; the T676S-Mps1 mutant recruited BubR1 and Mad2 at levels comparable to WT-Mps1 indicating that it is indeed an active kinase (**figure 4.8B**). Furthermore, cells were sensitive to nocodazole treatment and arrested in mitosis at identical levels to WT cells (**figure 4.8C**). Lastly, GFP T676S-Mps1 cells were synchronised by a thymidine block and release protocol and recorded during an unperturbed mitosis (**figure 4.9A**). Cells expressing GFP T676S-Mps1 spent no longer in mitosis than WT-Mps1 cells (**figure 4.9B**) and were phenotypically normal (**figure 4.9C**). Taken together, these results indicate that the T676S-Mps1 mutant, while an active kinase, does not act like a true phospho-mimetic mutant as kinase activity was not elevated. The most likely explanation is that the serine residue, like threonine, is both trans-autophosphorylated and dephosphorylated by PP2A-B56. Like others, we failed to generate a true phospho-mimetic mutant at T676. In future work, a different strategy could be employed, for example, modifying the stretch of amino acids neighbouring T676, that make up the PP2A-B56 consensus motif, so that this site is no longer recognised. Usually a second approach would be to stop dephosphorylation by blocking PP2A-B56, however, PP2A-B56 controls multiple kinetochore targets. Thus, it would be difficult to uncouple the phenotypic effects of T676 dephosphorylation from that of the KMN network. Due to the technical limitations and the presence of multiple PP2A-B56 targets, there are few options available beyond phosphomimetic mutants to study constitutively active Mps1.

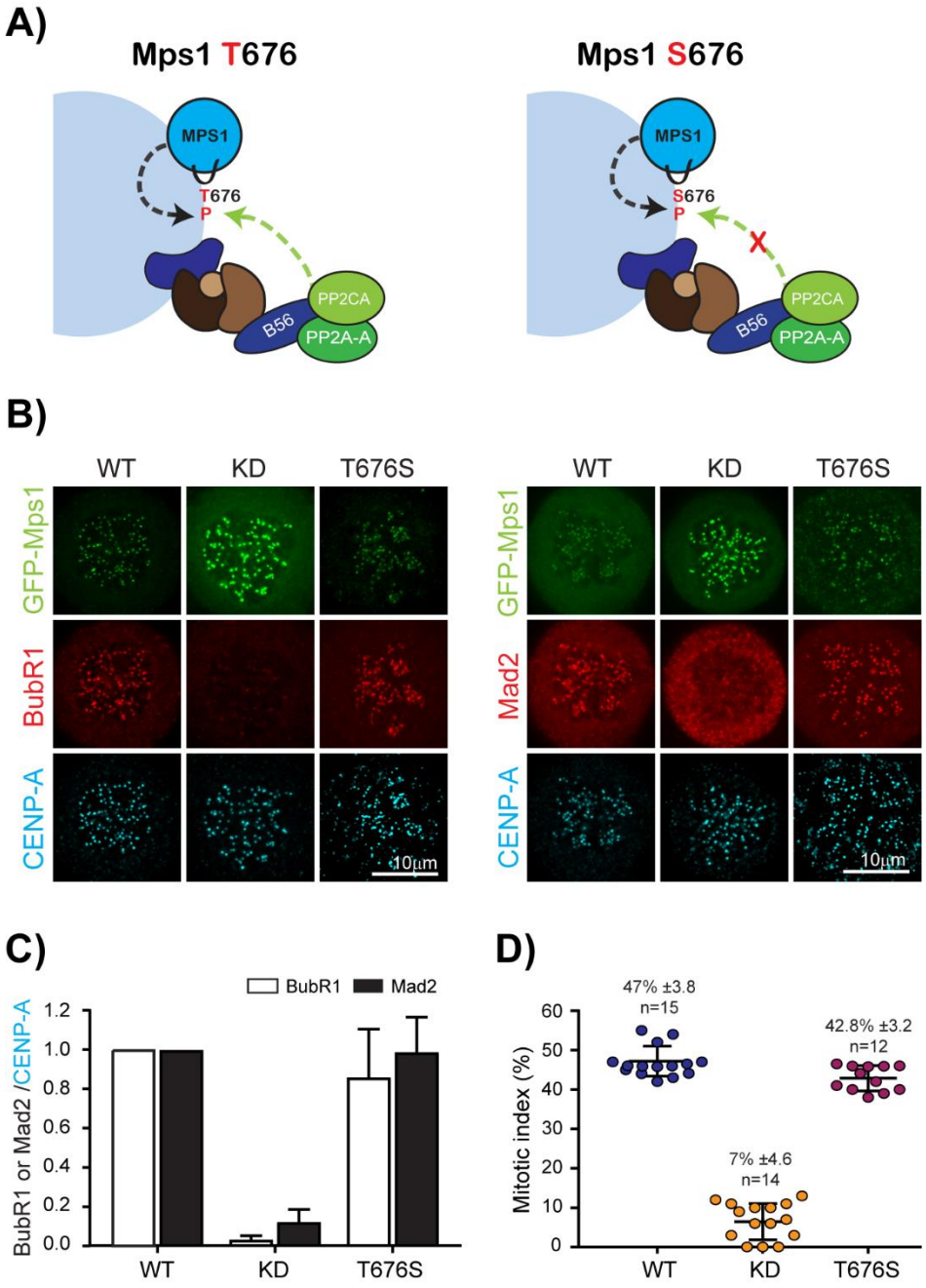

Figure 4.8. Analysis of the T676S-Mps1 mutant. (A) Schematic diagram showing the expected mechanics of T676S-Mps1 phosphorylation compared to WT-Mps1. **(B-C)** Mps1 rescue experiments were performed on T676S-Mps1 mutant cells and the checkpoint was assessed by immunofluorescence analysis of BubR1 and Mad2. Quantification of SAC proteins in representative cells expressing T676S-Mps1 shows that the SAC is active in the T676S mutant. **(D)** Mitotic rescue assays on WT, KD, and T676S demonstrated that T676S mutants can arrest in mitosis and therefore have a functional checkpoint.

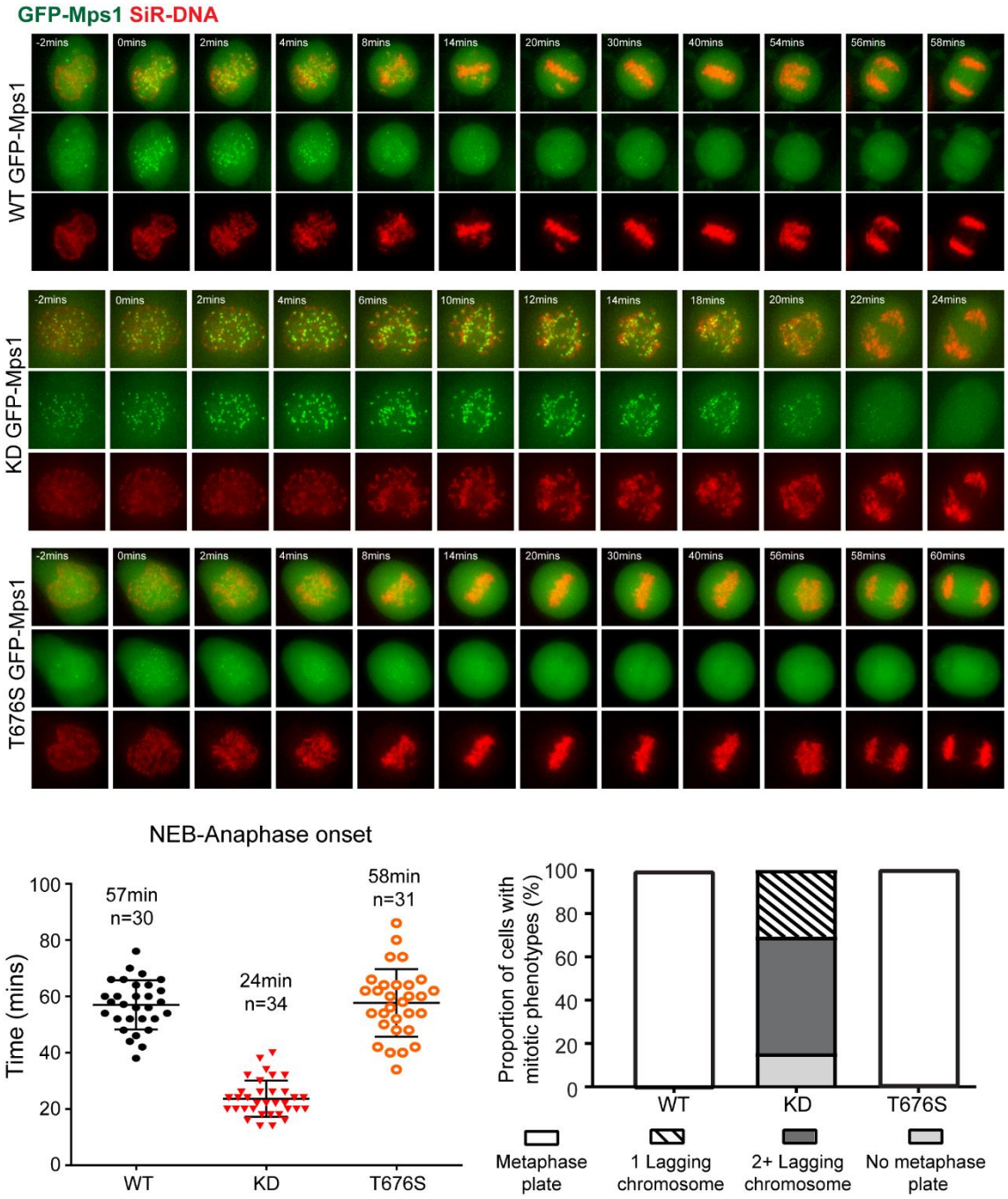

Figure 4.9. Live cell imaging of Mps1 T676S mutants. (A) Live cell imaging was performed on cells expressing GFP-Mps1 and stained with SiR-Hoechst to visualise DNA. Still images were taken during mitosis. **(B)** The length of time from nuclear envelope breakdown to anaphase was counted and plotted in the above graph. Like WT-Mps1, the Mps1-T676S cells undergo an organised mitosis with few chromosomal abnormalities and in roughly the same length of time as WT-Mps1 cells.

4.2.6 Mps1 and PP2A-B56 regulate K-MT attachments.

So far, my data show that Mps1 and PP2A-B56 act in complex negative feedback loops to influence each other's activity. Mps1 mediated phosphorylation of Knl1 is required to recruit PP2A-B56 to kinetochores. PP2A-B56 opposes its own recruitment by inactivating Mps1 and removing BubR1-docking sites on Knl1 (Espert et al., 2014). It has been shown that PP2A-B56 is needed for proper chromosome alignment and depleting the PP2A-B56 phosphatase destabilises K-fibres (Kruse et al., 2013; Foley et al., 2011). In previous studies this effect was assigned to an increase in the phosphorylation levels of Aurora B substrates when PP2A-B56 was depleted (Foley et al., 2011). It has been postulated that the Mps1 kinase plays a role in regulating K-MT attachments because its inhibition or depletion blocks chromosome alignment (Hewitt et al., 2010). Here, we aimed to determine how Mps1 kinase activity influenced PP2A-B56 mediated stabilisation of kinetochore-microtubule attachments.

Cells were synchronously released into mitosis, treated with MG132 and Mps1 or Aurora B inhibitors as indicated (**figure 4.10**), and stained for DNA, kinetochores and microtubules. In line with previous studies, B56 knockdown destabilised K-fibres and this could be rescued with the addition of Aurora B inhibitor, confirming that PP2A-B56 stabilises microtubule attachments by opposing Aurora B activity (Foley et al., 2011). Interestingly, inhibiting Mps1 restored the stability of K-fibres in B56 depleted cells. This result indicates that somehow Mps1 kinase negatively regulates the PP2A-B56 mediated stabilisation of microtubule attachments. During this work, an identical experiment was performed and reported by another group which confirmed the interplay between Mps1 and PP2A-B56 in controlling microtubule attachment stability (Maciejowski et al., 2017). Further to this, it was shown that the Ska complex was the major effector used by Mps1 to control K-MT attachments. Mutating Mps1 phospho-sites on Ska3 to mimic constitutively phosphorylated forms of Ska3 destabilised K-fibres. This is phenotypically similar to the effect of B56 knock-down on K-fibre stability. These results demonstrate that the opposing activities of the Mps1 kinase and PP2A-B56 phosphatase coordinate both SAC signalling and the stabilisation of K-MT attachments.

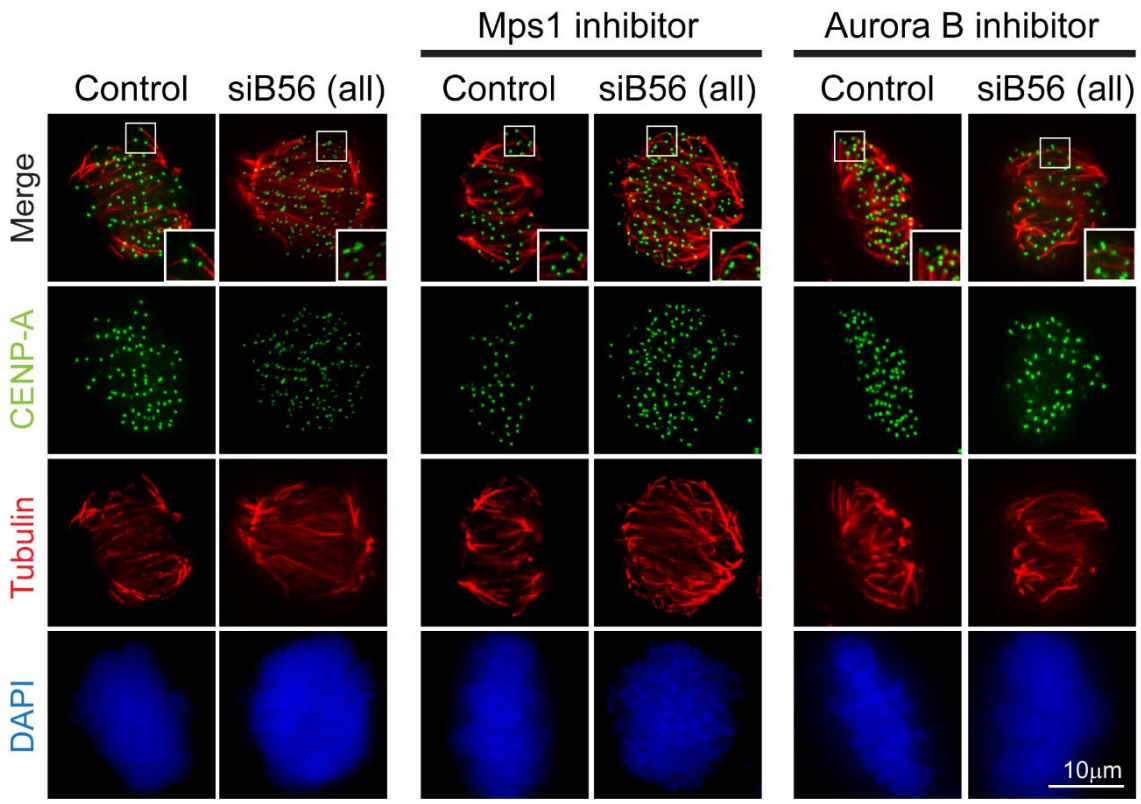

Figure 4.10. Mps1 and PP2A-B56 work antagonistically to control K-MT attachments. Cold stability assay of GFP-CENP-A cells depleted of B56 and treated with MG132 and Mps1 or Aurora B inhibitors. Additionally, cells were stained for tubulin and DAPI to visualise microtubules and chromosomes respectively. B56 depletion inhibited K-MT attachments, however, attachments could be rescued by inhibiting either Mps1 and Aurora B. This demonstrates that Mps1 activity is important for stabilising K-MT attachments. The smaller panels show a zoomed in version of K-MT attachments.

4.3. Discussion

4.3.1 Summary of results.

Here, I have uncovered a novel function for PP2A-B56 in controlling the phosphorylation status, and thus, the activity of Mps1 kinase during SAC signalling. Using chemical inhibitors and siRNA-based knock-down of the catalytic subunits of the PPP family of phosphatases I determined that a PP2A phosphatase was responsible for dephosphorylating pT676. Further analysis identified the components of this PP2A holoenzyme as the PP2Cα catalytic subunit and the B56 regulatory subunit. Mps1 was a direct substrate for PP2A phosphatases in *in vitro* dephosphorylation assays. In cells, the BubR1 associated pool of PP2A-B56 regulates this reaction. To test the consequence of blocking PP2A-B56 mediated dephosphorylation of T676 I created a new mutant T676S-Mps1. Although T676S-Mps1 was an active kinase, it did not behave like a true phospho-mimetic and consequently was phenotypically normal. The interplay between Mps1 and PP2A-B56 is important in establishing K-MT attachments. Mps1 activity destabilises microtubule binding, whereas the opposing action of PP2A-B56 promotes the formation of K-MT attachments.

4.3.2 Discussion

How the SAC is turned off at chromosome bi-orientation is a major unresolved problem in SAC signalling. In this thesis, it has been show that a fundamental step in SAC silencing is the inactivation of the most upstream checkpoint kinase Mps1. Over the past decade Mps1 kinase has emerged as the master regulator of SAC signalling. Mps1 is activated at unattached kinetochores by trans-autophosphorylation of the T-loop residue T676 (Kang et al., 2007; Mattison et al., 2007; Tyler et al., 2008). Importantly, as K-MT attachments mature Mps1 is dephosphorylated and released from kinetochores (Jelluma et al., 2010). Since the activation of Mps1 is a phosphorylation-dependent event, I hypothesised that the reverse reaction may be under the control of a protein phosphatase. The Mps1 T-loop is a direct target of PP2A-B56 both *in vivo* and *in vitro*. In cells, this relies on an interaction between the B56 regulatory subunit and the core SAC protein BubR1. PP2A-B56 antagonises Mps1 autophosphorylation to inactivate its kinase activity and the recruitment of downstream components.

While the release of Mps1 from kinetochores is an important step in SAC silencing (Jelluma et al., 2010), how Mps1 is turned off had not been studied. In the current model, one of the mechanisms the SAC is silenced is through the competition between Mps1 and microtubules for a single site on the Ndc80 complex (Ji et al., 2015; Hiruma et al., 2015). However, it is important to note that in budding yeast and human cells, a fraction of Mps1 is retained at attached kinetochores (Vázquez-Novelle and Petronczki, 2014; Aravamudhan et al., 2015). This residual pool of Mps1 must be switched off to completely extinguish the SAC signal. Additionally, while unattached kinetochores are the primary site for MCC production at prometaphase, pre-mitotic MCC complexes are produced from nuclear pores during late interphase and prophase (Rodriguez-Bravo et al., 2014). Inhibiting Mps1 at these stages decreases the concentration of pre-mitotic MCC in cells and is associated with a reduction in cyclin B levels. Interestingly, a truncated version of Mps1 unable to bind kinetochores was sufficient to generate MCC molecules and delay anaphase entry (Maciejowski et al., 2010) These

observations highlight the need for a mechanism to inactivate Mps1 before its release from kinetochores.

Using an unbiased siRNA-based approach we demonstrated that a BubR1 associated phosphatase holoenzyme consisting of the PP2Cα, PP2A-A and B56 subunits regulates pT676 on Mps1. During this period of research, two separate studies were published that reported partially similar results (Maciejowski et al., 2017; Moura et al., 2017). In agreement with my results, Maciejowski et al., 2017 found that PP2A-B56 dephosphorylates Mps1 in human cells. Another study showed that in Drosophila PP1 dephosphorylates the T-loop of Mps1 (Moura et al., 2017). In human cells depleting B56 increased the phosphorylation of two N-terminal residues pT360/T363 (Maciejowski et al., 2017). These residues are autophosphorylation sites on Mps1 expected to be important in regulating localisation, however, no change in localisation was observed (Wang et al., 2014). Importantly, this study did not analyse the T-loop of Mps1 and thus the results presented here still mark a key advancement in our understanding of how Mps1 is regulated in human cells.

In humans, the PP1 and PP2A-B56 phosphatases play overlapping functions and overall a more rigorous analysis is needed to define their individual contributions. A second study in Drosophila, identified PP1 as the mitotic phosphatase that controls T-loop phosphorylation (pT490) (Moura et al., 2017). In contrast, in mammalian cells, we were unable to detect any contribution from PP1 or combinations of PP1 subunits. Although PP1 may control the T-loop of Mps1 in drosophila, based on these results and others we argue that in humans PP2A-B56 seems to be the relevant phosphatase (Maciejowski et al., 2017; Espert et al., 2014). It is important to note that there are some major differences in SAC regulation in humans and Drosophila, for example, in the latter the recruitment of Bub proteins is not dependent on pMELT motifs. PP1 plays a more prominent role in yeast and Drosophila its function in mammalians is less pronounced. In humans cells, PP1 binding is promoted by PP2A-B56 which reverses phosphorylations on the SILK and RVSF motifs on Knl1 placed by Aurora B (Nijenhuis et al., 2014). As microtubule attachments are established, Aurora B

phosphorylations are lost and this enables PP1 to localise to kinetochores (Liu et al., 2010). The experiments carried out here have been conducted in the absence of microtubules on SAC activated cells. It is possible that a function for PP1 may have been overlooked due to the absence of microtubules. Comparing the phosphorylation status of SAC proteins such as Mps1, Bub1 and Knl1 in the absence or presence of microtubules may yield interesting results. Taking my results together with those of others, I propose that at least in humans PP2A-B56 plays a major role in regulating the T-loop of Mps1. However, the data presented in this study do not exclude a role for PP1 later in mitosis when microtubules are attached to kinetochores.

To understand the biological relevance of PP2A-B56-mediated dephosphorylation at T676 I attempted to create phosphomimetic versions of Mps1: T676D, T676E and T676S. Unfortunately, none of these mutants demonstrated increased kinase activity. While I was unable to generate a true phosphomimetic, my new findings tie into previous observations on the B56 binding mutants and T676A mutants (Kang et al., 2007; Mattison et al., 2007; Espert et al., 2014). When BubR1 was replaced with a BubR1 version unable to dock PP2A-B56, cells spent three times longer in mitosis and this was associated with increased checkpoint activity (Espert et al., 2014). A disadvantage of this mutant is that it shows the cumulative effect of stopping B56-mediated dephosphorylation of all its kinetochore substrates rather than at a specific residue. Nonetheless, an extended mitosis fits with increased levels of Mps1 phosphorylation and kinase activity. Conversely, from T676A Mps1 mutants, that rapidly exit mitosis, we can infer the effect of having too much PP2A-B56 activity is an inability to mount a checkpoint response. The findings presented here and previous work from our lab, demonstrate that the PP2A-B56 phosphatase contributes to SAC silencing by opposing Mps1 activity in a two-step process. Firstly, PP2A-B56 inactivates Mps1 to stop the addition of new phosphate groups on Knl1s MELT motifs, and secondly, it removes phosphate groups from MELT motifs to release the Bub proteins already present at kinetochores. Recent proteomic analysis has identified several new Mps1 substrates including Ndc80,

Bub1, Mad1 and the Ska3 complex. Whether these substrates are also regulated by PP2A-B56 is a necessary question to be answered.

The interplay between Mps1 kinase and PP2A-B56 phosphatase activity is critical in creating a complex signalling network involving multiple negative feedback loops, priming events and dynamic changes in kinetochore composition (Nijenhuis et al., 2014; Espert et al., 2014; Funabiki and Wynne, 2013). Mps1 and PP2A-B56 act in negative feedback loops to influence each other's function. Mps1 promotes the recruitment of BubR1:PP2A-B56 to prime its own inactivation. Similarly, by removing phosphate groups from the MELT motifs of Knl1 PP2A-B56 triggers its own release (Espert et al., 2014). In addition to this, this study shows that PP2A-B56 acts upstream by directly inactivating Mps1 to stop the further recruitment of BubR1. The model developing is one where Mps1 and PP2A-B56 are in a constant tug of war. At unattached kinetochores, Mps1 wins and phosphorylates multiple targets to assemble the SAC module and halt mitotic progression. At this point PP2A-B56 serves to hold Mps1 in check so that the SAC can be rapidly inactivated. The binding of microtubules signifies a shift in power, Mps1 is turned off by PP2A-B56 mediated dephosphorylation and then released from kinetochores. The PP2A-B56 phosphatase also reverses the phosphorylation of Knl1 to break the protein:protein interactions previously built by Mps1. The inactivation of Mps1 and release of SAC components blocks the further initiation of the SAC and production of the MCC. A lack of the wait anaphase signal leads to the activation of the APC/C complex and this in turn drives mitotic exit. The balance between Mps1 and PP2A-B56 activity must be tightly coupled to the formation of end-on attachments. Thus, a key question remains: how is the interplay between Mps1 and PP2A-B56 activity integrated with microtubule sensing?

Not only are Mps1 and PP2A-B56 master regulators of SAC signalling, but both have been implicated in regulating microtubule attachments. Previous studies have defined a role for PP2A-B56 in controlling the stability of K-MT attachments. Depleting PP2A-B56 destabilises K-fibres in cold stable assays and cells expressing B56 binding mutants mis-segregate chromosomes at a higher

frequency (Foley et al., 2011). The function of Mps1 in regulating K-MT attachments is less clear, but inhibiting Mps1 blocks chromosome alignment (Hewitt et al., 2010; Maure et al., 2007; Jelluma et al., 2008b). We hypothesised that in part Mps1 plays a role in regulating K-MT attachments may in part be due to the control of PP2A-B56. How Mps1 activity influences PP2A-B56 mediated stabilisation of K-MT attachments was an interesting question.

The stability of K-fibres depends on the phosphorylation status of kinetochores by mitotic kinases including Aurora B and Plk1 (Salimian et al., 2011; Ahonen et al., 2005). The phosphorylation of kinetochore proteins is associated with the destabilisation of microtubule binding (Welburn et al., 2010; Zaytsev et al., 2015; Guimaraes et al., 2008). PP2A-B56 works antagonistically to remove phosphate groups from Aurora B substrates and in doing so stabilises microtubule attachments. The disruption of K-MT attachments in PP2A-B56 depleted cells correlates with an increase in the phosphorylation of Aurora B substrates (Foley et al., 2011). Strikingly, Aurora B inhibition of B56 depleted cells largely rescues K-MT attachments. This indicates that a major way that PP2A-B56 controls K-MT is by dephosphorylating Aurora B targets. Now, we demonstrate that Mps1 inhibition also stabilises K-fibres in B56 depleted cells. This indicated that Mps1 and PP2A-B56 work antagonistically in controlling microtubule attachments. Previously, it was suggested that Mps1 promotes the activity of Aurora B by phosphorylating Borealin a member of the CPC (see 1.2.3.2) (Jelluma et al., 2008a). One explanation for this finding is that this phenotypic rescue is due to an increase in Aurora B activity. During the course of these experiments, another research group published an almost identical experiment (Maciejowski et al., 2017). Additionally, they found that Mps1 controlled microtubule stability, in an Aurora B independent mechanism, by phosphorylating pS34 on the Ska3 protein to stop its recruitment to kinetochores. The Ska complex is needed to stabilise the microtubule interface by clamping microtubules to the Ndc80 complex (Jeyaprakash et al., 2012; Zhang et al., 2012). Phosphomimetic mutants of Ska3 destabilise microtubule binding suggesting that dephosphorylation at this site is critical (Maciejowski et al., 2017). More recently, it was shown that PP1 and PP2A oppose the Mps1 mediated phosphorylation of Ska3. Depletion of either

phosphatase disrupted the kinetochore localisation of Ska3 (Sivakumar and Gorbsky, 2017). Intriguingly, a more overarching role for PP2A-B56 in regulating and integrating K-MT attachments with SAC silencing is unfolding. These findings together with previous studies, demonstrate that phosphorylation at the kinetochore-microtubule interface is tuned by the opposing activities of mitotic kinases, Mps1 and Aurora B, and mitotic phosphatases, PP1 and PP2.

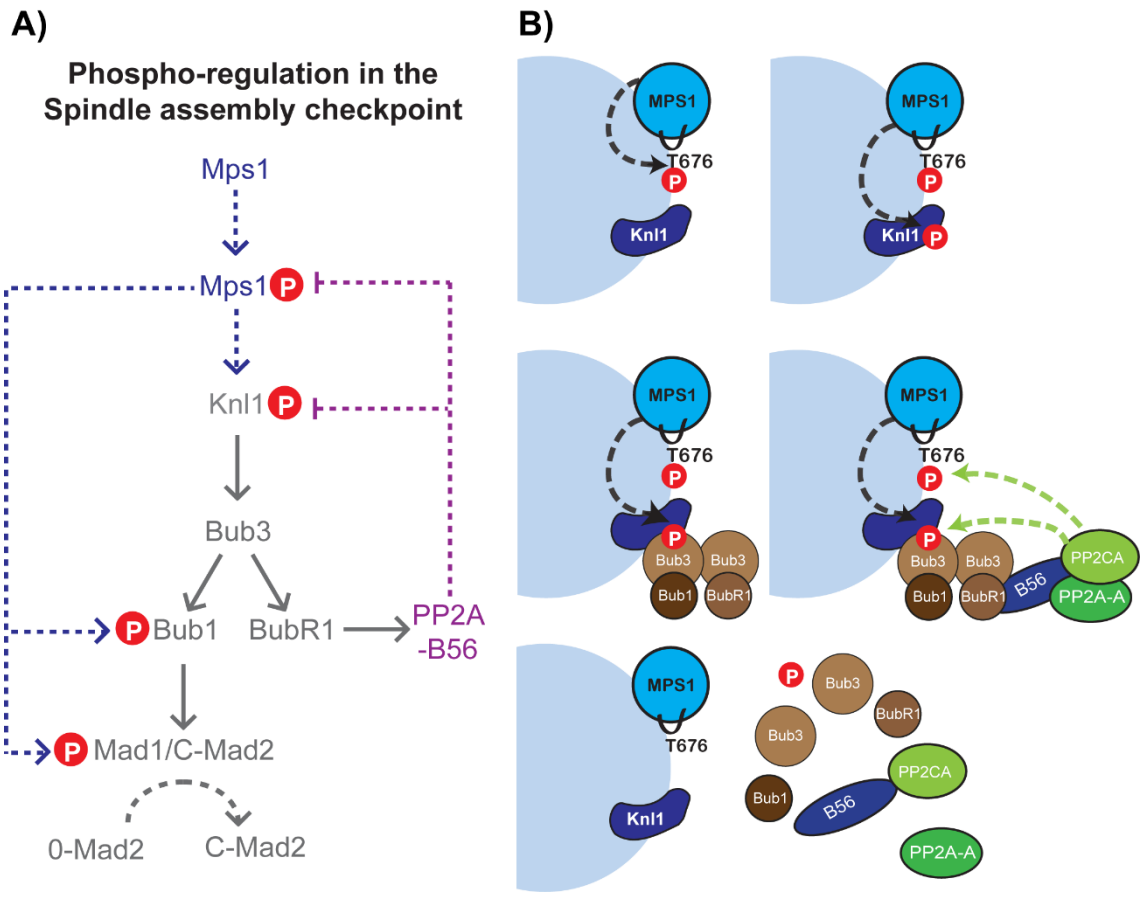

Figure 4.11. Model of the PP2A-B56 negative feedback loop modulating Mps1 activity and SAC signalling. A) Mps1 is activated by autophosphorylation and recruits downstream SAC components (grey) by phosphorylation of Knl1 and Bub1 (blue). The PP2A-B56 phosphatase (purple) is recruited by BubR1 binding and negatively regulates the function of Mps1 by two ways. It was shown previously that PP2A-B56 dephosphorylates the MELT motifs to ablate the binding site of the Bub complex (Espert et al., 2014). **B)** Now, we have identified a second regulatory step in this feedback loop in which PP2A-B56 directly inactivates Mps1 to stop all subsequent phosphorylation events.

5.
A GLOBAL ANALYSIS OF MPS1 PHOSPHORYLATION

5.1 Introduction.

When the SAC is active, Mps1 is hyperphosphorylated and activated at unattached kinetochores. The development of K-MT attachments induces the loss of phosphate groups from Mps1 so that it is fully dephosphorylated around the time cells exit mitosis (Stucke et al., 2002). How Mps1 is dephosphorylated and inactivated as the SAC is turned off is still unknown. Previous studies have shown that Mps1 is autophosphorylated at many residues during mitosis (**figure 5.1**) (Tyler et al., 2008; Dou et al., 2011; Jelluma et al., 2008b). In addition to this, Mps1 is phosphorylated by other mitotic kinases including Cdk1, Plk1 and Aurora B (Dou et al., 2011; von Schubert et al., 2015). The functional importance of some sites is known, for example, T676 autophosphorylation and Cdk1 dependent phosphorylation of S281 are important for Mps1 activity (Mattison et al., 2007; Jelluma et al., 2008b; Kang et al., 2007; Morin et al., 2012). The importance of other phosphosites is yet to be determined. Outside of the kinase domain the functional significance of phosphorylation events is less clear, although the phosphorylation of the N-terminal kinetochore binding region of Mps1 has been suggested to be important for controlling its localisation.

Early studies on Mps1 described a tight link between its activity and localisation. When Mps1 is inhibited it accumulates at kinetochores suggesting that somehow Mps1 negatively regulates its own localisation (Jelluma et al., 2010; Hewitt et al., 2010). Precise details of this negative feedback are lacking, but it has been postulated that autophosphorylation on sites at the N-terminal are key in controlling Mps1 localisation. The autophosphorylation of eight N-terminal residues on Mps1 are associated with the regulation of Mps1 localisation (Wang et al., 2014). A phospho-mimetic mutant with mutations at these eight sites (Mps1-8D) had slightly reduced kinetochore localisation, whereas, a non-phosphorylatable mutant, Mps1-8A, displayed slightly increased kinetochore localisation. Phospho-mimicking mutations of these phosphorylation sites caused errors in chromosome segregation, suggesting that they have a biological relevance. Based on these results, Wang et al., 2014 concluded that phosphorylated Mps1 has reduced affinity for kinetochores.

Here, I aimed to determine exactly which autophosphorylation sites on Mps1 were targeted by the PP2A-B56 phosphatase. I reasoned that phosphosites dynamically regulated by autophosphorylation and PP2A-B56-mediated dephosphorylation should be functionally important. A greater understanding of PP2A-B56-mediated dephosphorylation of Mps1 may provide insight into how changes in Mps1 phosphorylation status result in its release and overall SAC silencing.

Aims:

- Analyse other sites on Mps1 controlled by PP2A-B56.
- Establish an immunoprecipitation and mass spectrometry based approach to determine the phosphorylation status of Mps1 when the SAC is switched on and off.
- Determine which sites on Mps1 are controlled by PP2A-B56 by mass spectrometry.

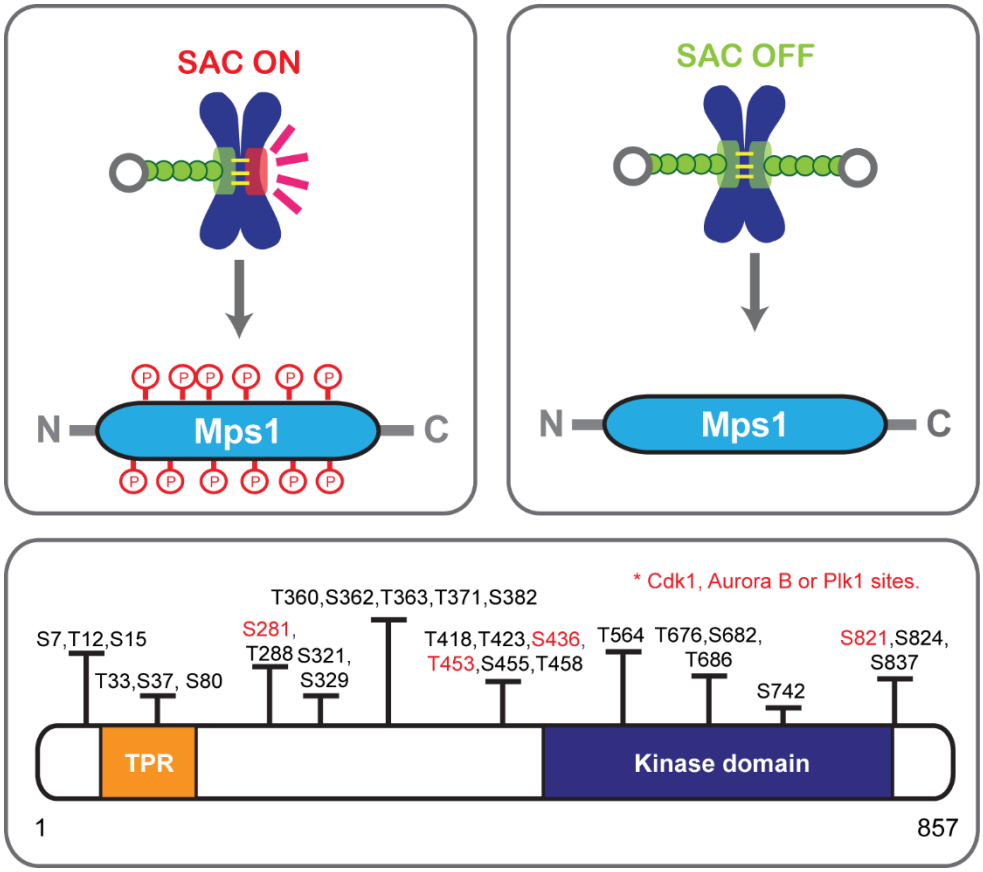

Figure 5.1. Phosphorylation of Mps1 during mitosis. The structure of Mps1 and phosphorylation sites as determined by mass spectrometry analysis of *in vivo* Mps1 extracted from SAC active cells. Figure was adapted from Dou et al., 2011. At unattached kinetochores, Mps1 is phosphorylated when the SAC is active. The attachment of microtubules turns the SAC off and Mps1 is dephosphorylated. This dephosphorylation is likely to be down to PP2A-B56 activity and we aimed to determine the precise sites controlled by it.

5.2.1 PP2A-B56 dephosphorylates pT33/S37 on Mps1.

So far, the PP2A-B56 phosphatase was shown to dephosphorylate pT676 a T-loop residue on Mps1 and in doing so it modulated Mps1 activity. Proteomic analysis of mitotic cells has revealed that Mps1 is heavily phosphorylated during mitosis (Dou et al., 2011; Jelluma et al., 2008b; Kang et al., 2007; Tyler et al., 2008; Wang et al., 2009). While Mps1 dependent trans-autophosphorylations make up the bulk of phosphorylations on Mps1, other kinases including Cdk1, MAPK and Plk1 are known to phosphorylate some sites on Mps1 (Dou et al., 2011; von Schubert et al., 2015). When Mps1 was dephosphorylated *in vitro* I observed a considerable downshift in its molecular weight (**figure 4.6**) indicating that multiple phosphate groups are lost. Next, it was tested whether PP2A-B56 plays a more general role in dephosphorylating other residues on Mps1. We were particularly interested to see whether PP2A-B56 exclusively removed phosphate groups placed by Mps1.

The phosphorylation of two N-terminal Mps1 autophosphorylation sites was assessed by immunofluorescence analysis, using a commercially available dual phospho-specific antibody recognising pT33 and pS37 on Mps1. These residues are found at the N-terminal kinetochore-binding domain of Mps1 and their phosphorylation is expected to be important for regulating Mps1 localisation. It had been postulated that the autophosphorylation of T33, S37 and six other N-terminal sites causes the dissociation of Mps1 from kinetochores (Wang et al., 2014). As before, synchronised mitotic cells were treated with or without Mps1 inhibitor to block Mps1-dependent autophosphorylation and as a result the p33/37 signal was lost (**figure 5.2A-B**). Like pT676, a short pulse of the PPP family inhibitor Calyculin restored p33/37 signal when Mps1 is inhibited indicating that this phosphosite is also under the control of a PPP family phosphatase (**figure 5.2A-B**). As expected, further siRNA experiments confirmed that the PP2A-B56 was the relevant phosphatase responsible for dephosphorylating p33/37. Surprisingly, I found that Mps1 could be hyperphosphorylated at T33/S37 and was still enriched at kinetochores after Mps1 inhibition. This contradicts the idea that phosphorylated Mps1 is less stably bound at kinetochores (Wang et al.,

2014) These results along with those of Maciejowski et al., 2017, show that PP2A-B56 dephosphorylates at least five different residues on Mps1 including T33, S37 and T676 presented here as well as T360 and T363 described elsewhere (Maciejowski et al., 2017). To identify all Mps1 sites controlled by PP2A-B56 a phospho-proteomic based approach was developed.

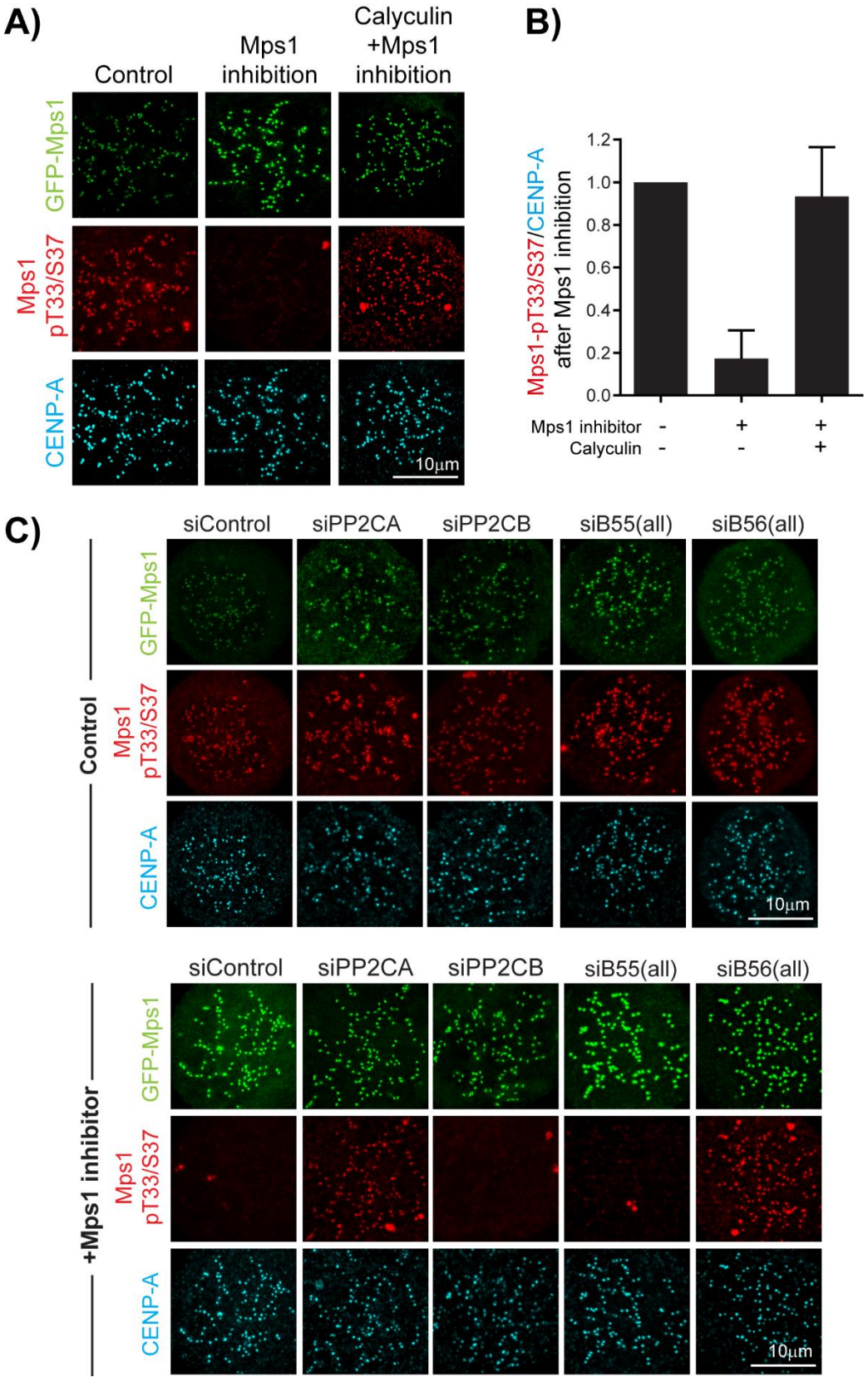
A)
Control
Mps1 inhibition
Calyculin +Mps1 inhibition
GFP-Mps1
Mps1 pT33/S37
CENP-A
10μm
B)
Mps1-pT33/S37/CENP-A after Mps1 inhibition
1.2
1.0
0.8
0.6
0.4
0.2
0.0
Mps1 inhibitor - + +
Calyculin - - +
C)
siControl
siPP2CA
siPP2CB
siB55(all)
siB56(all)
Control
+Mps1 inhibitor
GFP-Mps1
Mps1 pT33/S37
CENP-A
10μm

Figure 5.2. PP2A-B56 controls other phosphosites on Mps1. PP2A-B56 controls dephosphorylation at other sites on Mps1. **(A)** As before, GFP-Mps1 cells were synchronised in mitosis by nocodazole-induced arrest and were treated with MG132 to block exit. Control cells were not treated with additional inhibitors. Next, AZ3146 was added for 5 mins or Calyculin A was added for 3 mins and AZ3146 after for a further 5 mins. Cells were analysed using antibodies for Mps1 pT33/S37 and CENP-A. **(B)** Quantification of (A), the pMps1 signal was quantified for 300 kinetochores in 15 cells. **(C)** Depletion of PP2A catalytic and regulatory subunits defined the relevant phosphatase as PP2A-B56.

5.2.2 Establishing a mass spectrometry-based approach to analyse Mps1 phosphorylation status.

A mass spectrometry-based approach was established to identify phosphorylations on immunoprecipitated Mps1 (outlined in **figure 5.3**). As a prerequisite to future Mps1 IP experiments, the IP protocol was optimised to release greater amounts of Mps1 into the supernatant. The optimal lysis condition involved digesting chromosomes with the endo-exonuclease, micrococcal nuclease, for 30 mins on ice and a further 20 mins at 25^{o}C (**figure 5.4**).

Having established optimal Mps1 IP conditions, I determined Mps1 phosphorylation status in cells where the SAC is turned on and off. The analysis of cells passing through an unperturbed mitosis from prometaphase (SAC on) to metaphase (SAC off) would have been the most informative experiment. However, work by others in the lab demonstrated that there were considerable technical hurdles in achieving highly synchronous cells at these specific stages on such a large scale. With this in mind, I opted to activate the checkpoint by treating cells with nocodazole and then recapitulated checkpoint inactivation by inhibiting Mps1 activity with AZ3146. Nocodazole-arrested cells were treated with MG132, to block mitotic exit, or MG132 and AZ3146 to inhibit Mps1 activity and recapitulate an inactive checkpoint (**figure 5.5A**). The length of AZ3146 treatment was extended to 1 hour in larger scale experiments and its effectiveness was assessed by immunofluorescence analysis (**figure 5.5B**). Both the p33/37 and BubR1 kinetochore signals were lost in individual cells after Mps1 inhibition indicating that the AZ3146 treatment was efficient. Moreover, changes in phosphorylation was assessed across the pool of cells, in western blot analysis the p33/37 band was reduced in Mps1 inhibited cells (**figure 5.5C**) and the total Mps1 band was downshifted on a coomassie gel (**figure 5.5D**). Following immunoprecipitation, Mps1 was eluted from Dynabeads using a glycine elution protocol (**figure 5.5E**). The SDS elution method was also tested, however, glycine elution is preferred because this method avoids introducing detergent into the eluate which interferes with the tryptic digest. Mps1 was effectively eluted

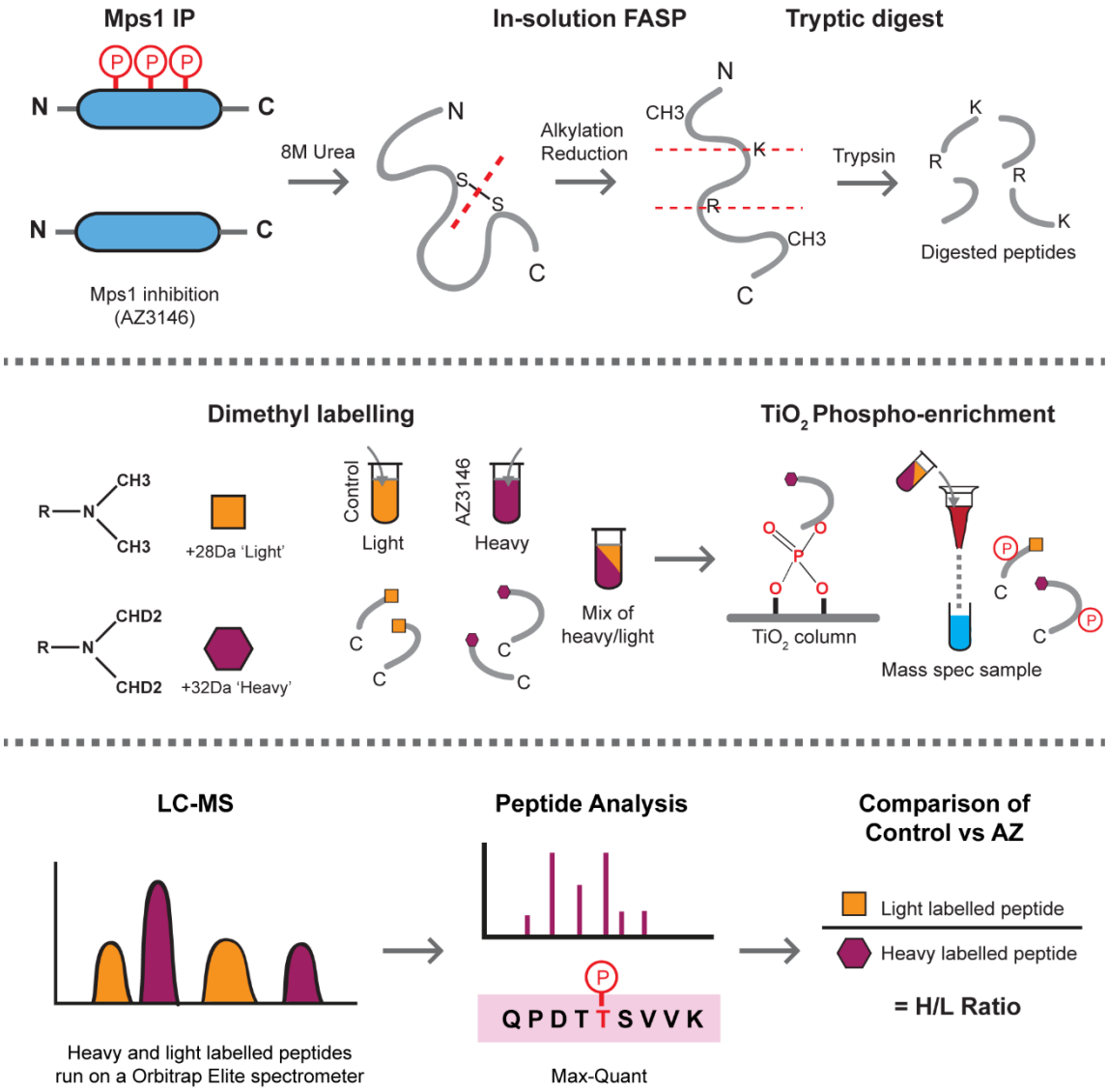

Figure 5.3. Mass spectrometry pipeline Schematic diagram of the mass spectrometry approach used. Mps1 was immunoprecipitated from cells after inhibitor treatment, eluted from Dynabeads by glycine elution and denatured by the addition of 8M Urea. The eluted material was alkylated, reduced and digested with trypsin on a FASP column. Control and Mps1 inhibitor treated samples were labelled light and heavy by di-methyl labelling and phospho-peptides were enriched using a TiO_2 column. Samples were loaded onto a mass spectrometer. Peptides were analysed in Max-Quant and their intensity was compared to identify changes in phosphorylation between control and Mps1 inhibited cells.

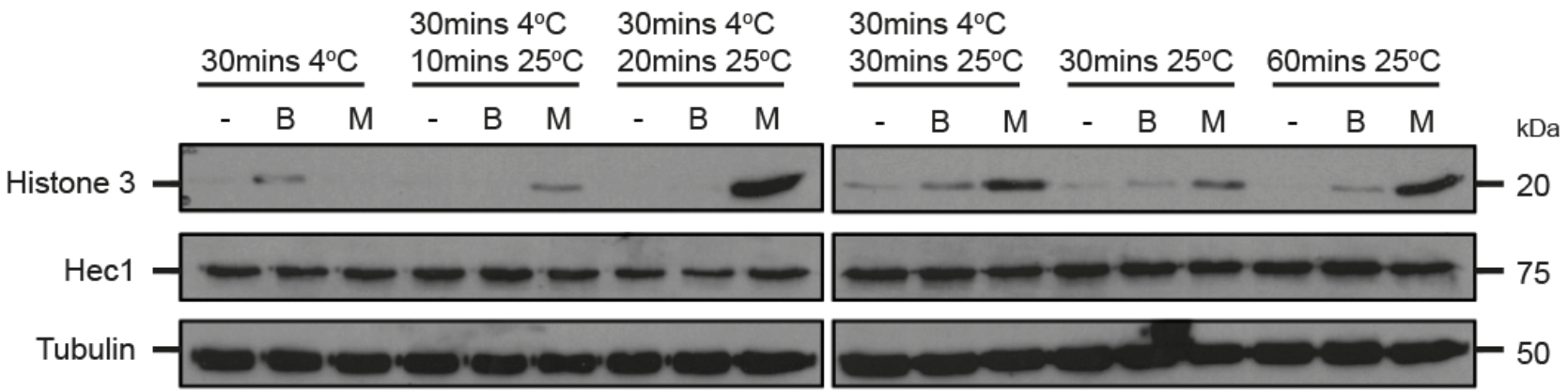

Figure 5.4. Optimisation of kinetochore immunoprecipitation. Mitotic cells were harvested and lysed for different lengths of time at 4°C and/or 25°C. Micrococcal-nuclease (M) and Benzonase (B) were added to the lysis buffer as indicated and western blot samples were taken for each condition. Samples were analysed for Histone 3 (centromeric protein), Hec1 (kinetochore protein) and tubulin (microtubules) by western blot analysis.

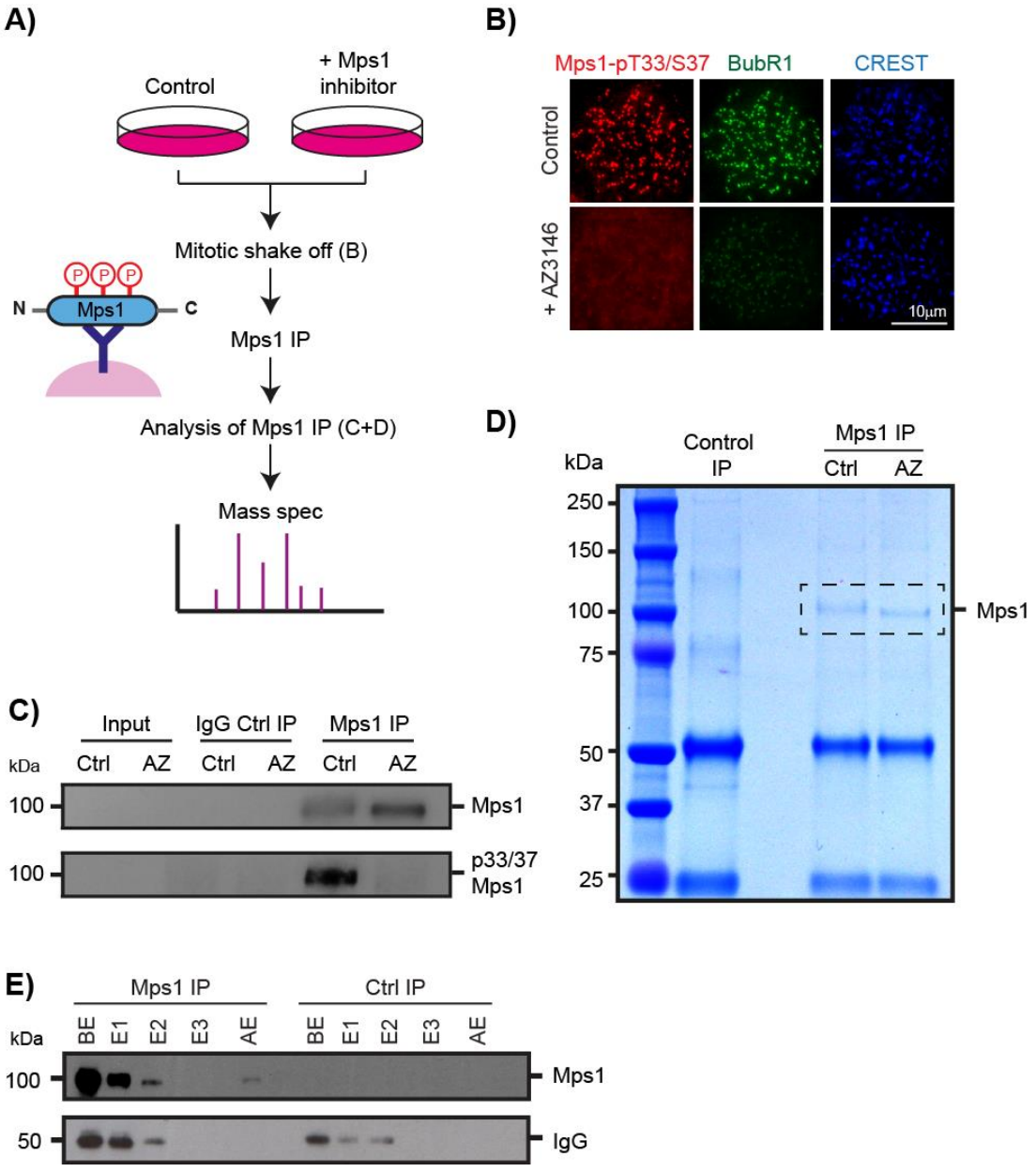

Figure 5.5. Mps1 phosphorylation in an Mps1 IP at different stages. (A) Schematic showing the basic steps in the mass spectrometry process. **(B)** After Mps1 inhibitor treatment, mitotic cells were harvested by shake-off and analysed for p33/37 and BubR1. **(C)** Mps1 was immunoprecipitated and western blot analysis demonstrated that p33/37 is lost after inhibitor treatment. **(D)** A sample of the Mps1 IP was run on an SDS-PAGE gel and the gel was stained with Coomassie blue. This showed that Mps1 was downshifted when inhibited. **(E)** Immunoprecipitated Mps1 was eluted using glycine, samples were taken for beads before elution (BE), after elution (AE) and for each elution (E1-E3).

using glycine and almost nothing was left on the dynabeads (**figure 5.5E**). Samples were processed for mass spectrometry and the intensity of phosphorylated Mps1 peptides were compared between cells with an active or inactive checkpoint. The mass spectrometry procedure was carried and the results were analysed in collaboration with Christina. H. Y. Barnard.

5.2.3. Mps1-dependent phosphorylations are lost after Mps1 inhibition

Using a mass spectrometry-based approach on Mps1 immunoprecipitates we observed changes in Mps1 phosphorylation when the SAC is switched on and off (**figure 5.6A**). In SAC activated cells with phosphorylated Mps1, we detected 31 phosphorylations of which 9 phosphorylation sites were novel to this study (**figure 5.6B**). The S268, a previously unidentified residue, lies at the MR domain and is potentially interesting because this domain plays a role in controlling Mps1 localisation (Ji et al., 2015). Most of the other newly identified residues are concentrated between residues 300-450 flanking the MR domain. Although several studies have identified multiple phosphorylation sites on Mps1 by proteomic analysis, the functional significance of these phosphorylation events remains elusive (Dou et al., 2011; von Schubert et al., 2015; Jelluma et al., 2008b; Mattison et al., 2007). A systematic knockdown of individual or stretches of Mps1 phosphosites is required to determine whether phosphorylation at all 31 phospho-residues is important for Mps1 function. If a phosphosite is phosphorylated when the SAC is active and dephosphorylated when the SAC is inactive we would logically expect them to be key phosphorylations because they are dynamically regulated in mitosis.

To identify key or ‘driving’ phosphorylations we compared the phosphorylation profile of Mps1 in human cells when the SAC was active or inactive. As described before, Mps1 was phosphorylated in nocodazole arrested cells, but the addition of Mps1 inhibitor caused the loss of most phosphate groups (**figure 5.5C**). Consistent with previous data, the level of pT33, pS37 and pT676 were all reduced after Mps1 inhibition, as well as, pT363 reported by Maciejowski et al., 2017. These data suggest that Mps1 undergoes global dephosphorylation, rather

than dephosphorylation at a subset of residues, during SAC silencing. I postulate that dephosphorylation outside of the kinase domain of Mps1 is critical for Mps1 function. A possible future experiment might be to mutate all these phosphosites to alanine or aspartate to see the physiological consequence of changes in Mps1 phosphorylation. To uncouple this from kinase activity, the T676 and the P+1 loop site T686 could be excluded. However, mutating this number of phosphosites is likely to destabilise protein structure. While most phosphate groups were lost, some phosphosites remained after Mps1 inhibition. Some of the phosphorylations that were unchanged are not Mps1 autophosphorylations, for example S281 and S333 have been identified as Cdk1 and Plk1 sites respectively (Dou et al., 2011; von Schubert et al., 2015). Thus, the loss in phosphorylation was specific to Mps1 autophosphorylation sites and it seems likely this was caused by a mitotic phosphatase. PP2A-B56 is likely to dephosphorylate other sites on Mps1 than the five aforementioned phosphosites, however, it is yet to be determined precisely what phosphorylations are sensitive to PP2A-B56. To gain a greater understanding of what residues are targeted by the PP2A-B56 phosphatase, we expanded our mass spectrometry analysis to include phosphorylations on B56 depleted cells.

A)

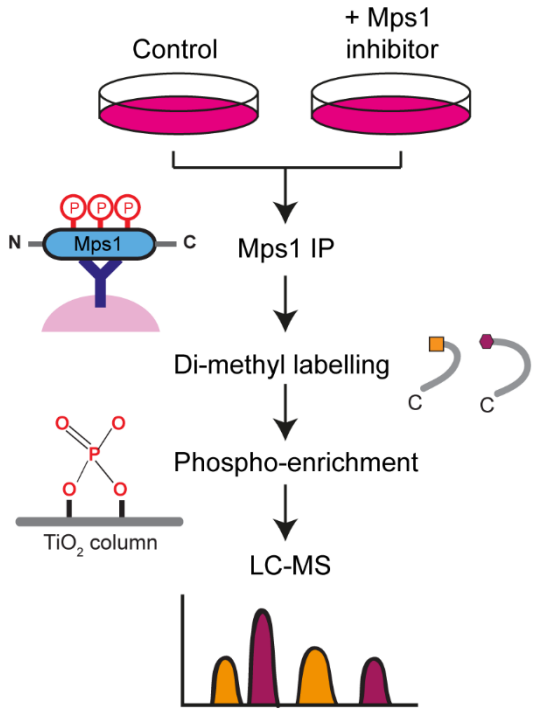

B)

Novel phosphosites	Peptide sequence
S268	TKQSCPFGR
S314	LVVPGSKPSGN
S403	QNPAASSNHWQ
S404	QNPAASSNHWQ
S430	EQPVFSVSKQS
S441	PPISTSKWFDP
S448	WFDPKSICK
S843	GESHNSSSSK
S844	GESHNSSSSK

C)

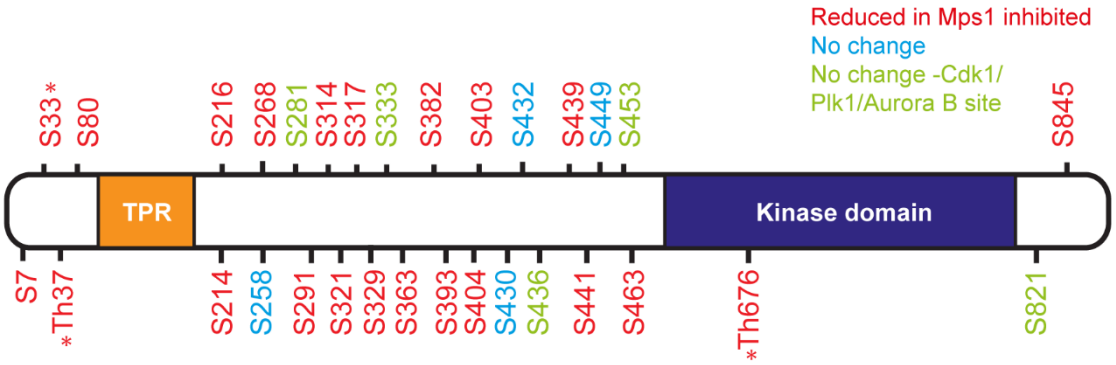

D)

Phosphosite	Peptide sequence	Expt1 Az/Ctrl	Expt2 Az/Ctrl	Expt3 Az/Ctrl	Average ratio
S7	MESEDLSGR	0.00	-	0.00	0.00
T33	EDLTDELS	-	0.45	0.00	0.22
S37	LTDELSLNK	0.05	-	0.00	0.02
S281	VNLLNSPDCDV	0.80	-	0.77	0.78
S321	PSGNDSCELR	0.03	0.00	0.04	0.03
S363	NKTESSLLAK	0.06	-	-	0.06
T676	MQPDTTSVVKD	0.00	0.00	0.00	0.00

Figure 5.6. **Comparison of phospho-peptide data for control and Mps1 inhibitor-treated cells**. **(A)** Schematic showing the main steps in the mass spectrometry process. **(B)** Novel Mps1 phosphosites found during this study **(C)** Overall analysis of the change in Mps1 phosphorylation status. Sites in red have a large fold decrease in AZ3146 samples, sites in blue do not show a significant change in phosphorylation and green sites are phosphorylated by other mitotic kinases. **(D)** Mps1 phosphosites were compared control and Mps1 inhibitor-treated samples. Examples of specific phosphosites including previously studied sites like T33, S37 and T676 as well as the CDK site 281 are shown.

5.2.4. Mps1 phosphorylations are retained in B56 depleted cells.

Proteomic analysis of Mps1 phosphorylations revealed that many auto-phosphorylation sites are lost after Mps1 inhibition. This indicated that Mps1 undergoes global dephosphorylation when the SAC is inactivated. As described previously, we have defined a major role for PP2A-B56 in regulating pT676, pT33 and pS37. Having established a mass spectrometry approach to observe the global phosphorylation status of Mps1 I sought to define the phosphorylation sites controlled by PP2A-B56.

Initial small-scale experiments on B56 depleted cells were carried out on lysates from a single 10cm dish to optimise the conditions before larger scale experiments. Mitotic cells treated with control or B56 siRNA were lysed in the presence or absence of phosphatase inhibitors and Mps1 inhibitor as indicated (**figure 5.7A**). Western blot analysis showed that Mps1 was smeared and upshifted in the presence of phosphatase inhibitors when cells were untreated. In the absence of phosphatases, phosphorylations on Mps1 were expected to be lost because the cellular phosphatases were active, however, depleting the relevant phosphatase should prevent Mps1 dephosphorylation. As expected, the Mps1 band was downshifted when cells were lysed in the absence of phosphatase inhibitors because of the activity of cellular phosphatases. The Mps1 band ran at the same molecular weight as dephosphorylated Mps1 pretreated with Mps1 inhibitor. When B56 depleted cells were lysed in the absence of phosphatase inhibitors, Mps1 was upshifted to produce two Mps1 bands. This result highlights that B56 is the relevant phosphatase responsible for controlling many phosphorylations on Mps1. Mps1 appears as two bands, Mps1 and pMps1 (upshifted band), in B56 depleted cells demonstrating that phosphorylation is retained to some extent but is not fully retained.

Next, I attempted to scale up this experiment to carry out Mps1 immunoprecipitations followed by mass spectrometry in PP2A-B56 depleted cells. The aim of this analysis was to define the specific phospho-residues regulated by PP2A-B56. As before, Mps1 was phosphorylated in the presence of

phosphatase inhibitors, which was confirmed by blotting for pT33/pS37. The pT33/pS37 was lost in Mps1 immunoprecipitates lysed from cells treated with AZ3146 or in the absence of phosphatase inhibitors. Large-scale depletion of B56 proved to be more difficult than anticipated and as a result depletion efficiency varied greatly between experiments. Encouragingly, in a preliminary experiment when cells were fully depleted of B56 and lysed in the absence of phosphatase inhibitors, the pT33/pS37signal was stabilised and Mps1 was upshifted (**figure 5.7B**). Preliminary experiments demonstrate that B56 depletion protects a number of phosphosites, however, a more reliable method is needed to identify these phosphosites by mass spectrometry. Further work is required to establish a protocol to reliably deplete B56 for an experiment of this scale. Following this, mass spectrometry analysis should reveal which specific sites are controlled by the PP2A-B56 phosphatase.

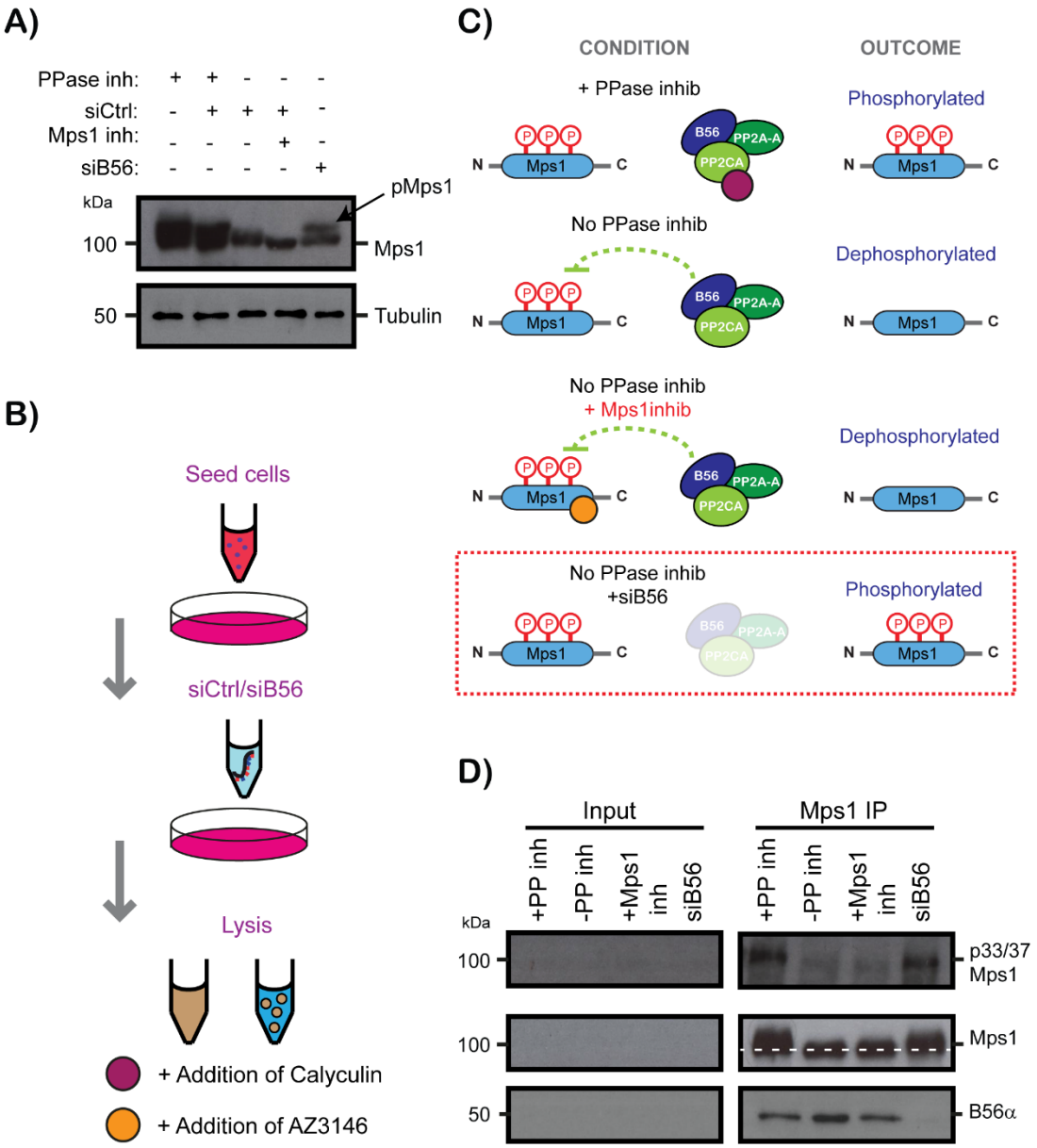

Figure 5.7. Mps1 IP in B56 depleted cells suggests that multiple sites on Mps1 are regulated by PP2A-B56. (A) Analysis of Mps1 in lysates treated as indicated with PPase inhibitors, Mps1 inhibitor and siB56. Mps1 appears as two bands in B56 depleted cells, Mps1 and pMps1 (upshifted band), demonstrating that phosphorylation is retained to some extent. **(B)** Diagram to show the experimental set up. **(C)** Schematic showing the experimental conditions and the expected outcomes. **(D)** Mps1 IPs were carried out on the cells treated as indicated and analysed by western blot analysis for p33/37 and total Mps1. The pMps1 signal is retained and total Mps1 is upshifted in cells depleted of B56 despite there being no PPase inhibitors added.

5.3. Discussion

5.3.1 Summary

I have shown that the PP2A-B56 mediated dephosphorylation of T676 on Mps1 is essential for controlling activity. Mps1 is phosphorylated at many residues during mitosis most of which are autophosphorylation sites. These results revealed that at least two other autophosphorylation sites T33 and S37 are modulated by PP2A-B56. Using mass spectrometry, we demonstrated that most autophosphorylations on Mps1 are lost when the SAC is turned off because of the activity of cellular phosphatases. Depleting the relevant phosphatase PP2A-B56 protected Mps1 from dephosphorylation. Additional mass spectrometry analysis is needed to define the specific Mps1 phosphosites controlled by PP2A-B56.

5.3.2 Discussion

Mps1 is a cell cycle regulated protein kinase whose phosphorylation and subsequent activation occurs concomitantly with mitotic entry. When Mps1 is extracted from mitotic extracts it is hyper-phosphorylated and this is associated with an increase in kinase activity of up to 30-fold (Stucke et al., 2002). In contrast, at interphase and after chromosomes are attached to microtubules Mps1 is dephosphorylated. The timely phosphorylation of Mps1 is important in regulating its activity and localisation. So far, myself and others have identified at least five sites controlled by the PP2A-B56 phosphatase: S33, T37, T360, T363 and T676 (Maciejowski et al., 2017). Proteomic analysis by multiple studies has demonstrated that Mps1 is phosphorylated at many residues across its surface (**figure 5.1**). Some of these residues are phosphorylated by other kinases such as Aurora B, Cdk1 and Plk1, however, the bulk of these have been designated as autophosphorylation sites (Dou et al., 2011; von Schubert et al., 2015). Although over 30 different phosphorylation sites on Mps1 have been reported, surprisingly little is known about their contribution to Mps1 regulation and overall SAC signalling. As confirmed here, T676 is essential for regulating Mps1 activity and its phosphorylation is reversed by PP2A-B56 to put the brakes on Mps1. Other studied residues include eight N-terminal residues, S7, T12, T33, S37, S321, T360, T363 and 371 that have been implicated in controlling Mps1 localisation (Wang et al., 2014). Some residues on Mps1, T12 and T15, have been reported to be non-functional phosphorylations that do not contribute towards Mps1 activity, localisation or overall SAC signalling (Xu et al., 2008a). In support of this idea, this seems to be the case for other SAC proteins, for example, only 6 out of 19 MELT motifs on Knl1 are needed to be phosphorylated for maximum checkpoint activity (Zhang et al., 2014). The idea emerging is that phosphorylation is ubiquitous in the SAC pathway. A major challenge in understanding phosphoregulation is differentiating ‘driver’ and ‘passenger’ phosphorylations. Important phosphorylation events, that we have coined as ‘driver’ phosphorylations, are critical for protein function and SAC signalling, whereas, ‘passenger’ phosphorylations have lost their functional importance due to redundancy or evolutionary changes. However, separating these

phosphorylation events is difficult because while some phosphosites may not contribute to SAC signalling individually, multisite phosphorylation is known to be a key mechanism for the fine-tuned regulation of protein function (Xu et al., 2008a). For example, phosphorylation at nine residues on the unstructured tail of Hec1 serves to finely tune its interaction with microtubules (Zaytsev et al., 2015). How Mps1 phosphorylation changes on a protein level when the SAC is on and off was an unresolved question.

To address this problem, I established a quantitative approach by coupling Mps1 immunoprecipitation with mass spectrometry. Using an elegant phospho-proteomic protocol we compared Mps1 phosphorylation when the SAC is active and inactive. The gold standard experiment would have been to immunoprecipiate Mps1 from cells at key stages during an unperturbed mitosis, however, work in our lab had already shown that this was a huge technical challenge. Instead we recapitulated SAC silencing by treating cells with the specific Mps1 inhibitor AZ3146. Mps1 is largely dephosphorylated when the SAC is turned off due to the activity of a cellular phosphatase. Preliminary experiments indicate that PP2A-B56 is likely to be regulating these phosphorylation events. The Mps1 band, produced from cells depleted of all B56 subunits, was smeared in western blot analysis indicating that phosphorylation is largely retained in the absence of PP2A-B56 (**figure 5.7**). It is important to specify which phosphosites on Mps1 are precisely controlled by PP2A-B56 given it's overlapping function with PP1. A critical and outstanding experiment, is the quantitation of Mps1 phosphorylations by mass spectrometry in cells depleted of PP2A-B56. Further optimisation is needed to overcome the technical challenge of depleting B56 at a larger scale. However, if this approach proves to not be feasible other strategies could be explored. A less stringent approach would be to treat cells with Calyculin A prior to the inactivation of the checkpoint. By inactivating the PPP phosphatases, we would expect to inhibit the dephosphorylation of all phosphosites on Mps1 controlled by PPP family members. Alternatively, we could analyse Mps1 phosphorylation in cells expressing the very specific B56 docking mutant BubR1$^{L699A/I672A}$. Although this method would still rely heavily on siRNA, we have found that depleting a single protein generally yields far better results.

An *in vitro* approach could also be used to dephosphorylate Mps1 immunoprecipitates with purified PP2A-B56 phosphatases.

Nonetheless, these results suggested that Mps1 undergoes dramatic changes in phosphorylation when the SAC was inactive. Given that Mps1 is dynamically phosphorylated and dephosphorylated it seems likely that such a drastic change in protein modification is important in regulating its function. Therefore, a greater understanding of the functional importance of these phosphosites is needed. To this end, systematic knockdown of individual or groups of Mps1 phosphosites may provide some clues about their biological relevance and identify driving phosphorylations. Understanding mechanistically how these phosphorylations control Mps1 function is a key challenge in Mps1 regulation. The analysis presented here could be further extended to gain insight about PP2A-B56 and its function in SAC silencing. Advancements in proteomics have provided an opportunity to reliably identify new substrates. For example, a recent study used global quantitative phospho-proteomics to identify many novel Mps1 substrates (Maciejowski et al., 2017). Importantly this study revealed that Mps1 phosphorylates far more substrates than originally thought including previously unknown targets such as Ndc80, CENP-E, Rod, Mad1, H2A, Ska3 and DYNLC1. Having established a reliable method to deplete B56, my analysis could similarly be extended to globally search for PP2A-B56 substrates. Although, the global analysis of PP2A-B56 substrates is satisfactory for the identification of new substrates, in-depth analysis of these interactions would still be required for a full understanding. As always, the devil lies in the detail.

It has been known for some time that the activity of Mps1 is intimately associated with its localisation. When Mps1 is inactivated by different means it accumulates at kinetochores, suggesting that somehow Mps1 negatively regulates its own kinetochore localisation. Two models have been suggested to explain this negative feedback loop: autophosphorylation-mediated release (Jelluma et al., 2010) and ARHGEF17-coupled release (Isokane et al., 2016). Of these, the autophosphorylation model has been more widely received despite a lack of detail into its mechanics. In this simplistic model, Mps1 autophosphorylates itself

and somehow these phosphorylations decrease its affinity for kinetochores. Wang et al., 2007, proposed that eight N-terminal Mps1 residues where needed for this release mechanism. A non-phosphorylatable mutant (Mps1-8A) was slightly enriched at kinetochores and consistently a phosphomimic mutant (Mps1-8D) was slightly decreased. While Mps1-8A mutants were phenotypically normal the Mps1-8D mutants divided with a higher frequency of mis-segregation. In contrast, we observed that hyperphosphorylated Mps1 at S33/T37 in B56 depleted cells could still accumulate at kinetochores when inhibited with Mps1 (**figure 5.2**). The results presented here strongly conflict with the idea of autophosphorylation decreasing Mps1 kinetochore association. In agreement with this, biochemical studies demonstrated that phosphorylating Mps1 increases its interaction with Hec1 (Hiruma et al., 2015). Thus, logic would dictate that phosphorylation of Mps1 in cells should increase its association with Hec1 and kinetochores. An explanation for these discrepancies could be that the Mps1-8D mutant is structurally altered, which may account for why its phenotype is substantially more pronounced than the related Mps1-8A mutant. The second model that has been proposed is a feedback mechanism involving an effector called ARGHEF17 (Isokane et al., 2016). In this model, cytoplasmic Mps1 binds ARHGEF17 and together they localise to kinetochores, where Mps1 is phosphorylated and activated. Active Mps1 kinase phosphorylates ARHGEF17 which primes their release from kinetochores. The specific contribution that T33 and S37 play in regulating Mps1 localisation is unclear, but the results presented here would best fit a model whereby phosphorylation of an effector protein induces Mps1 release.

Two key regulatory mechanisms are ubiquitous in the SAC pathway; phosphorylation and protein:protein interactions. Having analysed changes in the activity and phosphorylation status of Mps1 I turned my attention to how Mps1 interactors regulate its function. As a starting point, I carried out an unbiased immunoprecipitation experiment to identify novel Mps1 interactors. The results from this analysis will be discussed in the next chapter.

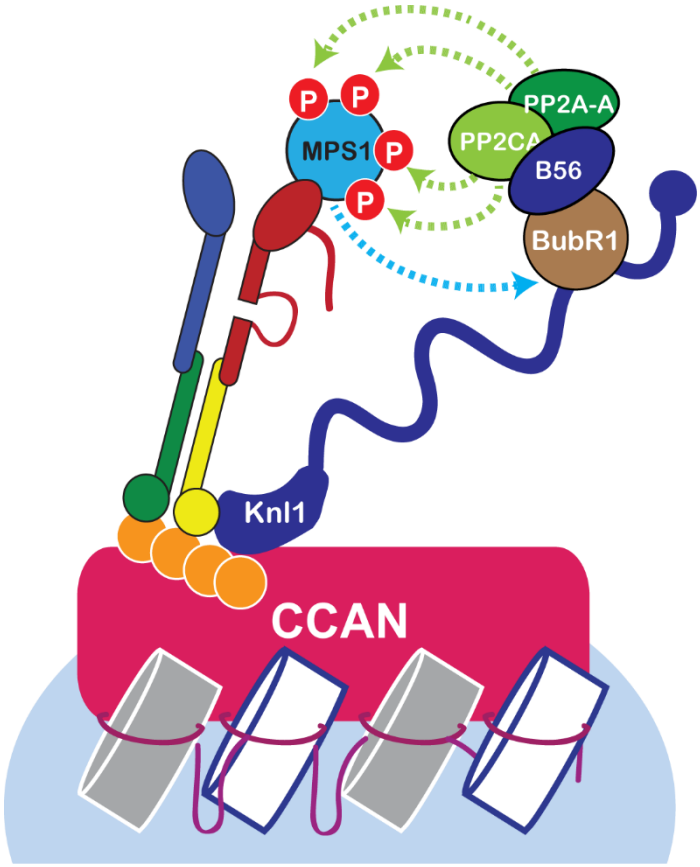

Figure 5.8. Multisite dephosphorylation of Mps1 by PP2A-B56. Diagram showing our current understanding of PP2A-B56 mediated dephosphorylation of Mps1. Mps1 recruits PP2A-B56 by BubR1 in a negative feedback loop. PP2A-B56 targets multiple sites on Mps1 to dephosphorylate and inactivate Mps1.

6.
IDENTIFICATION OF MPS1 KINETOCHORE INTERACTORS.

6.1 Introduction.

SAC signalling is dependent on the activity of kinetochore-localised Mps1 to further recruit other SAC proteins including Bub3, BubR1 and Mad2 which make up the anaphase inhibiting signal. Blocking the release of Mps1 from kinetochores stops the SAC from being turned off and perturbs anaphase onset (Ito et al., 2012; Jelluma et al., 2010; Maldonado and Kapoor, 2011). The Hec1 protein, a member of the Ndc80 complex, has been established as the major kinetochore receptor of Mps1 and is its only known interaction partner (Hiruma et al., 2015; Ji et al., 2015). The Hec1-Mps1 interaction is regulated by the upstream kinase Aurora B to integrate the EC pathway with the SAC network. There is convincing evidence from multiple studies to support this interaction, for example, inhibiting Aurora B with small molecule inhibitors or depleting Hec1 by siRNA blocks the recruitment of Mps1 to kinetochores (Martin-Lluesma et al., 2002; Saurin et al., 2011; Zhu et al., 2013). The interaction between Mps1 and Hec1 is weak and presumed to be transient to allow the dynamic recruitment and release of Mps1 from kinetochores. The tenuous nature of this interaction provides one explanation as to why it had not been detected in human cells before this study (Hiruma et al., 2015; Ji et al., 2015).

In addition to modulating the recruitment of Mps1, the Ndc80 complex is essential for mediating the interaction between kinetochores and microtubules (Long et al., 2017; Cheeseman et al., 2006; Foley and Kapoor, 2013). Both the Ndc80:Mps1 and Ndc80:microtubule interactions are made through the N-terminal calponin homology (CH) domain of Hec1. Previous studies demonstrated that, Mps1 localises to kinetochores, by its N-terminal extension (NTE) and tetratricopeptide repeat (TPR) domain. In line with this, truncated versions of Mps1 lacking these domains fail to bind kinetochores (Nijenhuis et al., 2013). To interact with Hec1, Mps1 relies on its NTE domain which directly contacts the CH domain of Hec1. The Hec1-Mps1 interaction can be promoted *in vitro* by the phosphorylation of both proteins (Hiruma et al., 2015). Recently it was shown that engineering mutations at four key Hec1 residues at the Hec1-Mps1 interface, based on structural data, disrupted this interaction in human cells (Hiruma et al., 2015).

Additionally, work by the Yu lab demonstrated that molecules of Mps1 are also bound to the CH domain of Nuf2. This interaction relies on a third region of Mps1 coined the middle region (MR) domain. Disrupting this interaction by expressing the N126A Nuf2 mutant abrogated the phosphorylation of Knl1 and the binding of downstream SAC proteins (Ji et al., 2015). Since Hec1 and Nuf2 are components of the same complex, one could imagine that the binding of Mps1 molecules to these sites orients them for trans-autophosphorylation. Recent studies have built on these observations, to demonstrate that microtubules directly disrupt the Ndc80 complex -Mps1 interaction (Ji et al., 2015; Hiruma et al., 2015). In this model, Mps1 binding is the critical step in microtubule sensing. Mps1 dynamically cycles on and off the kinetochore until eventually the formation of end-on attachments prevents its rebinding. This suggests that a crucial step in SAC inactivation is the binding of microtubules at the Ndc80 complex. Thus, kinetochores sense microtubule binding through the competition between Mps1 and microtubules. It is thought that Mps1 is an evolutionarily conserved sensor of K-MT attachments.

In addition to being regulated by microtubules, the Hec1-Mps1 interaction is controlled by Aurora B kinase the major effector of the EC pathway. Aurora B phosphorylates the N-terminal tail of Hec1 at nine serine residues to decrease its affinity for microtubules (Martin-Lluesma et al., 2002; Nijenhuis et al., 2013; Saurin et al., 2011; Zhu et al., 2013; Hiruma et al., 2015; Ji et al., 2015; DeLuca et al., 2011). Thus, Aurora B promotes the Hec1-Mps1 interaction. As end-on attachments arise, Aurora B is spatially separated from the Ndc80 complex. Reduced phosphorylation of the Ndc80 complex is associated with the release of Mps1 from kinetochores. Biochemical experiments and molecular dynamic simulations demonstrated that the nine phosphorylation events are additively integrated to fine-tune the Ndc80-microtubule interaction (Zaytsev et al., 2015). Consistent with these ideas, treating cells with the specific Aurora B inhibitor, ZM447439, perturbs Mps1 kinetochore localisation (Zhu et al., 2013; Saurin et al., 2011). A non-phosphorylatable Hec1 mutant, Hec1-9A, had reduced Mps1 kinetochore binding. Furthermore, a phospho-mimicking mutant, Hec1-9D, had increased Mps1 kinetochore signal (Zhu et al., 2013). Taken together these

results present a strong case for an interaction between Hec1 and Mps1 that is under the regulation of Aurora B.

Many kinases interact with binding partners to achieve maximum activity. Cdks are perhaps the best example of a kinase activated by the binding of a regulatory interaction partner. Cyclins have a central role in substrate recognition (see 1.1.2). Other kinases such as the Aurora kinases use the binding of interactors as an activation mechanism. Aurora A associates with the microtubule based protein TPX2 which triggers the phosphorylation of its T-loop (Bayliss et al., 2003). Work from our lab showed that this phosphorylation event is reversed by the action of the PP6 phosphatase (Zeng et al., 2010). Likewise, the catalytic activity of the Aurora B kinase is controlled by its interaction with INCENP a component of the CPC complex (Carmena et al., 2012). In addition to a gain of function, some interaction partners inhibit kinase activity for example p21 is a biological inhibitor of a subset of Cdks (Abbas and Dutta, 2009). The role of interactors in the regulation of Mps1 function had not been investigated. We hypothesised that the identification of novel binding partners would provide new insight in to how Mps1 functions at kinetochores. To this end, we carried out an Mps1 immunoprecipitation coupled to mass spectrometry to find other Mps1 interactors.

Aims:

- Establish the tools needed to study Mps1 interactors by first confirming that the Hec1-Mps1 interaction occurs in human cells.
- Carry out Mps1 immunoprecipitation followed by mass spectrometry to identify novel Mps1 interactors.
- Knock-down experiments to understand how these interactors influence Mps1 function.

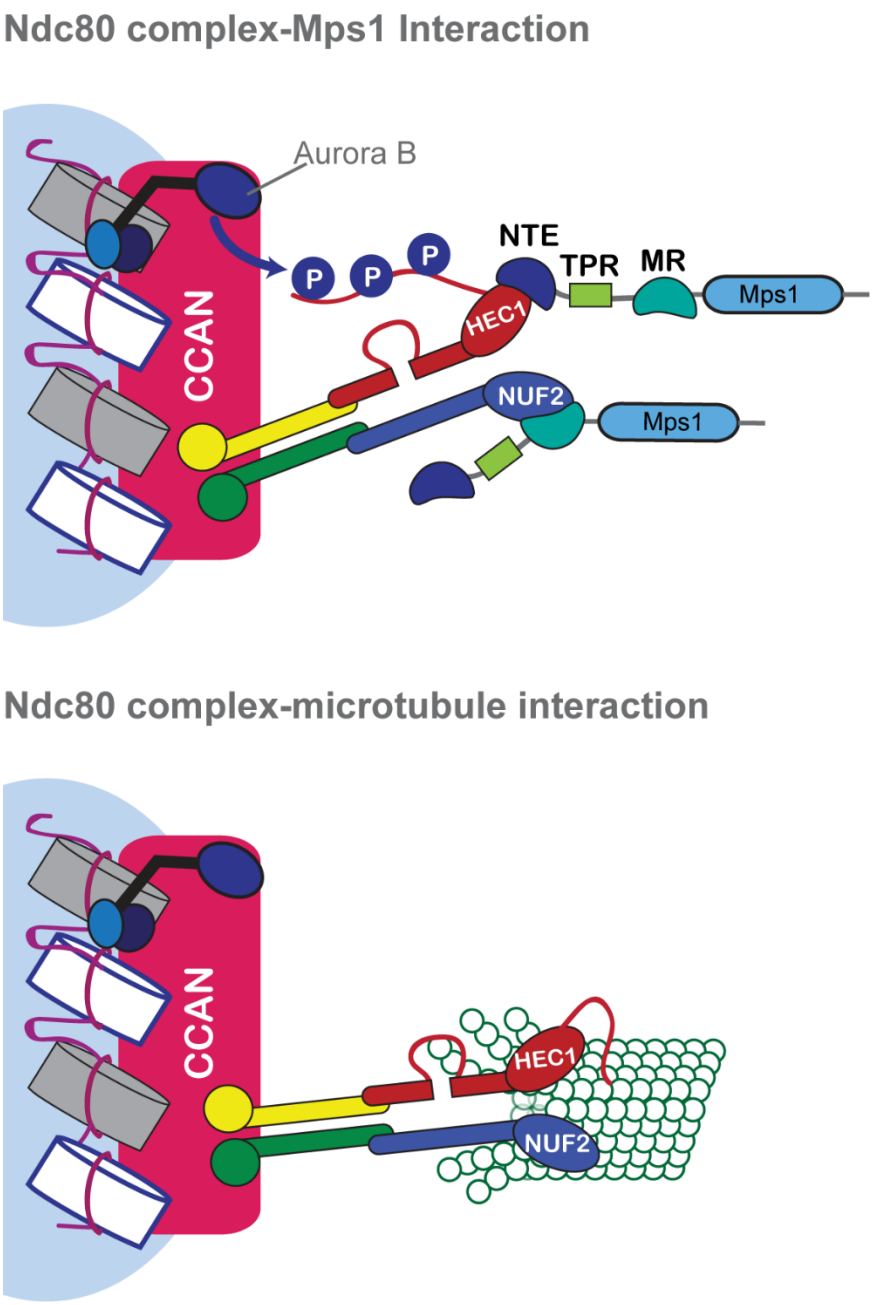

Figure 6.1. Current model for Mps1 kinetochore binding. Hec1 and Nuf2 are required for Mps1 binding. **(A)** Aurora B phosphorylates Hec1 to promotes its interaction with Mps1. The NTE domain of Mps1 binds to the CH-domain of Hec1 and the MR domain binds to Nuf2. **(B)** The binding of microtubules to Hec1 and Nuf2 blocks Aurora B phosphorylation of Hec1 and this leads to the release of Mps1 from kinetochores. Adapted from Hiruma et al., 2015 and Ji et al., 2015.

6.2.1 Aurora B and Hec1 are needed to localise Mps1 to kinetochores.

As a prerequisite to immunoprecipitation experiments investigating Mps1 interactions, I aimed to develop the tools needed to detect its interaction with Hec1, a known interactor. It had been proposed that Aurora B kinase activity and Hec1 were needed for kinetochores to bind Mps1 (Nijenhuis et al., 2013; Zhu et al., 2013; Saurin et al., 2011). In this model, when the SAC is active Aurora B kinase phosphorylates multiple N-terminal serine residues on Hec1 to promote the Hec-Mps1 interaction. The attachment of microtubules to kinetochores inactivates Aurora B leading to the dephosphorylation of Hec1 and the release of Mps1 from kinetochores (DeLuca et al., 2011; Saurin et al., 2011; Zhu et al., 2013). Abrogating Aurora B activity using the chemical inhibitor ZM447439 reduced GFP-Mps1 kinetochore localisation (**figure 6.2A-B**). Next, Hec1 was knocked-down to assess its role in controlling Mps1 kinetochore binding (**figure 6.2C-D**). Hec1 depletion, like Aurora B inhibition, prevented GFP-Mps1 from binding to kinetochores. These results support the current model (**figure 6.2E**) in which Hec1 and Aurora B are required to localise Mps1 to kinetochores. However, evidence of a direct interaction between Mps1 and Hec1 is lacking.

Other studies have described the Mps1-Hec1 interaction based on *in vitro* experiments between purified fragments (Zhu et al., 2013; Hiruma et al., 2015; Ji et al., 2015). However, an interaction between endogenous full-length proteins had not been reported to date. Here, an *in vivo* approach was taken to find out whether the Mps1-Hec1 interaction occurs between endogenous proteins in human cells using immunoprecipitation. As described previously (figure 5.3 and section 2.6.3), I optimised my immunoprecipitation protocol to release kinetochore assemblies into the supernatant using the micrococcal nuclease enzyme. Hec1 complexes were immunoprecipitated and Mps1 and Nuf2, known interactors, were pulled-down (**figure 6.3A**). A small level of the SAC protein Bub1 was also detected, whereas a negative control Eg5 was completely absent. Hec1 was enriched in a reciprocal Mps1 IP providing additional support for a potential interaction between Mps1 and Hec1 in cells. While an interaction between purified Hec1 and Mps1 fragments had been described *in vitro* (Zhu et

al., 2013), this is the first demonstration of a clear interaction between endogenous proteins. In line with the current model, the ability for Hec1 to pull-down Mps1 was sensitive to Aurora B inhibition (**figure 6.3B**). So far, my results confirm that Hec1 is needed for the kinetochore binding of Mps1 and this interaction is promoted by Aurora B dependent phosphorylation of kinetochore targets.

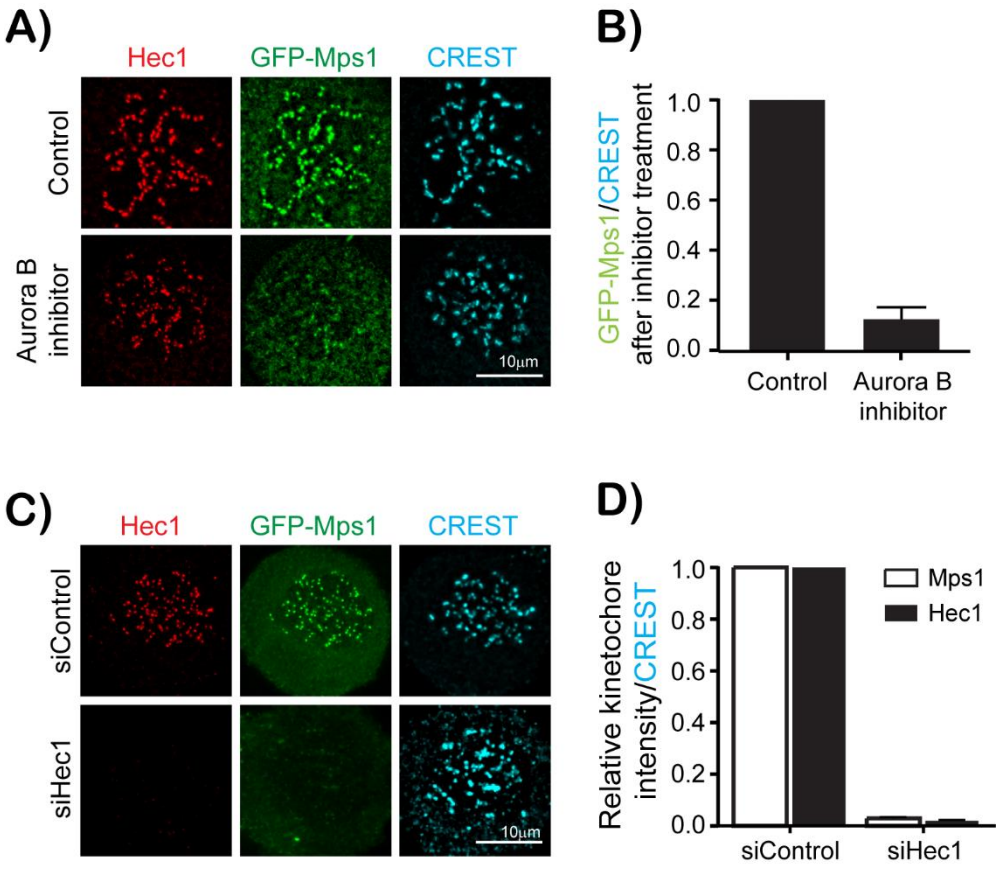

Figure 6.2. Aurora B activity and Hec1 are important for Mps1 localisation. **(A)** Mitotic cells were treated with MG132 or MG132 and Aurora B inhibitor and stained for GFP-Mps1, anti-Hec1 and anti-CREST. **(B)** Quantification of GFP-Mps1 kinetochore signal in control and Aurora B inhibited cells. **(C)** Cells were treated with siControl or siHec1 and stained as before. **(D)** Quantification of GFP-Mps1 and Hec1 kinetochore signals in siControl or siHec1 cells.

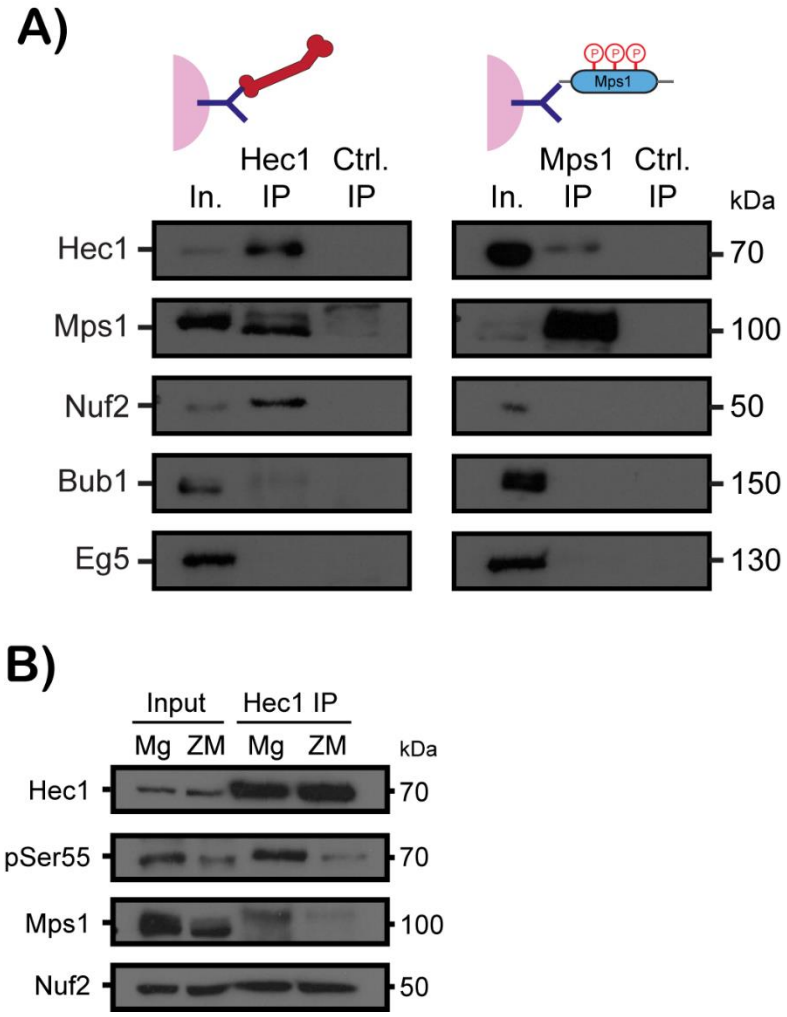

Figure 6.3. The Mps1-Hec1 interaction is sensitive to Aurora B inhibition. **(A)** Hec1 and Mps1 IPs were carried out and analysed for Nuf2, Bub1 and as a negative control, the microtubule motor protein, Eg5. **(B)** Aurora B inhibition prevents Mps1 from associating with the Hec1 complex, but not Nuf2.

6.2.2 Identification of novel Mps1 interactors.

Thus far, Hec1 had been identified as the major kinetochore receptor of Mps1. Many kinases bind to interaction partners, and this can influence their activity, localisation or the recognition of a subset of substrates. Before this study, the idea of Mps1 having additional interactors had not been tested. I postulated that finding novel binding partners would give new insight into Mps1 function. To answer this question, I carried out Mps1 immunoprecipitation followed by mass spectrometry to uncover novel Mps1 interactors at kinetochores. Mps1 complexes were immunoprecipitated from HeLa cells, samples were run on an SDS-PAGE gel and the gel was analysed by staining with Coomassie blue before mass spectrometry (**figure 6.4A**). There were two bands present in Mps1 IPs at 100kDa and 260kDa that were absent in the control IP. The 100kDa band corresponded to the molecular weight of Mps1 and although the identity of the 260kDa band was yet to be determined, it corresponded to the molecular weight of Knl1. Intriguingly, mass spectrometry analysis of Mps1 complexes in two separate experiments identified Knl1 (CASC5) and Shugoshin 2 (SGO2) as the top Mps1 interactors (**figure 6.4B**). Therefore, the 260kDa band was likely to correspond to Knl1 (**figure 6.4A-B**). In both experiments, Knl1 produced a strong signal in Mps1 IPs, but was almost absent in control IPs (**figure 6.4C**). These results suggest that Knl1 is potentially a main interactor for Mps1. Surprisingly, only a single peptide of Hec1 or Nuf2 was detected by mass spectrometry. Why Hec1 was seen in western blot analysis, but not by mass spectrometry was unclear. A direct interaction between Hec1 and Mps1 had been described *in vitro* by several studies (Martin-Lluesma et al., 2002; Saurin et al., 2011; Hiruma et al., 2015; Ji et al., 2015; Zhu et al., 2013). However, it is important to note that owing to the transient nature of Mps1 localisation at kinetochores its interaction with Hec1 had never been proven in cells. It was possible that unknown technical difficulties could account for these discrepancies and therefore, it was essential that we tested the Mps1-Hec1 and Mps1-Knl1 interactions by other techniques.

The second highest candidate protein SGO2 was only enriched in a single Mps1 IP experiment. I tested whether SGO2 was indeed an Mps1 interactor by western

blot analysis, but this interaction was not investigated further due to a lack of a satisfactory antibody. Recently, it was reported that Mps1 and Bub1 activity was needed for the recruitment of SGO2 to centromeres in mouse oocytes (El Yakoubi et al., 2017). Although a direct interaction between Mps1 and SGO2 was not identified, further investigation of this interaction in human cells should be considered. The Bub proteins and Nuf2 were also detected at low levels, however, this was likely to be due to their interaction with Knl1. The mass spectrometry data presented here have possibly uncovered Knl1 as a major Mps1 interaction partner (**figure 6.4**).

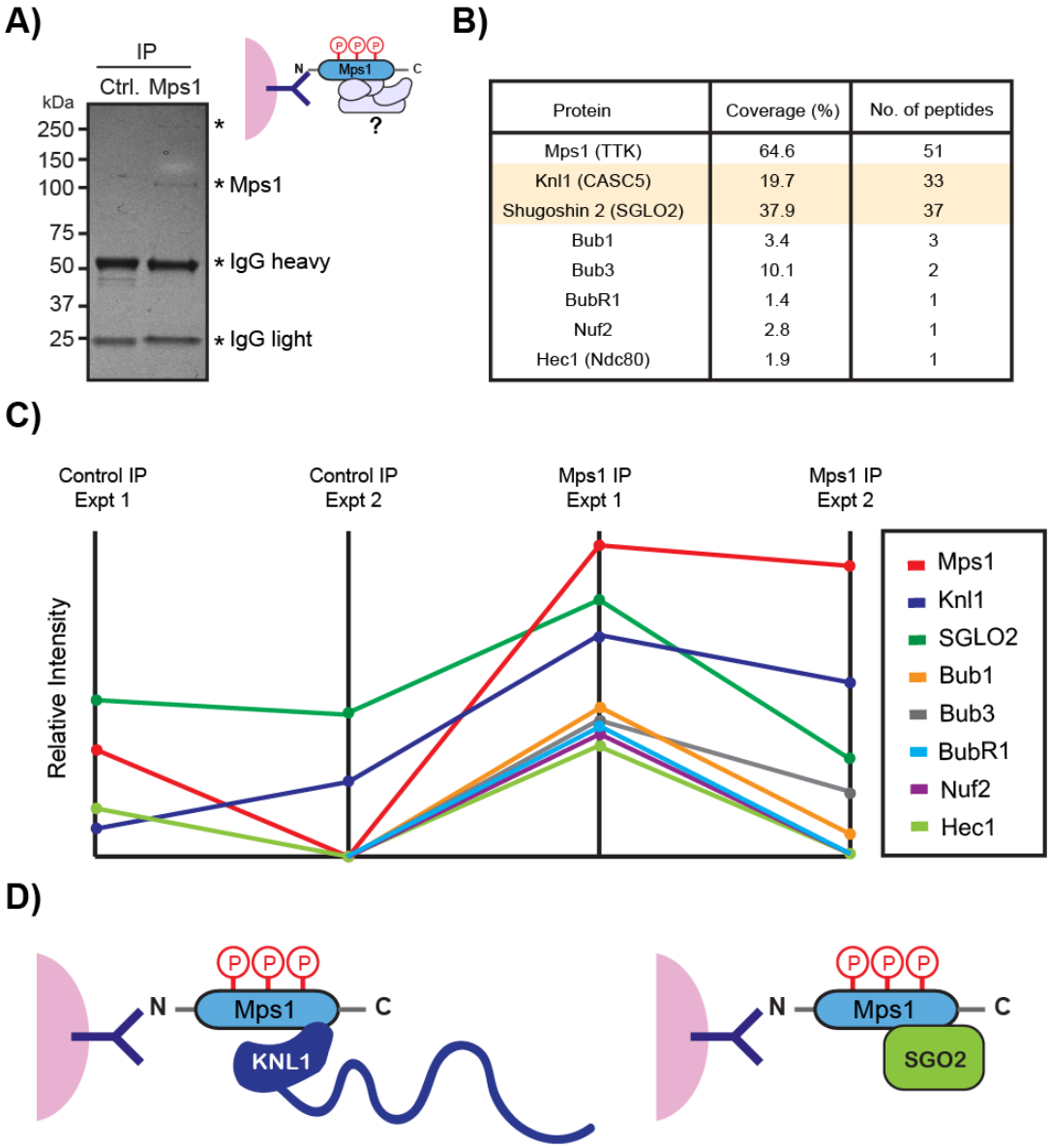

Protein	Coverage (%)	No. of peptides
Mps1 (TTK)	64.6	51
Knl1 (CASC5)	19.7	33
Shugoshin 2 (SGLO2)	37.9	37
Bub1	3.4	3
Bub3	10.1	2
BubR1	1.4	1
Nuf2	2.8	1
Hec1 (Ndc80)	1.9	1

Figure 6.4. Knl1 and Shugoshin2 were the top interactors in the Mps1 IP. Mps1 complexes were immunoprecipitated and mass spectrometry was performed in two separate experiments. **(A)** Control and Mps1 IPs were initially analysed by staining protein gels with Coomassie blue dye before mass spectrometry. **(B)** A table showing the coverage and number of peptides for the top Mps1 interactors. Mps1, Knl1 and SGO2 were the most enriched proteins when compared to the species-specific control. **(C)** Comparison of the relative intensity of different proteins between control and Mps1 IPs from two separate experiments. Proteins were labelled as indicated in the key. **(D)** Knl1 and SGO2 are the top interactors that came down by this method.

6.2.3 Knl1 regulates Mps1 kinetochore localisation.

Following the mass spectrometry results, further Mps1 IPs were performed for validation and indeed Knl1 was consistently enriched by western blot analysis. Hec1 was significantly enriched, albeit to a lesser extent than Knl1, and Bub1 showed up after long exposures. It was unclear why Hec1 was detected in Mps1 IPs by western blot analysis but not by mass spectrometry (**figure 6.5A**), whereas, both mass spectrometry and western blot analysis demonstrated that the Mps1-Knl1 interaction was the most stable (**figures 6.4&6.5**). Knl1 is a substrate of Mps1 that is phosphorylated at multiple residues however despite this, we would not expect a kinase-substrate interaction to be so stable. Based on these results, we hypothesised that perhaps a pool of Mps1 may also bind to Knl1 to localise to kinetochores.

To understand how Knl1 controls Mps1 localisation I used siRNA to deplete cells of Hec1 and Knl1 and investigated changes in their localisation. GFP-Mps1 cells were synchronously released into mitosis, mitotic exit was blocked by the addition of MG132 and the SAC was activated by nocodazole treatment. Hec1 depletion blocked Mps1 from binding to kinetochores. In addition to this, Hec1 depletion reduced Knl1 at kinetochores to 32% of that of control cells (**figure 6.5B-C**). Importantly, the knockdown of Knl1 was sufficient to evict Mps1 from kinetochores despite the presence of ~70% of Hec1. It was possible that the 30% of Hec1 lost in Knl1-depleted cells may represent a functionally important pool of Hec1 required for Mps1 binding. Based on these results, Knl1 is important for Mps1 to associate to kinetochores. To bind kinetochores Knl1 interacts with the C-terminal tail of the Mis12 complex subunit Nsl1. Disruption of the Mis12:Knl1 interaction by siRNA mediated depletion of Dsn1 blocks Knl1 localisation (Cheeseman et al., 2004, 2008). These results contrast previous studies, because others have not been able to detect a reduction in Knl1 in human cells depleted of Hec1 or through biochemical experiments (Cheeseman et al., 2006, 2008; Pagliuca et al., 2009; Petrovic et al., 2010). There are some disparities in studies focused on co-dependency, for example, Cheeseman et al, 2008 reported that the Mis12 proteins dissociate from kinetochores after Knl1

depletion. However, despite a reduction in the Mis12-complex they did not see the logically expected loss of Hec1 in human cells. In the same study they observed a 45% reduction in Hec1 at kinetochores in chicken cells (Cheeseman et al., 2008). Consistent with these results a more recent study showed that Hec1 levels are decreased by ~40% after Knl1 depletion in human cells (Caldas et al., 2013). Moreover, Hec1 is needed for the kinetochore localisation of Zwint1 which is supposed to contribute to Knl1 localisation (Lin et al., 2006). Further investigation is needed to determine the reciprocal kinetochore binding mechanism of Hec1 and Knl1. Nevertheless, these siRNA experiments clearly demonstrate that the removal of either Knl1 or Hec1 significantly decreases ability of Mps1 to bind to kinetochores. Understanding how Mps1 binds to kinetochores is somewhat complicated because of the co-dependency of Hec1 and Knl1 on kinetochore binding.

6.2.4 The N-terminus of Knl1 is important for Mps1 binding.

So far, mass spectrometry and siRNA-based experiments pointed towards an interaction between Knl1 and Mps1. Next, I aimed to define the specific region on Knl1 needed for this interaction. While searching the literature we noticed that a previously published paper found that Mps1 is pulled-down in IP experiments on an N-terminal Knl1 fragment Knl1$^{1-250}$ (Krenn et al., 2014). To validate whether Mps1 indeed binds to the N-terminal of Knl1, I performed a similar experiment on an available N-terminal fragment Knl1$^{1-350}$. This fragment consists of several motifs including the PP1 binding motif, KI1, KI2, and MELTs 1-4, but importantly the kinetochore binding domain is lacking (**figure 6.6A**). As expected, when Knl1$^{1-350}$ is immunoprecipitated from HEK293T cells, known Knl1 interactors such as Bub1, BubR1 and PP1 are bought down (**figure 6.6B**). Importantly, Mps1 was pulled-down in this IP and was enriched at least as much as PP1, a known interactor. Hec1 was not present in the IP sample because this fragment of Knl1 does not bind to kinetochores. This provides further support to the idea that the Knl1-Mps1 interaction is not dependent on Hec1.

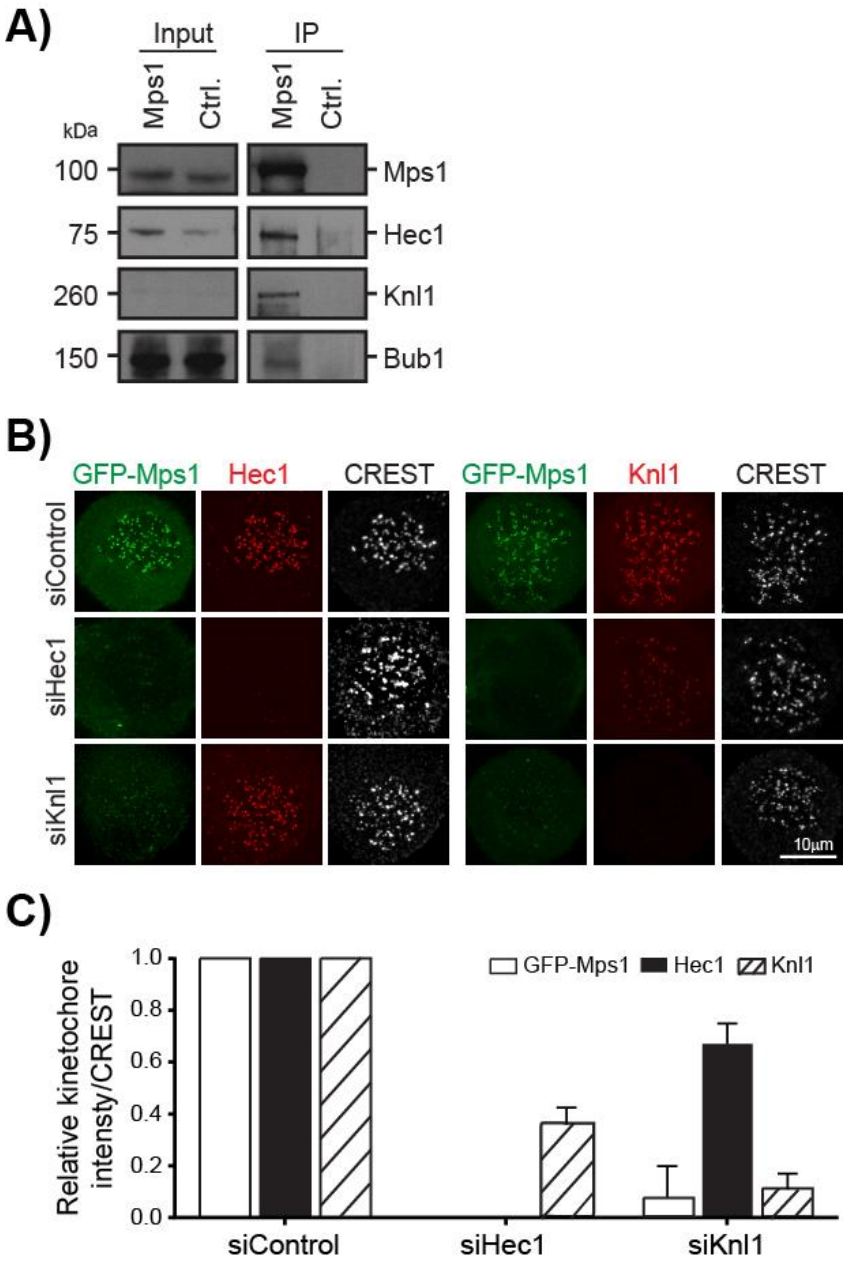

Figure 6.5. Depletion of Knl1 disrupts Mps1 from localising to kinetochores. **(A)** Immunofluorescence analysis of cells depleted of Hec1 and Knl1. Cells were stained for GFP-Mps1, anti-Hec1, anti-Knl1 and anti-CREST. **(B)** Quantification of GFP-Mps1, Hec1 and Knl1 staining demonstrated that GFP-Mps1 was significantly reduced when either Hec1 or Knl1 were depleted. It also revealed that Hec1 and Knl1 influence one another's localisation.

While IP experiments demonstrate that two proteins may be part of a complex they do not provide evidence for a direct protein:protein interaction. Next, using an *in vitro* approach I aimed to demonstrate direct binding between recombinant Mps1 and purified Knl1 fragments. Two fragments of Knl1 were purified to investigate if this interaction was dependent on MELT motifs, Knl1$^{1-350}$ as described previously and Knl1$^{350-728}$ which only contains MELT motifs (**figure 6.7A**). Similar *in vitro* binding assays had been successfully performed on Hec1 and Mps1 fragments, and therefore, I used purified Hec1 fragments as a positive control (Zhu et al., 2013; Ji et al., 2015). GST-tagged Hec1 or Knl1 fragments were bound to GST beads and incubated with purified His-Mps1 for an hour. Western blot analysis showed that Mps1 was not bound in any condition that we tested (**figure 6.7C**) including in the positive control Hec1 1-196. The interaction between Knl1$^{1-350}$ and Mps1 was shown *in vivo* (**figure 6.6B**) and it is possible that we were unable to see this *in vitro* because of a lack of modifications on Knl1 fragment for example phosphorylations on MELT motifs. Further optimisation is needed to establish an *in vitro* binding assay, and this should indicate which specific Hec1 and Knl1 fragments are able to bind Mps1.

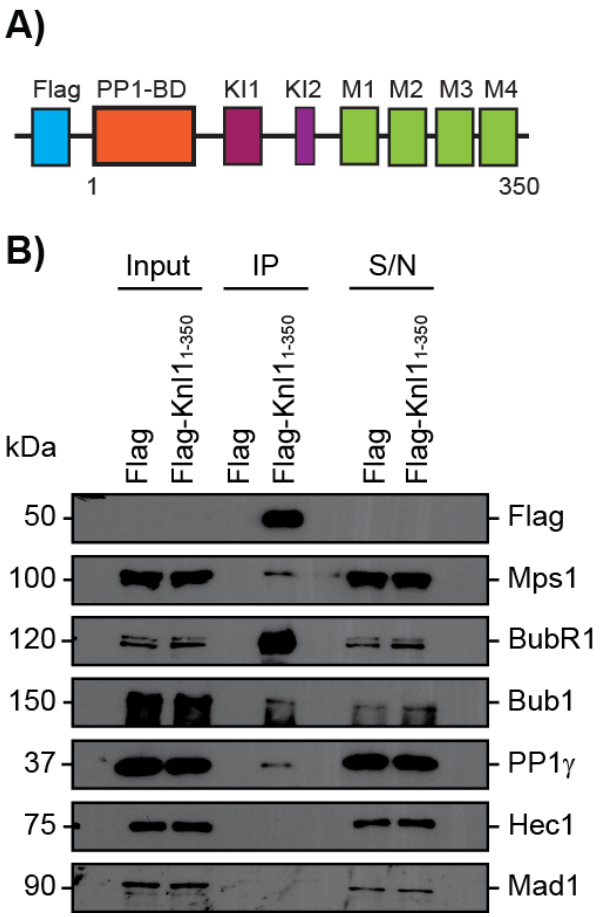

Figure 6.6. The Knl1 fragment$^{1-350}$ pulls down Mps1. (A) Diagram showing the motifs in the Knl1$^{1-350}$ fragment. The motifs include the PP1 binding domain (PP1-BD), KI1 and KI2 and MELT motifs (M1-M4). **(B)** The flag-Knl1$_{1-350}$ fragment was transfected into HEK293T cells and a flag immunoprecipitation was carried out. Several SAC components are pulled down in the flag IP most importantly Mps1.

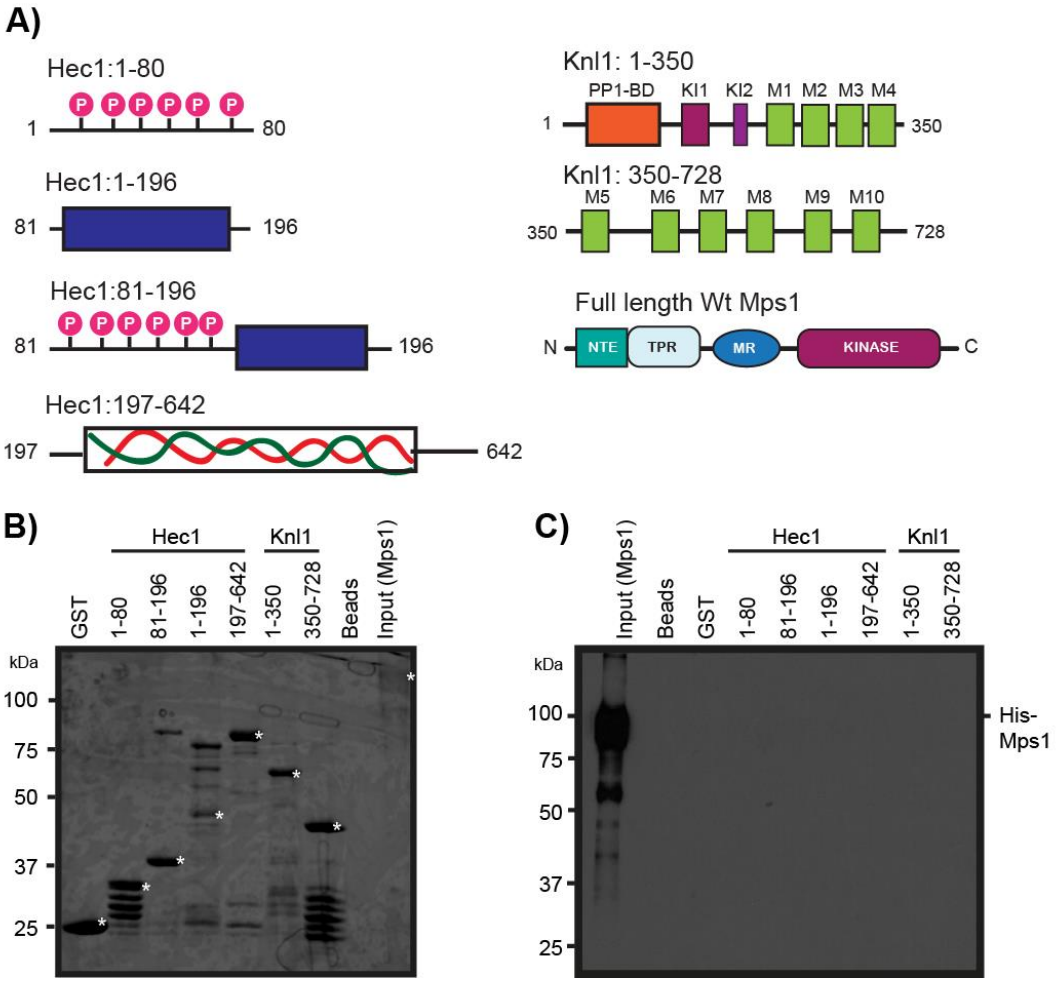

Figure 6.7. *In vitro* binding assay of Hec1 and Knl1 fragments with full length Mps1. (A) The indicated fragments were purified and **(B)** a binding assay was performed *in vitro.* Purified Hec1 and Knl1 fragments were each incubated with His-Mps1 coupled to His-beads. Samples were run on a Coomassie gel to determine whether Mps1 was pulled down by any of the fragments. Asterisks highlight the bands corresponding to the purified proteins. **(C)** Western blot analysis confirmed that Mps1 did not interact with any of these fragments.

6.3 Discussion

Summary

Proteomic analysis of Mps1 complexes identified two novel interactors Knl1 and SGO2, whereas proposed interactors such as Hec1 and Nuf2 were absent in Mps1 IPs (**figure 6.8**). Knock-down of Hec1 and Knl1 revealed that Mps1 was indeed lost from kinetochores when these proteins are absent. Intriguingly this study provided support to a model in which Hec1 and Knl1 are co-dependent in binding to kinetochores. Knl1 was dependent on Hec1 to bind kinetochores and vice versa. Mps1 was pulled-down with an N-terminal Knl1 fragment that was unable to bind kinetochores indicating that the Mps1-Knl1 interaction does not require Hec1. Confirmation of a direct interaction between Mps1 and Knl1 and exact details about the specific domains involved should be the focus of future work.

6.3.2 Discussion

The binding of interaction partners is a common mechanism used to regulate kinases (Bayliss et al., 2012). Here, we investigated whether Mps1 interacted with other proteins besides its kinetochore receptor the Ndc80 complex. The identification of new interactors would provide important insight into Mps1 function and regulation. To this end, we conducted Mps1 immunoprecipitation followed by mass spectrometry to search for novel interactors.

The composition of Mps1 complexes, immunoprecipitated from cell lysates of mitotic cells, was resolved by mass spectrometry (**figure 6.4**). Proteomic analysis identified Knl1 and SGO2 as possible Mps1 interactors that had not been previously characterised. It is important to note that previously trusted Mps1 interactors like Hec1 and Nuf2 were not detected by mass spectrometry, however, it is widely believed that this interaction is weak and transient in nature. Next, we confirmed the Mps1-Knl1 interaction occurred in cells by immunoprecipitation (**figure 6.5A**). Further to this, using Knl1 siRNA we demonstrated that in addition to Hec1, Knl1 is also critical in regulating the localisation of Mps1. There are three possibilities to explain my results in context with those of others: 1) Knl1 is a distinct binding receptor for Mps1, 2) Knl1 and Hec1 cooperate to bind Mps1 (**figure 6.8**) and 3) unknown technical problems are influencing these assays.

Research over the past decade has provided key insight into the mechanism of Mps1 localisation. Several observations can be made about the localisation of Mps1: it is controlled upstream by the Aurora B kinase, it requires Hec1 to bind to kinetochores, phosphorylation of Mps1 influences its localisation and importantly its binding is inhibited by microtubule binding. Consistent with these results, a potential Mps1-Knl1 interaction would fit with these observations. Firstly, the N-terminal tail of Knl1 is phosphorylated by Aurora B and dephosphorylated by PP2A-B56 in response to microtubule binding (Cheeseman et al., 2006; M. Kapoor, 2013; Foley et al., 2011). Moreover, the dephosphorylation of Knl1 by PP2A-B56 is predicted to stabilise microtubule

binding (Foley et al., 2011). Secondly, the loss of Mps1 from kinetochores in Hec1 depleted cells could in part be explained by its co-dependency with Knl1 (**figure 6.5**) (Cheeseman et al., 2008; Lin et al., 2006; Caldas et al., 2013). Thirdly, while the Ndc80 complex is the major microtubule binding centre it has also been suggested from biochemical experiments that Knl1 directly functions in microtubule binding (Cheeseman et al., 2006). Knl1 is likely to control K-MT attachments in different species and its depletion results in a partial alignment phenotype, in which a significant number of chromosomes fail to congress and remain stranded at spindle poles (Desai et al., 2003; Cheeseman et al., 2008; Pagliuca et al., 2009; Caldas et al., 2013). Thus, when placed in the context of other studies, it is conceivable that Knl1 may represent a third kinetochore receptor of Mps1. This third binding site would inhibit the Knl1-microtubule interaction and would be sensitive to Aurora B activity.

Another possible binding strategy could be a cooperative binding mechanism whereby the Ndc80 complex and Knl1 bind Mps1 together. Intriguingly we didn't detect Hec1 by mass spectrometry in this assay and even in western blot analysis it was less enriched than Knl1. Others have provided considerable evidence to support the Mps1-Hec1 interaction (Martin-Lluesma et al., 2002; Zhu et al., 2013; Saurin et al., 2011; Hiruma et al., 2015; Ji et al., 2015). Most of these data have been in the form of biochemical experiments between recombinant fragments of Mps1 and Hec1 or Nuf2. However, mutating key residues at predicted binding interfaces, for example, in the N126A Nuf2 mutant or C4 Hec1 mutant, Mps1 was delocalised from kinetochores (Hiruma et al., 2015; Ji et al., 2015). Although it was suggested that these sites represent two distinct binding sites for Mps1, an alternative model could be that a single Mps1 interacts with both Hec1 and Nuf2 using different interaction domains. This could be extended to include Knl1 as a third point of contact. In this possible model, a single Mps1 protein could bind to three sites on the KMN (Knl1, Nuf2, Hec1) and in doing so would block the entire microtubule binding interface. Knl1 may be required to more stably bind Mps1 at kinetochores. The Mps1-Knl1 interaction was considerably more stable than its interaction with Hec1 (**figure 6.5**). An interesting observation from FRAP analysis was that only ~70% of Mps1 is rapidly turned over at kinetochores (**figure 3.8**).

This suggests that the remaining 30% is stably bound to kinetochores by a different mechanism, perhaps by interacting with Knl1. In this possible model, the two pools may have two distinct functions, the transient pool may be critical for microtubule sensing and turning on the SAC, whereas, the stably bound pool may be needed to maintain the SAC signal.

Although these preliminary results are potentially interesting it is important to note that this analysis differs from published data. Thus, we must consider possible technical issues to explain these results. Since, we did not detect Hec1, a trusted Mps1 interactor, one possibility to explain these results is that the homemade Mps1 antibody may cross-react with Knl1. However, we have also confirmed the Mps1-Knl1 interaction by IP using a commercially available antibody. Moreover, we saw this interaction in a different system involving HEK-293T expressing the Flag-Knl1$^{1-350}$ (**figure 6.6**). Another possibility is that we have stabilised a normally transient kinase-substrate interaction between Mps1 and Knl1. However, this seems unlikely and still cannot explain how Knl1 depletion removes Mps1 from kinetochores. So far, I have been unable to establish the correct conditions for *in vitro* binding assays (**figure 6.7**). This is likely due to differences in experimental set-up, for example, others have found that phosphorylation of Mps1 *in vitro* enables its interaction with Hec1 (Ji et al., 2015). Key future experiments are to confirm and map the Mps1-Knl1 interaction using purified fragments of these proteins

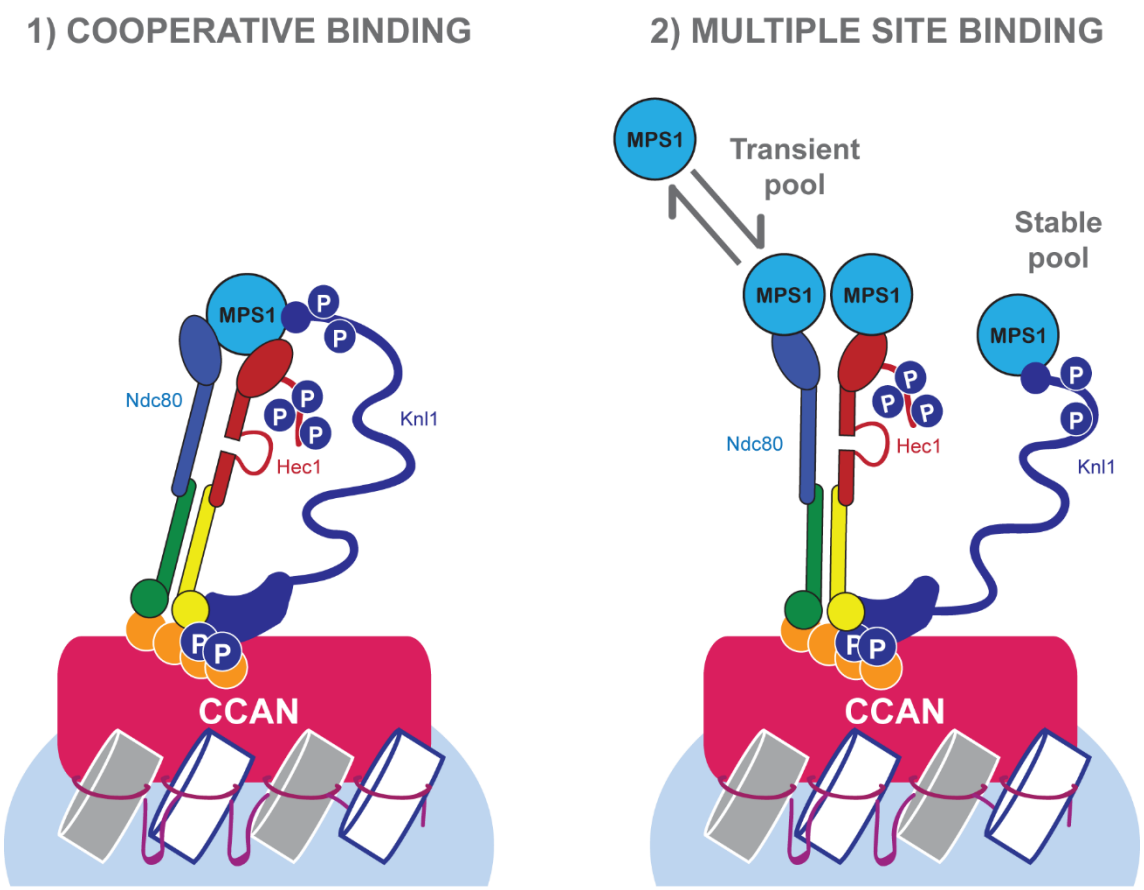

Figure 6.8 Binding mechanisms for Mps1. Two possible binding mechanisms for Mps1 based on ours and others results. Hec1, Nuf2 and Knl1 cooperate to bind a single Mps1 molecule. Alternatively, Mps1 binds to three different sites on the KMN network. Overall, the binding of Mps1 sterically blocks the KMN-microtubule interface.

7.

CONCLUDING REMARKS

7. CONCLUDING REMARKS

In the third decade of our investigation into the spindle checkpoint, one of the major challenges has been dissecting the function of Mps1. Mps1 has emerged as a master regulator of the SAC pathway. Now, after substantial research we have made some progress in deciphering function of Mps1. Mps1 phosphorylates multiple kinetochore targets, to positively regulate protein:protein interactions and in doing so it assembles the SAC module. At present, there are some gaps in our understanding of how this happens, however, it seems that a detailed model of how Mps1 builds the SAC module is just around the corner. So far, key milestones have included realising that Mps1 is required for the recruitment of all downstream SAC proteins (Tighe et al., 2008; Sliedrecht et al., 2010; Hewitt et al., 2010; Kwiatkowski et al., 2010; Santaguida et al., 2010; Maciejowski et al., 2010), the identification of Knl1 as a critical substrate (Yamagishi et al., 2012; London et al., 2012; Shepperd et al., 2012), that Mps1 acts as a microtubule sensor through competitive binding (Hiruma et al., 2015; Ji et al., 2015) and more recently the discovery of new Mps1 substrates by advanced proteomics (Maciejowski et al., 2017). While the function of Mps1 is an active area of research very little is known about how it is regulated. Given that Mps1 has a critical function in SAC signalling I hypothesised that there must be regulatory mechanisms in place to modulate its function. Logically Mps1 may be regulated at four points: its recruitment to, activation and inactivation at, and release from kinetochores. Thus, the primary aim of this study was to understand how Mps1 is regulated. In this concluding section, I will discuss how my results fit into the wider context, how ideas emerging from this work may lead onto new avenues of research and finally the pressing questions that remain in SAC regulation.

7.1.1 SAC INACTIVATION

While the SAC is critical for delaying anaphase when kinetochores are unattached, it is equally important that it is turned off so that chromosomes can be segregated to opposite spindle poles. The SAC is inactivated by three ways including dynein-mediated stripping, inhibition by p31-comet and dephosphorylation by the SAC phosphatases (Lara-Gonzalez et al., 2012). Together these mechanisms negatively regulate key events in the SAC pathway including the loading of the Mad1:Mad2 template (Howell et al., 2001), the conversion of O-Mad2 to C-Mad2 (Mapelli et al., 2006) and the Knl1:Bub3 interaction (London et al., 2012; Espert et al., 2014; Nijenhuis et al., 2014). During prometaphase, the kinetochore is phosphorylated by SAC kinases and this turns the checkpoint on. At metaphase, the kinases are turned off and SAC phosphatases rapidly reverse these phosphorylations. The PP1 and PP2A-B56 are thought to be the critical phosphatases responsible for turning the SAC signal off (Espert et al., 2014; Nijenhuis et al., 2014).

Recently, work in our lab showed that a BubR1 associated pool of PP2A-B56 phosphatase opposes Mps1 function by directly reversing phosphorylations on the MELT motifs of Knl1 (Espert et al., 2014). The removal of phospho-MELT sites released the Bub proteins from kinetochores and turned the SAC off. Reversible protein phosphorylation is a central theme in most signalling networks. Based on the fact that phosphorylation is ubiquitous in the SAC pathway, it seemed likely that many of these phosphorylation events may be controlled by mitotic phosphatases. The most upstream phosphorylation event in the checkpoint is the autoactivation of Mps1 kinase by trans-autophosphorylation. In this study, we found that the PP2A-B56 phosphatase directly dephosphorylates the T-loop of Mps1, both *in vitro* and *in vivo.* PP2A-B56 mediated dephosphorylation of Mps1 inactivates its kinase domain and in turn negatively regulates the SAC pathway. Disrupting the PP2A-B56 mediated dephosphorylation of Mps1, increases its activity, the recruitment of SAC proteins and the length of time cells spend in mitosis. Thus, PP2A-B56 silences the SAC signal through a two-step process. Firstly, PP2A-B56 dephosphorylates the T-

loop of Mps1 and this switches Mps1 into an inactive configuration. Secondly, PP2A-B56 removes phosphate groups from Knl1 to release Bub proteins already docked at kinetochores (Espert et al., 2014). Together this inhibits the loading of the Mad1:Mad2 template and the production of the MCC at kinetochores. These findings are a significant advance in understanding how PP2A-B56 silences the mitotic checkpoint. In agreement, with these results a separate study showed that PP2A-B56 dephosphorylates N-terminal sites on Mps1 (Maciejowski et al., 2017). Whereas, in drosophila PP1 was identified as the major SAC phosphatase that regulates Mps1 T-loop phosphorylation (Moura et al., 2017). The PP1 and PP2A-B56 play overlapping functions in humans and therefore, a more rigorous analysis is needed to determine their individual contributions. The next important step is building on the preliminary experiments presented here to define which specific phosphosites on Mps1 are regulated by PP2A-B56. Secondly, a systematic analysis of these sites is needed to define their biological significance.

Currently our work and those of others on the SAC phosphatases, has been limited to only two phosphorylation events, pKnl1 and pMps1, both of which are controlled by Mps1 kinase (Rosenberg et al., 2011; Nijenhuis et al., 2014; Espert et al., 2014; Moura et al., 2017; Maciejowski et al., 2017). This has largely been due to a lack of detailed information on Mps1 kinetochores substrates. Towards the end of this project, another research group carried out a phospho-proteomic analysis to identify novel Mps1 substrates. The results of this screen emphasised that Mps1 has many targets at the kinetochore including the SAC proteins Bub1, BubR1, Mad1, Mad2, Rod and the Ndc80 complex, as well as, other proteins important in chromosome segregation such as Ska3, Cenp-E, H2A and DYNLC1 (Maciejowski et al., 2017). Overall, this new information highlights that it has not been fully appreciated that Mps1 has a much more overarching function in regulating chromosome segregation. Consistent with the cold stability experiments shown here (**figure 4.10**), they found that PP2A-B56 stabilised K-MT attachments by opposing the Mps1-mediated phosphorylation of Ska3.

Thus, I hypothesise that PP2A-B56 plays a more global role in regulating other, if not all, Mps1 kinetochore substrates. To address such a question, future

experiments could expand on our current phospho-proteomic analysis of B56-depleted cells. In addition to specifically looking at changes in Mps1 phosphorylation when B56 is depleted, we could search more widely at other Mps1 substrates by immunoprecipitating entire kinetochores or analysing the entire phosphoproteome of a cell. A model study recently answered a similar question for the PP2A-B55 phosphatase (Cundell et al., 2016). In this study phospho-proteomics combined with kinetic modelling was used to identify novel substrates as well as the dephosphorylation rate and temporal properties of each substrate. The idea of temporal control is an interesting point because it seems likely that the phosphorylation at and composition of kinetochores is highly dynamic as microtubule attachments are initiated, tested and matured. Understanding the timing of phosphorylation and dephosphorylation events will be essential for determining the sequence of events of when SAC proteins are bound and released from kinetochores. This elegant approach should be considered in the future, however, currently it is more urgent that we fill in the gaps by identifying the unknown PP2A-B56 substrates. The analysis of PP2A-B56 substrates may provide more clues into its function and how it recognises its substrates.

Our understanding of how kinases and phosphatases regulate the SAC pathway is still in its infancy. While, new information has highlighted a greater role for Mps1, the function of other kinases such as Plk1 remains a point of debate (Ikeda and Tanaka, 2017; von Schubert et al., 2015). In addition to this, whether PP2A-B56 also reverses phosphorylations by other kinases such as Cdk1, Bub1 or Plk1 is an open question. Another problem is the discrepancies reported about the functional importance of PP1 versus PP2A-B56 (Nijenhuis et al., 2014; Espert et al., 2014; Moura et al., 2017; Maciejowski et al., 2017). It seems likely that these two phosphatases play overlapping functions, however, it is probable that they function at different stages in SAC silencing. The urgent question to be answered in the remaining decade of checkpoint research is how these kinases and phosphatases interact to regulate the checkpoint. Answering this question requires the identification of all of their substrates, temporal knowledge of when these phosphorylation or dephosphorylation events occur and importantly

determining which specific phosphorylations are ‘drivers.’ More widely, we need to consider how these events are then coordinated with other silencing mechanisms. For example, while PP2A-B56 may negatively regulate the recruitment of Mad1:Mad2 by releasing Bub1 from kinetochores, the dynein-mediated stripping of Mad1:Mad2 upon microtubule binding is still needed for complete SAC inactivation (Howell et al., 2001; Maldonado and Kapoor, 2011; Karess, 2005; Gassmann et al., 2010; Griffis et al., 2007). Additionally, the PP2A-B56 control of SAC signalling may not be limited to kinetochores and may be as far reaching as the dephosphorylation of components of the MCC-APC/C complex.

7.1.2 THE MPS1-KNL1 INTERACTION

Mps1 must be continuously cycled on and off kinetochores for microtubule attachments to form, however, precisely how this happens is unclear. The recruitment and release of Mps1 are key regulatory steps in the SAC pathway. Recent progress has advanced our understanding of how Mps1 localises to kinetochores, but very little is known about its release (Hiruma et al., 2015; Ji et al., 2015). To localise to kinetochores Mps1 interacts with Nuf2 and Hec1 of the Ndc80 complex. Here, we aimed to identify novel Mps1 interactors to gain additional clues into its function. By combining Mps1 immunoprecipitation with mass spectrometry I found that Knl1 is a previously unidentified interaction partner of Mps1. Intriguingly, Knl1 meets many of the requirements to be a third Mps1 receptor. In the past decade, research has shown that Mps1 localisation requires Hec1, is sensitive to Aurora B activity and is competitive with microtubule binding (Martin-Lluesma et al., 2002; Zhu et al., 2013; Saurin et al., 2011; Hiruma et al., 2015; Ji et al., 2015). Knl1 is also phosphorylated by Aurora B, is a microtubule binding site and somehow influences the localisation of Hec1 (Cheeseman et al., 2006; Caldas et al., 2013; Foley et al., 2011; Cheeseman and Desai, 2008; Pagliuca et al., 2009). While these results are still preliminary, the Mps1-Knl1 interaction is supported by three lines of evidence, 1) immunoprecipitation and mass spectrometry of Mps1 complexes pulls down Knl1, 2) a Knl1$^{1-350}$ fragment interacts with Mps1 and 3) Knl1 depletion inhibits

the localisation of Mps1 to kinetochores. To confirm this protein:protein interaction additional assays could be used such as yeast-two hybrid, iso-thermal calorimetry and NMR techniques. Despite this, coimmunoprecipitation is arguably the gold standard in demonstrating that a protein:protein interaction occurs in an actual cell. So far, we have been unable to provide detailed information of the Mps1-Knl1 interaction at the domain and amino acid levels. Following confirmation of this interaction, the next important step will be gaining biochemical and structural data on the Mps1-Knl1 interface.

These results taken together with those of others indicate that Mps1 binds to three components of the KMN network: Hec1, Nuf2 and Knl1 (Martin-Lluesma et al., 2002; Zhu et al., 2013; Saurin et al., 2011; Hiruma et al., 2015; Ji et al., 2015). How Mps1 interacts with these proteins is an important question. On one hand, the KMN network may cooperate to bind Mps1 by interacting with three distinct domains on Mps1. On the other hand, individual Mps1 molecules may bind to each of these three sites separately. Although this remains an open question, the idea of three distinct binding domains may be consistent with observations on the FRAP kinetics of GFP-Mps1 (**figure 3.8**). The FRAP analysis presented here demonstrated that only ~65% of Mps1 is dynamically turned over at kinetochores consistent with another study (Isokane et al., 2016). This suggests that a third of Mps1 is stably bound at kinetochores and thus, it is possible that the Mps1-Knl1 we have uncovered represents a previously unknown stably bound pool. In contrast, a different study in drosophila reported an almost 100% recovery in WT-Mps1, but ~70% in KD-Mps1 (Moura et al., 2017). Thus, it is perhaps too early to speculate much about the concept of two distinct pools of Mps1. Nonetheless in this possible model, a transient pool of Mps1 might function as a microtubule sensor to turn the checkpoint on, whereas, the stable pool might be needed for continued SAC signalling. The binding of Mps1 to kinetochores is the first step in SAC signalling and therefore, elucidating how this occurs is critical to further our knowledge of the SAC pathway.

7.2 Conclusion

The regulatory mechanisms that control the checkpoint kinase Mps1 are fundamental in the activation and inactivation of the SAC. In this project, we investigated how Mps1 function is modulated by protein phosphatases and interaction partners. I have found a novel regulatory step where BubR1 associated PP2A-B56 inactivates Mps1 by removing a critical phosphate group from its T-loop and disables the SAC signalling cascade. Thus, PP2A-B56 inactivates the SAC by antagonising Mps1 through the inactivation of its T-loop and the dephosphorylation of MELT motifs on Knl1. The picture developing is one where Mps1 and PP2A-B56 play a more overarching role in controlling SAC activation and silencing respectively. Future work outlined in this thesis should provide greater insight into how PP2A-B56 opposes Mps1 more globally to silence the checkpoint. Intriguingly, my search for novel Mps1 interactors uncovered an interaction between Mps1 and the scaffold protein Knl1. Knl1 meets the known requirements to be a third kinetochore receptor for Mps1 and its interaction with Mps1 is surprisingly stable. These results are still preliminary and considerable work is needed to further validate them as well as, to define the domains and core amino acids required at the Knl1-Mps1 interface. This work has bought us a step closer in understanding how the function of Mps1 is regulated during mitosis.

REFERENCES

Abbas, T., and A. Dutta. 2009. p21 in cancer: intricate networks and multiple activities. *Nat. Rev. Cancer*. 9:400–414.

Abrieu, A., L. Magnaghi-Jaulin, J.A. Kahana, M. Peter, A. Castro, S. Vigneron, T. Lorca, D.W. Cleveland, and J.-C. Labbé. 2001. Mps1 Is a Kinetochore-Associated Kinase Essential for the Vertebrate Mitotic Checkpoint. *Cell*. 106:83–93.

Ahonen, L.J., M.J. Kallio, J.R. Daum, M. Bolton, I.A. Manke, M.B. Yaffe, P.T. Stukenberg, and G.J. Gorbsky. 2005. Polo-like Kinase 1 Creates the Tension-Sensing 3F3/2 Phosphoepitope and Modulates the Association of Spindle-Checkpoint Proteins at Kinetochores. *Curr. Biol.* 15:1078–1089.

Alberts B et al. 2014. Molecular Biology of The Cell. Garland Science. 963-1019 pp.

Alfieri, C., L. Chang, Z. Zhang, J. Yang, S. Maslen, M. Skehel, and D. Barford. 2016. Molecular basis of APC/C regulation by the spindle assembly checkpoint. *Nature*. 536:431–436.

Alushin, G.M., V. Musinipally, D. Matson, J. Tooley, P.T. Stukenberg, and E. Nogales. 2012. Multimodal microtubule binding by the Ndc80 kinetochore complex. 19:1161.

Alushin, G.M., V.H. Ramey, S. Pasqualato, D.A. Ball, N. Grigorieff, A. Musacchio, and E. Nogales. 2010. The Ndc80 kinetochore complex forms oligomeric arrays along microtubules. *Nature*. 467:805–810.

Andersen, J.S., C.J. Wilkinson, T. Mayor, P. Mortensen, E.A. Nigg, and M. Mann. 2003. Proteomic characterization of the human centrosome by protein correlation profiling. *Nature*. 426:570–574.

De Antoni, A., C.G. Pearson, D. Cimini, J.C. Canman, V. Sala, L. Nezi, M. Mapelli, L. Sironi, M. Faretta, E.D. Salmon, and A. Musacchio. 2005. The Mad1/Mad2 Complex as a Template for Mad2 Activation in the Spindle Assembly Checkpoint. *Curr. Biol.* 15:214–225.

Aravamudhan, P., A.A. Goldfarb, and A.P. Joglekar. 2015. The kinetochore encodes a mechanical switch to disrupt spindle assembly checkpoint signalling. *Nat. Cell Biol.* 17:868.

Arquint, C., A.-M. Gabryjonczyk, and E. A Nigg. 2014. Centrosomes as signalling centres. 369.

Axton, J.M., V. Dombrádi, P.T.W. Cohen, and D.M. Glover. 1990. One of the protein phosphatase 1 isoenzymes in Drosophila is essential for mitosis. *Cell*. 63:33–46.

Barisic, M., B. Sohm, P. Mikolcevic, C. Wandke, V. Rauch, T. Ringer, M. Hess, G. Bonn, and S. Geley. 2010. Spindly/CCDC99 Is Required for

Efficient Chromosome Congression and Mitotic Checkpoint Regulation. *Mol. Biol. Cell* . 21:1968–1981.

Barr, F.A., P.R. Elliott, and U. Gruneberg. 2011. Protein phosphatases and the regulation of mitosis. *J. Cell Sci.* . 124:2323–2334.

Barros, T.P., K. Kinoshita, A.A. Hyman, and J.W. Raff. 2005. Aurora A activates D-TACC–Msps complexes exclusively at centrosomes to stabilize centrosomal microtubules. *J. Cell Biol.* 170:1039 LP-1046.

Bayliss, R., A. Fry, T. Haq, and S. Yeoh. 2012. On the molecular mechanisms of mitotic kinase activation. *Open Biol.* 2.

Bayliss, R., T. Sardon, I. Vernos, and E. Conti. 2003. Structural Basis of Aurora-A Activation by TPX2 at the Mitotic Spindle. *Mol. Cell*. 12:851–862.

Besson, A., S.F. Dowdy, and J.M. Roberts. 2008. CDK Inhibitors: Cell Cycle Regulators and Beyond. *Dev. Cell*. 14:159–169.

Biggins, S., and A.W. Murray. 2001. The budding yeast protein kinase Ipl1/Aurora allows the absence of tension to activate the spindle checkpoint. *Genes Dev.* 15:3118–3129.

Blajeski, A.L., V.A. Phan, T.J. Kottke, and S.H. Kaufmann. 2002. G(1) and G(2) cell-cycle arrest following microtubule depolymerization in human breast cancer cells. *J. Clin. Invest.* 110:91–99.

Boersema, P.J., R. Raijmakers, S. Lemeer, S. Mohammed, and A.J.R. Heck. 2009. Multiplex peptide stable isotope dimethyl labeling for quantitative proteomics. *Nat. Protoc.* 4:484–494.

Bollen, M., W. Peti, M.J. Ragusa, and M. Beullens. 2010. The extended PP1 toolkit: designed to create specificity. *Trends Biochem. Sci.* 35:450–458.

Bondoc, J.M.G., N.M. Wolf, M. Ndichuck, C. Abad-Zapatero, and F. Movahedzadeh. 2017. Mutagenesis of threonine to serine in the active site of Mycobacterium tuberculosis fructose-1,6-bisphosphatase (Class II) retains partial enzyme activity. *Biotechnol. Reports*. 15:48–54.

Brady, D.M., and K.G. Hardwick. 2000. Complex formation between Mad1p, Bub1p and Bub3p is crucial for spindle checkpoint function. *Curr. Biol.* 10:675–678.

Buffin, E., C. Lefebvre, J. Huang, M.E. Gagou, and R.E. Karess. 2005. Recruitment of Mad2 to the Kinetochore Requires the Rod/Zw10 Complex. *Curr. Biol.* 15:856–861.

Caldas, G. V, K.F. DeLuca, and J.G. DeLuca. 2013. KNL1 facilitates phosphorylation of outer kinetochore proteins by promoting Aurora B kinase activity. *J. Cell Biol.* 203:957–969.

V Caldas, G., J. G Deluca, G. Caldas, and J. DeLuca. 2013. KNL1: Bringing Order to the Kinetochore. 123. Springer Berlin Heidelberg. 1-13 pp.

Caldas, G. V, T.R. Lynch, R. Anderson, S. Afreen, D. Varma, and J.G. DeLuca. 2015. The RZZ complex requires the N-terminus of KNL1 to mediate optimal Mad1 kinetochore localization in human cells. *Open Biol.* 5.

Carmena, M., M. Wheelock, H. Funabiki, and W.C. Earnshaw. 2012. The Chromosomal Passenger Complex (CPC): From Easy Rider to the Godfather of Mitosis. *Nat. Rev. Mol. Cell Biol.* 13:789–803.

Carroll, C.W., K.J. Milks, and A.F. Straight. 2010. Dual recognition of CENP-A nucleosomes is required for centromere assembly. *J. Cell Biol.* 189:1143 LP-1155.

Carroll, C.W., M.C.C. Silva, K.M. Godek, L.E.T. Jansen, and A.F. Straight. 2009. Centromere assembly requires the direct recognition of CENP-A nucleosomes by CENP-N. *Nat Cell Biol*. 11:896–902.

Chan, Y.W., A.A. Jeyaprakash, E.A. Nigg, and A. Santamaria. 2012. Aurora B controls kinetochore–microtubule attachments by inhibiting Ska complex–KMN network interaction. *J. Cell Biol.* 196:563 LP-571.

Chao, W.C.H., K. Kulkarni, Z. Zhang, E.H. Kong, and D. Barford. 2012. Structure of the mitotic checkpoint complex. *Nature*. 484:208–213.

Cheeseman, I.M., J.S. Chappie, E.M. Wilson-Kubalek, and A. Desai. 2006. The Conserved KMN Network Constitutes the Core Microtubule-Binding Site of the Kinetochore. *Cell*. 127:983–997.

Cheeseman, I.M., and A. Desai. 2008. Molecular architecture of the kinetochore-microtubule interface. *Nat Rev Mol Cell Biol*. 9:33–46.

Cheeseman, I.M., T. Hori, T. Fukagawa, and A. Desai. 2008. KNL1 and the CENP-H/I/K Complex Coordinately Direct Kinetochore Assembly in Vertebrates. *Mol. Biol. Cell* . 19:587–594.

Cheeseman, I.M., S. Niessen, S. Anderson, F. Hyndman, J.R. Yates, K. Oegema, and A. Desai. 2004. A conserved protein network controls assembly of the outer kinetochore and its ability to sustain tension. *Genes Dev.* 18:2255–2268.

Ciferri, C., S. Pasqualato, E. Screpanti, G. Varetti, S. Santaguida, G. Dos Reis, A. Maiolica, J. Polka, J.G. De Luca, P. De Wulf, M. Salek, J. Rappsilber, C.A. Moores, E.D. Salmon, and A. Musacchio. 2008. Implications for Kinetochore-Microtubule Attachment from the Structure of an Engineered Ndc80 Complex. *Cell*. 133:427–439.

Colombo, R., M. Caldarelli, M. Mennecozzi, M.L. Giorgini, F. Sola, P. Cappella, C. Perrera, S.R. Depaolini, L. Rusconi, U. Cucchi, N. Avanzi, J.A. Bertrand, R.T. Bossi, E. Pesenti, A. Galvani, A. Isacchi, F. Colotta, D. Donati, and J. Moll. 2010. Targeting the Mitotic Checkpoint for Cancer Therapy with NMS-P715, an Inhibitor of MPS1

Kinase. *Cancer Res.* 70:10255 LP-10264.

Conduit, P.T., Z. Feng, J.H. Richens, J. Baumbach, A. Wainman, S.D. Bakshi, J. Dobbelaere, S. Johnson, S.M. Lea, and J.W. Raff. 2014. The Centrosome-Specific Phosphorylation of Cnn by Polo/Plk1 Drives Cnn Scaffold Assembly and Centrosome Maturation. *Dev. Cell*. 28:659–669.

Conduit, P.T., A. Wainman, and J.W. Raff. 2015. Centrosome function and assembly in animal cells. *Nat Rev Mol Cell Biol*. 16:611–624.

Coudreuse, D., and P. Nurse. 2010. Driving the cell cycle with a minimal CDK control network. *Nature*. 468:1074–1079.

Cundell, M.J., R.N. Bastos, T. Zhang, J. Holder, U. Gruneberg, B. Novak, and F.A. Barr. 2013. The BEG (PP2A-B55/ENSA/Greatwall) Pathway Ensures Cytokinesis follows Chromosome Separation. *Mol. Cell*. 52:393–405.

Cundell, M.J., L.H. Hutter, R. Nunes Bastos, E. Poser, J. Holder, S. Mohammed, B. Novak, and F.A. Barr. 2016. A PP2A-B55 recognition signal controls substrate dephosphorylation kinetics during mitotic exit. *J. Cell Biol.*

Défachelles, L., N. Raich, R. Terracol, X. Baudin, B. Williams, M. Goldberg, and R.E. Karess. 2015. RZZ and Mad1 dynamics in Drosophila mitosis. *Chromosom. Res.* 23:333–342.

DeLuca, K.F., S.M.A. Lens, and J.G. DeLuca. 2011. Temporal changes in Hec1 phosphorylation control kinetochore–microtubule attachment stability during mitosis. *J. Cell Sci.* 124:622 LP-634.

Desai, A., S. Rybina, T. Müller-Reichert, A. Shevchenko, A. Shevchenko, A. Hyman, and K. Oegema. 2003. KNL-1 directs assembly of the microtubule-binding interface of the kinetochore in C. elegans. *Genes Dev.* . 17:2421–2435.

Dick, A.E., and D.W. Gerlich. 2013. Kinetic framework of spindle assembly checkpoint signalling. 15:1370.

Dimitrova, Y.N., S. Jenni, R. Valverde, Y. Khin, and S.C. Harrison. 2016. Structure of the MIND Complex Defines a Regulatory Focus for Yeast Kinetochore Assembly. *Cell*. 167:1014–1027.e12.

Dominguez-Brauer, C., K.L. Thu, J.M. Mason, H. Blaser, M.R. Bray, and T.W. Mak. 2015. Targeting Mitosis in Cancer: Emerging Strategies. *Mol. Cell*. 60:524–536.

Dou, Z., C. von Schubert, R. Körner, A. Santamaria, S. Elowe, and E.A. Nigg. 2011. Quantitative Mass Spectrometry Analysis Reveals Similar Substrate Consensus Motif for Human Mps1 Kinase and Plk1. *PLoS One*. 6:e18793.

Dubrovsky, J.G., and V.B. Ivanov. 2003. Celebrating 50 years of the cell cycle. *Nature*. 426:759.

Dunsch, A.K., E. Linnane, F.A. Barr, and U. Gruneberg. 2011. The astrin–kinastrin/SKAP complex localizes to microtubule plus ends and facilitates chromosome alignment. *J. Cell Biol.* 192:959 LP-968.

Dzhindzhev, N.S., G. Tzolovsky, Z. Lipinszki, S. Schneider, R. Lattao, J. Fu, J. Debski, M. Dadlez, and D.M. Glover. 2014. Plk4 Phosphorylates Ana2 to Trigger Sas6 Recruitment and Procentriole Formation. *Curr. Biol.* 24:2526–2532.

Ems-McClung, S.C., S.G. Hainline, J. Devare, H. Zong, S. Cai, S.K. Carnes, S.L. Shaw, and C.E. Walczak. 2013. Aurora B Inhibits MCAK Activity Through a Phospho-conformational Switch that Reduces Microtubule Association. *Curr. Biol.* 23:2491–2499.

Espert, A., P. Uluocak, R.N. Bastos, D. Mangat, P. Graab, and U. Gruneberg. 2014. PP2A-B56 opposes Mps1 phosphorylation of Knl1 and thereby promotes spindle assembly checkpoint silencing. *J. Cell Biol.* . 206:833–842.

Espeut, J., P. Lara-Gonzalez, M. Sassine, A.K. Shiau, A. Desai, and A. Abrieu. 2015. Natural Loss of Mps1 Kinase in Nematodes Uncovers a Role for Polo-like Kinase 1 in Spindle Checkpoint Initiation. *Cell Rep.* 12:58–65.

Eytan, E., K. Wang, S. Miniowitz-Shemtov, D. Sitry-Shevah, S. Kaisari, T.J. Yen, S.-T. Liu, and A. Hershko. 2014. Disassembly of mitotic checkpoint complexes by the joint action of the AAA-ATPase TRIP13 and p31comet. *Proc. Natl. Acad. Sci.* . 111:12019–12024.

Fachinetti, D., H. Diego Folco, Y. Nechemia-Arbely, L.P. Valente, K. Nguyen, A.J. Wong, Q. Zhu, A.J. Holland, A. Desai, L.E.T. Jansen, and D.W. Cleveland. 2013. A two-step mechanism for epigenetic specification of centromere identity and function. *Nat Cell Biol*. 15:1056–1066.

Faesen, A.C., M. Thanasoula, S. Maffini, C. Breit, F. Müller, S. van Gerwen, T. Bange, and A. Musacchio. 2017. Basis of catalytic assembly of the mitotic checkpoint complex. *Nature*. 542:498–502.

Falk, S.J., J. Lee, N. Sekulic, M.A. Sennett, T.-H. Lee, and B.E. Black. 2016. CENP-C directs a structural transition of CENP-A nucleosomes mainly through sliding of DNA gyres. 23:204.

Fededa, J.P., and D.W. Gerlich. 2012. Molecular control of animal cell cytokinesis. *Nat Cell Biol*. 14:440–447.

Foley, E.A., and T.M. Kapoor. 2013. Microtubule attachment and spindle assembly checkpoint signalling at the kinetochore. *Nat Rev Mol Cell Biol*. 14:25–37.

Foley, E.A., M. Maldonado, and T.M. Kapoor. 2011. Formation of stable attachments between kinetochores and microtubules depends on the B56-PP2A phosphatase. *Nat Cell Biol*. 13:1265–1271.

Funabiki, H., and D. Wynne. 2013. Making an effective switch at the kinetochore by phosphorylation and dephosphorylation. *Chromosoma*. 122:135–158.

Gama, J.B., C. Pereira, P.A. Simões, R. Celestino, R.M. Reis, D.J. Barbosa, H.R. Pires, C. Carvalho, J. Amorim, A.X. Carvalho, D.K. Cheerambathur, and R. Gassmann. 2017. Molecular mechanism of dynein recruitment to kinetochores by the Rod–Zw10–Zwilch complex and Spindly. *J. Cell Biol.* 216:943 LP-960.

Gascoigne, K.E., and S.S. Taylor. 2009. How do anti-mitotic drugs kill cancer cells? *J. Cell Sci.* 122:2579 LP-2585.

Gassmann, R., A.J. Holland, D. Varma, X. Wan, F. Çivril, D.W. Cleveland, K. Oegema, E.D. Salmon, and A. Desai. 2010. Removal of Spindly from microtubule-attached kinetochores controls spindle checkpoint silencing in human cells. *Genes Dev.* . 24:957–971.

Gharbi-Ayachi, A., J.-C. Labbé, A. Burgess, S. Vigneron, J.-M. Strub, E. Brioudes, A. Van-Dorsselaer, A. Castro, and T. Lorca. 2010. The Substrate of Greatwall Kinase, Arpp19, Controls Mitosis by Inhibiting Protein Phosphatase 2A. *Science (80-.).* 330:1673 LP-1677.

Godek, K.M., L. Kabeche, and D.A. Compton. 2015. Regulation of kinetochore-microtubule attachments through homeostatic control during mitosis. *Nat Rev Mol Cell Biol*. 16:57–64.

Gönczy, P. 2015. Centrosomes and cancer: revisiting a long-standing relationship. *Nat. Rev. Cancer*. 15:639.

Green, R.A., E. Paluch, and K. Oegema. 2012. Cytokinesis in Animal Cells. *Annu. Rev. Cell Dev. Biol.* 28:29–58.

Griffis, E.R., N. Stuurman, and R.D. Vale. 2007. Spindly, a novel protein essential for silencing the spindle assembly checkpoint, recruits dynein to the kinetochore. *J. Cell Biol.* 177:1005 LP-1015.

Grishchuk, E.L., I.S. Spiridonov, V.A. Volkov, A. Efremov, S. Westermann, D. Drubin, G. Barnes, F.I. Ataullakhanov, and J.R. McIntosh. 2008. Different assemblies of the DAM1 complex follow shortening microtubules by distinct mechanisms. *Proc. Natl. Acad. Sci.* . 105:6918–6923.

Guimaraes, G.J., Y. Dong, B.F. McEwen, and J.G. DeLuca. 2008. Kinetochore-Microtubule Attachment Relies on the Disordered N-Terminal Tail Domain of Hec1. *Curr. Biol.* 18:1778–1784.

Guttinger, S., E. Laurell, and U. Kutay. 2009. Orchestrating nuclear envelope disassembly and reassembly during mitosis. *Nat Rev Mol Cell Biol*. 10:178–191.

Haering, C.H., A.-M. Farcas, P. Arumugam, J. Metson, and K. Nasmyth. 2008. The cohesin ring concatenates sister DNA

molecules. *Nature*. 454:297–301.

Hagan, R.S., M.S. Manak, H.K. Buch, M.G. Meier, P. Meraldi, J. V Shah, P.K. Sorger, and S.J. Doxsey. 2011. p31(comet) acts to ensure timely spindle checkpoint silencing subsequent to kinetochore attachment. *Mol. Biol. Cell*. 22:4236–4246.

Hanahan, D., and R.A. Weinberg. 2011. Hallmarks of Cancer: The Next Generation. *Cell*. 144:646–674.

Hanisch, A., H.H.W. Silljé, and E.A. Nigg. 2006. Timely anaphase onset requires a novel spindle and kinetochore complex comprising Ska1 and Ska2. *EMBO J.* 25:5504 LP-5515.

Hanks, S., K. Coleman, S. Reid, A. Plaja, H. Firth, D. FitzPatrick, A. Kidd, K. Méhes, R. Nash, N. Robin, N. Shannon, J. Tolmie, J. Swansbury, A. Irrthum, J. Douglas, and N. Rahman. 2004. Constitutional aneuploidy and cancer predisposition caused by biallelic mutations in BUB1B. 36:1159.

Hartwell, L.H., and T.A. Weinert. 1989. Checkpoints: controls that ensure the order of cell cycle events. *Science (80-.).* 246:629 LP-634.

Hauf, S., R.W. Cole, S. LaTerra, C. Zimmer, G. Schnapp, R. Walter, A. Heckel, J. van Meel, C.L. Rieder, and J.-M. Peters. 2003. The small molecule Hesperadin reveals a role for Aurora B in correcting kinetochore–microtubule attachment and in maintaining the spindle assembly checkpoint. *J. Cell Biol.* 161:281 LP-294.

Heald, R., and A. Khodjakov. 2015. Thirty years of search and capture: The complex simplicity of mitotic spindle assembly. *J. Cell Biol.* 211:1103 LP-1111.

Heim, A., A. Konietzny, and T.U. Mayer. 2015. Protein phosphatase 1 is essential for Greatwall inactivation at mitotic exit. *EMBO Rep.* 16:1501–1510.

Hertz, E.P.T., T. Kruse, N.E. Davey, B. López-Méndez, J.O. Sigurðsson, G. Montoya, J. V. Olsen, and J. Nilsson. 2016. A Conserved Motif Provides Binding Specificity to the PP2A-B56 Phosphatase. *Mol. Cell*. 63:686–695.

Heun, P., S. Erhardt, M.D. Blower, S. Weiss, A.D. Skora, and G.H. Karpen. 2006. Mislocalization of the Drosophila Centromere-Specific Histone CID Promotes Formation of Functional Ectopic Kinetochores. *Dev. Cell*. 10:303–315.

Hewitt, L., A. Tighe, S. Santaguida, A.M. White, C.D. Jones, A. Musacchio, S. Green, and S.S. Taylor. 2010. Sustained Mps1 activity is required in mitosis to recruit O-Mad2 to the Mad1–C-Mad2 core complex. *J. Cell Biol.* 190:25–34.

Hirano, T. 2005. Condensins: Organizing and Segregating the Genome. *Curr. Biol.* 15:R265–R275.

Hiruma, Y., C. Sacristan, S.T. Pachis, A. Adamopoulos, T. Kuijt, M. Ubbink, E.

von Castelmur, A. Perrakis, and G.J.P.L. Kops. 2015. Competition between MPS1 and microtubules at kinetochores regulates spindle checkpoint signaling. *Sci.* . 348:1264–1267.

Hochegger, H., S. Takeda, and T. Hunt. 2008. Cyclin-dependent kinases and cell-cycle transitions: does one fit all? *Nat Rev Mol Cell Biol*. 9:910–916.

Hori, T., M. Amano, A. Suzuki, C.B. Backer, J.P. Welburn, Y. Dong, B.F. McEwen, W.-H. Shang, E. Suzuki, K. Okawa, I.M. Cheeseman, and T. Fukagawa. 2008. CCAN Makes Multiple Contacts with Centromeric DNA to Provide Distinct Pathways to the Outer Kinetochore. *Cell*. 135:1039–1052.

Howell, B.J., B.F. McEwen, J.C. Canman, D.B. Hoffman, E.M. Farrar, C.L. Rieder, and E.D. Salmon. 2001. Cytoplasmic dynein/dynactin drives kinetochore protein transport to the spindle poles and has a role in mitotic spindle checkpoint inactivation. *J. Cell Biol.* 155:1159 LP-1172.

Howell, B.J., B. Moree, E.M. Farrar, S. Stewart, G. Fang, and E.D. Salmon. 2004. Spindle Checkpoint Protein Dynamics at Kinetochores in Living Cells. *Curr. Biol.* 14:953–964.

Howman, E. V, K.J. Fowler, A.J. Newson, S. Redward, A.C. MacDonald, P. Kalitsis, and K.H.A. Choo. 2000. Early disruption of centromeric chromatin organization in centromere protein A (Cenpa) null mice. *Proc. Natl. Acad. Sci.* . 97:1148–1153.

Hoyt, M.A., L. Totis, and B.T. Roberts. 1991. S. cerevisiae genes required for cell cycle arrest in response to loss of microtubule function. *Cell*. 66:507–517.

Huis in 't Veld, P.J., S. Jeganathan, A. Petrovic, P. Singh, J. John, V. Krenn, F. Weissmann, T. Bange, and A. Musacchio. 2016. Molecular basis of outer kinetochore assembly on CENP-T. *Elife*. 5:e21007.

Hunter, A.W., M. Caplow, D.L. Coy, W.O. Hancock, S. Diez, L. Wordeman, and J. Howard. 2003. The Kinesin-Related Protein MCAK Is a Microtubule Depolymerase that Forms an ATP-Hydrolyzing Complex at Microtubule Ends. *Mol. Cell*. 11:445–457.

Hunter, T. 2012. Why nature chose phosphate to modify proteins. *Philos. Trans. R. Soc. B Biol. Sci.* 367:2513 LP-2516.

Ikeda, M., and K. Tanaka. 2017. Plk1 bound to Bub1 contributes to spindle assembly checkpoint activity during mitosis. *Sci. Rep.* 7:8794.

Isokane, M., T. Walter, R. Mahen, B. Nijmeijer, J.-K. Hériché, K. Miura, S. Maffini, M.P. Ivanov, T.S. Kitajima, J.-M. Peters, and J. Ellenberg. 2016. ARHGEF17 is an essential spindle assembly checkpoint factor that targets Mps1 to kinetochores. *J. Cell Biol.* . 212:647–659.

Ito, D., Y. Saito, and T. Matsumoto. 2012.

Centromere-tethered Mps1 pombe homolog (Mph1) kinase is a sufficient marker for recruitment of the spindle checkpoint protein Bub1, but not Mad1. *Proc. Natl. Acad. Sci. U. S. A.* 109:209–214.

Izawa, D., and J. Pines. 2015. The mitotic checkpoint complex binds a second CDC20 to inhibit active APC/C. *Nature*. 517:631–634.

Jakobsen, L., K. Vanselow, M. Skogs, Y. Toyoda, E. Lundberg, I. Poser, L.G. Falkenby, M. Bennetzen, J. Westendorf, E.A. Nigg, M. Uhlen, A.A. Hyman, and J.S. Andersen. 2011. Novel asymmetrically localizing components of human centrosomes identified by complementary proteomics methods. *EMBO J.* 30:1520 LP-1535.

Jelluma, N., A.B. Brenkman, N.J.F. van den Broek, C.W.A. Cruijsen, M.H.J. van Osch, S.M.A. Lens, R.H. Medema, and G.J.P.L. Kops. 2008a. Mps1 Phosphorylates Borealin to Control Aurora B Activity and Chromosome Alignment. *Cell*. 132:233–246.

Jelluma, N., A.B. Brenkman, I. McLeod, J.R. Yates III, D.W. Cleveland, R.H. Medema, and G.J.P.L. Kops. 2008b. Chromosomal Instability by Inefficient Mps1 Auto-Activation Due to a Weakened Mitotic Checkpoint and Lagging Chromosomes. *PLoS One*. 3:e2415.

Jelluma, N., T.B. Dansen, T. Sliedrecht, N.P. Kwiatkowski, and G.J.P.L. Kops. 2010. Release of Mps1 from kinetochores is crucial for timely anaphase onset. *J. Cell Biol.* 191:281–290.

Jemaa, M., L. Galluzzi, O. Kepp, L. Senovilla, M. Brands, U. Boemer, M. Koppitz, P. Lienau, S. Prechtl, V. Schulze, G. Siemeister, A.M. Wengner, D. Mumberg, K. Ziegelbauer, A. Abrieu, M. Castedo, I. Vitale, and G. Kroemer. 2013. Characterization of novel MPS1 inhibitors with preclinical anticancer activity. *Cell Death Differ*. 20:1532–1545.

Jeyaprakash, A.A., C. Basquin, U. Jayachandran, and E. Conti. 2011. Structural Basis for the Recognition of Phosphorylated Histone H3 by the Survivin Subunit of the Chromosomal Passenger Complex. *Structure*. 19:1625–1634.

Jeyaprakash, A.A., A. Santamaria, U. Jayachandran, Y.W. Chan, C. Benda, E.A. Nigg, and E. Conti. 2012. Structural and Functional Organization of the Ska Complex, a Key Component of the Kinetochore-Microtubule Interface. *Mol. Cell*. 46:274–286.

Ji, Z., H. Gao, L. Jia, B. Li, and H. Yu. 2017. A sequential multi-target Mps1 phosphorylation cascade promotes spindle checkpoint signaling. *Elife*. 6:e22513.

Ji, Z., H. Gao, and H. Yu. 2015. Kinetochore attachment sensed by competitive Mps1 and microtubule binding to Ndc80C. *Sci.* . 348:1260–1264.

Jia, L., B. Li, R.T. Warrington, X. Hao, S. Wang, and H. Yu. 2011. Defining pathways of spindle checkpoint silencing: functional redundancy between Cdc20 ubiquitination and p31comet. *Mol. Biol. Cell* . 22:4227–4235.

Kalantzaki, M., E. Kitamura, T. Zhang, A. Mino, B. Novák, and T.U. Tanaka. 2015. Kinetochore–microtubule error correction is driven by differentially regulated interaction modes. 17:421.

Kallio, M.J., M.L. McCleland, P.T. Stukenberg, and G.J. Gorbsky. 2002. Inhibition of Aurora B Kinase Blocks Chromosome Segregation, Overrides the Spindle Checkpoint, and Perturbs Microtubule Dynamics in Mitosis. *Curr. Biol.* 12:900–905.

Kang, J., Y. Chen, Y. Zhao, and H. Yu. 2007. Autophosphorylation-dependent activation of human Mps1 is required for the spindle checkpoint. *Proc. Natl. Acad. Sci.* 104:20232–20237.

Karess, R. 2005. Rod–Zw10–Zwilch: a key player in the spindle checkpoint. *Trends Cell Biol.* 15:386–392.

Kastan, M.B., and J. Bartek. 2004. Cell-cycle checkpoints and cancer. *Nature*. 432:316–323.

Kato, H., J. Jiang, B.-R. Zhou, M. Rozendaal, H. Feng, R. Ghirlando, T.S. Xiao, A.F. Straight, and Y. Bai. 2013. A Conserved Mechanism for Centromeric Nucleosome Recognition by Centromere Protein CENP-C. *Science (80-.).* 340:1110 LP-1113.

Kawashima, S.A., Y. Yamagishi, T. Honda, K. Ishiguro, and Y. Watanabe. 2010. Phosphorylation of H2A by Bub1 Prevents Chromosomal Instability Through Localizing Shugoshin. *Science (80-.).* 327:172 LP-177.

Kellogg, D.R. 2003. Wee1-dependent mechanisms required for coordination of cell growth and cell division. *J. Cell Sci.* 116:4883 LP-4890.

Khodjakov, A., and T. Kapoor. 2005. Microtubule Flux: What Is It Good for? *Curr. Biol.* 15:R966–R968.

Kim, S., and H. Yu. 2015. Multiple assembly mechanisms anchor the KMN spindle checkpoint platform at human mitotic kinetochores. *J. Cell Biol.* 208:181 LP-196.

Kinoshita, K., T.L. Noetzel, L. Pelletier, K. Mechtler, D.N. Drechsel, A. Schwager, M. Lee, J.W. Raff, and A.A. Hyman. 2005. Aurora A phosphorylation of TACC3/maskin is required for centrosome-dependent microtubule assembly in mitosis. *J. Cell Biol.* 170:1047 LP-1055.

Kirschner, M., and T. Mitchison. 1986. Beyond self-assembly: From microtubules to morphogenesis. *Cell*. 45:329–342.

Kitajima, T.S., T. Sakuno, K. Ishiguro, S. Iemura, T. Natsume, S.A. Kawashima, and Y. Watanabe. 2006. Shugoshin collaborates with protein phosphatase 2A to protect cohesin. *Nature*. 441:46–

52.

Kollman, J.M., A. Merdes, L. Mourey, and D.A. Agard. 2011. Microtubule nucleation by γ-tubulin complexes. *Nat Rev Mol Cell Biol*. 12:709–721.

Kops, G.J.P.L., D.R. Foltz, and D.W. Cleveland. 2004. Lethality to human cancer cells through massive chromosome loss by inhibition of the mitotic checkpoint. *Proc. Natl. Acad. Sci. United States Am.* . 101:8699–8704.

Kops, G.J.P.L., Y. Kim, B.A.A. Weaver, Y. Mao, I. McLeod, J.R. Yates, M. Tagaya, and D.W. Cleveland. 2005a. ZW10 links mitotic checkpoint signaling to the structural kinetochore. *J. Cell Biol.* 169:49–60.

Kops, G.J.P.L., B.A.A. Weaver, and D.W. Cleveland. 2005b. On the road to cancer: aneuploidy and the mitotic checkpoint. *Nat Rev Cancer*. 5:773–785.

Kratz, A.-S., F. Bärenz, K.T. Richter, and I. Hoffmann. 2015. Plk4-dependent phosphorylation of STIL is required for centriole duplication. *Biol. Open*. 4:370 LP-377.

Krenn, V., and A. Musacchio. 2015. The Aurora B Kinase in Chromosome Bi-Orientation and Spindle Checkpoint Signaling. *Front. Oncol.* 5:225.

Krenn, V., K. Overlack, I. Primorac, S. van Gerwen, and A. Musacchio. 2014. KI Motifs of Human Knl1 Enhance Assembly of Comprehensive Spindle Checkpoint Complexes around MELT Repeats. *Curr. Biol.* 24:29–39.

Krenn, V., A. Wehenkel, X. Li, S. Santaguida, and A. Musacchio. 2012. Structural analysis reveals features of the spindle checkpoint kinase Bub1–kinetochore subunit Knl1 interaction. *J. Cell Biol.* 196:451–467.

Kruse, T., G. Zhang, M.S.Y. Larsen, T. Lischetti, W. Streicher, T. Kragh Nielsen, S.P. Bjørn, and J. Nilsson. 2013. Direct binding between BubR1 and B56–PP2A phosphatase complexes regulate mitotic progression. *J. Cell Sci.* . 126:1086–1092.

Kulukian, A., J.S. Han, and D.W. Cleveland. 2009. Unattached Kinetochores Catalyze Production of an Anaphase Inhibitor that Requires a Mad2 Template to Prime Cdc20 for BubR1 Binding. *Dev. Cell*. 16:105–117.

Kwiatkowski, N., N. Jelluma, P. Filippakopoulos, M. Soundararajan, M.S. Manak, M. Kwon, H.G. Choi, T. Sim, Q.L. Deveraux, S. Rottmann, D. Pellman, J. V Shah, G.J.P.L. Kops, S. Knapp, and N.S. Gray. 2010. Small-molecule kinase inhibitors provide insight into Mps1 cell cycle function. *Nat Chem Biol*. 6:359–368.

Lan, W., and D.W. Cleveland. 2010. A chemical tool box defines mitotic and interphase roles for Mps1 kinase. *J. Cell Biol.* 190:21–24.

Lara-Gonzalez, P., F.G. Westhorpe, and

S.S. Taylor. 2012. The Spindle Assembly Checkpoint. *Curr. Biol.* 22:R966–R980.

Lee, K., and K. Rhee. 2011. PLK1 phosphorylation of pericentrin initiates centrosome maturation at the onset of mitosis. *J. Cell Biol.* 195:1093—1101.

Li, R., and A.W. Murray. 1991. Feedback control of mitosis in budding yeast. *Cell*. 66:519–531.

Li, X., and R.B. Nicklas. 1995. Mitotic forces control a cell-cycle checkpoint. *Nature*. 373:630–632.

Lin, Y.-C., C.-W. Chang, W.-B. Hsu, C.-J.C. Tang, Y.-N. Lin, E.-J. Chou, C.-T. Wu, and T.K. Tang. 2013. Human microcephaly protein CEP135 binds to hSAS-6 and CPAP, and is required for centriole assembly. *EMBO J.* 32:1141–1154.

Lin, Y.-T., Y. Chen, G. Wu, and W.-H. Lee. 2006. Hec1 sequentially recruits Zwint-1 and ZW10 to kinetochores for faithful chromosome segregation and spindle checkpoint control. *Oncogene*. 25:6901.

Liu, D., O. Davydenko, and M.A. Lampson. 2012. Polo-like kinase-1 regulates kinetochore–microtubule dynamics and spindle checkpoint silencing. *J. Cell Biol.* 198:491 LP-499.

Liu, D., M. Vleugel, C.B. Backer, T. Hori, T. Fukagawa, I.M. Cheeseman, and M.A. Lampson. 2010. Regulated targeting of protein phosphatase 1 to the outer kinetochore by KNL1 opposes Aurora B kinase. *J. Cell Biol.* 188:809 LP-820.

Liu, J., and J.N. Onuchic. 2006. A driving and coupling “Pac-Man” mechanism for chromosome poleward translocation in anaphase A. *Proc. Natl. Acad. Sci.* . 103:18432–18437.

Liu, S.-T., J.B. Rattner, S.A. Jablonski, and T.J. Yen. 2006. Mapping the assembly pathways that specify formation of the trilaminar kinetochore plates in human cells. *J. Cell Biol.* 175:41–53.

Liu Hang, S.-T. The mitotic checkpoint complex (MCC): looking back and forth after 15 years. *AIMS Mol. Sci.* 3:597–634.

London, N., and S. Biggins. 2014. Mad1 kinetochore recruitment by Mps1-mediated phosphorylation of Bub1 signals the spindle checkpoint. *Genes Dev.*

London, N., S. Ceto, J.A. Ranish, and S. Biggins. 2012. Phosphoregulation of Spc105 by Mps1 and PP1 Regulates Bub1 Localization to Kinetochores. *Curr. Biol.* 22:900–906.

Long, A.F., D.B. Udy, and S. Dumont. 2017. Hec1 Tail Phosphorylation Differentially Regulates Mammalian Kinetochore Coupling to Polymerizing and Depolymerizing Microtubules. *Curr. Biol.* 27:1692–1699.e3.

Lück-Vielmetter, D., M. Schleicher, B. Grabatin, J. Wippler, and G. Gerisch. 1990. Replacement of threonine residues by serine and alanine in a phosphorylatable heavy chain

fragment of Dictyostelium myosin II. *FEBS Lett.* 269:239–243.

Luo, X., Z. Tang, J. Rizo, and H. Yu. 2002. The Mad2 Spindle Checkpoint Protein Undergoes Similar Major Conformational Changes Upon Binding to Either Mad1 or Cdc20. *Mol. Cell*. 9:59–71.

M. Kapoor, E.A.F.& T. 2013. Microtubule attachment and spindle assembly checkpoint signalling at the kinetochore. *Nat. Rev. Mol. Cell Biol.* 14:25–37.

Maciejowski, J., H. Drechsler, K. Grundner-Culemann, E.R. Ballister, J.-A.A. Rodriguez-Rodriguez, V. Rodriguez-Bravo, M.J.K.K. Jones, E. Foley, M.A. Lampson, H. Daub, A.D. McAinsh, and P. V. Jallepalli. 2017. Mps1 Regulates Kinetochore-Microtubule Attachment Stability via the Ska Complex to Ensure Error-Free Chromosome Segregation. *Dev. Cell*. 41:143–156.e6.

Maciejowski, J., K.A. George, M.-E. Terret, C. Zhang, K.M. Shokat, and P. V Jallepalli. 2010. Mps1 directs the assembly of Cdc20 inhibitory complexes during interphase and mitosis to control M phase timing and spindle checkpoint signaling. *J. Cell Biol.* 190:89–100.

Maia, A., J. de Man, U. Boon, A. Janssen, J.-Y. Song, M. Omerzu, J. Gerard Sterrenburg, M. B W Prinsen, N. Willemsen-Seegers, J. A D M de Roos, A. M van Doornmalen, J. Uitdehaag, G. Kops, J. Jonkers, R. C Buijsman, G. Zaman, and R. Medema. 2015. Inhibition of the spindle assembly checkpoint kinase TTK enhances the efficacy of docetaxel in a triple negative breast cancer model. 26.

Maiato, H., C.L. Rieder, and A. Khodjakov. 2004a. Kinetochore-driven formation of kinetochore fibers contributes to spindle assembly during animal mitosis. *J. Cell Biol.* 167:831 LP-840.

Maiato, H., P. Sampaio, and C.E.B.T.-I.R. of C. Sunkel. 2004b. Microtubule-Associated Proteins and Their Essential Roles During Mitosis. Academic Press. 53–153.

Maldonado, M., and T.M. Kapoor. 2011. Constitutive Mad1 targeting to kinetochores uncouples checkpoint signalling from chromosome biorientation. *Nat Cell Biol*. 13:475–482.

Malureanu, L.A., K.B. Jeganathan, M. Hamada, L. Wasilewski, J. Davenport, and J.M. van Deursen. 2009. BubR1 N Terminus Acts as a Soluble Inhibitor of Cyclin B Degradation by APC/CCdc20 in Interphase. *Dev. Cell*. 16:118–131.

Malvezzi, F., G. Litos, A. Schleiffer, A. Heuck, K. Mechtler, T. Clausen, and S. Westermann. 2013. A structural basis for kinetochore recruitment of the Ndc80 complex via two distinct centromere receptors. *EMBO J.* 32:409–423.

Manchado, E., M. Guillamot, and M.

Malumbres. 2012. Killing cells by targeting mitosis. *Cell Death Differ*. 19:369–377.

Mapelli, M., F. V Filipp, G. Rancati, L. Massimiliano, L. Nezi, G. Stier, R.S. Hagan, S. Confalonieri, S. Piatti, M. Sattler, and A. Musacchio. 2006. Determinants of conformational dimerization of Mad2 and its inhibition by p31(comet). *EMBO J.* 25:1273–1284.

Martin-Lluesma, S., V.M. Stucke, and E.A. Nigg. 2002. Role of Hec1 in Spindle Checkpoint Signaling and Kinetochore Recruitment of Mad1/Mad2. *Science (80-.).* 297:2267–2270.

Mattison, C.P., W.M. Old, E. Steiner, B.J. Huneycutt, K.A. Resing, N.G. Ahn, and M. Winey. 2007. Mps1 Activation Loop Autophosphorylation Enhances Kinase Activity. *J. Biol. Chem.* 282:30553–30561.

Maure, J.-F., E. Kitamura, and T.U. Tanaka. 2007. Mps1 Kinase Promotes Sister-Kinetochore Bi-orientation by a Tension-Dependent Mechanism. *Curr. Biol.* 17:2175–2182.

McAinsh, A.D., and P. Meraldi. 2011. The CCAN complex: Linking centromere specification to control of kinetochore–microtubule dynamics. *Semin. Cell Dev. Biol.* 22:946–952.

McHugh, T., and J.P.I. Welburn. 2017. Dynein at kinetochores: Making the connection. *J. Cell Biol.*

Meadows, J.C., L.A. Shepperd, V. Vanoosthuyse, T.C. Lancaster, A.M. Sochaj, G.J. Buttrick, K.G. Hardwick, and J.B.A. Millar. 2011. Spindle Checkpoint Silencing Requires Association of PP1 to Both Spc7 and Kinesin-8 Motors. *Dev. Cell*. 20:739–750.

Michaelis, C., R. Ciosk, and K. Nasmyth. 1997. Cohesins: Chromosomal Proteins that Prevent Premature Separation of Sister Chromatids. *Cell*. 91:35–45.

Mochida, S., S.L. Maslen, M. Skehel, and T. Hunt. 2010. Greatwall Phosphorylates an Inhibitor of Protein Phosphatase 2A That Is Essential for Mitosis. *Science (80-.).* 330:1670 LP-1673.

Morgan, D.O. 2007. The Cell Cycle: Principles of control. New Science Press, London.

Morin, V., S. Prieto, S. Melines, S. Hem, M. Rossignol, T. Lorca, J. Espeut, N. Morin, and A. Abrieu. 2012. CDK-Dependent Potentiation of MPS1 Kinase Activity Is Essential to the Mitotic Checkpoint. *Curr. Biol.* 22:289–295.

Mosalaganti, S., J. Keller, A. Altenfeld, M. Winzker, P. Rombaut, M. Saur, A. Petrovic, A. Wehenkel, S. Wohlgemuth, F. Müller, S. Maffini, T. Bange, F. Herzog, H. Waldmann, S. Raunser, and A. Musacchio. 2017. Structure of the RZZ complex and molecular basis of its interaction with Spindly. *J. Cell Biol.* 216:961 LP-981.

Moura, M., M. Osswald, N. Leça, J. Barbosa, A.J. Pereira, H. Maiato, C.E. Sunkel, and C. Conde. 2017. Protein Phosphatase 1 inactivates Mps1 to ensure efficient Spindle Assembly Checkpoint silencing. *Elife*. 6:e25366.

Moyle, M.W., T. Kim, N. Hattersley, J. Espeut, D.K. Cheerambathur, K. Oegema, and A. Desai. 2014. A Bub1–Mad1 interaction targets the Mad1–Mad2 complex to unattached kinetochores to initiate the spindle checkpoint. *J. Cell Biol.* . 204:647–657.

Musacchio, A. 2015. The Molecular Biology of Spindle Assembly Checkpoint Signaling Dynamics. *Curr. Biol.* 25:R1002–R1018.

Musacchio, A., and A. Desai. 2017. A Molecular View of Kinetochore Assembly and Function. *Biology (Basel).* 6:5.

Nasmyth, K., and C.H. Haering. 2005. THE STRUCTURE AND FUNCTION OF SMC AND KLEISIN COMPLEXES. *Annu. Rev. Biochem.* 74:595–648.

Nasmyth, K., and C.H. Haering. 2009. Cohesin: Its Roles and Mechanisms. *Annu. Rev. Genet.* 43:525–558.

Naud, S., I.M. Westwood, A. Faisal, P. Sheldrake, V. Bavetsias, B. Atrash, K.-M.J. Cheung, M. Liu, A. Hayes, J. Schmitt, A. Wood, V. Choi, K. Boxall, G. Mak, M. Gurden, M. Valenti, A. de Haven Brandon, A. Henley, R. Baker, C. McAndrew, B. Matijssen, R. Burke, S. Hoelder, S.A. Eccles, F.I. Raynaud, S. Linardopoulos, R.L.M. van Montfort, and J. Blagg. 2013. Structure-Based Design of Orally Bioavailable 1H-Pyrrolo[3,2-c]pyridine Inhibitors of Mitotic Kinase Monopolar Spindle 1 (MPS1). *J. Med. Chem.* 56:10045–10065.

Nigg, E.A. 2007. Centrosome duplication: of rules and licenses. *Trends Cell Biol.* 17:215–221.

Nigg, E.A., and T. Stearns. 2011. The centrosome cycle: Centriole biogenesis, duplication and inherent asymmetries. *Nat Cell Biol*. 13:1154–1160.

Nijenhuis, W., E. von Castelmur, D. Littler, V. De Marco, E. Tromer, M. Vleugel, M.H.J. van Osch, B. Snel, A. Perrakis, and G.J.P.L. Kops. 2013. A TPR domain–containing N-terminal module of MPS1 is required for its kinetochore localization by Aurora B. *J. Cell Biol.* 201:217–231.

Nijenhuis, W., G. Vallardi, A. Teixeira, G.J.P.L. Kops, and A.T. Saurin. 2014. Negative feedback at kinetochores underlies a responsive spindle checkpoint signal. *Nat Cell Biol*. advance on.

Nishino, T., F. Rago, T. Hori, K. Tomii, I.M. Cheeseman, and T. Fukagawa. 2013. CENP-T provides a structural platform for outer kinetochore assembly. *EMBO J.* 32:424 LP-436.

Nunes Bastos, R., M. Cundell, and F. A Barr. 2014. KIF4A and PP2A–B56 form a

spatially restricted feedback loop opposing Aurora B at the anaphase central spindle. 207.

Ohta, M., T. Ashikawa, Y. Nozaki, H. Kozuka-Hata, H. Goto, M. Inagaki, M. Oyama, and D. Kitagawa. 2014. Direct interaction of Plk4 with STIL ensures formation of a single procentriole per parental centriole. 5:5267.

Overlack, K., I. Primorac, M. Vleugel, V. Krenn, S. Maffini, I. Hoffmann, G.J.P.L. Kops, and A. Musacchio. 2015. A molecular basis for the differential roles of Bub1 and BubR1 in the spindle assembly checkpoint. *Elife*. 4.

Pagliuca, C., V.M. Draviam, E. Marco, P.K. Sorger, and P. De Wulf. 2009. Roles for the Conserved Spc105p/Kre28p Complex in Kinetochore-Microtubule Binding and the Spindle Assembly Checkpoint. *PLoS One*. 4:e7640.

Peters, J.-M. 2006. The anaphase promoting complex/cyclosome: a machine designed to destroy. *Nat Rev Mol Cell Biol*. 7:644–656.

Petrovic, A., J. Keller, Y. Liu, K. Overlack, J. John, Y.N.N. Dimitrova, S. Jenni, S. van Gerwen, P. Stege, S. Wohlgemuth, P. Rombaut, F. Herzog, S.C.C. Harrison, I.R.R. Vetter, A. Musacchio, S. van Gerwen, P. Stege, S. Wohlgemuth, P. Rombaut, F. Herzog, S.C.C. Harrison, I.R.R. Vetter, and A. Musacchio. 2016. Structure of the MIS12 Complex and Molecular Basis of Its Interaction with CENP-C at Human Kinetochores. *Cell*. 167:1028–1040.e15.

Petrovic, A., S. Mosalaganti, J. Keller, M. Mattiuzzo, K. Overlack, V. Krenn, A. De Antoni, S. Wohlgemuth, V. Cecatiello, S. Pasqualato, S. Raunser, and A. Musacchio. 2014. Modular Assembly of RWD Domains on the Mis12 Complex Underlies Outer Kinetochore Organization. *Mol. Cell*. 53:591–605.

Petrovic, A., S. Pasqualato, P. Dube, V. Krenn, S. Santaguida, D. Cittaro, S. Monzani, L. Massimiliano, J. Keller, A. Tarricone, A. Maiolica, H. Stark, and A. Musacchio. 2010. The MIS12 complex is a protein interaction hub for outer kinetochore assembly. *J. Cell Biol.* 190:835 LP-852.

Picard, A., J.P. Capony, D.L. Brautigan, and M. Dorée. 1989. Involvement of protein phosphatases 1 and 2A in the control of M phase-promoting factor activity in starfish. *J. Cell Biol.* 109:3347–3354.

Pinsky, B.A., C. V Kotwaliwale, S.Y. Tatsutani, C.A. Breed, and S. Biggins. 2006. Glc7/Protein Phosphatase 1 Regulatory Subunits Can Oppose the Ipl1/Aurora Protein Kinase by Redistributing Glc7. *Mol. Cell. Biol.* . 26:2648–2660.

Primorac, I., J.R. Weir, E. Chiroli, F. Gross, I. Hoffmann, S. van Gerwen, A. Ciliberto, A. Musacchio, and J. Pines. 2013. Bub3 reads phosphorylated MELT repeats to promote spindle assembly checkpoint signaling. *Elife*. 2.

Rago, F., K.E. Gascoigne, and I.M. Cheeseman. 2015. Distinct Organization and Regulation of the Outer Kinetochore KMN Network Downstream of CENP-C and CENP-T. *Curr. Biol.* 25:671–677.

Rieder, C.L., R.W. Cole, A. Khodjakov, and G. Sluder. 1995. The checkpoint delaying anaphase in response to chromosome monoorientation is mediated by an inhibitory signal produced by unattached kinetochores. *J. Cell Biol.* 130:941 LP-948.

Rieder, C.L., A. Schultz, R. Cole, and G. Sluder. 1994. Anaphase onset in vertebrate somatic cells is controlled by a checkpoint that monitors sister kinetochore attachment to the spindle. *J. Cell Biol.* 127:1301 LP-1310.

Rodriguez-Bravo, V., J. Maciejowski, J. Corona, H.K. Buch, P. Collin, M.T. Kanemaki, J. V. Shah, and P. V. Jallepalli. 2014. Nuclear Pores Protect Genome Integrity by Assembling a Premitotic and Mad1-Dependent Anaphase Inhibitor. *Cell*. 156:1017–1031.

Rosenberg, J.S., F.R. Cross, and H. Funabiki. 2011. KNL1/Spc105 Recruits PP1 to Silence the Spindle Assembly Checkpoint. *Curr. Biol.* 21:942–947.

Salimian, K.J., E.R. Ballister, E.M. Smoak, S. Wood, T. Panchenko, M.A. Lampson, and B.E. Black. 2011. Feedback Control in Sensing Chromosome Biorientation by the Aurora B Kinase. *Curr. Biol.* 21:1158–1165.

Salmela, A.-L., and M. Kallio. 2013. Mitosis as an anti-cancer drug target. *Chromosoma*. 122:431–449.

Salvatore, G., T.C. Nappi, P. Salerno, Y. Jiang, C. Garbi, C. Ugolini, P. Miccoli, F. Basolo, M.D. Castellone, A.M. Cirafici, R.M. Melillo, A. Fusco, M.L. Bittner, and M. Santoro. 2007. A Cell Proliferation and Chromosomal Instability Signature in Anaplastic Thyroid Carcinoma. *Cancer Res.* 67:10148 LP-10158.

Santaguida, S., and A. Musacchio. 2009. The life and miracles of kinetochores. *EMBO J.* 28:2511 LP-2531.

Santaguida, S., A. Tighe, A.M. D'Alise, S.S. Taylor, and A. Musacchio. 2010. Dissecting the role of MPS1 in chromosome biorientation and the spindle checkpoint through the small molecule inhibitor reversine. *J. Cell Biol.* 190:73–87.

Saurin, A.T., M.S. van der Waal, R.H. Medema, S.M.A. Lens, and G.J.P.L. Kops. 2011. Aurora B potentiates Mps1 activation to ensure rapid checkpoint establishment at the onset of mitosis. *Nat Commun*. 2:316.

Schleiffer, A., M. Maier, G. Litos, F. Lampert, P. Hornung, K. Mechtler, and S. Westermann. 2012. CENP-T proteins are conserved centromere receptors of the Ndc80 complex. *Nat Cell Biol*. 14:604–613.

Schmidt, J.C., T. Kiyomitsu, T. Hori, C.B.

Backer, T. Fukagawa, and I.M. Cheeseman. 2010. Aurora B kinase controls the targeting of the Astrin–SKAP complex to bioriented kinetochores. *J. Cell Biol.* 191:269 LP-280.

Scholey, M.J., G. Civelekoglu-Scholey, and I. Brust-Mascher. 2016. Anaphase B. *Biol.* . 5.

von Schubert, C., F. Cubizolles, J.M. Bracher, T. Sliedrecht, G.J.P.L. Kops, and E.A. Nigg. 2015. Plk1 and Mps1 Cooperatively Regulate the Spindle Assembly Checkpoint in Human Cells. *Cell Rep.* 12:66–78.

Shepperd, L.A., J.C. Meadows, A.M. Sochaj, T.C. Lancaster, J. Zou, G.J. Buttrick, J. Rappsilber, K.G. Hardwick, and J.B.A. Millar. 2012. Phosphodependent Recruitment of Bub1 and Bub3 to Spc7/KNL1 by Mph1 Kinase Maintains the Spindle Checkpoint. *Curr. Biol.* 22:891–899.

Shichiri, M., K. Yoshinaga, H. Hisatomi, K. Sugihara, and Y. Hirata. 2002. Genetic and Epigenetic Inactivation of Mitotic Checkpoint Genes hBUB1 and hBUBR1 and Their Relationship to Survival. *Cancer Res.* 62:13 LP-17.

Shrestha, R.L., and V.M. Draviam. 2013. Lateral to End-on Conversion of Chromosome-Microtubule Attachment Requires Kinesins CENP-E and MCAK. *Curr. Biol.* 23:1514–1526.

Silió, V., A.D. McAinsh, and J.B. Millar. 2015. KNL1-Bubs and RZZ Provide Two Separable Pathways for Checkpoint Activation at Human Kinetochores. *Dev. Cell*. 35:600–613.

Simonetta, M., R. Manzoni, R. Mosca, M. Mapelli, L. Massimiliano, M. Vink, B. Novak, A. Musacchio, and A. Ciliberto. 2009. The Influence of Catalysis on Mad2 Activation Dynamics. *PLOS Biol.* 7:e1000010.

Sironi, L., M. Mapelli, S. Knapp, A. De Antoni, K.-T. Jeang, and A. Musacchio. 2002. Crystal structure of the tetrameric Mad1–Mad2 core complex: implications of a “safety belt” binding mechanism for the spindle checkpoint. *EMBO J.* 21:2496–2506.

Sivakumar, S., and G.J. Gorbsky. 2017. Phosphatase-regulated recruitment of the spindle- and Kinetochore-Associated (Ska) Complex to kinetochores. *Biol. Open*.

Sliedrecht, T., C. Zhang, K.M. Shokat, and G.J.P.L. Kops. 2010. Chemical Genetic Inhibition of Mps1 in Stable Human Cell Lines Reveals Novel Aspects of Mps1 Function in Mitosis. *PLoS One*. 5:e10251.

Stucke, V.M., H.H.W. Sillje, L. Arnaud, and E.A. Nigg. 2002. Human Mps1 kinase is required for the spindle assembly checkpoint but not for centrosome duplication. *EMBO J*. 21:1723–1732.

Sudakin, V., G.K.T. Chan, and T.J. Yen.

2001. Checkpoint inhibition of the APC/C in HeLa cells is mediated by a complex of BUBR1, BUB3, CDC20, and MAD2. *J. Cell Biol.* . 154:925–936.

Suijkerbuijk, S.J.E., M. Vleugel, A. Teixeira, and G.J.P.L. Kops. 2012. Integration of Kinase and Phosphatase Activities by BUBR1 Ensures Formation of Stable Kinetochore-Microtubule Attachments. *Dev. Cell*. 23:745–755.

Sullivan, K.F., M. Hechenberger, and K. Masri. 1994. Human CENP-A contains a histone H3 related histone fold domain that is required for targeting to the centromere. *J. Cell Biol.* 127:581 LP-592.

Suzuki, A., B.L. Badger, and E.D. Salmon. 2015. A quantitative description of Ndc80 complex linkage to human kinetochores. 6:8161.

Tanaka, K., H. Li Chang, A. Kagami, and Y. Watanabe. 2009. CENP-C Functions as a Scaffold for Effectors with Essential Kinetochore Functions in Mitosis and Meiosis. *Dev. Cell*. 17:334–343.

Tanaka, T.U., N. Rachidi, C. Janke, G. Pereira, M. Galova, E. Schiebel, M.J.R. Stark, and K. Nasmyth. 2002. Evidence that the Ipl1-Sli15 (Aurora Kinase-INCENP) Complex Promotes Chromosome Bi-orientation by Altering Kinetochore-Spindle Pole Connections. *Cell*. 108:317–329.

Tang, C.C., S. Lin, W. Hsu, Y. Lin, C. Wu, Y. Lin, C. Chang, K. Wu, and T.K. Tang. 2011. The human microcephaly protein STIL interacts with CPAP and is required for procentriole formation. *EMBO J.* 30:4790 LP-4804.

Tang, N.H., and T. Toda. 2013. Ndc80 Loop as a protein-protein interaction motif. *Cell Div.* 8:2.

Tardif, K.D., A. Rogers, J. Cassiano, B.L. Roth, D.M. Cimbora, R. McKinnon, A. Peterson, T.B. Douce, R. Robinson, I. Dorweiler, T. Davis, M.A. Hess, K. Ostanin, D.I. Papac, V. Baichwal, I. McAlexander, J.A. Willardsen, M. Saunders, H. Christophe, D. V Kumar, D.A. Wettstein, R.O. Carlson, and B.L. Williams. 2011. Characterization of the cellular and antitumor effects of MPI-0479605, a small-molecule inhibitor of the mitotic kinase Mps1. *Mol. Cancer Ther.* 10:2267–2275.

Teichner, A., E. Eytan, D. Sitry-Shevah, S. Miniowitz-Shemtov, E. Dumin, J. Gromis, and A. Hershko. 2011. p31(comet) promotes disassembly of the mitotic checkpoint complex in an ATP-dependent process. *Proc. Natl. Acad. Sci. U. S. A.* 108:3187–3192.

Tighe, A., O. Staples, and S. Taylor. 2008. Mps1 kinase activity restrains anaphase during an unperturbed mitosis and targets Mad2 to kinetochores. *J. Cell Biol.* 181:893–901.

Tooley, J., and P.T. Stukenberg. 2011. The Ndc80 complex: integrating the kinetochore's many movements. *Chromosom. Res.* 19:377–391.

Torres, E.M., B.R. Williams, and A. Amon. 2008. Aneuploidy: Cells Losing Their Balance. *Genet.* . 179:737–746.

Tyler, R.K., M.L.H. Chu, H. Johnson, E.A. McKenzie, S.J. Gaskell, and P.A. Eyers. 2008. Phosphoregulation of human Mps1 kinase. *Biochem. J.* 417:173 LP-184.

Uhlmann, F., D. Wernic, M.-A. Poupart, E. V Koonin, and K. Nasmyth. 2000. Cleavage of Cohesin by the CD Clan Protease Separin Triggers Anaphase in Yeast. *Cell*. 103:375–386.

Varma, D., and E.D. Salmon. 2012. The KMN protein network – chief conductors of the kinetochore orchestra. *J. Cell Sci.* 125:5927–5936.

Varma, D., X. Wan, D. Cheerambathur, R. Gassmann, A. Suzuki, J. Lawrimore, A. Desai, and E.D. Salmon. 2013. Spindle assembly checkpoint proteins are positioned close to core microtubule attachment sites at kinetochores. *J. Cell Biol.* 202:735–746.

Vázquez-Novelle, M.D., and M. Petronczki. 2014. Relocation of the Chromosomal Passenger Complex Prevents Mitotic Checkpoint Engagement at Anaphase. *Curr. Biol.* 20:1402–1407.

Vleugel, M., M. Omerzu, V. Groenewold, M.A. Hadders, S.M.A. Lens, and G.J.P.L. Kops. 2015. Sequential Multisite Phospho-Regulation of KNL1-BUB3 Interfaces at Mitotic Kinetochores. *Mol. Cell*. 57:824–835.

Vleugel, M., E. Tromer, M. Omerzu, V. Groenewold, W. Nijenhuis, B. Snel, and G.J.P.L. Kops. 2013. Arrayed BUB recruitment modules in the kinetochore scaffold KNL1 promote accurate chromosome segregation. *J. Cell Biol.* 203:943–955.

Walczak, C.E., S. Cai, and A. Khodjakov. 2010. Mechanisms of chromosome behaviour during mitosis. *Nat Rev Mol Cell Biol*. 11:91–102.

Wang, F., J. Dai, J.R. Daum, E. Niedzialkowska, B. Banerjee, P.T. Stukenberg, G.J. Gorbsky, and J.M.G. Higgins. 2010. Histone H3 Thr-3 Phosphorylation by Haspin Positions Aurora B at Centromeres in Mitosis. *Science (80-.).* 330:231 LP-235.

Wang, H., X. Zhang, L. Teng, and R.J. Legerski. 2015. DNA damage checkpoint recovery and cancer development. *Exp. Cell Res.* 334:350–358.

Wang, W., Y. Yang, Y. Gao, Q. Xu, F. Wang, S. Zhu, W. Old, K. Resing, N. Ahn, M. Lei, and X. Liu. 2009. Structural and mechanistic insights into Mps1 kinase activation. *J. Cell. Mol. Med.* 13:1679–1694.

Wang, X., H. Yu, L. Xu, T. Zhu, F. Zheng, C. Fu, Z. Wang, and Z. Dou. 2014. Dynamic Autophosphorylation of Mps1 Kinase Is Required for Faithful Mitotic Progression. *PLoS One*. 9:e104723.

Wei, R.R., J. Al-Bassam, and S.C. Harrison. 2006. The Ndc80/HEC1 complex is a contact point for kinetochore-

microtubule attachment. 14:54.

Weir, J.R., A.C. Faesen, K. Klare, A. Petrovic, F. Basilico, J. Fischböck, S. Pentakota, J. Keller, M.E. Pesenti, D. Pan, D. Vogt, S. Wohlgemuth, F. Herzog, and A. Musacchio. 2016. Insights from biochemical reconstitution into the architecture of human kinetochores. *Nature*. 537:249–253.

Welburn, J.P.I., E.L. Grishchuk, C.B. Backer, E.M. Wilson-Kubalek, J.R. Yates III, and I.M. Cheeseman. 2009. The Human Kinetochore Ska1 Complex Facilitates Microtubule Depolymerization-Coupled Motility. *Dev. Cell*. 16:374–385.

Welburn, J.P.I., M. Vleugel, D. Liu, J.R. Yates III, M.A. Lampson, T. Fukagawa, I.M. Cheeseman, J.R. Yates III, M.A. Lampson, T. Fukagawa, and I.M. Cheeseman. 2010. Aurora B Phosphorylates Spatially Distinct Targets to Differentially Regulate the Kinetochore-Microtubule Interface. *Mol. Cell*. 38:383–392.

Westhorpe, F.G., A. Tighe, P. Lara-Gonzalez, and S.S. Taylor. 2011. p31-mediated extraction of Mad2 from the MCC promotes efficient mitotic exit. *J. Cell Sci.* 124:3905 LP-3916.

White-Gilbertson, S., D.T. Kurtz, and C. Voelkel-Johnson. 2009. The role of protein synthesis in cell cycling and cancer. *Mol. Oncol.* 3:402–408.

Winey, M., L. Goetsch, P. Baum, and B. Byers. 1991. MPS1 and MPS2: novel yeast genes defining distinct steps of spindle pole body duplication. *J. Cell Biol.* 114:745–754.

Wollman, R., E.N. Cytrynbaum, J.T. Jones, T. Meyer, J.M. Scholey, and A. Mogilner. 2005. Efficient Chromosome Capture Requires a Bias in the “Search-and-Capture” Process during Mitotic-Spindle Assembly. *Curr. Biol.* 15:828–832.

Wood, E., and P. Nurse. 2015. Sizing up to Divide: Mitotic Cell-Size Control in Fission Yeast. *Annu. Rev. Cell Dev. Biol.* 31:11–29.

Wu, J.Q., J.Y. Guo, W. Tang, C.-S. Yang, C.D. Freel, C. Chen, A.C. Nairn, and S. Kornbluth. 2009. PP1-mediated dephosphorylation of phosphoproteins at mitotic exit is controlled by inhibitor-1 and PP1 phosphorylation. *Nat. Cell Biol.* 11:644.

Xu, Q., S. Zhu, W. Wang, X. Zhang, W. Old, N. Ahn, and X. Liu. 2008a. Regulation of Kinetochore Recruitment of Two Essential Mitotic Spindle Checkpoint Proteins by Mps1 Phosphorylation. *Mol. Biol. Cell*. 20:10–20.

Xu, Y., Y. Chen, P. Zhang, P.D. Jeffrey, and Y. Shi. 2008b. Structure of a Protein Phosphatase 2A Holoenzyme: Insights into B55-Mediated Tau Dephosphorylation. *Mol. Cell*. 31:873–885.

El Yakoubi, W., E. Buffin, D. Cladière, Y. Gryaznova, I. Berenguer, S.A. Touati,

R. Gómez, J.A. Suja, J.M. van Deursen, and K. Wassmann. 2017. Mps1 kinase-dependent Sgo2 centromere localisation mediates cohesin protection in mouse oocyte meiosis I. *Nat. Commun.* 8:694.

Yamagishi, Y., T. Honda, Y. Tanno, and Y. Watanabe. 2010. Two Histone Marks Establish the Inner Centromere and Chromosome Bi-Orientation. *Science (80-.).* 330:239 LP-243.

Yamagishi, Y., C.-H. Yang, Y. Tanno, and Y. Watanabe. 2012. MPS1/Mph1 phosphorylates the kinetochore protein KNL1/Spc7 to recruit SAC components. *Nat Cell Biol*. 14:746–752.

Yamaguchi, M., R. VanderLinden, F. Weissmann, R. Qiao, P. Dube, N.G. Brown, D. Haselbach, W. Zhang, S.S. Sidhu, J.-M. Peters, H. Stark, and B.A. Schulman. 2016. Cryo-EM of Mitotic Checkpoint Complex-Bound APC/C Reveals Reciprocal and Conformational Regulation of Ubiquitin Ligation. *Mol. Cell*. 63:593–607.

Yang, M., B. Li, D.R. Tomchick, M. Machius, J. Rizo, H. Yu, and X. Luo. 2007a. p31(comet) Blocks Mad2 Activation through Structural Mimicry. *Cell*. 131:744–755.

Yang, Y., F. Wu, T. Ward, F. Yan, Q. Wu, Z. Wang, T. McGlothen, W. Peng, T. You, M. Sun, T. Cui, R. Hu, Z. Dou, J. Zhu, W. Xie, Z. Rao, X. Ding, and X. Yao. 2008. Phosphorylation of HsMis13 by Aurora B Kinase Is Essential for Assembly of Functional Kinetochore. *J. Biol. Chem.* 283:26726–26736.

Yang, Z., U.S. Tulu, P. Wadsworth, and C.L. Rieder. 2007b. Kinetochore Dynein Is Required for Chromosome Motion and Congression Independent of the Spindle Checkpoint. *Curr. Biol.* 17:973–980.

Zaytsev, A. V, J.E. Mick, E. Maslennikov, B. Nikashin, J.G. DeLuca, and E.L. Grishchuk. 2015. Multisite phosphorylation of the NDC80 complex gradually tunes its microtubule-binding affinity. *Mol. Biol. Cell*. 26:1829–1844.

Zaytsev, A. V, D. Segura-Peña, M. Godzi, A. Calderon, E.R. Ballister, R. Stamatov, A.M. Mayo, L. Peterson, B.E. Black, F.I. Ataullakhanov, M.A. Lampson, and E.L. Grishchuk. 2016. Bistability of a coupled Aurora B kinase-phosphatase system in cell division. *Elife*. 5:e10644.

Zaytsev, A. V, L.J.R. Sundin, K.F. DeLuca, E.L. Grishchuk, and J.G. DeLuca. 2014. Accurate phosphoregulation of kinetochore–microtubule affinity requires unconstrained molecular interactions. *J. Cell Biol.* 206:45 LP-59.

Zeng, K., R.N. Bastos, F.A. Barr, and U. Gruneberg. 2010. Protein phosphatase 6 regulates mitotic spindle formation by controlling the T-loop phosphorylation state of Aurora A bound to its activator TPX2. *J. Cell Biol.* . 191:1315–1332.

Zhang, G., C. D Kelstrup, X.-W. Hu, M. J. Kaas Hansen, M. R Singleton, J.

Olsen, and J. Nilsson. 2012. The Ndc80 internal loop is required for recruitment of the Ska complex to establish end-on microtubule attachment to kinetochores. 125. 3243-3253 pp.

Zhang, G., T. Kruse, B. López-Méndez, K.B. Sylvestersen, D.H. Garvanska, S. Schopper, M.L. Nielsen, and J. Nilsson. 2017. Bub1 positions Mad1 close to KNL1 MELT repeats to promote checkpoint signalling. 8:15822.

Zhang, G., T. Lischetti, D.G. Hayward, and J. Nilsson. 2015. Distinct domains in Bub1 localize RZZ and BubR1 to kinetochores to regulate the checkpoint. *Nat. Commun.* 6:7162.

Zhang, G., T. Lischetti, and J. Nilsson. 2014. A minimal number of MELT repeats supports all the functions of KNL1 in chromosome segregation. *J. Cell Sci.* 127:871 LP-884.

Zhu, T., Z. Dou, B. Qin, C. Jin, X. Wang, L. Xu, Z. Wang, L. Zhu, F. Liu, X. Gao, Y. Ke, Z. Wang, F. Aikhionbare, C. Fu, X. Ding, and X. Yao. 2013. Phosphorylation of microtubule-binding protein Hec1 by mitotic kinase Aurora B specifies spindle checkpoint kinase Mps1 signaling at the kinetochore. *J. Biol. Chem.*